



TECHNISCHE UNIVERSITÄT MÜNCHEN

Lehrstuhl für Erneuerbare und Nachhaltige Energiesysteme

Drivers of energy storage demand in the German power system: an analysis of the influence of methodology and parameters on modelling results

Maximilian R. Kühne

Vollständiger Abdruck der von der Fakultät für Elektrotechnik und Informationstechnik der Technischen Universität München zur Erlangung des akademischen Grades eines

Doktor-Ingenieurs

genehmigten Dissertation.

Vorsitzender: Univ.-Prof. Dr.-Ing. Wolfgang Kellerer

Prüfer der Dissertation: 1. Univ.-Prof. Dr. rer. nat. Thomas Hamacher
2. Univ.-Prof. Dr.-Ing. Hermann-Josef Wagner,
Ruhr-Universität Bochum

Die Dissertation wurde am 09.11.2015 bei der Technischen Universität München eingereicht und durch die Fakultät für Elektrotechnik und Informationstechnik am 22.04.2016 angenommen.

Abstract

This thesis assesses the influence of methodology and parameters on modelling results on storage demand in the power system. The investigation is based on both qualitative analysis and – using Germany as an example – model-based sensitivity analysis. While it is shown that the share of renewable energy, meteorological conditions as well as storage and fuel costs are important drivers of storage demand in general, sensitivity is found to differ significantly between storage technologies. The uncertainty about storage demand is furthermore evaluated from an investor's perspective. Only the profitability of pumped-storage hydro power plants proves robust to varying boundary conditions.

Zusammenfassung

Die Arbeit untersucht den Einfluss von Methodik und Parametern auf Modellierungsergebnisse zum Speicherbedarf im Stromsystem. Die Untersuchung basiert sowohl auf qualitativen Analysen als auch auf einer modellgestützten Sensitivitätsanalyse am Beispiel Deutschlands. Während sich der Anteil erneuerbarer Energien, die Wetterverhältnisse sowie Speicher- und Brennstoffkosten allgemein als wichtige Einflussfaktoren des Speicherbedarfs erweisen, unterscheidet sich die Sensitivität der verschiedenen Speichertechnologien sehr deutlich. Die Unsicherheit bezüglich des Speicherbedarfs wird zudem aus Investorensicht bewertet. Lediglich die Rentabilität von Pumpspeicherwerken erweist sich als robust gegenüber variierenden Rahmenbedingungen.

Contents

| | | |
|----------|---|-----------|
| 1 | INTRODUCTION | 9 |
| 1.1 | ENERGY STORAGE AND THE ENERGY TRANSITION | 9 |
| 1.2 | RELATED WORK..... | 12 |
| 1.3 | MAIN CONTRIBUTIONS..... | 13 |
| 1.4 | OUTLINE..... | 14 |
| 2 | REVIEW OF STUDIES ON THE DEMAND FOR ENERGY STORAGE IN POWER SYSTEMS | 17 |
| 2.1 | COMPARISON OF METHODOLOGY AND RESULTS OF SELECTED STUDIES | 17 |
| 2.1.1 | <i>General scope.....</i> | <i>17</i> |
| 2.1.2 | <i>Methodology and results</i> | <i>20</i> |
| 2.2 | COMPARISON OF RESULTS ON ENERGY STORAGE DEMAND IN THE GERMAN POWER SYSTEM | 31 |
| 3 | THE WHOLE-SYSTEMS COST MINIMISATION MODEL IMAKUS.. | 35 |
| 3.1 | THE EXISTING MODEL AND ITS SCOPE | 35 |
| 3.2 | METHODOLOGICAL APPROACH AND MODEL FORMULATION | 37 |
| 3.2.1 | <i>Submodel MOWIKA: generation capacity expansion</i> | <i>37</i> |
| 3.2.2 | <i>Submodel MESTAS: storage capacity expansion</i> | <i>54</i> |
| 3.2.3 | <i>Submodel MOGLIE: ensuring system firm capacity</i> | <i>73</i> |
| 3.2.4 | <i>The iterative approach.....</i> | <i>81</i> |
| 3.3 | EXTENSIONS TO THE MODEL IMAKUS | 87 |
| 3.3.1 | <i>Calculating the salvage value by using the annuity method for depreciation</i> | <i>87</i> |
| 3.3.2 | <i>Optimisation of initial and final storage levels</i> | <i>93</i> |
| 3.3.3 | <i>Constraining emissions over the whole planning horizon</i> | <i>96</i> |
| 4 | QUALITATIVE ANALYSIS OF THE INFLUENCE OF METHODOLOGY AND ASSUMPTIONS ON MODELLING RESULTS..... | 99 |
| 4.1 | RESOLVING SPACE | 99 |

| | | |
|----------|---|------------|
| 4.2 | RESOLVING TIME | 101 |
| 4.2.1 | <i>Representative time slices vs. annual time series</i> | 101 |
| 4.2.2 | <i>Hourly resolution of time series</i> | 103 |
| 4.3 | SYSTEM BOUNDARIES..... | 104 |
| 4.3.1 | <i>Geographic scope</i> | 104 |
| 4.3.2 | <i>Sectoral scope</i> | 106 |
| 4.4 | FORESIGHT AND PLANNING HORIZONS | 108 |
| 4.4.1 | <i>Planning with perfect foresight</i> | 108 |
| 4.4.2 | <i>Intertemporal approach vs. snapshot years</i> | 109 |
| 4.5 | DISCOUNTING THE FUTURE | 113 |
| 4.6 | CARBON PRICES VS. CARBON EMISSIONS TARGETS..... | 117 |
| 4.7 | MODELLING OF POWER PLANTS AND ENERGY STORAGE | 122 |
| 4.7.1 | <i>Simplified modelling of unit commitment</i> | 122 |
| 4.7.2 | <i>Curtailment of generation from RES and CHP</i> | 123 |
| 4.7.3 | <i>Must-run of conventional generation</i> | 125 |
| 4.7.4 | <i>Independent rating of storage dimensions</i> | 127 |
| 4.7.5 | <i>Optimising vs. exogenously fixing initial storage levels</i> | 130 |
| 4.8 | DISCUSSION AND CONCLUSION | 132 |
| 5 | SENSITIVITY ANALYSIS OF ENERGY STORAGE DEMAND IN THE GERMAN POWER SYSTEM | 135 |
| 5.1 | SCENARIO FRAMEWORK FOR SENSITIVITY ANALYSIS | 135 |
| 5.2 | DEFINING THE REFERENCE SCENARIO | 137 |
| 5.2.1 | <i>General assumptions</i> | 137 |
| 5.2.2 | <i>Electricity demand</i> | 137 |
| 5.2.3 | <i>Share and structure of RES</i> | 138 |
| 5.2.4 | <i>Time series of demand and generation</i> | 140 |
| 5.2.5 | <i>Existing power plant portfolio</i> | 146 |
| 5.2.6 | <i>Existing storage portfolio</i> | 148 |
| 5.2.7 | <i>Fuels</i> | 150 |
| 5.2.8 | <i>Technical and economic parameters of new build power plants</i> | 152 |
| 5.2.9 | <i>Technical and economic parameters of new build storage</i> | 154 |
| 5.2.10 | <i>Overall emissions target</i> | 156 |
| 5.3 | SELECTING A METEOROLOGICAL REFERENCE YEAR | 158 |
| 5.3.1 | <i>Characterising annual time series of demand and generation</i> | 158 |
| 5.3.2 | <i>Characterising annual time series of residual demand</i> | 165 |
| 5.3.3 | <i>Approach to selecting a reference year</i> | 167 |
| 5.4 | RESULTS FROM THE REFERENCE SCENARIO | 176 |
| 5.4.1 | <i>Economic savings of storage expansion</i> | 176 |
| 5.4.2 | <i>Curtailment of generation from RES and CHP</i> | 177 |
| 5.4.3 | <i>Storage expansion and operation</i> | 178 |

| | | |
|----------|--|------------|
| 5.4.4 | <i>Generation expansion and operation</i> | 182 |
| 5.5 | DEFINING THE VARIATION SCENARIOS | 186 |
| 5.5.1 | <i>Variation of annual time series</i> | 186 |
| 5.5.2 | <i>Variation of RES share</i> | 188 |
| 5.5.3 | <i>Variation of RES structure</i> | 190 |
| 5.5.4 | <i>Variation of fuel costs</i> | 193 |
| 5.5.5 | <i>Variation of the bonus on storage costs</i> | 194 |
| 5.5.6 | <i>Variation of storage investment costs</i> | 195 |
| 5.6 | OVERVIEW OF RESULTS FROM THE VARIATION SCENARIOS..... | 197 |
| 5.6.1 | <i>Sensitivity of total storage expansion</i> | 197 |
| 5.6.2 | <i>Sensitivity of PSP expansion</i> | 201 |
| 5.6.3 | <i>Sensitivity of AA-CAES expansion</i> | 204 |
| 5.6.4 | <i>Sensitivity of H₂-CCGT expansion</i> | 208 |
| 5.7 | DETAILED DISCUSSION OF RESULTS FROM THE VARIATION SCENARIOS | 213 |
| 5.7.1 | <i>Variation of annual time series</i> | 213 |
| 5.7.2 | <i>Variation of RES share</i> | 219 |
| 5.7.3 | <i>Variation of RES structure</i> | 223 |
| 5.8 | DISCUSSION AND CONCLUSION | 229 |
| 6 | INTERPRETATION OF RESULTS ON ENERGY STORAGE DEMAND FROM AN INVESTOR'S PERSPECTIVE | 233 |
| 6.1 | ARE RESULTS FROM WHOLE-SYSTEMS COST MINIMISATION OF ANY USE TO INVESTORS? | 233 |
| 6.2 | ADAPTING THE DISCOUNT RATE TO THE INVESTOR'S PERSPECTIVE..... | 235 |
| 6.3 | RESULTS FROM THE REFERENCE SCENARIO | 235 |
| 6.4 | PROFITABILITY OF INVESTMENTS INTO STORAGE UNDER VARIATION SCENARIOS | 238 |
| 6.4.1 | <i>Approach to determining profitability under variation scenarios</i> . | 238 |
| 6.4.2 | <i>Overview of earned IRR</i> | 239 |
| 6.4.3 | <i>Earned IRR under scenarios varying annual time series</i> | 241 |
| 6.4.4 | <i>Earned IRR under scenarios varying RES share</i> | 242 |
| 6.4.5 | <i>Earned IRR under scenarios varying RES structure</i> | 244 |
| 6.5 | DISCUSSION AND CONCLUSION | 245 |
| 7 | CONCLUSION..... | 247 |
| 7.1 | SUMMARY OF RESULTS..... | 247 |
| 7.2 | PERSPECTIVES | 249 |
| A | LITERATURE REVIEW..... | 253 |
| A.1 | COMPLEMENTARY ASPECTS OF METHODOLOGY OF SELECTED STUDIES..... | 253 |
| B | VARIABILITY INDICES | 255 |

| | | |
|----------|--|------------|
| B.1 | DETERMINING VARIABILITY INDICES OF GENERATION AND DEMAND TIME SERIES | 255 |
| B.2 | DETERMINING VARIABILITY INDICES OF RESIDUAL DEMAND TIME SERIES.... | 260 |
| C | DATA..... | 263 |
| C.1 | PARAMETERS OF EXISTING PSP IN GERMANY | 263 |
| C.2 | DEVELOPMENT OF RES AND CHP GENERATION CAPACITY..... | 264 |
| | ABBREVIATIONS | 267 |
| | NOMENCLATURE | 269 |
| | LIST OF TABLES..... | 279 |
| | LIST OF FIGURES..... | 283 |
| | REFERENCES..... | 289 |

1 Introduction

In this first chapter, the motivation for analysing the influence of methodology and parameters on modelling results on storage demand is described. The related work is discussed and the main contributions of this thesis are presented. An outline of this thesis is provided at the end of the chapter.

1.1 Energy storage and the energy transition

While the history of the German “Energiewende” can be traced back to the oil price crisis and the German anti-nuclear movement of the 1970s (vide Hake *et al.* 2015), the guiding principles of the current energy transition policy in Germany were proclaimed more recently in the so-called “Energiekonzept”, a policy package drafted by the German government in 2010 (BMWi & BMU 2010).

Whereas the original concept stipulated to prolong the lifetimes of existing nuclear power plants in Germany, this policy was already abandoned in 2011, when the German government decided to phase out nuclear power (BGBL 2011) as an immediate reaction to accidents in the Japanese nuclear power plant of Fukushima following the earthquake and tsunami of 11 March 2011 (Norio *et al.* 2011). With this exception, Germany has since committed to the principal goals of the “Energiekonzept”, namely reducing greenhouse gas (GHG) emissions by 80 % until 2050 (on 1990 levels) and substantially increasing the share of renewable energy sources (RES) in total energy consumption and, particularly, in electricity consumption (BMWi & BMU 2010).

However, the intended energy transition does not come without challenges. For instance, due to the high variability of electricity generation from major RES like wind power and solar photovoltaics (PV), a combination of measures will be required to effectively balance electricity generation and demand in power systems with high shares of RES: Besides expanding transmission and distribution networks and increasing the flexibility of demand and conventional backup capacities, also the expansion of energy storage capacities could facilitate the integration of RES into the power system (vide e. g. Delucchi & Jacobson 2011, Schaber 2013).

As electricity prices vary, storages have always been used in conventional power systems to perform energy arbitrage (vide e. g. Graves *et al.* 1999): Storage operators can generate revenues by charging storages during times of low demand – i. e. low prices – and discharging storages to substitute expensive generation from peaking plants (referred to as peak shaving). Assuming that electricity prices reflect the marginal costs of electricity generation (vide Schweppe *et al.* 1988), the described dispatch of storages also reduces the total costs of electricity generation from a system point of view.

While storage dispatch follows the same rationale in power systems that accommodate high shares of RES, energy arbitrage opportunities are even more plentiful: Due to the high variability of RES generation, the residual demand – i. e. the original consumer electricity demand minus electricity generation from RES and combined heat and power (CHP) – is subject to strong fluctuations that can be smoothed by storages. In case of extremely high shares of RES, renewable electricity feed-in might even exceed demand occasionally. By charging storages, the curtailment – and, thus, wasting – of these cost-free energy surpluses can be avoided.

Apart from the German energy transition, similar concepts for a future low-carbon and largely renewable-based energy supply have been proposed in other countries, e. g. in the United Kingdom (DECC 2011) and Denmark (KEMIN 2011). Also, the majority of US states have implemented policies to further promote renewable electricity generation (Delmas & Montes-Sancho 2011).

As a consequence, a multitude of studies have been published lately which address the topic of energy storage demand in future power systems with high shares of RES. However, as different studies convey quite contradictory impressions of storage demand, political and private-sector decision makers may find it hard to draw any conclusions from these often model-based analyses. By picking only a few examples from the bulk of recently published studies on storage demand, Figure 1.1 shall illustrate the problems of interpreting results in the light of alternative studies.

After consulting the analysis by Pieper & Rubel (2011), which estimates a global potential of 1895 GWh of additional storage capacity until 2030, one might be surprised that – according to Strbac *et al.* (2012), who report up to 14.9 GW of charging and discharging capacity and a 24-h storage duration – the additional demand for storage capacity in Great Britain (358 GWh) equals almost 19 % of the global value.

Results by Adamek *et al.* (2012) might cause even more confusion: The study reports a demand of 2191 GWh of additional storage capacity in Germany until 2025, which well exceeds the global value found in Pieper & Rubel (2011). An alternative value for Germany – 40 GWh specified in Kuhn *et al.* (2012) – appears to be better in line with the global potential but will probably no longer put the reader's mind at ease.

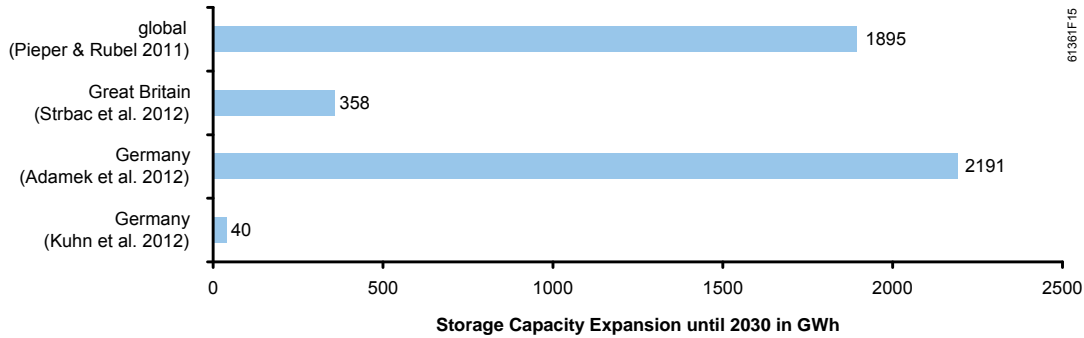


Figure 1.1: Selected study results on the expansion of storage capacity until 2030

At least some of this confusion can be easily resolved: As Pieper & Rubel (2011) take an investor’s perspective and assess market potential, they naturally come up with lower estimates of storage capacity than the other three studies which adopt a system point of view. Furthermore, a closer look at assumptions in Kuhn *et al.* (2012) reveals that the comparably small storage capacity of 40 GWh in this study actually equals an exogenously defined limit.

However, it remains unclear whether the very high level of storage demand in Germany found in Adamek *et al.* (2012) is actually comparable to results reported for Great Britain and whether it could, in principle, be reproduced with methods employed, for instance, in Kuhn *et al.* (2012).

Unfortunately, studies seldom offer direct comparisons of their findings with results from related studies. It is thus up to the reader to compare the respective methodological approaches and input parameters. This leaves researchers and, in particular, political and private-sector decision makers who might not be familiar with the applied methods in an unsatisfying situation: While interpreting results from a single study is often difficult enough, judging the impact of alternative approaches can be even more challenging and requires transparency of methodology and assumptions. Grasping the influence of varying input parameters without conducting a proper sensitivity analysis is, however, all but impossible.

To remedy this situation in the realm of studies on storage demand, this thesis provides systematic analyses that address the following questions:

- How do assumptions and methodological approaches affect modelling results?
- How strongly dependent are modelling results on input parameters?
- How, if at all, can results from system level studies be interpreted from an investor’s perspective?

1.2 Related work

A considerable number of publications have tried to remedy the uncertainty created by the multitude of methodological approaches and their potential influence on results by classifying models. For energy systems models in general, one such example is the review by Connolly *et al.* (2010), where 37 models are grouped into commonly used categories, like e. g. simulation tools, equilibrium approaches, top-down and bottom-up approaches. Connolly *et al.* (2010) furthermore distinguish between operation and investment optimisation tools.

An alternative classification of energy systems models is presented by Pfenninger *et al.* (2014). Three fundamental approaches are identified: simulation techniques to facilitate forecasts (predictive); optimisation methods to provide scenarios (normative); and qualitative or mixed methods. Models employing any of these approaches but with an exclusive focus on power systems are grouped into a fourth category.

Pfenninger *et al.* (2014) acknowledge the need to compare and validate modelling results and point to the widespread criticism against energy systems models: In the past, models were often criticised as being intransparent in terms of methodology and inaccessible regarding both model code and input data. In order to facilitate independent review and allow for reproducible results, modellers are thus reminded to increase transparency and accessibility in the future.

A review of methodologies by Zucker *et al.* (2013) only considers models focusing on energy storage in the power system. Models are grouped into two main categories, namely engineering models, which assess the techno-economic feasibility of a given storage asset under given boundary conditions (“price taker approach”), and system models, where storage operation is subject to minimising total system costs.

Beyond the cited principal categories, all three publications discuss further characteristics along which models can be differentiated, like e. g. geographic and sectoral scope or temporal and spatial resolution. While similar criteria are used in an attempt to roughly classify studies on storage demand in this thesis (vide Chapter 2), the influence of assumptions and methodology on modelling results shall also be analysed on a more detailed level.

Such an analysis – albeit for energy systems models in general – has been conducted by Mai *et al.* (2013). While this study covers the main types of energy systems models and characterises the nature of their results, it also discusses the impact of central assumptions, like e. g. the discount rate. It thus represents a helpful work of reference for the target audience of energy systems models, which is complemented in this thesis with regard to specific aspects of storage modelling and the influence of assumptions and methodology on results on storage demand (vide Chapter 4). In contrast to the purely qualitative assessment by Mai *et al.* (2013), the analysis in this

thesis is underpinned by comparing actual results obtained from different methodological approaches.

Results on storage demand from different studies have already been compared in a number of reviews. For instance, 14 publications focusing on the German power system are compared by Wenzel & Kunz (2015) with regard to future storage capacities. Zucker *et al.* (2013) contrast studies with very different geographic scopes. A selection of 13 studies that assess the techno-economic feasibility of pumped-storage hydro power plants (PSP) and compressed air energy storages (CAES) are compared in terms of earned contribution margins. Furthermore, twelve system studies are compared with regard to the system benefits of storage.

Although reviewers are aware of the limited comparability of results from different studies, the possible causes for the identified differences – i. e. methodological approaches, assumptions and input parameters – are seldom analysed thoroughly.

Moreover, only few of the primary studies on storage demand discuss the impact of their methodological choices or provide a sensitivity analysis of their results to input parameters. Many studies only investigate a rather small number of scenarios (e. g. Adamek *et al.* 2012, Klaus *et al.* 2010, Kuhn *et al.* 2012). A more systematic analysis of the sensitivity of storage demand to one input parameter – namely storage costs – has been conducted by Strbac *et al.* (2012). This thesis intends to further improve the understanding of the sensitivity of storage demand and, thus, analyses the impact of a broad range of parameters on modelling results (vide Chapter 5).

1.3 Main contributions

This thesis sets out to systematically and coherently assess the influence of methodological approaches, assumptions and input parameters on modelling results on energy storage demand in the power system. By this means, the understanding of the causes for potentially contradictory results from different studies shall be improved and the drivers of storage demand shall be identified.

The main contributions of this thesis can be summarised as follows:

- As a complement to existing analyses for energy systems models in general, methodology and assumptions are analysed qualitatively with regard to their influence on modelling results on storage demand. This analysis is underpinned by a comparison of different approaches with the whole-systems cost minimisation model IMAKUS. Findings are summarised in the form of a quickly accessible guide to better evaluate and compare modelling results on storage demand in the future.

- As modelling results on storage demand are largely dependent on the meteorological conditions reflected by input parameters, a method is proposed to select a representative set of time series of renewable electricity generation and electricity demand. The time series are characterised with regard to full load hours, surplus energy and residual energy demand as well as intra-annual variability.
- Using Germany as an example, the sensitivity of modelling results on storage demand to input parameters is analysed with the whole-systems cost minimisation model IMAKUS. The analysis demonstrates that all of the tested input parameters are important drivers of storage demand. Sensitivity is however found to differ significantly between storage technologies.
- By determining the internal rate of return on storage investments under varying input parameters, the uncertainty about cost-optimal storage demand is also evaluated from an investor’s perspective. Only the profitability of PSP proves comparably robust to varying boundary conditions.

1.4 Outline

As the rather bold comparison of results on energy storage demand in the introductory chapter leaves many questions unanswered, Chapter 2 takes a closer look at the cited studies and reviews further studies on storage demand with regard to scope and methodology. A detailed comparison of results on storage demand in the German power system leads to the conclusion that the influence of methodology and parameters on modelling results needs further analysis.

Chapter 3 describes methodology and formulation of the whole-systems cost minimisation model IMAKUS, which shall be used in this thesis to analyse the influence of methodology and parameters on modelling results on storage demand. Both the existing model and extensions within the scope of this thesis are presented.

Chapter 4 discusses how methodological approaches affect modelling results on storage demand. Wherever possible, the qualitative analysis is complemented by comparing results obtained from the whole-systems cost minimisation model IMAKUS for different approaches and assumptions.

In Chapter 5, the model IMAKUS is used to analyse the sensitivity of results on storage demand to changes in selected input parameters. Initially, the general framework for this sensitivity analysis is introduced and all input parameters are presented in detail. A reference scenario is defined and a meteorological reference year – which represents the typical characteristics of time series of renewable electricity genera-

tion and electricity demand – is identified. Storage capacity expansion is optimised under the reference scenario as well as under varying input parameters.

Chapter 6 discusses the general relevance of modelling results from whole-systems cost minimisation to investors and evaluates the uncertainty about cost-optimal storage demand from an investor's perspective. The profitability of storage investments optimised under the reference scenario is analysed for varying boundary conditions.

Finally, Chapter 7 summarises the main results and discusses several perspectives for future research.

Appendix A provides complementary information on the methodology of studies that are reviewed in Chapter 2. The methods used in this thesis to measure the variability of time series of generation, demand and residual demand are described in Appendix B. Additional data on existing PSP in Germany and the assumed development of RES and CHP generation capacity can be found in Appendix C.

2 Review of studies on the demand for energy storage in power systems

As already the selection of literature accounts in the introductory chapter showed, different studies convey quite contradictory impressions of the future demand for energy storage. This chapter takes a closer look at eleven recent studies on energy storage demand and discusses to what extent results from different studies are comparable. In the first section, the selected studies are presented and compared with regard to their general scope, methodology and results. While most of the selected studies focus on Germany, the geographic scope ranges from other countries and regions to a global scale. This general review is followed by a detailed comparison of results on energy storage demand in the German power system in Section 2.2.

2.1 Comparison of methodology and results of selected studies

2.1.1 General scope

As energy storage is considered to be one of the key elements of future low-carbon power systems, a multitude of studies have been published lately on storage technologies, the technical and economic feasibility of storage and storage demand. In this chapter, eleven recent studies on energy storage demand are reviewed. Therefore, the crucial criterion for studies to be considered in this review was whether future storage capacities are determined and specified.

Whereas studies with a clear focus on energy storage demand were preferred, some of the selected studies consider storage as merely one of several elements of future power systems. Depending on the primary objective – i. e. either identifying storage

demand on a system level, determining the cost-optimal structure of power systems, assessing the market potential of storage or analysing the technical feasibility of power systems with high shares of RES –, studies take very different methodological approaches. Moreover, even studies with the same objective may still employ different methods.

Table 2.1 presents the general scope of the eleven studies that were selected for review. Besides information on geographic scope, sectoral scope and time perspective, the table offers a brief overview of the primary objectives and the methodological approaches of the different studies.

While most of the selected studies focus on Germany, the review also includes studies with other geographic scopes: EPRI (2012) and Hand *et al.* (2012) cover the United States and Strbac *et al.* (2012) analyse storage demand in Great Britain. In Scholz (2012), the geographic scope comprises Europe and North Africa. By contrast, Pieper & Rubel (2011) present a global perspective. The sectoral scope of most studies extends beyond the power sector, including e. g. partial representations of the transport and heating sectors.

The majority of studies offer a long-term perspective until 2050. However, only a small number of studies – namely Hand *et al.* (2012), Kuhn (2012) and Kuhn *et al.* (2012) – explore the whole pathway until 2050 by modelling the power system over a planning horizon of several decades. In EPRI (2012), the pathway of the power system is explored over a mid-term planning horizon until 2030. By contrast, other studies only analyse one or more snapshot years.

Six out of eleven studies focus on identifying energy storage demand and are modelling the power system, namely Adamek *et al.* (2012), Agora Energiewende (2014), EPRI (2012), Kuhn (2012), Kuhn *et al.* (2012) and Strbac *et al.* (2012). However, only four – EPRI (2012), Kuhn (2012), Kuhn *et al.* (2012) and Strbac *et al.* (2012) – are using whole-systems cost minimisation to determine the optimal storage portfolio. In Adamek *et al.* (2012) and Agora Energiewende (2014), approaches to identify storage demand are only partly predicated on cost minimisation: System benefits of either estimated or arbitrarily chosen storage capacities are analysed by means of a cost minimisation model of the power system.

Hand *et al.* (2012), Scholz (2010) and Scholz (2012) also use whole-systems cost minimisation models to determine the cost-optimal structure of the power system, i. e. the expansion of generation, storage and transmission capacities. While these studies offer a broader scope, they do not place special emphasis on the storage issue. Thus, the applied methods may not always allow for detailed storage modelling: For instance, Hand *et al.* (2012) employ representative time slices instead of annual time series (vide Sections 2.1.2 and 4.2.1).

Table 2.1: General scope of studies selected for review

| reference | geographic scope | sectoral scope | time perspective | primary objective | method |
|-----------------------------|-------------------------------------|--|--|---|---|
| Adamek <i>et al.</i> (2012) | Germany | power sector | long-term, snapshots of 2025 and 2050 | identifying storage demand on system level | analysing system benefits of storage based on cost minimisation |
| Agora Energiewende (2014) | Germany, interconnected with Europe | power sector, partial representation of heating sector ¹⁾ | long-term, snapshots of 2023, 2033 and 90 % RES system | identifying storage demand on system level | analysing system benefits of storage based on cost minimisation |
| EPRI (2012) | Midwestern United States | power sector | mid-term, pathway until 2030 | identifying storage demand on system level | whole-systems cost minimisation |
| Hand <i>et al.</i> (2012) | United States ²⁾ | power sector, partial representations of transport and heating sectors | long-term, pathway until 2050 | determining generation, storage and transmission capacities | whole-systems cost minimisation |
| Klaus <i>et al.</i> (2010) | Germany | power sector, partial representations of transport and heating sectors | long-term, snapshot of 2050 | assessing technical feasibility of 100 % RES system | simulation |
| Kuhn (2012) | Germany | power sector | long-term, pathway until 2050 | identifying storage demand on system level | whole-systems cost minimisation (iterative approach) |
| Kuhn <i>et al.</i> (2012) | Germany | power sector, partial representations of transport and heating sectors | long-term, pathway until 2050 | identifying storage demand on system level | whole-systems cost minimisation (iterative approach) |
| Pieper & Rubel (2011) | global | power sector | mid-term, until 2030 | assessing market potential of storage technologies | business case analysis |
| Scholz (2010) | Germany, interconnected with Europe | power sector, partial representation of heating sector | long-term, snapshot of 2050 | determining generation, storage and transmission capacities | whole-systems cost minimisation |
| Scholz (2012) | Europe and North Africa | power sector, partial representation of heating sector | long-term, snapshot of 2050 | determining generation, storage and transmission capacities | whole-systems cost minimisation |
| Strbac <i>et al.</i> (2012) | Great Britain | power sector, partial representations of transport and heating sectors | long-term, snapshots of 2020, 2030 and 2050 | identifying storage demand on system level | whole-systems cost minimisation |

1) complementary analysis of market potential extends to transport sector and chemicals industry

2) not including Alaska and Hawaii

Whereas in most of the studies the relevant criterion in determining storage demand is the economic benefit for the considered power system, two studies take distinctly different approaches: Klaus *et al.* (2010) assess the technical feasibility of a power system based on 100 % RES and determine necessary storage and conventional backup capacities, using a simulation model. Costs are not considered. Pieper & Rubel (2011) adopt an investor's perspective and assess the market potential of energy storage by conducting a business case analysis of storage applications.

It should be noted that two pairs of studies are using identical models: The model IMAKUS is used both in Kuhn (2012) and Kuhn *et al.* (2012), although Kuhn (2012) does not consider competing flexible options in the transport and heating sectors. Moreover, results in both Scholz (2010) and Scholz (2012) are obtained from the model REMix. While the selection of studies using identical models does not further enhance the diversity of the reviewed methodological approaches, it allows to identify the impact of different input parameters on modelling results (vide Section 2.2).

2.1.2 *Methodology and results*

In the previous section, the selected studies were briefly presented with regard to their general scope, primary objective and the general methodological approach. While the following review is intended to offer a general idea of applied methods and obtained results, it enlarges upon energy storage, which is the focus of this thesis. Further details of methodology – for instance, whether competing flexible options are considered and how the provision of operating reserve is modelled – are addressed in Appendix A.1.

Adamek *et al.* (2012)

In this study, a sequential approach is used to identify storage demand in the German power system. First, demand for short- and long-duration storage is estimated based on an analysis of time series of residual demand. For this purpose, the time series in hourly resolution is decomposed into its high- and low-frequency components (comprising periodic times less than and greater than 24 hours respectively). Charging and discharging capacity and storage capacity are dimensioned to enable the balancing of all short- and long-term fluctuations. However, the rating is afterwards adjusted to generic values of storage duration.

Secondly, the economic feasibility of the obtained storage capacities is analysed. The chronological dispatch of storages is optimised in hourly resolution, using a unit commitment model based on mixed-integer quadratic programming. Four cases of storage expansion are considered: either short- or long-duration storage; both short-

and long-duration storage; only 50 % of short- and long-duration capacities. The existing storage portfolio and the generation portfolio are exogenously fixed. In order to determine system benefits, savings through storage are compared with annualised investment costs of storage, which are calculated assuming an arbitrarily defined portfolio of storage technologies (at an interest rate of 9 %).

Whereas storages are initially rated to balance all fluctuations of residual demand, curtailment of surplus generation is allowed in the unit commitment model. The rating of storages is therefore adjusted according to the actual utilisation of capacities in the optimisation model. All results on storage demand are based on snapshot years.

While Adamek *et al.* (2012) determine storage demand using a single-node model (i. e. transmission constraints are neglected), a secondary goal of this study is to analyse the impact of storage on transmission capacity expansion. Thus, the technical feasibility of system operation according to the unit commitment model is tested *ex post* for each hour by means of load flow analysis. For this purpose, the German high voltage network is modelled with 18 nodes, also considering equivalent models of interconnections with the European transmission system.

As results show, the total utilised short- and long-duration storage capacity reaches 2 TWh in 2025, at a share of RES of 40 %. If a share of RES of 80 % is assumed in 2050, the total utilised storage capacity reaches 8 TWh. In case of 100 % RES, total utilised storage capacity increases threefold compared to the 80 % scenario. According to Adamek *et al.* (2012), the total annual system costs increase in all four cases of storage expansion compared to a system without storage expansion, i. e. storage investment costs exceed the generated savings.

However, storage demand which is determined by analysing time series of residual demand represents an upper estimate, as storage losses are neglected and the balancing of all fluctuations is assumed. By contrast, the storage capacities that are actually utilised by the optimisation model can differ significantly from rated values, as losses are considered and the balancing of fluctuations is only economically feasible to a certain extent. Although stated differently by Adamek *et al.* (2012), the applied method is not suitable to identify cost-optimal storage demand: While the utilisation of exogenously – i. e. in fact arbitrarily – fixed storage capacities might not lead to a net system benefit, storage capacity expansion could still turn out economically feasible if optimised with a whole-systems cost minimisation model.

Agora Energiewende (2014)

As in Adamek *et al.* (2012), the approach employed by Agora Energiewende (2014) to identify storage demand on the transmission network level is only partly based on cost minimisation: System benefits of arbitrarily chosen short- and long-duration storage capacities are analysed by comparing scenarios with and without storage,

using a cost minimisation model of the power system. The considered short- and long-duration storage technologies are characterised by efficiency, range of costs and generic values of storage duration. Results are only based on snapshot years.

While the study focuses on Germany, the whole European power system is modelled, assuming 21 European market regions (nodes) that are linked via net transfer capacities (NTC). Transmission of power between these nodes is modelled as a transport problem. However, within individual market regions (e. g. Germany) transmission constraints are not considered.

The chronological dispatch of exogenously defined generation and storage capacities is determined in hourly resolution in a three-stage process: First, electricity exchange between the market regions is optimised neglecting integer decisions of unit commitment. Secondly, assuming the determined electricity exchange, power plant dispatch is optimised with a mixed-integer unit commitment model employing decomposition. Thirdly, based on the unit commitment decisions, dispatch of power plants and storages is simultaneously optimised, using linear programming.

The curtailment of surplus electricity generation is allowed. By assigning opportunity costs to the curtailed energy, Agora Energiewende (2014) intends to take into account the system benefit of integrating additional surplus generation.

Besides the analysis of large-scale storage demand in the transmission system, the study also investigates system benefits of battery storage on the distribution level. For this purpose, network analysis methods are applied. Scenarios with and without storage are compared with regard to the need for capacity expansion in the distribution network, considering thermal limitation and voltage-drop limitation of power lines. The analysis is conducted for representative distribution networks and results are extrapolated to obtain estimates for Germany.

Moreover, the study is complemented by an analysis of the market potential of energy storage outside the power sector, namely in the transport sector and the chemicals industry. Market potential is estimated based on rough calculations, literature review and expert knowledge.

Results show that, at a share of RES of 43 % in Germany in 2023, there is no demand for storage on the transmission level. For 2033, at an RES share of 60 %, a charging and discharging capacity of 3 GW of long-duration storage is found to be feasible, if low flexibility of the power system, low storage investment costs and high opportunity costs of curtailed energy are assumed. In case of 90 % RES in Germany, storage demand is observed for low storage investment costs, even in case of high flexibility of the power system: Out of several arbitrarily defined storage portfolios, a portfolio of 16 GW long- and 7 GW short-duration capacity yields the largest cost savings com-

pared to a scenario without storage expansion. The resulting storage portfolio is economically feasible in spite of several competing flexible options being considered.

EPRI (2012)

In contrast to the previously described studies – which only optimise the operation of exogenously defined storage capacities to determine system benefits –, storage demand is identified by means of whole-systems cost minimisation in EPRI (2012). The employed model EGEAS simultaneously optimises the expansion of storage and generation capacities, using a dynamic programming approach. While investment decisions are determined intertemporally across a mid-term planning horizon, dispatch is not modelled chronologically but based on monthly load duration curves. Transmission constraints are not considered.

In EPRI (2012), three competing storage technologies are available for endogenous capacity expansion: PSP, CAES and batteries. Due to the intertemporal approach, investment decisions into storage are optimal with respect to the whole planning horizon. The curtailment of surplus electricity generation is allowed.

Moreover, the mixed-integer unit commitment model PLEXOS is used for a more detailed analysis of the economic feasibility of storage capacities resulting from optimisation. Whereas capacity expansion in EGEAS is only driven by energy arbitrage, PLEXOS allows for the co-optimisation of storage revenues from energy arbitrage and ancillary services, based on time series from hourly up to five-minute resolution. In PLEXOS, transmission constraints are modelled using the DC (literally “direct current”) power flow method.

The results obtained in EPRI (2012) describe the least-cost pathway for the power system of the Midwestern United States during the period 2010–2030. If energy arbitrage is the only source of revenue, investment into storage is only observed for a small number of scenarios and is limited to CAES. Against expectations, storage demand declines with increasing shares of RES. When benefits from the ancillary services market are also considered in PLEXOS, all three storage technologies are observed to become economically feasible.

Hand *et al.* (2012)

As already pointed out in Section 2.1.1, the primary objective of Hand *et al.* (2012) is not to identify storage demand but to investigate the structure and feasibility of a future power system with high penetrations of RES. For this purpose, investment decisions into RES, conventional generation, storage and transmission assets and demand side flexibility options are simultaneously optimised using linear programming. A detailed description of the applied whole-systems cost minimisation model ReEDS is provided by Short *et al.* (2011).

The expansion of generation, storage and transmission capacities as well as the deployment of demand side technologies is optimised for successive two-year periods, with capacities being carried over to subsequent periods. The model also accounts for the elasticity of electricity demand, which is adjusted between solves of two-year periods based on the deviations between resulting and expected electricity prices. Instead of using annual time series, each year is modelled by 17 time slices, representing seasons, times of day and the summer peak load period.

Three competing storage technologies are considered for capacity expansion: PSP, CAES and a generic high-energy battery technology. Storage duration is exogenously fixed to 8 h for PSP and batteries and 15 h for CAES. The transmission network is modelled as a transport problem with 134 nodes, which represent balancing areas. Curtailment of surplus electricity generation is allowed.

Hand *et al.* (2012) furthermore employ the unit commitment model GridView for a more detailed analysis of the operational implications of high shares of RES. Based on time series in hourly resolution, the linear programming model co-optimises a given power system with regard to electricity generation and the provision of ancillary services. The transmission of power between the 134 balancing areas is modelled using the DC power flow method.

The results obtained from the model ReEDS represent the least-cost pathway for the power system of the United States during the period 2010–2050. However, it should be noted that capacity expansion is optimised with limited foresight, i. e. investment decisions are only optimal for each two-year period. Although storage capacity expansion is determined for individual technologies, results in Hand *et al.* (2012) are aggregated to show the total amount of installed capacity.

While investment into storage is observed for all scenarios, storage capacity expansion is greater for higher shares of RES. Under scenarios with low demand and an RES share of 80 % by 2050, 80–130 GW of charging and discharging capacity are added to the existing 20 GW of PSP capacity over the planning horizon. The highest level of expansion is observed when the availability of competing flexible options (e. g. demand response) is limited. CAES are reported to make up the largest portion of new build capacity. By contrast, the share of batteries is very limited due to high costs and the fact that benefits from short-term peak shaving or deployment on the distribution level cannot be evaluated with ReEDS.

Klaus *et al.* (2010)

In contrast to the other reviewed studies, the study by Klaus *et al.* (2010) does not build on any kind of economic analysis. Instead, a simulation model is used to assess the technical feasibility of a power system based on 100 % RES. By this means, necessary storage and backup generation capacities are determined. Electricity supply in

the considered year 2050 is simulated based on time series in hourly resolution, using a rolling horizon of four days. In order to achieve more robust results, the simulation is conducted for four different meteorological years.

The dispatch of demand side technologies, storage, backup capacities and electricity import is consecutively optimised (in the listed order) so that the residual demand is balanced in the best possible way, i. e. demand is covered at all times and curtailment is reduced to a maximum of 1 % of the original surplus energy. Transmission constraints are not considered.

The PSP capacity installed in 2050 is estimated based on planned projects and expected repowering. Either hydrogen or methane storage is deployed as a second storage technology. In order to allow for the nearly complete integration of surplus energy, the installed charging and discharging power of hydrogen or methane storage is rated accordingly. The required storage capacity results from simulation.

The results presented by Klaus *et al.* (2010) are valid for a snapshot of the German power system in 2050, however considering different meteorological conditions. According to simulations, 44 GW of electrolyser capacity are necessary. The required storage capacity amounts to 85 TWh in the hydrogen case and 75 TWh in the methane case. While permitting the nearly complete integration of surplus energy, the determined storage capacities are not cost-optimal.

Kuhn (2012) and Kuhn *et al.* (2012)

Both in Kuhn (2012) and Kuhn *et al.* (2012), the whole-systems cost minimisation model IMAKUS is used to identify energy storage demand in the German power system over a planning horizon of several decades. In contrast to models solving whole-systems cost minimisation problems as single optimisation problems (e. g. EPRI 2012, Hand *et al.* 2012, Scholz 2012, Strbac *et al.* 2012), IMAKUS takes an iterative approach to determine generation and storage capacity expansion. Transmission constraints are not considered. A detailed description of the model IMAKUS and the model formulation are given in Chapter 3.

Investment decisions into generation and storage assets are determined in two separate submodels, using linear programming. First, the expansion of conventional generation capacity is optimised intertemporally, based on discretised annual load duration curves of residual demand. Secondly, the expansion of storage capacity is optimised on a yearly basis along with the economic dispatch of power plants and storages, which is modelled in hourly resolution.

As the impact of storage operation on load duration curves is considered during the optimisation of generation capacity expansion in the next iterative step, the generation and storage portfolios adapt to each other iteratively and the submodel solutions converge to the whole-systems cost minimum (vide Section 3.2.4).

In IMAKUS, three competing storage technologies are considered for capacity expansion: PSP, advanced adiabatic compressed air energy storage (AA-CAES) and hydrogen storage. Instead of assuming generic storage durations, the three dimensions of new build storages – i. e. storage capacity, charging and discharging capacity – can be rated independently. The curtailment of surplus electricity generation is allowed.

As the expansion of storage capacity is optimised on a yearly basis, investment decisions are only optimal for individual years. Consequently, annualised investment costs are considered and storage capacities are not carried over to subsequent years. As storage modelling in IMAKUS only allows for energy arbitrage, non-variable costs of storage are by default reduced by 50 % to account for potential contribution margins from the ancillary services market. A consistent real interest rate of 3 % is used throughout the model.

Both Kuhn (2012) and Kuhn *et al.* (2012) investigate the least-cost pathway of the German power system over the planning horizon 2010–2050. Despite employing the same model, the two studies report very different results on storage demand under – at least on the face of it – similar assumptions: For a share of RES of 80 % in 2050, total storage capacity reaches almost 12 TWh in Kuhn (2012), whereas, according to Kuhn *et al.* (2012), total storage capacity only amounts to 4.1 TWh. A more detailed comparison of these results is given in Section 2.2.

Kuhn (2012) shows that, regardless of the availability of other storage technologies, hydrogen storage is the most suitable technology to cover long-duration storage demand. Moreover, the integration of large amounts of surplus energy is observed to be only feasible at all if hydrogen storage is available. Kuhn *et al.* (2012) also examine an RES share of only 60 % in 2050. Under this scenario, storage demand is significantly lower and, notably, hydrogen storage is not economically feasible. Whereas Kuhn (2012) does not consider competing flexible options in the transport and heating sectors, Kuhn *et al.* (2012) show that technologies like electric vehicles or storage heating help to integrate surplus electricity generation, while, at the same time, reducing the economic potential of large-scale energy storage.

Pieper & Rubel (2011)

In this study, the global market potential of energy storage until 2030 is assessed by conducting a business case analysis of storage applications. For this purpose, eight specific applications of storage in power systems are considered. Starting from an estimation of the overall demand for these applications, Pieper & Rubel (2011) determine the actual market potential of storage technologies by calculating the financial attractiveness (i. e. the internal rate of return) of using a certain storage technology for an application and by analysing the complexity of implementation as well as the availability of alternatives to storage.

Each business case, i. e. each technology–application pair, is analysed individually, assuming that a given storage facility will only be used for a single storage application. However, as in reality storages can generate revenues from different sources, the actual market potential could be higher than estimated.

The study considers PSP, CAES, AA-CAES and hydrogen storage as well as three battery technologies. According to the results, the application of storages for energy arbitrage is not attractive due to only small differences in electricity price levels. Furthermore, residential storage applications are found to be uneconomical. By contrast, the following applications are identified to be already attractive today or to become attractive until 2030: provision of operating reserve and black start services; stabilising of conventional generation; island and off-grid storage; avoidance or deferral of investments into grid infrastructure; as well as industrial peak shaving.

In addition to approximately 100 GW and 1000 GWh of storage capacity already existing on a global scale, Pieper & Rubel (2011) estimate a market potential of 330 GW and 1895 GWh of storage capacity until 2030. About one third of this global potential is driven by the provision of operating reserve. While batteries account for 50 % of the market potential in terms of financial investment, they only represent a small portion of the estimated storage capacity.

Scholz (2010) and Scholz (2012)

The whole-systems cost minimisation model REMix is used in Scholz (2010) and Scholz (2012). In both studies, the primary objective is to determine the cost-optimal structure of a future power system based on 100 % RES. For this purpose, investment decisions into RES, conventional backup generation, storage and transmission assets are optimised using linear programming. While both studies investigate a geographic scope that covers Europe and North Africa, Scholz (2010) explicitly focuses on results for Germany.

The geographic scope is subdivided into 36 regions. The model allows to select any arbitrary number and combination of regions for investigation. Either the inter-regional transmission of power is permitted – in this case, the transmission network is modelled as a transport problem – or regions are treated as island grids.

However, as time series in hourly resolution are used, treating a network of several nodes as a single optimisation problem can quickly exceed computational limitations. Therefore, a spatial decomposition approach is used if more than ten regions are considered: First, electricity exchange between nine aggregated super-regions is optimised. Secondly, assuming the previously determined electricity exchange, generation and storage capacity expansion is optimised within each super-region. In a final step, the expansion of transmission capacities between original regions is optimised with exogenously fixed generation and storage capacities.

The model optimises investment into three competing storage technologies, namely PSP, AA-CAES and hydrogen storage. Storage dimensions – i. e. charging capacity, discharging capacity and storage capacity – are rated independently, except for PSP, where storage duration is fixed to 8 h. Investment decisions are only optimal for the considered snapshot year, i. e. 2050. The curtailment of surplus electricity generation is allowed.

It should be noted that results obtained with REMix do not necessarily represent the cost-optimal structure of the power system, as generation, storage and transmission are not optimised simultaneously. Scholz (2010) reports a total storage capacity of 0.8 TWh if Germany is considered separately from other European regions. When transmission between regions is permitted, 0.24 TWh of storage capacity is installed in Germany. Under a scenario of increasing electricity demand, a total storage capacity of just over 1 TWh is reported for Germany in the isolated case, whereas capacity decreases to 0.1 TWh if transmission is permitted. Under all scenarios, storage capacity expansion is limited to PSP and AA-CAES.

By contrast, Scholz (2012) reports significantly higher levels of total storage capacity. When regions are treated as island grids, a capacity of 19.4 TWh is installed in Germany, 19 TWh of which are hydrogen storage capacity. Total capacity in Germany decreases slightly to 19 TWh if transmission between regions is permitted. Results from Scholz (2010) and Scholz (2012) are also compared in detail in Section 2.2.

Strbac *et al.* (2012)

The last study selected for review, Strbac *et al.* (2012), identifies the future energy storage demand in Great Britain based on whole-systems cost minimisation and analyses system benefits and the value of storage. For this purpose, investment decisions into storage, conventional generation, transmission and distribution assets are simultaneously optimised employing the mixed-integer linear programming model DSIM. In order to determine system benefits, i. e. the savings through storage, the optimised power system is compared with a system where storage is not available.

The analysis is conducted for individual snapshot years – namely 2020, 2030 and 2050 –, which are modelled based on time series in hourly resolution. Power plant dispatch takes into account start-up costs, a minimum generation constraint, minimum up and down time constraints and ramping constraints. By default, the provision of operating reserve is exogenously fixed. However, the provision of operating reserve as well as the uncertainty of wind generation, demand and power plant outages can also be considered by using a stochastic programming. The curtailment of surplus electricity generation is allowed.

Strbac *et al.* (2012) consider generic storage technologies, which are characterised by storage duration, round-trip efficiency, storage costs and the grid level of connection,

i. e. either bulk storage at the transmission level or distributed storage at the distribution level. Investment into the different storage technologies is optimised one at a time in separate scenarios. Thus, results do not provide direct insight into the cost-optimal allocation of capacity between short- and long-duration storage or between transmission and distribution level.

Investment costs for generation and transmission assets are annualised using technology-specific values of weighted average cost of capital (WACC) and economic lifetime. As WACC and lifetime cannot be generalised for generic storage technologies, annual returns are assumed instead of annualised costs. The maximum permissible investment costs could be calculated for given values of WACC and lifetime.

The transmission network is modelled as a transport problem, comprising seven nodes: five regions in Great Britain plus two neighbouring regions (Ireland and Continental Europe). Within each of the five regions of Great Britain, the distribution network is modelled using representative network topologies. The expansion of distribution capacities is implemented by constraining distribution network peak load.

Strbac *et al.* (2012) investigate storage demand in Great Britain under different developments of electricity demand and generation portfolio as well as under different assumptions regarding fuel costs, competing flexible technologies or the level of interconnection with other regions. The obtained result is the cost-optimal capacity and location of storage for an individual snapshot year.

In 2030, the transmission level demand for storages with 24-hour storage duration ranges between 2 GW and 15 GW of charging and discharging capacity, depending on the assumed level of storage costs. At the distribution level, more capacity is installed for the same level of costs. While the net system benefit of storage is higher in the distributed case, the contribution to integrating surplus energy tends to be lower. Generally, the system benefit of storage increases with higher storage durations.

In 2020, storage is only installed in case of significantly lower storage costs. In 2050, the transmission level demand for storages with 24-hour storage duration ranges between 5 GW and 25 GW (in the high and low cost case respectively). By also applying a stochastic programming approach, Strbac *et al.* (2012) furthermore demonstrate that the average value of storage increases by more than 50 % if storage resources can be optimally allocated between energy arbitrage and operating reserve.

Comparison of studies

As this review shows, the majority of studies base their analyses completely or at least in large part on computational models of the power system. Usually, some kind of optimisation technique – such as linear programming, mixed-integer programming or quadratic programming – is employed. Mere simulation models are an exception (e. g. Klaus *et al.* 2010). The chosen optimisation technique largely deter-

mines the achievable level of detail of the model, for instance, whether or not unit commitment constraints can be considered.

An important axis along which optimisation-based approaches can be distinguished is whether storage capacity expansion is endogenously optimised or exogenously defined. In the latter case, only the dispatch of storages is optimised. While determining the system benefits of storage as compared to a system without storage is a viable approach to assess the profitability of a given storage portfolio, it is actually not a suitable method to evaluate the economic feasibility of storage in general. Nevertheless, this approach is used by some studies (Adamek *et al.* 2012, Agora Energiewende 2014) to identify storage demand.

Among the seven studies which employ a whole-systems cost minimisation model to optimise storage capacity expansion endogenously, three different approaches can be identified: In EPRI (2012), Hand *et al.* (2012) and Strbac *et al.* (2012), all decisions of capacity expansion and operation are optimised simultaneously. By contrast, an iterative approach is used in Kuhn (2012) and Kuhn *et al.* (2012) to determine investment decisions into generation and storage assets. The third approach, which is applied in Scholz (2010) and Scholz (2012), is the consecutive optimisation of generation and storage capacity expansion on the one hand and transmission capacity expansion on the other hand.

While transmission expansion is not optimised simultaneously with generation and storage expansion in Scholz (2010) and Scholz (2012), the transmission network is not considered at all in the single-node models used in EPRI (2012), Kuhn (2012) and Kuhn *et al.* (2012). Only Hand *et al.* (2012) and Strbac *et al.* (2012) take into account transmission constraints and allow for the simultaneous optimisation of generation, storage and transmission expansion.

The majority of studies use annual time series in hourly resolution. By contrast, storage capacity expansion is optimised based on monthly load duration curves in EPRI (2012) and based on 17 representative time slices per year in Hand *et al.* (2012). It should be noted that, with regard to storage modelling, the latter approaches are less suitable than time series in hourly resolution (vide Section 4.2).

When storage capacity expansion is optimised, studies usually consider several competing storage technologies and, thus, the cost-optimal storage portfolio is determined. Only Strbac *et al.* (2012) optimise investment into the different storage technologies one at a time in separate scenarios.

While some models allow for the independent rating of storage dimensions (e. g. Kuhn 2012, Scholz 2012), there are several studies that reduce the number of degrees of freedom of the optimisation problem by exogenously fixing storage duration (EPRI 2012, Hand *et al.* 2012, Strbac *et al.* 2012). Generic values of storage duration

are also used to characterise the exogenously fixed storage portfolios in Adamek *et al.* (2012) and Agora Energiewende (2014).

Moreover, the majority of studies assume the economic integration of surplus electricity generation: Curtailment is allowed and, thus, surplus energy is only integrated to the extent that measures like storage capacity expansion are economically feasible. However, the review also includes two studies where curtailment is restricted. While Klaus *et al.* (2010) limit curtailment to 1 % of the original surplus energy, Adamek *et al.* (2012) initially rate storage new builds to enable the complete integration of surplus electricity generation.

This review illustrates quite well the diversity of methodologies and assumptions that are applied to assess storage demand in power systems. Aside from exceptions like Klaus *et al.* (2010) and Pieper & Rubel (2011) – one taking a pure technical perspective and one an investor’s perspective –, even the group of studies where the economic benefit for the power system is the relevant criterion in determining storage demand is very heterogeneous. Against this background, non-conformity of results among different studies is not surprising.

2.2 Comparison of results on energy storage demand in the German power system

As this thesis investigates energy storage demand in the German power system, results from studies focusing on Germany are compared in detail. While seven of the studies reviewed in Section 2.1 specify future storage capacities in Germany, only six studies determine storage demand based on some kind of economic analysis and are thus considered comparable. By contrast, storage capacities identified for Germany in Klaus *et al.* (2010) are based on the analysis of technical feasibility and, naturally, exceed the level of economically feasible capacity.

From each of the six studies, one scenario is selected. The comparison is performed for the year 2050. While Adamek *et al.* (2012), Agora Energiewende (2014), Scholz (2010) and Scholz (2012) only consider snapshot years, the year 2050 represents the last year of the modelled planning horizon in Kuhn (2012) and Kuhn *et al.* (2012). Table 2.2 lists the selected scenarios and specifies RES share, annual electricity consumption and annual RES generation. The selection of scenarios comprises the analysis of power systems with RES shares ranging from 80 % to 100 % in 2050.

As electricity exchange between Germany and neighbouring countries either is neglected or can only be considered insufficiently in Adamek *et al.* (2012), Kuhn (2012) and Kuhn *et al.* (2012), the scenarios selected for comparison from Scholz (2010) and

Scholz (2012) also assume an isolated German power system. However, a comparable scenario is not available in Agora Energiewende (2014). The scenario selected from this study considers the transmission of power between Germany and several other European market regions.

Table 2.2: Selected scenarios of storage demand in the German power system and general assumptions for the year 2050

| reference | scenario | RES share ¹⁾ | annual consumption ²⁾ | annual RES generation | shares in RES generation |
|-----------------------------|--|-------------------------|----------------------------------|-----------------------|--------------------------|
| Adamek <i>et al.</i> (2012) | 80 %-Szenario, Variante D | 80 % | 501 TWh | 432 TWh | 60 % wind, 14 % solar PV |
| Agora Energiewende (2014) | 90 Prozent / 60 Prozent, Variante K:7–L:16 | 90 % | 561 TWh | 575 TWh | 66 % wind, 20 % solar PV |
| Kuhn (2012) | Standard | 80 % | 560 TWh | 482 TWh | 62 % wind, 12 % solar PV |
| Kuhn <i>et al.</i> (2012) | 80/minus15 | 80 % | 510 TWh | 427 TWh | 63 % wind, 12 % solar PV |
| Scholz (2010) | 100SVp_DEDKNO (low demand case) | 100 % | 509 TWh | 579 TWh | 68 % wind, 15 % solar PV |
| Scholz (2012) | EUNA_10ods | 100 % | 549 TWh | 612 TWh | 58 % wind, 5 % solar PV |

1) usually specified in % of gross electricity consumption
2) usually corresponds to net electricity consumption

In Figure 2.1, the selected scenarios are compared with regard to installed charging, discharging and storage capacities in 2050. A few values presented in this figure are not explicitly specified in the studies: For instance, Scholz (2010) does not report the installed charging and discharging capacity of PSP, but the value is specified in a follow-up study by Faulstich *et al.* (2011). Furthermore, the storage capacities of short- and long-duration storages are not reported in Agora Energiewende (2014). However, based on the reported discharging capacities, storage capacities are calculated using the values specified for storage duration and discharging efficiency. As only a possible range of 1500–2000 h is given for the storage duration of long-duration storage, the lower value is assumed in order to calculate storage capacity. Analogously, the storage capacity of PSP is also calculated for Scholz (2012).

Whereas Kuhn *et al.* (2012), Kuhn (2012), Scholz (2010) and Scholz (2012) model three specific storage technologies, only two generic storage types – short- and long-duration storage – are considered in Adamek *et al.* (2012) and Agora Energiewende (2014). In both studies, the short-duration type is assumed to represent batteries,

PSP and CAES, while the long-duration type represents chemical energy storage, like e. g. hydrogen storage.

The examined scenarios show that significantly more long-duration storage capacity than short-duration storage capacity is required in case of high shares of RES. Only in Scholz (2010) – where total storage capacity is much smaller than in the other scenarios –, the storage portfolio does not include a long-duration technology like hydrogen storage.

Figure 2.1 furthermore illustrates that, if rated independently, installed discharging capacity tends to be significantly smaller than installed charging capacity. This characteristic can be observed in results from Kuhn *et al.* (2012), Kuhn (2012) and Adamek *et al.* (2012). In case of high shares of RES, surplus generation typically occurs in the form of short-term power peaks. In order to integrate this energy, large charging capacities are required, whereas the discharging of storages can usually be distributed over several – equally profitable – hours.

However, in absolute terms, large deviations of results are apparent: In case of 80 % RES share, the reported total charging, discharging and storage capacities differ by as much as two- or threefold. For an RES share of 100 %, total storage capacity in Scholz (2012) even exceeds storage capacity in Scholz (2010) by a factor of 24.

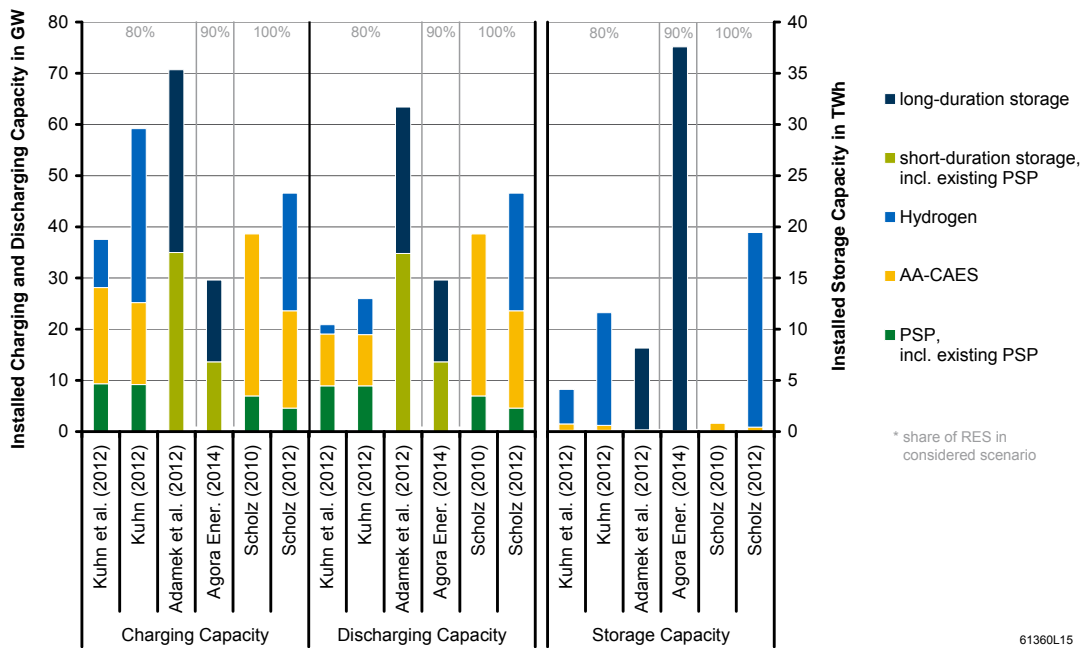


Figure 2.1: Comparison of study results on charging, discharging and storage capacity in Germany in 2050

The large charging and discharging capacities reported in Adamek *et al.* (2012) as well as the extremely large storage capacity obtained for the scenario by Agora Energiewende (2014) could be due to the respective methodological approaches: Adamek *et al.* (2012) initially rate storage new builds to enable the complete integration of surplus electricity generation and only afterwards reduce capacities to the level of actual utilisation in a cost-minimisation model. In Agora Energiewende (2014), storage capacities are defined arbitrarily and generic storage durations are assumed.

Moreover, the pairwise comparison of 80 % scenarios by Kuhn *et al.* (2012) and Kuhn (2012) as well as of 100 % scenarios by Scholz (2010) and Scholz (2012) shows that, despite employing the same model and examining – at least on the face of it – similar scenarios, different studies can yield very different results.

While the ratio of RES generation to consumption and the proportions of wind and solar generation are virtually equal (vide Table 2.2), different sets of annual time series are used in Kuhn *et al.* (2012) and Kuhn (2012). As a result, Kuhn (2012) reports 77 TWh of surplus energy in 2050, which is almost twice as much as the 44 TWh reported in Kuhn *et al.* (2012) and, presumably, causes higher storage demand.

Similar attempts to explain the significantly higher investment into storage in Scholz (2012) fail. Again, the ratio of RES generation to consumption is virtually equal in both studies (vide Table 2.2). However, with a share of wind and solar of 83 % in total RES generation, variable renewable generation technologies take up a much larger proportion in Scholz (2010) than in Scholz (2012) (63 %). This would be expected to lead to higher storage demand in Scholz (2010) rather than in Scholz (2012). In addition, lower storage efficiencies and higher storage costs in Scholz (2012) are also not in line with the observed higher storage demand.

Conclusion

To put it in a nutshell: Results are difficult to compare. While studies on storage demand make use of a multitude of methodological approaches and assumptions, even identical approaches can yield highly contradictory results. To better understand the broad range of results on storage demand stemming from different studies or even only a single model, both the influence of methodology and assumptions and the influence of input parameters on modelling results need further analysis.

Therefore, a qualitative analysis of how assumptions and the choice of methodological approaches affect modelling results on storage demand is conducted in Chapter 4. Afterwards, Chapter 5 analyses the sensitivity of results to changes in selected input parameters with the whole-systems cost minimisation model IMAKUS.

3 The whole-systems cost minimisation model IMAKUS

In this chapter, the methodology and formulation of the model IMAKUS and its sub-models are described in detail. The whole-systems cost minimisation model is used in this thesis to analyse the influence of methodology, assumptions and input parameters on modelling results on energy storage demand. While the existing model is presented in the first two sections of this chapter, the last section describes how the model was improved and extended in this thesis to enable the further variation of methodology and assumptions.

3.1 The existing model and its scope

IMAKUS is a deterministic model of the German power system, which takes an iterative approach to identifying investment decisions both into storage and conventional generation assets over a planning horizon of several decades. While, to a certain extent, scope and method of IMAKUS were already discussed in Chapter 2, a detailed description of the approach and the model formulation are given in this chapter. The functionality of the model is described to the extent that is used in this thesis. This comprises most of the existing model as it was presented in Kuhn (2012).

Figure 3.1 is a schematic representation of this core model. It consists of three iteratively coupled submodels, MOWIKA, MESTAS and MOGLIE, with the most important input parameters being annual amounts and time series of electricity consumption and generation from RES and CHP, the existing generation and storage portfolio as well as technical and economic parameters of generation and storage new builds. While investment decisions into conventional generation and storage assets are de-

terminated in the submodels MOWIKA and MESTAS respectively, the firm capacity of the whole power system is calculated in the submodel MOGLIE.

As the impact of storage operation on load duration curves is considered during the optimisation of generation capacity expansion, the generation and storage portfolios adapt to each other iteratively and the submodel solutions converge to the whole-systems cost minimum. Whereas the expansion of generation capacities is optimised intertemporally in the submodel MOWIKA, MESTAS only optimises storage capacities on a yearly basis. Due to the large size of the considered optimisation problems, a linear programming approach is used in both submodels. For a comprehensive overview of the theory of linear programming, vide Hillier & Lieberman (2014).

By comparing the firm capacity of the power system with peak demand and adjusting the minimum installed conventional generation capacity in each iterative step, it is furthermore ensured that the resulting generation and storage portfolio meets the requirements of security of supply. The obtained result is the least-cost pathway of the power system for the examined planning horizon, considering that investment decisions into storage assets are only optimal for individual years.

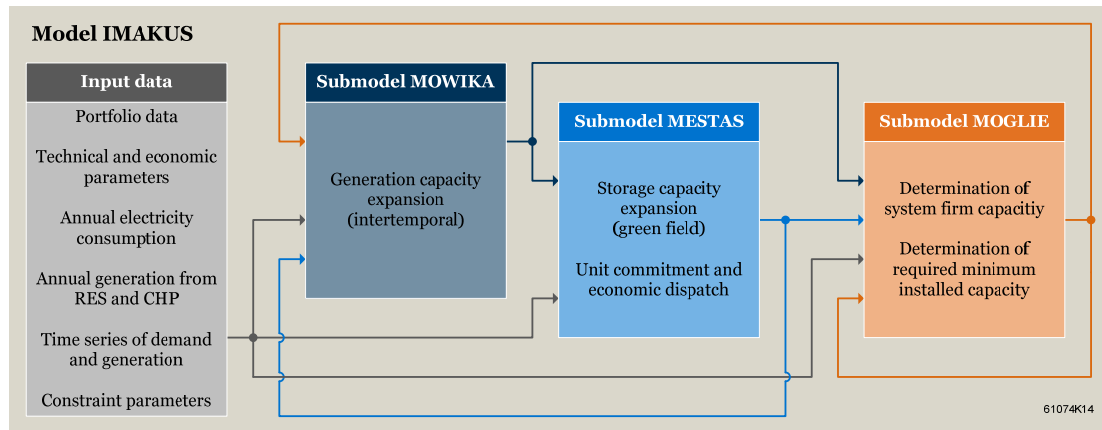


Figure 3.1: Schematic representation of the whole-systems cost minimisation model IMAKUS

With regard to spatial resolution, Germany is modelled as a single region, i. e. transmission constraints are not considered in IMAKUS. While neighbouring countries are not modelled in IMAKUS – the German power system is considered to be self-sufficient –, Kuhn (2012) also described a generalised approach to optionally model the export of surplus electricity generation at exogenously fixed prices. However, within the scope of this thesis, electricity export is not considered to be part of the functionality of IMAKUS. Moreover, the approaches presented in Kuhn *et al.* (2012)

to optionally optimise the charging and discharging of electric vehicles as well as the operation of flexible loads like refrigerators and storage heating are not considered in this thesis.

Section 3.2 gives a detailed description of the methodology and the formulation of the existing model IMAKUS, excluding the abovementioned features. In contrast to Kuhn (2012), where a graphical matrix representation of linear programming problems is provided, only a generic algebraic representation is used in this thesis to describe the submodels MOWIKA and MESTAS. The model IMAKUS is implemented in MATLAB® and uses CPLEX® to solve the linear programming problems. In order to allow for the variation of certain assumptions, some extensions to the existing model IMAKUS have to be implemented, which are described in Section 3.3.

3.2 Methodological approach and model formulation

3.2.1 Submodel MOWIKA: generation capacity expansion

The expansion of generation capacity is optimised in the submodel MOWIKA with regard to minimising the cost of covering electricity demand over the considered planning horizon. As electricity generation from RES and CHP is defined exogenously, only the operation and expansion of conventional generation capacities is planned within the scope of the submodel MOWIKA. The demand to be covered in MOWIKA is thus the residual demand, which is defined as the original consumer electricity demand minus electricity generation from RES and CHP.

Moreover, the residual demand can be modified to also represent the impact of energy storage, which can be determined exogenously, e. g. in the submodel MESTAS. For this purpose, any electricity generated by storages when discharging is subtracted from residual demand, while the amount of electricity consumed by storages when charging is added.

As storages are not endogenously modelled, time series of demand do not necessarily have to be considered in chronological order in MOWIKA. Instead, the planning of operation and expansion of conventional power plants is based on the annual duration curves of residual demand. Although neglecting the chronological order of demand and thus not considering start-up costs, minimum generation as well as minimum up and down time constraints, this approach allows an adequate estimation of the utilisation level of power plants (Roth 2008, Kuhn 2012).

The unavailability of generation capacity due to planned maintenance and unplanned outages is considered implicitly by constraining power output to a maximum value

smaller than rated power, thus limiting the capacity factor of power plants. For this purpose, Roth (2008) introduced a reduction coefficient that is used to weight the installed generation capacity and which is determined based on historical data on the availability of power plants. The reduction coefficient of a power plant is equal to its energy availability:

$$\xi = A = 1 - (U_p + U_{up}) = (1 - FOR) \cdot (1 - U_p) \quad (3-1)$$

| | |
|-------------|--|
| where ξ | reduction coefficient to consider the unavailability of generation capacity due to planned maintenance and unplanned outages |
| A | energy availability |
| U_p | planned energy unavailability |
| U_{up} | unplanned energy unavailability |
| FOR | forced outage rate |

Definitions of energy availability as well as planned and unplanned energy unavailability can be found in VGB (2010). Billinton & Allan (1984) give a definition of the forced outage rate, which is the probability of finding a generating unit on forced outage. In contrast to the unplanned energy unavailability, the forced outage rate is exclusively based on time periods when the generating unit is not maintained. It can be used to calculate the reduction coefficient according to equation (3-1), which is in part adopted from Roth (2008). By constraining the power output of power plants to a reduced generation capacity, the model is forced to install more generation capacity than actually necessary to cover peak load. With regard to the amount of electricity produced annually, this approach is equivalent to considering the rated power of power plants and endogenously modelling the uncertainty of forced outages.

As aforementioned, the expansion of generation capacities is optimised intertemporally in MOWIKA, i. e. each investment decision depends on present and future boundary conditions and is influenced by previous and future investment decisions. As investment decisions are made simultaneously across the planning horizon of several decades, the model “can act strategically” (Mai *et al.* 2013). The planning horizon is subdivided into years. All technical and economic parameters of power plants are defined on an annual basis. New build power plants go into service at the beginning of a year, while the end of the lifetime is always reached on the last day of the year. Thus, for each simulation year, a distinct generation portfolio is obtained, com-

prising exogenously fixed existing power plants as well as new build power plants installed in the current simulation year or in previous years.

Discretised annual load duration curves

Despite the already limited scope of the submodel MOWIKA, the size of the linear programming problem and thus the computational burden would increase dramatically if each single hour of the whole planning horizon of several decades was considered. However, the optimisation of generation capacity expansion has not to be based necessarily on time series in hourly resolution. As argued in Kuhn & Kühne (2011) and Kuhn (2012), the obtained modelling results are still satisfying if discretised annual load duration curves are used. In this case, it is however essential that the form of the annual load duration curves is approximated as accurately as possible.

Instead of simply taking the mean of a given number of adjacent hours of the annual load duration curve, a dynamic algorithm is used to discretise duration curves (Kuhn & Kühne 2011, Kuhn 2012). For a given number of discretisation intervals, the best approximation of the original duration curve is obtained by choosing smaller discretisation intervals in steeper regions of the curve and larger intervals in flatter sections (vide Figure 3.2). Which intervals have to be further divided is decided dynamically based on the root-mean-square deviation from the original curve. The amount of energy contained in the discretised annual load duration curve is equal to the energy contained in the original curve. In order to preserve the information about the magnitude of annual peak load, one discretisation interval of one hour's duration is pre-defined for each annual load duration curve, which contains the peak load value.

According to Kuhn (2012), annual load duration curves are already sufficiently approximated with 200 discretisation intervals. This means that the number of time slices which represent a planning horizon from 2010 to 2050 (41 years) in MOWIKA can be reduced from 359160 hours to 8200 intervals, without suffering a significant loss of accuracy in modelling results on generation expansion.

It should be noted that the applied method of discretised annual load duration curves is a special form of representative time slices approaches, which are quite commonly used in energy systems modelling to reduce temporal resolution (e. g. Short *et al.* 2011, Schaber 2013, Nahmmacher *et al.* 2014). In this case however, time slices do not represent contiguous periods like time of day, days or weeks, but are constituted of an arbitrary number of adjacent hours of the annual load duration curve. As for all other representative time slices approaches, the discretisation intervals are weighted. In order to allow for the correct determination of energy, costs and emissions, the model formulation therefore has to account for the different durations of discretisation intervals.

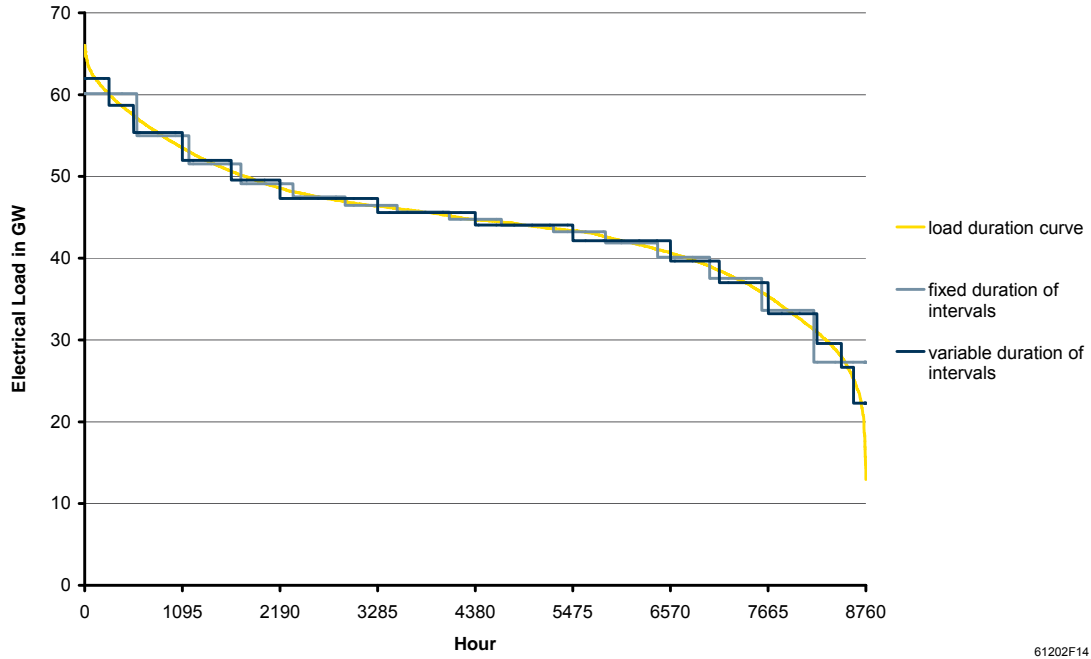


Figure 3.2: Approximation of an annual load duration curve using 15 discretisation intervals of fixed duration vs. using 15 discretisation intervals of variable duration

Model formulation

The expansion and dispatch of power plants in the submodel MOWIKA is driven by the demand for electricity. In each time step of the planning horizon, i. e. in each discretisation interval di in each year ys , the residual demand has to be met jointly by existing power plants pe and new build power plants pn :

$$\sum_{pe} P_{pe,ys,di}^{gen} + \sum_{pn} P_{pn,ys,di}^{gen} = d_{ys,di} \quad (3-2)$$

where $P_{pe,ys,di}^{gen}$ mean value of generating power of existing power plant pe in discretisation interval di in simulation year ys

$P_{pn,ys,di}^{gen}$ mean value of generating power of new build power plant pn in discretisation interval di in simulation year ys

$d_{ys,di}$ mean value of residual demand in discretisation interval di

| | |
|------|--|
| | in simulation year ys |
| ys | set of simulation years |
| pe | set of existing power plants operational in simulation year ys |
| pn | set of new build power plants operational in simulation year ys |
| di | set of discretisation intervals in simulation year ys |

The set of existing power plants pe comprises all power plants which were exogenously defined as existing generation capacity in Germany and which are operational in a specific simulation year ys . Whether an existing power plant is still operational in a specific year depends on the lifetime, which is also defined exogenously. The set of new build power plants pn comprises the new build power plants that are operational in a specific simulation year ys , i. e. the new build power plants installed in the simulation year itself as well as all new build power plants that were already installed in previous years and did not yet reach the end of their lifetime. The end of lifetime for each new build power plant is determined based on the characteristic lifetime of the respective technology, which is an exogenously defined parameter.

All generation capacities are assumed to be net capacities, i. e. gross capacities decreased by the auxiliary consumption of power plants. Thus, when the residual demand is determined, the net rather than the gross electricity demand has to be used. In order to account for transmission losses (which do not occur endogenously, as transmission constraints are not modelled), the net electricity demand can optionally be increased by the estimated amount of transmission losses.

While the residual demand can take negative values when RES and CHP generation exceed consumer demand, generating power (as all other variables) is defined to be non-negative. As information on surplus generation is not directly relevant to the expansion planning of conventional generation capacity, the solvability of equation (3-2) is ensured by simply setting all negative values of residual demand to zero. By contrast, surplus generation is explicitly considered in MESTAS (vide Section 3.2.2).

If must-run of conventional generation is assumed, i. e. if the total generating power of existing and new build power plants must not fall below a certain threshold power at any given time, all values of residual demand which are lower than the assumed must-run level are simply set to the threshold value.

The generating power of existing power plants pe and new build power plants pn in each discretisation interval di is constrained by their respective installed net generation capacities:

$$P_{pe,ys,di}^{gen} \leq \xi_{pe} \cdot C_{pe}^{gen} \quad (3-3)$$

$$P_{pn,ys,di}^{gen} \leq \xi_{pn} \cdot C_{pn}^{gen} \quad (3-4)$$

| | |
|----------------------------|---|
| where $P_{pe,ys,di}^{gen}$ | mean value of generating power of existing power plant pe in discretisation interval di in simulation year ys |
| ξ_{pe} | reduction coefficient to consider the unavailability of existing power plant pe due to planned maintenance and unplanned outages |
| C_{pe}^{gen} | generation capacity of existing power plant pe |
| $P_{pn,ys,di}^{gen}$ | mean value of generating power of new build power plant pn in discretisation interval di in simulation year ys |
| ξ_{pn} | reduction coefficient to consider the unavailability of new build power plant pn due to planned maintenance and unplanned outages |
| C_{pn}^{gen} | generation capacity of new build power plant pn |
| ys | set of simulation years |
| pe | set of existing power plants operational in simulation year ys |
| pn | set of new build power plants operational in simulation year ys |
| di | set of discretisation intervals in simulation year ys |

Whereas the generation capacities of existing power plants are exogenously fixed, the generation capacity of each new build power plant is a variable that is determined endogenously in MOWIKA. As already mentioned above, in order to account for the unavailability of generation capacity, a reduction coefficient is used to further constrain power output.

A set of new build power plants pi which are available for installation can be defined for each simulation year ys . Thus, the expansion of certain power plant technologies can be prohibited in the future, while other technologies might only be made available for installation in later years. Whereas existing power plants are modelled at

plant level, the new build capacity is only classified with regard to technology and the year of installation, but not broken down into individual power plants. For each simulation year ys and for each technology, the generation capacity is constrained to a maximum capacity available for installation:

$$C_{pi}^{gen} \leq c_{pi}^{gen,max} \quad (3-5)$$

where C_{pi}^{gen} generation capacity of new build power plant pi
 $c_{pi}^{gen,max}$ maximum generation capacity available for installation of new build power plant pi
 pi set of new build power plants available for installation in simulation year ys

Considering these constraints and the objective of minimising costs, only as much generation capacity as necessary to meet the peak residual load would be installed by the model. Due to constraining power output to a reduced generation capacity, the total installed generation capacity of all power plants operational in a specific year will actually already exceed the annual peak load. However, if more backup capacity is required, equation (3-6) can optionally be introduced. It ensures that for each simulation year ys the total installed generation capacity is greater than a certain minimum capacity. If MOWIKA is used iteratively within the model IMAKUS, this constraint becomes mandatory (vide Section 3.2.4).

$$\sum_{pe} c_{pe}^{gen} + \sum_{pn} C_{pn}^{gen} \geq c_{ys}^{gen,total,min} \quad (3-6)$$

where c_{pe}^{gen} generation capacity of existing power plant pe
 C_{pn}^{gen} generation capacity of new build power plant pn
 $c_{ys}^{gen,total,min}$ minimum installed total generation capacity in simulation year ys
 ys set of simulation years
 pe set of existing power plants operational in simulation year ys

pn set of new build power plants operational
in simulation year ys

A few further constraints can be introduced optionally in the submodel MOWIKA. For instance, the amount of fuels available for consumption can be limited for each simulation year ys :

$$\sum_{di} \left(\sum_{pefl} \frac{1}{\eta_{pefl}} \cdot P_{pefl,ys,di}^{gen} \cdot \delta_{di} + \dots \right. \\ \left. \sum_{pnfl} \frac{1}{\eta_{pnfl}} \cdot P_{pnfl,ys,di}^{gen} \cdot \delta_{di} \right) \leq w_{fl,ys}^{therm,max} \quad (3-7)$$

where η_{pefl} net efficiency of existing power plant $pefl$
 $P_{pefl,ys,di}^{gen}$ mean value of generating power of
existing power plant $pefl$ in discretisation
interval di in simulation year ys
 δ_{di} duration of discretisation interval di
in hours
 η_{pnfl} net efficiency of new build
power plant $pnfl$
 $P_{pnfl,ys,di}^{gen}$ mean value of generating power of new
build power plant $pnfl$ in discretisation
interval di in simulation year ys
 $w_{fl,ys}^{therm,max}$ maximum amount of thermal energy
of fuel fl available for consumption
in simulation year ys
 ys set of simulation years
 $pefl$ set of existing power plants operational
in simulation year ys burning fuel fl
 $pnfl$ set of new build power plants operational
in simulation year ys burning fuel fl
 fl set of fuel types
 di set of discretisation intervals
in simulation year ys

The constraint, which has to be implemented separately for each fuel, specifies the annual maximum amount of fuels as thermal energy. The total fuel consumption of

existing and new build power plants has to be calculated based on their power output. For this purpose, net efficiencies are used. The net efficiency of a power plant already accounts for the auxiliary consumption of the plant. Furthermore, the different durations of discretisation intervals di have to be considered when calculating the amount of thermal energy consumed.

While annual carbon emissions can be limited implicitly in MOWIKA by exogenously fixing a carbon price for each year (which is then considered as an additional component of the variable costs of power plants), it is also possible to instead constrain carbon emissions directly by introducing annual emissions targets:

$$\sum_{di} \left(\sum_{pe} \varepsilon_{pe}^{electr} \cdot P_{pe,ys,di}^{gen} \cdot \delta_{di} + \sum_{pn} \varepsilon_{pn}^{electr} \cdot P_{pn,ys,di}^{gen} \cdot \delta_{di} \right) \leq e_{ys}^{max} \quad (3-8)$$

| | |
|-----------------------------------|--|
| where $\varepsilon_{pe}^{electr}$ | emissions of existing power plant pe per unit of electricity generated |
| $P_{pe,ys,di}^{gen}$ | mean value of generating power of existing power plant pe in discretisation interval di in simulation year ys |
| δ_{di} | duration of discretisation interval di in hours |
| $\varepsilon_{pn}^{electr}$ | emissions of new build power plant pn per unit of electricity generated |
| $P_{pn,ys,di}^{gen}$ | mean value of generating power of new build power plant pn in discretisation interval di in simulation year ys |
| e_{ys}^{max} | maximum amount of emissions permitted in simulation year ys |
| ys | set of simulation years |
| pe | set of existing power plants operational in simulation year ys |
| pn | set of new build power plants operational in simulation year ys |
| di | set of discretisation intervals in simulation year ys |

Thus, the total amount of carbon emissions produced by existing and new build power plants in a certain simulation year ys is limited to an exogenously defined maximum amount of emissions. Emissions are calculated for each power plant in

each time step by multiplying the power output by a factor representing emissions per unit of electricity generated, which is the quotient of the emission intensity of the burned fuel divided by the net efficiency of the respective power plant. Again, the different durations of discretisation intervals di have to be accounted for.

The objective function of the submodel MOWIKA, which is subject to minimisation, covers the total cost associated with the operation and expansion of conventional generation capacities over the whole planning horizon:

$$\begin{aligned} \text{minimise } \sum_{ys} \left\{ \sum_{pi} \tilde{\kappa}_{pi}^{nv} \cdot C_{pi}^{gen} + \dots \right. \\ \left. \sum_{di} \left(\sum_{pe} \tilde{\kappa}_{pe}^v \cdot P_{pe,ys,di}^{gen} \cdot \delta_{di} + \dots \right. \right. \\ \left. \left. \sum_{pn} \tilde{\kappa}_{pn}^v \cdot P_{pn,ys,di}^{gen} \cdot \delta_{di} \right) \right\} \end{aligned} \quad (3-9)$$

| | |
|----------------------------------|--|
| where $\tilde{\kappa}_{pi}^{nv}$ | present value of non-variable costs of new build power plant pi |
| C_{pi}^{gen} | generation capacity of new build power plant pi |
| $\tilde{\kappa}_{pe}^v$ | present value of variable costs of existing power plant pe |
| $P_{pe,ys,di}^{gen}$ | mean value of generating power of existing power plant pe in discretisation interval di in simulation year ys |
| δ_{di} | duration of discretisation interval di in hours |
| $\tilde{\kappa}_{pn}^v$ | present value of variable costs of new build power plant pn |
| $P_{pn,ys,di}^{gen}$ | mean value of generating power of new build power plant pn in discretisation interval di in simulation year ys |
| ys | set of simulation years |
| pe | set of existing power plants operational in simulation year ys |
| pi | set of new build power plants available for installation in simulation year ys |
| pn | set of new build power plants operational in simulation year ys |

di set of discretisation intervals
in simulation year ys

When costs incurring in different simulation years are summed up, the time value of money has to be considered. Thus, all cost components are discounted to the present value in a given base year. In MOWIKA, the first year of the planning horizon is defined as the base year.

The objective function sums up non-variable costs associated with the installation of new build power plants over all simulation years ys . While non-variable costs like annual fixed costs actually occur periodically over the lifetime of a power plant, these costs can also be converted to a single cost term that is valid in the year of investment (vide infra). This approach allows a very convenient formulation and implementation of the objective function. Furthermore, the variable costs caused by the operation of both existing and new build power plants in each time step of the planning horizon are added to the total. As in case of determining energy or emissions, the different durations of discretisation intervals di have to be considered when calculating the variable costs of electricity generation. All non-variable costs of existing power plants are considered to be sunk costs and are not included in the objective function.

Modelling of costs

The non-variable costs of new build power plants are a capacity-dependent cost term. The present value of non-variable costs comprises the present values of investment costs, total fixed costs as well as total decommissioning costs and is reduced by a potential salvage value of the power plant at the end of the planning horizon:

$$\tilde{\kappa}_{pi}^{nv} = \tilde{\kappa}_{pi}^{inv} + \tilde{\kappa}_{pi}^{fix,total} + \tilde{\kappa}_{pi}^{dec,total} - \tilde{\kappa}_{pi}^{sal} \quad (3-10)$$

where $\tilde{\kappa}_{pi}^{nv}$ present value of non-variable costs of
new build power plant pi

$\tilde{\kappa}_{pi}^{inv}$ present value of investment costs of
new build power plant pi

$\tilde{\kappa}_{pi}^{fix,total}$ present value of total fixed costs of
new build power plant pi

$\tilde{\kappa}_{pi}^{dec,total}$ present value of total decommissioning
costs of new build power plant pi

$\tilde{\kappa}_{pi}^{sal}$ present value of salvage value of
new build power plant pi

pi set of new build power plants available
for installation in simulation year ys

The present value of investment costs is calculated by discounting the investment costs valid in simulation year ys , i. e. the future value, to a given base year y^{base} :

$$\tilde{\kappa}_{pi}^{inv} = \frac{1}{(1+i)^{ys-y^{base}}} \cdot \kappa_{pi}^{inv} \quad (3-11)$$

where $\tilde{\kappa}_{pi}^{inv}$ present value of investment costs
of new build power plant pi
 i real discount rate
 y^{base} base year
 κ_{pi}^{inv} investment costs of new build
power plant pi
 ys set of simulation years
 pi set of new build power plants available
for installation in simulation year ys

A comprehensive overview of the concept of time value of money as well as related formulae of present value, future value and annuity can be found in Van Horne & Wachowicz (2004). Due to the assumption of a perfect market, a single interest rate is applied in IMAKUS and its submodels (vide Roth 2008). As all costs are assumed to be inflation-adjusted real values of costs, a real discount rate has to be used to calculate present values.

It is assumed that investment costs for a new build power plant fall due at the time of installation, i. e. at the beginning of the corresponding simulation year ys . Given that the first year of the planning horizon is defined as the base year y^{base} , investment costs of a power plant installed in the first simulation year are not discounted in equation (3-11), while investment costs of a new build power plant in the second simulation year will be discounted over one year, investment costs in the third simulation year over two years, etc.

The second cost component of the present value of non-variable costs is the present value of total fixed costs. Fixed costs are the capacity-dependent costs for the operation and maintenance (O&M) of a power plant. In MOWIKA, it is assumed that fixed costs occur on an annual basis and, more concisely, that they fall due at the begin-

ning of each year. It is furthermore assumed that the annual fixed costs of a given power plant are constant over its whole lifetime.

In order to determine the present value of total fixed costs in the base year y^{base} , the series of annual fixed costs is first discounted to the simulation year ys in which the power plant is installed and then further discounted to the base year y^{base} :

$$\begin{aligned} \tilde{\kappa}_{pi}^{fix,total} &= \frac{1}{(1+i)^{ys-y^{base}}} \cdot \kappa_{pi}^{fix,a} \cdot \left\{ 1 + \sum_{n=1}^{l_{pi}^{rel}-1} \frac{1}{(1+i)^n} \right\} \\ &= \frac{1}{(1+i)^{ys-y^{base}}} \cdot \kappa_{pi}^{fix,a} \cdot \left\{ 1 + \left(\frac{1}{i} - \frac{1}{i \cdot (1+i)^{l_{pi}^{rel}-1}} \right) \right\} \end{aligned} \quad (3-12)$$

where $\tilde{\kappa}_{pi}^{fix,total}$ present value of total fixed costs of new build power plant pi
 i real discount rate
 y^{base} base year
 $\kappa_{pi}^{fix,a}$ annual fixed costs of new build power plant pi
 l_{pi}^{rel} relevant lifetime of new build power plant pi
 n number of payment periods (years)
 ys set of simulation years
 pi set of new build power plants available for installation in simulation year ys

As the annual fixed costs represent a series of equal payments that occur at the beginning of each period, equation (3-12) is based on the calculation of the present value of an annuity due (vide Van Horne & Wachowicz 2004). Only the costs that occur during the relevant lifetime of the power plant are included in the total. The relevant lifetime of a power plant is the share of lifetime within the planning horizon. Fixed costs for any years beyond the planning horizon are not taken into account.

The present value of total decommissioning costs is the last cost component that adds to the present value of non-variable costs of a new build power plant. It is assumed that all costs required for decommissioning will fall due when the power plant is put out of service at the end of its lifetime. These target costs for decommissioning can be accrued over the whole lifetime of the power plant by periodically paying an equal amount of money into a savings account with interest rate i . Like investment

costs and annual fixed costs, the annual savings for decommissioning are also assumed to fall due at the beginning of the year:

$$\begin{aligned}\kappa_{pi}^{dec,target} &= \kappa_{pi}^{dec,a} \cdot \sum_{n=1}^{l_{pi}} (1+i)^n \\ &= \kappa_{pi}^{dec,a} \cdot (1+i) \cdot \frac{(1+i)^{l_{pi}} - 1}{i}\end{aligned}\quad (3-13)$$

where $\kappa_{pi}^{dec,target}$ target costs for decommissioning of new build power plant pi
 $\kappa_{pi}^{dec,a}$ annual savings for decommissioning of new build power plant pi
 l_{pi} lifetime of new build power plant pi
 n number of payment periods (years)
 i real discount rate
 pi set of new build power plants available for installation in simulation year ys

After solving equation (3-13) for the amount to be saved annually, the present value of total decommissioning costs of a new build power plant can be calculated:

$$\begin{aligned}\tilde{\kappa}_{pi}^{dec,total} &= \frac{1}{(1+i)^{ys-y^{base}}} \cdot \kappa_{pi}^{dec,a} \cdot \left\{ 1 + \sum_{n=1}^{l_{pi}^{rel}-1} \frac{1}{(1+i)^n} \right\} \\ &= \frac{1}{(1+i)^{ys-y^{base}}} \cdot \kappa_{pi}^{dec,a} \cdot \left\{ 1 + \left(\frac{1}{i} - \frac{1}{i \cdot (1+i)^{l_{pi}^{rel}-1}} \right) \right\}\end{aligned}\quad (3-14)$$

where $\tilde{\kappa}_{pi}^{dec,total}$ present value of total decommissioning costs of new build power plant pi
 i real discount rate
 y^{base} base year
 $\kappa_{pi}^{dec,a}$ annual savings for decommissioning of new build power plant pi
 l_{pi}^{rel} relevant lifetime of new build power plant pi
 n number of payment periods (years)
 ys set of simulation years

pi set of new build power plants available
for installation in simulation year ys

As the annual savings for decommissioning also represent a series of equal payments that occur at the beginning of each period, equation (3-14) can be formulated analogously to equation (3-12). Again, the series of annual savings is first discounted to the simulation year ys in which the power plant is installed and then further discounted to the base year y^{base} . Only the share of the target costs that can be accrued over the relevant lifetime of the power plant, i. e. within the planning horizon, is considered.

The present value of non-variable costs is finally reduced by a potential salvage value of the new build power plant at the end of the planning horizon. While annual fixed costs and annual savings for decommissioning are only considered over the relevant lifetime of the power plant, the full investment costs are charged at the time of installation, regardless of whether the power plant is built in the first simulation year or in the last year of the planning horizon. However, this approach apparently has a huge impact on evaluating the economic feasibility of a power plant: It leads to the tapering off of capacity expansion during the final years of the planning horizon and to the short-sighted preference of less capital-intensive peaking plants.

The described situation is typically encountered when planning over a finite horizon. As a matter of fact, model builders inevitably have to draw on finite – and in most cases rather short – planning horizons, not least due to the increase of computational costs and uncertainty of assumptions for longer horizons. Meanwhile, the problems associated with finite planning horizons are well-known. As the impact of decisions on post-horizon years is not modelled, errors occur compared to the optimal solution of the corresponding infinite horizon problem. These errors are referred to as “end effects” in literature (Grinold 1983, Hadjicostas & Adams 1992).

According to Grinold (1983), the “truncation technique” is the natural approach to dealing with finite planning horizons: Post-horizon years are simply ignored, thus turning a blind eye to abovementioned end effects. A common approach to mitigate end effects in generation expansion planning is to extend the simulation period beyond the actual planning horizon (e. g. EPRI 2012). If the simulation period is long enough, the economic feasibility of each asset installed within the planning horizon can be evaluated over its whole lifetime.

However, a central problem of this approach is that input parameters and assumptions are required for an even longer period. While this is often remedied by assuming all parameters to be constant over a so-called “static post-horizon” (Hadjicostas & Adams 1992), it has to be decided whether the increased computational burden of an extended simulation period is still acceptable.

Another approach to mitigate the end effects of finite-horizon planning problems is the “salvage technique”, which improves the truncation technique by placing a residual or salvage value on all assets that do not reach the end of lifetime within the planning horizon (Grinold 1983). There are several possibilities to estimate the salvage value. A common approach is to determine the “undepreciated investment” at the end of the planning horizon, although this neglects any possible future revenues (Hadjicostas & Adams 1992).

Kuhn (2012) proposed to calculate the salvage value of new build power plants in MOWIKA by using straight-line depreciation. The present value of the salvage value is obtained by first discounting the salvage value to the simulation year ys in which the power plant is installed and then further discounting to the base year y^{base} :

$$\tilde{\kappa}_{pi}^{sal} = \frac{1}{(1+i)^{ys-y^{base}}} \cdot \frac{1}{(1+i)^{l_{pi}^{rel}}} \cdot \left(1 - \frac{l_{pi}^{rel}}{l_{pi}}\right) \cdot \kappa_{pi}^{inv} \quad (3-15)$$

| | |
|-----------------------------------|--|
| where $\tilde{\kappa}_{pi}^{sal}$ | present value of salvage value of new build power plant pi |
| i | real discount rate |
| y^{base} | base year |
| l_{pi}^{rel} | relevant lifetime of new build power plant pi |
| l_{pi} | lifetime of new build power plant pi |
| κ_{pi}^{inv} | investment costs of new build power plant pi |
| ys | set of simulation years |
| pi | set of new build power plants available for installation in simulation year ys |

By reducing the present value of non-variable costs of new build power plants by this salvage value, the end effect of generation expansion is mitigated to a certain extent in MOWIKA. Kuhn (2012) however illustrated that average annual investment costs still increase systematically with every year that the lifetime of a power plant exceeds the planning horizon. Due to the resulting shift of weight towards investment costs, less capital-intensive peaking plants are still preferred during the final years of the planning horizon. An alternative depreciation approach is presented in Section 3.3.1, which allows to further mitigate the end effect of generation expansion.

Besides the non-variable costs of new build power plants, the objective function (3-9) also includes the present values of variable costs of existing and new build power plants. The variable costs can be defined for each set of power plants operational in a given simulation year ys and burning a given fuel fl :

$$\tilde{\kappa}_{pefl}^v = \frac{1}{(1+i)^{ys-y^{base}}} \cdot \left(\frac{1}{\eta_{pefl}} \cdot \kappa_{fl,ys}^{fuel} + \kappa_{pefl,ys}^{vO\&M} + \varepsilon_{pefl}^{electr} \cdot \kappa_{ys}^{emi} \right) \quad (3-16)$$

$$\tilde{\kappa}_{pnfl}^v = \frac{1}{(1+i)^{ys-y^{base}}} \cdot \left(\frac{1}{\eta_{pnfl}} \cdot \kappa_{fl,ys}^{fuel} + \kappa_{pnfl,ys}^{vO\&M} + \varepsilon_{pnfl}^{electr} \cdot \kappa_{ys}^{emi} \right) \quad (3-17)$$

| | |
|---------------------------------|---|
| where $\tilde{\kappa}_{pefl}^v$ | present value of variable costs of existing power plant $pefl$ |
| $\tilde{\kappa}_{pnfl}^v$ | present value of variable costs of new build power plant $pnfl$ |
| i | real discount rate |
| y^{base} | base year |
| η_{pefl} | net efficiency of existing power plant $pefl$ |
| η_{pnfl} | net efficiency of new build power plant $pnfl$ |
| $\kappa_{fl,ys}^{fuel}$ | costs for fuel fl in simulation year ys |
| $\kappa_{pefl,ys}^{vO\&M}$ | variable O&M costs of existing power plant $pefl$ in simulation year ys |
| $\kappa_{pnfl,ys}^{vO\&M}$ | variable O&M costs of new build power plant $pnfl$ in simulation year ys |
| $\varepsilon_{pefl}^{electr}$ | emissions of existing power plant $pefl$ per unit of electricity generated |
| $\varepsilon_{pnfl}^{electr}$ | emissions of new build power plant $pnfl$ per unit of electricity generated |
| κ_{ys}^{emi} | carbon emissions price in simulation year ys |
| ys | set of simulation years |
| $pefl$ | set of existing power plants operational in simulation year ys burning fuel fl |
| $pnfl$ | set of new build power plants operational in simulation year ys burning fuel fl |
| fl | set of fuel types |

The variable costs comprise the costs for fuel, variable O&M cost and – if carbon emissions are not directly limited by constraint (3-8) – emission costs. However, if annual emissions targets are used, the exogenously defined carbon emissions price in equations (3-16) and (3-17) has to be set to zero.

In this case, the carbon emissions price emerges endogenously and can be determined by consulting the dual problem of the optimisation problem: According to Hillier & Lieberman (2014), shadow prices can be obtained from the dual problem of a linear program, which represent the marginal values of resources that are constrained in the primal problem. Thus, the shadow price associated with the annual emissions constraint (3-8) equals the carbon emissions price.

Results

The main result obtained from the submodel MOWIKA is the intertemporally optimised development of the conventional generation portfolio for the whole planning horizon. Annual generation portfolios comprise the existing generation capacity at plant level as well as the new build capacity classified with regard to technology and the year of installation. When MOWIKA is used within the iterative process of the superordinate model IMAKUS, the resulting annual generation portfolios are utilised as input parameters to the submodels MESTAS and MOGLIE.

Further results include the annual non-variable and variable costs of electricity generation as well as the annual amounts of generated electricity, fuel consumption and carbon emissions per generation technology. If annual emissions are constrained by emissions targets, the carbon price can also be obtained for each simulation year. As the expansion and dispatch of generation capacity is based on discretised annual duration curves of residual demand, the temporal resolution of results is also restricted to mean values in discretisation intervals.

3.2.2 Submodel MESTAS: storage capacity expansion

Whereas MOWIKA optimises the expansion of conventional generation capacities, the submodel MESTAS is used to optimise the expansion of storage capacities. Although approaches to model storage expansion and operation based on either load duration curves (e. g. EPRI 2012) or representative time slices (e. g. Short *et al.* 2011) exist, models with a focus on energy storage are preferably based on chronological time series in at least hourly resolution (e. g. Strbac *et al.* 2012), allowing for more detailed modelling of storage dispatch. For this reason, the optimisation of storage capacity expansion in MESTAS is also based on chronological time series in hourly resolution (Kuhn 2012).

Compared to the optimisation of generation capacity expansion, the optimisation of storage capacity expansion imposes a significantly higher computational burden, as dispatch decisions in different time steps are not anymore independent. Moreover, if charging capacity, discharging capacity and storage capacity are rated independently, the number of degrees of freedom increases. Due to the higher complexity of the optimisation problem and the higher temporal resolution, the intertemporal approach is abandoned in MESTAS and each year of the considered planning horizon is optimised individually, only based on information available for the respective simulation year (Kuhn 2012). With regard to the categories proposed by Mai *et al.* (2013), the submodel MESTAS can thus be attributed to the class of “myopic models that make decisions in stages, with limited information about future conditions”.

The expansion of storage capacity is optimised with regard to minimising the cost of covering the residual demand over one year. As in MOWIKA, electricity generation from RES and CHP is defined exogenously in MESTAS. Furthermore, the conventional generation portfolio is defined exogenously for each year. Thus, only the operation of conventional power plants and the operation and expansion of storages is planned within the scope of the submodel MESTAS. While in contrast to MOWIKA power plant dispatch is modelled chronologically, start-up costs, minimum generation and minimum up and down time constraints are also not considered.

Due to the myopic approach, investment decisions into storage assets obtained in MESTAS are only optimal for individual years: The model will opt for an investment if it appears profitable under the circumstances given in the respective simulation year, unaware of the future development of parameters that could negatively affect the performance and profitability of the same investment.

Kuhn (2012) discusses two possible approaches to deal with these short-sighted investments in subsequent simulation years. A very natural approach is to simply carry over the storage capacities to subsequent years, i. e. to exogenously define all capacities from previous simulation years as pre-installed capacity. However, Kuhn (2012) points out that, in this case, suboptimal capacities are kept in the storage portfolio, which possibly prevent the model from installing alternative technologies in future years. By contrast, if previous investment decisions are ignored and storage capacities are not carried over, the model can design the optimal storage portfolio anew in each year. This approach is also referred to as “green-field approach”.

While the green-field approach allows to identify which developments will have a positive or negative impact on the economic feasibility of certain storage technologies, Kuhn (2012) states that in some cases the obtained results might not represent a realistic pathway of storage expansion, as the installed capacity of a certain storage technology can decrease in subsequent years. However, such cases are not a predominant problem in scenarios with increasing shares of RES, where storage de-

mand is generally expected to increase over the years (Kuhn 2012). Moreover, if capacities are not carried over, the individual years of the considered period are completely independent of each other and thus can be solved in parallel. Although the green-field approach is the default method used in MESTAS, previously installed storage capacities can optionally also be carried over to subsequent years.

In order to ensure the comparability of storage portfolios from different simulation years, all technical and economic parameters of new build storages are assumed to be constant across all years of the considered period. This assumption – although very restrictive – allows to identify capacities of the same storage technology that are installed in different years as being identical. If the development of technical and economic storage parameters needs to be reflected in the model, an additional new build storage technology has to be made available for each stage of development.

As for power plants in MOWIKA, new build storages go into service at the beginning of the respective simulation year. The existing storage portfolio, the conventional generation portfolio, demand, RES and CHP generation as well as all other technical and economic parameters are defined on an annual basis.

Model formulation

The submodel MESTAS is formulated for one simulation year in hourly resolution. As in MOWIKA, all variables are non-negative. The operation of conventional power plants and the operation and expansion of storage capacities is driven by the demand for electricity. In each time step ts of the respective simulation year the residual demand has to be met jointly by power plants pp , existing storages se and new build storages sn :

$$\sum_{pp} P_{pp,ts}^{gen} + \sum_{se} (P_{se,ts}^{discharge} - P_{se,ts}^{charge}) + \dots \quad (3-18)$$

$$\sum_{sn} (P_{sn,ts}^{discharge} - P_{sn,ts}^{charge}) - P_{ts}^{curtail} = d_{ts}$$

where $P_{pp,ts}^{gen}$ mean value of generating power of power plant pp in time step ts

$P_{se,ts}^{discharge}$ mean value of discharging power of existing storage se in time step ts

$P_{se,ts}^{charge}$ mean value of charging power of existing storage se in time step ts

$P_{sn,ts}^{discharge}$ mean value of discharging power of existing storage sn in time step ts

$P_{sn,ts}^{charge}$ mean value of charging power of

| | |
|--------------------|--|
| | existing storage sn in time step ts |
| $P_{ts}^{curtail}$ | mean value of curtailed power in time step ts |
| d_{ts} | mean value of residual demand in time step ts |
| pp | set of power plants |
| se | set of existing storages |
| sn | set of new build storages |
| ts | set of time steps (8760 hours) |

The set of power plants pp comprises the whole conventional generation portfolio that is defined exogenously for the respective simulation year. If MESTAS is used within the iterative process of the superordinate model IMAKUS, the annual generation portfolio is obtained from the submodel MOWIKA. As in MOWIKA, all generation capacities are assumed to be net capacities. The residual demand is defined as the net electricity demand decreased by RES and CHP generation. In order to account for transmission losses, the net electricity demand can optionally be increased by the estimated amount of transmission losses.

As the residual demand can take negative values when RES and CHP generation exceed consumer demand, the solvability of equation (3-18) is ensured by explicitly considering the power that, as the case may be, needs to be curtailed. However, curtailment is not the only option for the model to handle surplus generation. Generally, equation (3-18) also allows to charge and discharge the same storage plant simultaneously. By this means, surplus generation is dissipated, while the storage level can be kept constant. As long as no variable costs are associated with the operation of storages, this operating mode does not increase the objective function and thus is equivalent to the curtailment of surplus power in terms of costs.

Although simultaneous charging and discharging is technically feasible and commonly used in PSP to control pump power (Albrecht 2013), it should be avoided within the scope of the submodel MESTAS, as it skews the amount of surplus energy actually integrated by storages. By granting infinitesimal revenues for curtailed power (vide equation (3-40)), the model will always prefer the curtailment of surplus energy to the dissipation in storages. As only infinitesimal revenues are used, curtailment is however not generally favoured over integrating surplus energy with storages. If variable costs are imposed for the charging and discharging of storages, the dissipation of surplus energy in storages is no longer economically attractive and the arbitrary cost incentive for curtailment becomes redundant.

The generating power of power plants is constrained in each time step ts by the installed capacity. As in MOWIKA, a reduction coefficient is used in MESTAS to implicitly account for the unavailability of generation capacity due to planned maintenance and unplanned outages:

$$P_{pp,ts}^{gen} \leq \xi_{pp} \cdot c_{pp}^{gen} \quad (3-19)$$

| | |
|-------------------------|---|
| where $P_{pp,ts}^{gen}$ | mean value of generating power of power plant pp in time step ts |
| ξ_{pp} | reduction coefficient to consider the unavailability of power plant pp due to planned maintenance and unplanned outages |
| c_{pp}^{gen} | generation capacity of power plant pp |
| pp | set of power plants |
| ts | set of time steps (8760 hours) |

Analogously, the charging and discharging power of storages is also constrained in MESTAS. For all existing storages se , which are defined exogenously for the respective simulation year, charging and discharging power are constrained by fixed capacities multiplied by the corresponding reduction coefficient:

$$P_{se,ts}^{charge} \leq \xi_{se} \cdot c_{se}^{charge} \quad (3-20)$$

$$P_{se,ts}^{discharge} \leq \xi_{se} \cdot c_{se}^{discharge} \quad (3-21)$$

| | |
|----------------------------|--|
| where $P_{se,ts}^{charge}$ | mean value of charging power of existing storage se in time step ts |
| $P_{se,ts}^{discharge}$ | mean value of discharging power of existing storage se in time step ts |
| ξ_{se} | reduction coefficient to consider the unavailability of existing storage se due to planned maintenance and unplanned outages |
| c_{se}^{charge} | charging capacity of existing storage se |
| $c_{se}^{discharge}$ | discharging capacity of existing storage se |

| | |
|------|--------------------------------|
| se | set of existing storages |
| ts | set of time steps (8760 hours) |

Charging and discharging capacities of each new build storage sn are variables that are determined endogenously in MESTAS:

$$P_{sn,ts}^{charge} \leq \xi_{sn} \cdot C_{sn}^{charge} \quad (3-22)$$

$$P_{sn,ts}^{discharge} \leq \xi_{sn} \cdot C_{sn}^{discharge} \quad (3-23)$$

| | |
|----------------------------|--|
| where $P_{sn,ts}^{charge}$ | mean value of charging power of new build storage sn in time step ts |
| $P_{sn,ts}^{discharge}$ | mean value of discharging power of new build storage sn in time step ts |
| ξ_{sn} | reduction coefficient to consider the unavailability of new build storage sn due to planned maintenance and unplanned outages |
| C_{sn}^{charge} | charging capacity of new build storage sn |
| $C_{sn}^{discharge}$ | discharging capacity of new build storage sn |
| sn | set of new build storages |
| ts | set of time steps (8760 hours) |

In contrast to mutually independent decisions on hourly power plant dispatch, the operation of storages in different time steps is linked via an energy balance equation. For a given storage, the storage level in each time step ts is determined by the storage level of the previous time step $ts-1$ as well as the amount of energy charged or discharged in the respective time step ts .

As charging and discharging power are defined as the effective power input and output, the amount of energy by which the storage level is eventually increased or decreased has to be calculated considering the respective charging and discharging efficiencies of the storage. In MESTAS, it is assumed that the round-trip efficiency of a storage unit results in equal parts from charging and discharging losses, i. e. the charging and discharging efficiencies each amount to the square root of the storage's round-trip efficiency. Furthermore, the energy balance accounts for losses due to the self-discharge of storages by multiplying the storage level of the previous time step by the hourly rate of self-discharge.

The following equations represent the energy balances of existing storages se and new build storages sn , valid for all time steps ts except for the first hour of the simulation year:

$$S_{se,ts} = (1 - \lambda_{se}) \cdot S_{se,ts-1} + \dots - \frac{1}{\eta_{se}^{discharge}} \cdot P_{se,ts}^{discharge} + \eta_{se}^{charge} \cdot P_{se,ts}^{charge} \quad (3-24)$$

$$S_{sn,ts} = (1 - \lambda_{sn}) \cdot S_{sn,ts-1} + \dots - \frac{1}{\eta_{sn}^{discharge}} \cdot P_{sn,ts}^{discharge} + \eta_{sn}^{charge} \cdot P_{sn,ts}^{charge} \quad (3-25)$$

| | |
|-------------------------|---|
| where $S_{se,ts}$ | storage level of existing storage se in time step ts |
| $S_{sn,ts}$ | storage level of new build storage sn in time step ts |
| λ_{se} | hourly rate of self-discharge of existing storage se |
| λ_{sn} | hourly rate of self-discharge of new build storage sn |
| $S_{se,ts-1}$ | storage level of existing storage se in time step $ts-1$ |
| $S_{sn,ts-1}$ | storage level of new build storage sn in time step $ts-1$ |
| η_{se}^{charge} | charging efficiency of existing storage se |
| η_{sn}^{charge} | charging efficiency of new build storage sn |
| $P_{se,ts}^{charge}$ | mean value of charging power of existing storage se in time step ts |
| $P_{sn,ts}^{charge}$ | mean value of charging power of new build storage sn in time step ts |
| $\eta_{se}^{discharge}$ | discharging efficiency of existing storage se |
| $\eta_{sn}^{discharge}$ | discharging efficiency of new build storage sn |
| $P_{se,ts}^{discharge}$ | mean value of discharging power of existing storage se in time step ts |
| $P_{sn,ts}^{discharge}$ | mean value of discharging power of new build storage sn in time step ts |
| se | set of existing storages |

sn set of new build storages
 ts set of time steps (8760 hours)

For the first hour, the previous storage level cannot be determined endogenously. Thus, for ts equal to one, the energy balance equations are reformulated by exogenously defining the initial storage level as a certain share of storage capacity:

$$S_{se,1} = (1 - \lambda_{se}) \cdot \sigma_{se} \cdot c_{se}^{storage} + \dots - \eta_{se}^{charge} \cdot P_{se,1}^{charge} - \frac{1}{\eta_{se}^{discharge}} \cdot P_{se,1}^{discharge} \quad (3-26)$$

$$S_{sn,1} = (1 - \lambda_{sn}) \cdot \sigma_{sn} \cdot C_{sn}^{storage} + \dots - \eta_{sn}^{charge} \cdot P_{sn,1}^{charge} - \frac{1}{\eta_{sn}^{discharge}} \cdot P_{sn,1}^{discharge} \quad (3-27)$$

where $S_{se,1}$ storage level of existing storage se in first time step
 $S_{sn,1}$ storage level of new build storage sn in first time step
 λ_{se} hourly rate of self-discharge of existing storage se
 λ_{sn} hourly rate of self-discharge of new build storage sn
 σ_{se} relative storage level of existing storage se at the beginning of the simulation year
 σ_{sn} relative storage level of new build storage sn at the beginning of the simulation year
 $c_{se}^{storage}$ storage capacity of existing storage se
 $C_{sn}^{storage}$ storage capacity of new build storage sn
 η_{se}^{charge} charging efficiency of existing storage se
 η_{sn}^{charge} charging efficiency of new build storage sn
 $P_{se,1}^{charge}$ mean value of charging power of existing storage se in first time step
 $P_{sn,1}^{charge}$ mean value of charging power of new build storage sn in first time step
 $\eta_{se}^{discharge}$ discharging efficiency of existing storage se
 $\eta_{sn}^{discharge}$ discharging efficiency of new build storage sn

| | |
|------------------------|--|
| | storage sn |
| $P_{se,1}^{discharge}$ | mean value of discharging power of existing storage se in first time step |
| $P_{sn,1}^{discharge}$ | mean value of discharging power of new build storage sn in first time step |
| se | set of existing storages |
| sn | set of new build storages |

As there is no constraint for the storage level at the end of the simulation year, the minimum cost solution requires all storages to be completely emptied. If the initial storage level is set to a value greater than zero, this energy is used over the simulation year to substitute conventional power plants, thus skewing the annual energy balance. For this reason, the initial level is, by default, fixed to zero for all storages. Section 3.3.2 describes how the above equations are altered to ensure that the annual amounts of energy charged and discharged are always well-balanced and to optionally allow for the optimisation of initial and final storage levels.

Just as charging and discharging power, the storage level of existing storages se and new build storages sn is constrained by the storage capacity in each time step ts :

$$S_{se,ts} \leq c_{se}^{storage} \quad (3-28)$$

$$S_{sn,ts} \leq C_{sn}^{storage} \quad (3-29)$$

| | |
|--------------------|--|
| where $S_{se,ts}$ | storage level of existing storage se in time step ts |
| $S_{sn,ts}$ | storage level of new build storage sn in time step ts |
| $c_{se}^{storage}$ | storage capacity of existing storage se |
| $C_{sn}^{storage}$ | storage capacity of new build storage sn |
| se | set of existing storages |
| sn | set of new build storages |
| ts | set of time steps (8760 hours) |

Again, the capacities of existing storages are exogenously fixed, whereas the storage capacities of new build storages are variables that are determined endogenously. In contrast to charging and discharging power, the storage capacity is not weighted by a reduction coefficient to account for unavailability.

In order to minimise the total annual costs of electricity generation, MESTAS can install new build storages to expand the existing storage portfolio. While other models often consider only a single new build storage technology (e. g. Strbac *et al.* 2012), MESTAS optimises the investment into competing storage technologies. By default, three storage technologies are available for expansion: PSP, AA-CAES and a power-to-power hydrogen storage technology (H₂-CCGT). Although it is possible to define further new build storage technologies, every additional option will increase the computational burden of the optimisation problem.

In principle, the charging, discharging and storage capacities of new build storages sn can each be constrained to a maximum capacity available for installation in the respective simulation year:

$$C_{sn}^{charge} \leq c_{sn}^{charge,max} \quad (3-30)$$

$$C_{sn}^{discharge} \leq c_{sn}^{discharge,max} \quad (3-31)$$

$$C_{sn}^{storage} \leq c_{sn}^{storage,max} \quad (3-32)$$

| | |
|--------------------------|---|
| where C_{sn}^{charge} | charging capacity of new build storage sn |
| $c_{sn}^{charge,max}$ | maximum charging capacity available for installation of new build storage sn |
| $C_{sn}^{discharge}$ | discharging capacity of new build storage sn |
| $c_{sn}^{discharge,max}$ | maximum discharging capacity available for installation of new build storage sn |
| $C_{sn}^{storage}$ | storage capacity of new build storage sn |
| $c_{sn}^{storage,max}$ | maximum storage capacity available for installation of new build storage sn |
| sn | set of new build storages |

However, when MESTAS is used to optimise the expansion of storage capacity for several consecutive years, it has to be ensured that the capacity that has been installed in previous years can be rebuilt in subsequent years (if still part of the optimal storage portfolio). Thus, maximum charging, maximum discharging and maximum storage capacities are not used to constrain annual investment with regard to potential limits of annual economic productivity. Instead, the above equations are only

used to limit the overall potential of new build storage technologies in Germany, e. g. in case of geological or topographical limitations.

Whereas exogenously fixed storage durations are often used to characterise new build storage technologies (e. g. Strbac *et al.* 2012, Hand *et al.* 2012), MESTAS allows for the independent rating of charging, discharging and storage capacities. However, if desired, the rating of new build storages can be constrained by enabling one or more of the following equations:

$$\alpha_{sn}^{\min} \leq \frac{C_{sn}^{\text{discharge}}}{C_{sn}^{\text{charge}}} \leq \alpha_{sn}^{\max} \quad (3-33)$$

$$\beta_{sn}^{\min} \leq \frac{C_{sn}^{\text{storage}}}{C_{sn}^{\text{discharge}}} \leq \beta_{sn}^{\max} \quad (3-34)$$

$$\gamma_{sn}^{\min} \leq \frac{C_{sn}^{\text{storage}}}{C_{sn}^{\text{charge}}} \leq \gamma_{sn}^{\max} \quad (3-35)$$

| | |
|--------------------------------|--|
| where C_{sn}^{charge} | charging capacity of new build storage sn |
| $C_{sn}^{\text{discharge}}$ | discharging capacity of new build storage sn |
| C_{sn}^{storage} | storage capacity of new build storage sn |
| α_{sn}^{\min} | lower limit of ratio of discharging to charging capacity of new build storage sn |
| α_{sn}^{\max} | upper limit of ratio of discharging to charging capacity of new build storage sn |
| β_{sn}^{\min} | lower limit of ratio of storage to discharging capacity of new build storage sn |
| β_{sn}^{\max} | upper limit of ratio of storage to discharging capacity of new build storage sn |
| γ_{sn}^{\min} | lower limit of ratio of storage to charging capacity of new build storage sn |
| γ_{sn}^{\max} | upper limit of ratio of storage to charging capacity of new build storage sn |
| sn | set of new build storages |

The ratio of discharging to charging capacity, the ratio of storage to discharging capacity as well as the ratio of storage to charging capacity can be either constrained to

a certain range or – if the respective lower and upper limits are assumed equal – fixed to a specific value. For instance, as discharging and charging units of modern PSP are usually combined in one pump-turbine (Albrecht 2013), equation (3-33) can be used to limit the ratio of discharging to charging capacity to a technically feasible range. Kuhn (2012) suggests a range from 0.8 to 1.2, which is the standard range implemented for new build PSP in MESTAS. Furthermore, equation (3-34) can be used to fix the storage duration of any technology to a generic or empirical value.

As in MOWIKA, further constraints can be introduced optionally. For instance, the amount of fuels available for consumption can be limited for the respective simulation year (vide equation (3-36)). The total fuel consumption of all power plants $ppfl$ burning fuel fl is limited by an annual maximum amount (given as thermal energy). Net efficiencies are used to calculate the fuel consumption of the power plants.

$$\sum_{ts} \left(\sum_{ppfl} \frac{1}{\eta_{ppfl}} \cdot P_{ppfl,ts}^{gen} \cdot \delta_{ts} \right) \leq w_{fl}^{therm,max} \quad (3-36)$$

| | |
|----------------------|--|
| where η_{ppfl} | net efficiency of power plant $ppfl$ |
| $P_{ppfl,ts}^{gen}$ | mean value of generating power of power plant $ppfl$ in time step ts |
| δ_{ts} | duration of time step ts (one hour) |
| $w_{fl}^{therm,max}$ | maximum amount of thermal energy of fuel fl available for consumption in simulation year |
| $ppfl$ | set of power plants burning fuel fl |
| fl | set of fuel types |
| ts | set of time steps (8760 hours) |

As in MOWIKA, annual carbon emissions in MESTAS are either limited implicitly by exogenously fixing a carbon price or are constrained directly by introducing an annual emissions target. Emissions are calculated for each power plant in each time step by multiplying the power output by a factor representing emissions per unit of electricity generated, which is the quotient of the emission intensity of the burned fuel divided by the net efficiency of the respective power plant:

$$\sum_{ts} \left(\sum_{pp} \varepsilon_{pp}^{electr} \cdot P_{pp,ts}^{gen} \cdot \delta_{ts} \right) \leq e^{max} \quad (3-37)$$

| | |
|-----------------------------------|--|
| where $\varepsilon_{pp}^{electr}$ | emissions of power plant pp per unit of electricity generated |
| $P_{pp,ts}^{gen}$ | mean value of generating power of power plant pp in time step ts |
| δ_{ts} | duration of time step ts (one hour) |
| e^{max} | maximum amount of emissions permitted in simulation year |
| pp | set of power plants |
| ts | set of time steps (8760 hours) |

Whereas in MOWIKA must-run of conventional generation can only be implemented by adjusting the duration curve of residual demand, the observance of a lower bound of total generating power is ensured in MESTAS by introducing the following equation for each time step ts :

$$\sum_{pp} P_{pp,ts}^{gen} \geq P^{mustrun} \quad (3-38)$$

| | |
|-------------------------|--|
| where $P_{pp,ts}^{gen}$ | mean value of generating power of power plant pp in time step ts |
| $P^{mustrun}$ | conventional must-run capacity in each time step ts |
| pp | set of power plants |
| ts | set of time steps (8760 hours) |

Another optional constraint in MESTAS is the limitation of curtailment of surplus generation from RES and CHP. If curtailment is not restricted, surplus generation will only be integrated to the extent that storage expansion is economically feasible. While this economic integration of surplus generation is the default case in MESTAS, the annual total of curtailed energy can also be constrained by means of equation (3-39). If the maximum amount of curtailed energy permitted in the respective simulation year is set to zero, storage has to be expanded in terms of capacity and power until every MWh of surplus generation can be utilised.

$$\sum_{ts} P_{ts}^{curtail} \cdot \delta_{ts} \leq w^{curtail,max} \quad (3-39)$$

| | |
|--------------------------|--|
| where $P_{ts}^{curtail}$ | mean value of curtailed power in time step ts |
| δ_{ts} | duration of time step ts (one hour) |
| $w^{curtail,max}$ | maximum amount of curtailed energy permitted in simulation year |
| ts | set of time steps (8760 hours) |

Equation (3-40) represents the objective function of the submodel MESTAS, which is subject to minimisation. It covers the total cost associated with the operation of conventional power plants as well as the operation and expansion of storages over the simulated year. All costs are assumed to reflect the current value in the respective simulation year. If MESTAS is used to simulate more than one year, e. g. when a planning horizon of several decades is optimised with the superordinate model IMAKUS, costs incurring in different years have to be discounted to a given base year in order to be comparable.

$$\begin{aligned}
 \text{minimise } & \sum_{sn} \left(\kappa_{sn}^{nv,charge} \cdot C_{sn}^{charge} + \dots \right. \\
 & \left. \kappa_{sn}^{nv,discharge} \cdot C_{sn}^{discharge} + \dots \right. \\
 & \left. \kappa_{sn}^{nv,storage} \cdot C_{sn}^{storage} \right) + \dots \\
 & \sum_{ts} \left\{ \sum_{pp} \kappa_{pp}^v \cdot P_{pp,ts}^{gen} \cdot \delta_{ts} + \dots \right. \\
 & \left. \sum_{se} \left(\kappa_{se}^{v,charge} \cdot P_{se,ts}^{charge} \cdot \delta_{ts} + \dots \right. \right. \quad (3-40) \\
 & \left. \left. \kappa_{se}^{v,discharge} \cdot P_{se,ts}^{discharge} \cdot \delta_{ts} \right) + \dots \right. \\
 & \left. \sum_{sn} \left(\kappa_{sn}^{v,charge} \cdot P_{sn,ts}^{charge} \cdot \delta_{ts} + \dots \right. \right. \\
 & \left. \left. \kappa_{sn}^{v,discharge} \cdot P_{sn,ts}^{discharge} \cdot \delta_{ts} \right) - \dots \right. \\
 & \left. \kappa^{curtail} \cdot P_{ts}^{curtail} \cdot \delta_{ts} \right\}
 \end{aligned}$$

| | |
|---------------------------------|---|
| where $\kappa_{sn}^{nv,charge}$ | non-variable costs of charging capacity of new build storage sn |
| C_{sn}^{charge} | charging capacity of new build storage sn |
| $\kappa_{sn}^{nv,discharge}$ | non-variable costs of discharging capacity of new build storage sn |
| $C_{sn}^{discharge}$ | discharging capacity of |

| | |
|-----------------------------|---|
| | new build storage sn |
| $\kappa_{sn}^{nv,storage}$ | non-variable costs of storage capacity of new build storage sn |
| $C_{sn}^{storage}$ | storage capacity of new build storage sn |
| κ_{pp}^v | variable costs of power plant pp |
| $P_{pp,ts}^{gen}$ | mean value of generating power of power plant pp in time step ts |
| δ_{ts} | duration of time step ts (one hour) |
| $\kappa_{se}^{v,charge}$ | variable costs of charging of existing storage se |
| $P_{se,ts}^{charge}$ | mean value of charging power of existing storage se in time step ts |
| $\kappa_{se}^{v,discharge}$ | variable costs of discharging of existing storage se |
| $P_{se,ts}^{discharge}$ | mean value of discharging power of existing storage se in time step ts |
| $\kappa_{sn}^{v,charge}$ | variable costs of charging of new build storage sn |
| $P_{sn,ts}^{charge}$ | mean value of charging power of new build storage sn in time step ts |
| $\kappa_{sn}^{v,discharge}$ | variable costs of discharging of new build storage sn |
| $P_{sn,ts}^{discharge}$ | mean value of discharging power of new build storage sn in time step ts |
| $\kappa^{curtail}$ | revenues of curtailment |
| $P_{ts}^{curtail}$ | mean value of curtailed power in time step ts |
| pp | set of power plants |
| se | set of existing storages |
| sn | set of new build storages |
| ts | set of time steps (8760 hours) |

To begin with, the objective function sums up non-variable costs associated with the installation of new build storages in the respective simulation year. As charging, discharging and storage capacities are rated independently in MESTAS, non-variable costs of storage also have to be split up into cost components rather than considering system unit costs that already account for a specific rating of power conversion and storage units. Thus, power-related costs (per kW) associated with the installation of the charging and discharging units and energy-related costs (per kWh) associated with the installation of the storage unit are used to weight installed capacities.

Furthermore, the variable costs caused in each time step by the operation of power plants and storages are added to the total. Non-variable costs of power plants and existing storages are considered to be sunk costs and are not included in the objective function in MESTAS. The objective function is eventually decreased by revenues that are granted for curtailed power (vide supra). As only infinitesimal revenues are used, the value of the objective function is however not significantly influenced.

Modelling of costs

As mentioned above, the objective function separately accounts for non-variable costs that are dependent on the charging, discharging and storage capacity of new build storages. Equations (3-41), (3-42) and (3-43) give the corresponding definitions of non-variable costs. Since MESTAS optimises the power system over a single simulation year, the objective function should only include the fraction of costs that actually incurs within the respective simulation year. Therefore, annualised costs are used to correctly account for the investment cost of new build storages.

Both the annual fixed costs for O&M and the annual savings for decommissioning are assumed to be power-related costs associated with the expansion of charging and discharging capacity, but are not contributing to the non-variable costs of storage capacity. As fixed costs and decommissioning costs are usually not specified separately for charging and discharging capacity, it is assumed that costs are caused in equal parts by charging and discharging units.

$$\kappa_{sn}^{nv,charge} = \left(\kappa_{sn}^{inv,a,charge} + \frac{\kappa_{sn}^{fix,a}}{2} + \frac{\kappa_{sn}^{dec,a}}{2} \right) \cdot (1-b) \quad (3-41)$$

$$\kappa_{sn}^{nv,discharge} = \left(\kappa_{sn}^{inv,a,discharge} + \frac{\kappa_{sn}^{fix,a}}{2} + \frac{\kappa_{sn}^{dec,a}}{2} \right) \cdot (1-b) \quad (3-42)$$

$$\kappa_{sn}^{nv,storage} = \kappa_{sn}^{inv,a,storage} \cdot (1-b) \quad (3-43)$$

| | |
|---------------------------------|--|
| where $\kappa_{sn}^{nv,charge}$ | non-variable costs of charging capacity of new build storage sn |
| $\kappa_{sn}^{nv,discharge}$ | non-variable costs of discharging capacity of new build storage sn |
| $\kappa_{sn}^{nv,storage}$ | non-variable costs of storage capacity of new build storage sn |
| $\kappa_{sn}^{inv,a,charge}$ | annualised investment costs of charging capacity of new build storage sn |
| $\kappa_{sn}^{inv,a,discharge}$ | annualised investment costs of discharging capacity of new build |

| | |
|-------------------------------|---|
| | storage sn |
| $\kappa_{sn}^{inv,a,storage}$ | annualised investment costs of storage capacity of new build storage sn |
| $\kappa_{sn}^{fix,a}$ | annual fixed costs of new build storage sn |
| $\kappa_{sn}^{dec,a}$ | annual savings for decommissioning of new build storage sn |
| b | bonus on non-variable costs of new build storages |
| sn | set of new build storages |

Moreover, non-variable costs of charging, discharging and storage capacity can optionally be reduced by the bonus b . Whereas a 0 % bonus would not reduce the costs, only 75 % of the actual costs would be considered if a bonus of 25 % is used. It is thus possible to account for potential contribution margins earned on markets that are not endogenously modelled in MESTAS, like e. g. the ancillary services market (Kuhn 2012). The same bonus is valid for all new build storage technologies. As a default value, a bonus of 50 % is suggested in Kuhn (2012) and Kuhn *et al.* (2012).

The annualised investment costs of charging, discharging and storage capacity are determined according to equations (3-44), (3-45) and (3-46). Like fixed costs and savings for decommissioning, annualised investment costs are also assumed to incur at the beginning of the simulation year. Thus, the reciprocal of the present value interest factor of an annuity due is used to calculate the annual share of investment costs (Van Horne & Wachowicz 2004). As in MOWIKA, a real discount rate is used.

$$\kappa_{sn}^{inv,a,charge} = \frac{1}{1+i} \cdot \frac{i \cdot (1+i)^{l_{sn}}}{(1+i)^{l_{sn}} - 1} \cdot \kappa_{sn}^{inv,charge} \quad (3-44)$$

$$\kappa_{sn}^{inv,a,discharge} = \frac{1}{1+i} \cdot \frac{i \cdot (1+i)^{l_{sn}}}{(1+i)^{l_{sn}} - 1} \cdot \kappa_{sn}^{inv,discharge} \quad (3-45)$$

$$\kappa_{sn}^{inv,a,storage} = \frac{1}{1+i} \cdot \frac{i \cdot (1+i)^{l_{sn}}}{(1+i)^{l_{sn}} - 1} \cdot \kappa_{sn}^{inv,storage} \quad (3-46)$$

where $\kappa_{sn}^{inv,a,charge}$ annualised investment costs of charging capacity of new build storage sn
 $\kappa_{sn}^{inv,a,discharge}$ annualised investment costs of discharging capacity of new build storage sn

| | |
|-------------------------------|---|
| $\kappa_{sn}^{inv,a,storage}$ | annualised investment costs of storage capacity of new build storage sn |
| i | real discount rate |
| l_{sn} | lifetime of new build storage sn |
| $\kappa_{sn}^{inv,charge}$ | investment costs of charging capacity of new build storage sn |
| $\kappa_{sn}^{inv,discharge}$ | investment costs of discharging capacity of new build storage sn |
| $\kappa_{sn}^{inv,storage}$ | investment costs of storage capacity of new build storage sn |
| sn | set of new build storages |

Analogously to the calculation of annual savings for the decommissioning of power plants in MOWIKA (vide equation (3-13)), the annual savings for the decommissioning of new build storages are determined under the assumption that the target costs can be accrued over the whole lifetime:

$$\kappa_{sn}^{dec,a} = \kappa_{sn}^{dec,target} \cdot \frac{1}{1+i} \cdot \frac{i}{(1+i)^{l_{sn}} - 1} \quad (3-47)$$

| | |
|-----------------------------|--|
| where $\kappa_{sn}^{dec,a}$ | annual savings for decommissioning of new build storage sn |
| $\kappa_{sn}^{dec,target}$ | target costs for decommissioning of new build storage sn |
| i | real discount rate |
| l_{sn} | lifetime of new build storage sn |
| sn | set of new build storages |

The objective function also includes the variable costs of power plants and storages. Variable costs of storages are specified separately for the amounts of energy charged and discharged. For power plants, the variable costs are determined analogously to MOWIKA. They are defined for each set of power plants burning a given fuel fl and comprise the costs for fuel, variable O&M costs as well as emission costs:

$$\kappa_{ppfl}^v = \frac{1}{\eta_{ppfl}} \cdot \kappa_{fl}^{fuel} + \kappa_{ppfl}^{vO\&M} + \varepsilon_{ppfl}^{electr} \cdot \kappa^{emi} \quad (3-48)$$

| | | |
|-------|-------------------------------|--|
| where | κ_{ppfl}^v | variable costs of power plant $ppfl$ |
| | η_{ppfl} | net efficiency of power plant $ppfl$ |
| | κ_{fl}^{fuel} | costs for fuel fl |
| | $\kappa_{ppfl}^{vO\&M}$ | variable O&M costs of power plant $ppfl$ |
| | $\varepsilon_{ppfl}^{electr}$ | emissions of power plant $ppfl$ per unit of electricity generated |
| | κ^{emi} | carbon emissions price |
| | $ppfl$ | set of power plants burning fuel fl |
| | fl | set of fuel types |

If an annual emissions target is used and emissions are directly limited by constraint (3-37), the exogenously defined carbon emissions price in equation (3-48) has to be set to zero. The carbon emissions price is then determined endogenously.

Results

The main results obtained from the submodel MESTAS are the cost-optimal storage portfolio as well as the optimised hourly dispatch of conventional power plants, existing storages and new build storages for the considered simulation year. The obtained storage portfolio not only represents the optimal mix of several competing storage technologies, but – as charging, discharging and storage capacity are rated independently – new build storages are also optimally adapted to the requirements of the power system. However, due to the myopic approach, storage capacity expansion is only optimal for the respective simulation year.

In addition to hourly values, results include aggregated values such as the annual non-variable costs of new build storages and the annual variable costs of electricity generation (including both power plants and storages). Further results are the annual amounts of generated electricity, fuel consumption and carbon emissions per generation technology as well as the annual amounts of energy charged and discharged per storage technology. If annual emissions are constrained by an emissions target, the carbon price for the considered simulation year can be obtained. The hourly values of curtailed power are summed up to determine the total annual surplus generation from RES and CHP that could not be integrated.

By utilising storages for peak-shaving purposes and the integration of surplus generation, the residual demand that has to be covered by conventional power plants is smoothed, thus reducing the costs of electricity generation compared to a power system without storages. When MESTAS is used within the iterative process of the superordinate model IMAKUS, the smoothed time series of residual demand are used as an input to the submodel MOWIKA. By this means, the impact of storage

operation can also be considered during the optimisation of generation capacity expansion (vide Section 3.2.4).

3.2.3 Submodel MOGLIE: ensuring system firm capacity

In principle, only as much conventional generation capacity as necessary to meet the peak residual load is installed by the submodel MOWIKA. As the output of each power plant is limited by a reduction coefficient to implicitly consider planned maintenance and unplanned outages, the total installed conventional generation capacity actually exceeds the peak residual load to a certain extent. However, only the average unavailability of conventional generation capacity is taken into account.

Despite its dependency on non-dispatchable generation, the residual demand is furthermore treated deterministically in MOWIKA. This means that, if the actual renewable feed-in falls short of assumed generation values, the optimised conventional generation portfolio could prove inadequate to meet the peak residual load.

Thus, further measures are necessary to ensure that the generation portfolio determined with MOWIKA satisfies the requirements of security of supply, i. e. to guarantee continuity of service even in case of low renewable generation and one or more unplanned outages at the time of peak load. For this purpose, the total generation capacity of the power system has to be increased by a certain reserve capacity.

According to Billinton & Allan (1984), there are two common static approaches to determine the necessary reserve capacity: The reserve capacity either is defined as a certain percentage of peak load or is set to equal the capacity of the largest unit on the system. However, these approaches offer little additional value compared to the already increased generation capacity resulting from the application of reduction coefficients in MOWIKA.

Billinton & Allan (1984) also point out that, due to different types and sizes of generating units, two systems with peak loads of the same magnitude may still require quite different amounts of reserve to guarantee the same level of security of supply. They furthermore criticise that, by using static approaches, the probabilistic aspects of security of supply are completely neglected.

Security of supply and firm capacity

The submodel MOGLIE allows to evaluate whether the installed generation capacity of a given portfolio has to be increased with regard to security of supply (Kuhn 2012). In order to effectively account for the unavailability of conventional power plants as well as the intermittent character of non-dispatchable generation, a probabilistic

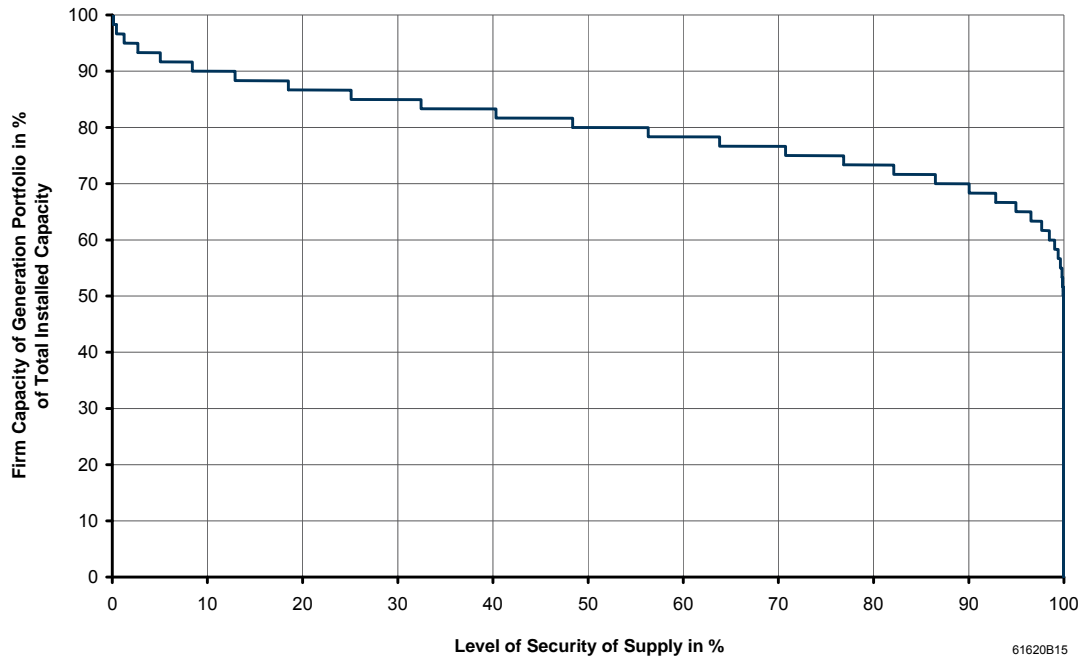


Figure 3.3: Complementary cumulative distribution function of available generation capacity in an exemplary generation portfolio

Based on the complementary cumulative distribution function of the whole generation portfolio, the firm capacity of a given power system is determined in the sub-model MOGLIE for a desired level of security of supply. The resulting firm capacity is then compared with the estimated peak load, which is the crucial factor with regard to security of supply. As a precaution, peak load is additionally augmented by 4 % (Kuhn 2012). If the firm capacity is greater than or equal to this worst-case peak load value, continuity of service is guaranteed at all times with the desired level of security. If the firm capacity is however lower, continuity of service is at risk and reserve capacity should be further increased.

Whereas a level of security of supply of 99.9 % was pursued in Germany before the European liberalisation of electricity markets (Brückl 2005), the installation of generation capacity is solely subject to economic considerations in today's liberalised markets (Kuhn 2012). However, Kuhn (2012) points out that in case of declining investments regulatory measures to increase installed capacity could become necessary in the future and assumes a default security level of 99.5 % in MOGLIE. As with regard to covering electricity demand, Germany is also assumed to be self-sufficient in terms of security of supply.

Determining probability distributions of available generation capacity

As there are significant differences with regard to the characteristics of availability of generation technologies, different approaches are required to determine the respective probability distributions of available generation capacity (Kuhn 2012). In case of conventional power plants, a simple “two-state model” as described by Billinton & Allan (1984) is used: Either the power plant’s total net generation capacity is available or the power plant is found on forced outage.

As it can be assumed that maintenance works are usually not scheduled for the fairly well-predictable time of peak load, only the technical reliability R of power plants is considered (Kuhn 2012). In contrast to the overall energy availability A , the technical reliability R , which is the complement of the forced outage rate of the power plant, is exclusively based on time periods when the generating unit is not maintained:

$$R = 1 - FOR \quad (3-50)$$

where R technical reliability
 FOR forced outage rate

Thus, the discrete probability distribution of a conventional power plant assigns the technical reliability to the power plant’s total net generation capacity, while the probability of available generation capacity being zero equals the forced outage rate.

As the outages of different power plants are assumed to be stochastically independent events, the overall probability distribution of the conventional generation portfolio can be calculated from individual probability distributions by means of stochastic convolution (Kuhn 2012). However, this requires conventional power plants to be modelled at plant level in MOGLIE. Thus, before generation portfolios that are obtained from the submodel MOWIKA can be analysed, the new build capacities – which are only classified with regard to technology and the year of installation – have to be broken down to plant level. For this purpose, new build capacities are split up into individual power plants assuming technology-specific minimum and maximum sizes of generating units.

For cogeneration technologies, i. e. fossil- and biomass-fired CHP and geothermal generation, the availability of generation capacity is not only subject to technical reliability but also dependent on heat demand (Kuhn 2012). However, due to a strong correlation between electricity and heat demand, cogeneration units are very likely to be committed at the time of peak electrical load (Kuhn 2012). As it is furthermore

assumed that maintenance works are usually not scheduled for the time of peak load, only the technical reliability of cogeneration units is considered (Kuhn 2012).

Based on the assumption that the installed cogeneration capacity is comprised of a very large number of very small generating units, Kuhn (2012) suggests a generalised approach to calculate the capacity credit of CHP and geothermal power plants: In case of an infinite number of units with infinitesimal capacity and identical technical reliability, the firm capacity of the portfolio equals the total generation capacity multiplied by the technical reliability of the individual generating units (irrespective of the desired level of security of supply). A default value of 95 % is used in MOGLIE to estimate the technical reliability of cogeneration units. The firm capacity of fossil- and biomass-fired CHP as well as geothermal generation can simply be added to the firm capacity that is calculated for the remaining generation portfolio.

For variable renewable generation technologies like wind, solar or hydro, availability of generation capacity is mainly influenced by the intermittent character of the natural resources rather than the technical reliability of the generating units. Thus, in contrast to the two-state model used to characterise conventional power plants, a “multi-state model” is applied to determine the probability distributions of available generation capacity (Kuhn 2012). The impact of technical reliability on the capacity credit of RES is neglected in MOGLIE.

The probability distributions for wind and hydro power can be derived from their respective hourly electricity generation patterns (Roth 2008): For this purpose, each discrete output power is assigned the probability that results from the analysis of the respective annual generation time series. However, in case of RES, electricity production from multiple generating units cannot be considered stochastically independent of each other. Therefore, the probability distributions are determined based on the aggregated time series of wind and hydro generation in Germany, which are also used as input parameters to the submodels MOWIKA and MESTAS.

In order to account for the correlation of onshore and offshore wind, the probability distribution for wind power is based on the accumulated time series of onshore and offshore wind generation. As the reliability of conventional power plants and the availability of generation capacity from wind or hydro power can be assumed independent, the respective probability distributions are combined by means of stochastic convolution to determine the overall probability distribution of the power system (Kuhn 2012).

While for wind and hydro power the available generation capacity can be considered time-independent (if seasonal variability is neglected), the available solar generation capacity is subject to a significant dependence on the time of day (Kuhn 2012). As the peak load usually occurs on a winter evening in Germany (ENTSO-E 2014), the capacity credit of solar generation is assumed to be zero (Kuhn 2012).

Furthermore, the capacity credit of storages is considered in the submodel MOGLIE. In contrast to conventional power plants, where the necessary fuel is assumed to be abundantly available, the ability of storages to provide generation capacity is limited by the amount of energy that is stored at a given point of time. On this account, analogously to wind and hydro power, a multi-state approach is used to characterise the availability of generation capacity from storages (Kuhn 2012).

The probability distribution of available generation (i. e. discharging) capacity from storages is based on an analysis of the hourly time series of storage level, which, for instance, can be obtained from economic dispatch optimisation in MESTAS. In order to determine the available generation capacity for a given storage unit in a given hour, the theoretical maximum discharging power is calculated based on the current storage level and compared to the actually installed discharging capacity. The available generation capacity equals the minimum of the two values (Kuhn 2012):

$$C_{ts}^{discharge,av} = \min \left(C^{discharge}, \frac{S_{ts} \cdot \eta^{discharge}}{\delta_{ts}} \right) \quad (3-51)$$

| | |
|-------------------------------|---|
| where $C_{ts}^{discharge,av}$ | available discharging capacity of a given storage in time step ts |
| $C^{discharge}$ | discharging capacity of a given storage |
| S_{ts} | storage level of a given storage in time step ts |
| $\eta^{discharge}$ | discharging efficiency of a given storage |
| δ_{ts} | duration of time step ts (one hour) |
| ts | set of time steps (8760 hours) |

As the economic dispatch of different storages is expected to be strongly correlated, the availability of generation capacity from these storage units also cannot be considered stochastically independent (Kuhn 2012). Therefore, the individual time series of available generation capacity are accumulated. The probability distribution of total available generation capacity from storages is derived from the resulting time series by evaluating the probability of discrete values of available discharging capacity (Kuhn 2012).

The technical reliability of storages is also taken into account in MOGLIE. For this purpose, each storage plant is assigned a discrete probability distribution characterising its technical reliability according to the two-state model (Kuhn 2012). As in case of conventional generation, this requires storages to be modelled at plant level. Storage portfolios that are obtained from the submodel MESTAS thus are split up assum-

ing technology-specific minimum and maximum sizes of discharging units. The overall probability distribution of the technically reliable generation capacity from storages is then calculated from individual probability distributions by means of stochastic convolution (Kuhn 2012).

Eventually, the overall probability distribution that considers both – the availability of stored energy and the technical reliability of storage units – has to be determined. As the forced outage of a storage unit can be assumed stochastically independent of its storage level, the two probability distributions can be combined by multiplying the probability of each discrete value of available discharging capacity with the probability that at least the respective capacity is also technically available (Kuhn 2012). The latter is obtained from the complementary cumulative distribution function of the technically reliable generation capacity from storages.

In order to determine the overall probability distribution of the power system, the probability distribution of available generation capacity from storages is combined with the respective probability distributions of conventional generation, wind and hydro power by means of stochastic convolution.

Kuhn (2012) points out that the described method to estimate the capacity credit of storages implicitly assumes that peak load occurs coincidentally, whereas in reality the time of peak load is fairly well-predictable and storage levels are likely to be increased in anticipation. Consequently, the capacity credit of storage is most probably underestimated in MOGLIE.

Adapting the generation portfolio to the requirements of security of supply

Besides the mere analysis whether a given power system satisfies the requirements of security of supply, MOGLIE also allows to estimate the amount of megawatts that the installed generation capacity needs to be increased by to reach the necessary firm capacity or, as the case may be, can be spared without undercutting the desired security level. If MOGLIE is used within the iterative process of IMAKUS, this information can be used in the submodel MOWIKA: As explained in Section 3.2.1, an additional equation in MOWIKA optionally constrains the conventional generation capacity to a minimum installed capacity. Depending on whether a capacity surplus or deficiency has been detected in MOGLIE, this minimum installed capacity is either decreased or increased in the next iterative step (vide Section 3.2.4).

As mentioned above, the complementary cumulative distribution function of a given generation portfolio is used to determine the firm capacity C^{firm} for the desired security level. Its deviation from the target value of firm capacity $C^{firm,target}$, i. e. the peak load plus 4 %, is defined as follows (Kuhn 2012):

$$\Delta C^{firm} = C^{firm,target} - C^{firm} \quad (3-52)$$

where ΔC^{firm} deviation of firm capacity from the target value of firm capacity
 $C^{firm,target}$ target value of firm capacity
 C^{firm} firm capacity of a given generation portfolio for a given level of security of supply

Thus, if the firm capacity is less than the target value, the deviation of firm capacity is positive. If the firm capacity is greater than the target value, the deviation of firm capacity is negative.

In order to increase or decrease the firm capacity of the generation portfolio by a certain amount, the installed generation capacity has to be increased or decreased by an even higher amount. As the firm capacity of the adapted generation portfolio will again depend on the number, size and the availability of the individual generating units, it is not possible to determine the exact amount of additional or spare generation capacity. However, as proposed by Kuhn (2012), the amount can be estimated based on the average capacity credit of installed generation capacity in the current generation portfolio:

$$\Delta C^{gen,conv} = \Delta C^{firm} \cdot \left(\frac{C^{firm,conv}}{C^{gen,conv}} \right)^{-1} \quad (3-53)$$

where $\Delta C^{gen,conv}$ amount of additional or spare conventional generation capacity
 ΔC^{firm} deviation of firm capacity from the target value of firm capacity
 $C^{firm,conv}$ firm capacity of the conventional generation portfolio for a given level of security of supply
 $C^{gen,conv}$ total installed conventional generation capacity

In the next iterative step, the calculated amount of additional or spare conventional generation capacity can be added to the minimum installed capacity in MOWIKA.

Analogously to the deviation of firm capacity, its sign is positive in case of a capacity deficiency and becomes negative in case of a capacity surplus.

As the minimum installed capacity constraint is only effective for conventional generation capacity, the only possibility to influence the firm capacity of the power system is through changes to the conventional generation portfolio. Consequently, equation (3-53) only considers the ratio of the capacity credit of power plants to the total installed conventional generation capacity to estimate the amount of additional or spare capacity.

3.2.4 *The iterative approach*

While the three models MOWIKA, MESTAS and MOGLIE can each be used for stand-alone analyses, they were actually developed as submodels of the superordinate model IMAKUS, which is used to iteratively determine the least-cost pathway of the whole power system for a given planning horizon. The idea for this iterative model was first presented in Kuhn & Kühne (2011) and the concept was further elaborated on in Kuhn (2012).

When planning the future design of the power system, a holistic optimisation model would be, in principle, desirable (Kuhn & Kühne 2011, Kuhn 2012): Thus, both long-term investment decisions into conventional power plants and storages and short-term decisions on the economic dispatch of these units could be optimised simultaneously, in due consideration of their mutual interdependencies. However, the computational burden of solving such an optimisation problem would increase dramatically for a planning horizon of several decades. As the reduction of temporal resolution (e. g. by using representative time slices) is not a viable option with regard to the desired detail of modelling storage dispatch, the original optimisation problem was instead split up into subproblems.

Whereas mathematical decomposition methods could be applied for this purpose, the knowledge about strong and rather weak interdependencies can also be used to identify subproblems that initially can be solved independently (Kuhn & Kühne 2011, Kuhn 2012): Naturally, there is a strong interdependency between capacity expansion and operation of power plants as well as between capacity expansion and operation of storages. Storage operation and power plant dispatch are also strongly interdependent and thus have to be optimised simultaneously.

By contrast, the impact of storage on generation capacity planning is supposed to be rather weak (Kuhn & Kühne 2011, Kuhn 2012). The economic feasibility of a power plant is largely determined by the level of capacity utilisation, i. e. the achieved ca-

capacity factor. Due to the typically large proportion of non-variable costs to total costs, base-load power plants require a high level of utilisation. On the other hand, peaking plants offer low non-variable costs at the expense of high variable costs, which makes them the cheapest option for low levels of utilisation.

As storages are used to store energy at low prices and substitute expensive conventional generation, the utilisation of base-load capacity increases, while the capacity factor of peaking plants is reduced. Thus, investment decisions into power plants that were made without considering storage can usually be confirmed when storage is taken into account afterwards (Kuhn & Kühne 2011, Kuhn 2012). Only in narrow ranges of annual utilisation time could storages tip the balance to investment into either the lower or the higher ranking technology in the merit order.

Figure 3.4, which is based on Kuhn (2012), illustrates the general effect of storage on the annual load duration curve and how the utilisation of power plants is influenced.

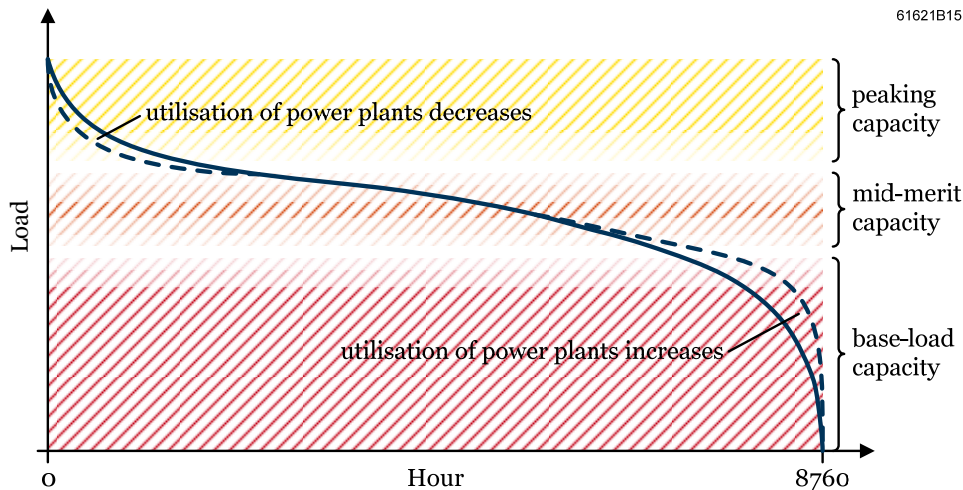


Figure 3.4: General effect of storage on annual load duration curves and its impact on the level of utilisation of power plants

Due to these considerations, the original problem of optimising the whole power system is split up into two subproblems in IMAKUS (Kuhn & Kühne 2011, Kuhn 2012): the expansion of generation capacity, which is addressed in the submodel MOWIKA, and the expansion of storage capacity, which is optimised along with the economic dispatch of power plants and storages in MESTAS. In order to account for the possible (if small) impact of storage on the structure of the generation portfolio, the two submodels are however iteratively coupled.

Starting from the second iterative step, the annual load duration curves used in MOWIKA are not based on the original time series of residual demand anymore. Instead, the smoothed time series of residual demand obtained from MESTAS in the previous step are used as an input. Depending on the extent of storage utilisation for peak-shaving purposes and surplus integration, the annual load duration curves of residual demand are deformed in a similar way as illustrated in Figure 3.4.

Thus, the impact of storages on the utilisation of conventional power plants is considered during the optimisation of generation capacity expansion in MOWIKA. The adapted annual generation portfolios are, in turn, used as an input during the next run of MESTAS. Here, the original time series of residual demand are used and storage capacity expansion is optimised considering the improved generation portfolios. Based on the assumption that investment decisions into power plants are usually confirmed if storages are considered, it is expected that the generation and storage portfolios adapt to each other iteratively and that submodel solutions consequently converge to the whole-systems cost minimum (Kuhn & Kühne 2011, Kuhn 2012).

The implementation of an iterative process also makes it possible to gradually adapt the generation portfolio to the requirements of security of supply (Kuhn & Kühne 2011, Kuhn 2012). Whereas it is impossible to determine *ex ante* the necessary amount of generation capacity to meet the desired level of security, the submodel MOGLIE allows to calculate the current firm capacity of the power system and estimates the amount by which the minimum installed conventional generation capacity either can be decreased or has to be increased in the next iterative step.

Therefore, if a certain security level is desired, the otherwise optional equation (3-6) needs to be included in MOWIKA to constrain the conventional generation capacity to a minimum installed capacity. At the beginning of the iterative process, an initial value has to be set for the minimum installed capacity. A suitable value is, for instance, the annual peak load of the original consumer demand. Whereas firm capacity will exceed the requirements considerably at the beginning, it iteratively converges to the target value of firm capacity (Kuhn & Kühne 2011, Kuhn 2012).

Thus, IMAKUS can also be used to determine a power system which meets a given level of security of supply. It should be noted that different scenarios only become comparable if the same level of security of supply is imposed on the respective power systems (Kuhn 2012).

Evaluating the convergence of the iterative process

Although it is expected that the solutions to the subproblems of generation and storage capacity expansion converge iteratively to the whole-systems cost minimum, the quality of results obtained from IMAKUS has to be further investigated. The convergence of the iterative process can be evaluated with regard to the following criteria:

- Is a stable generation and storage portfolio established after an acceptable number of iterative steps?
- Does the mutual adaptation of generation and storage capacities lead to lower overall costs of the power system?
- How closely is the global optimum of the original optimisation problem approximated by the iterative process?

The question whether the iterative process converges towards lower overall costs of the power system is addressed in Kuhn & Kühne (2011) and Kuhn (2012). The overall costs of the power system in a given iterative step have to be calculated based on the relevant costs from both submodels, MOWIKA and MESTAS. Actually, for each iterative step, two substeps can be distinguished where different methods of calculation are valid. Figure 3.5 illustrates the iterative process schematically.

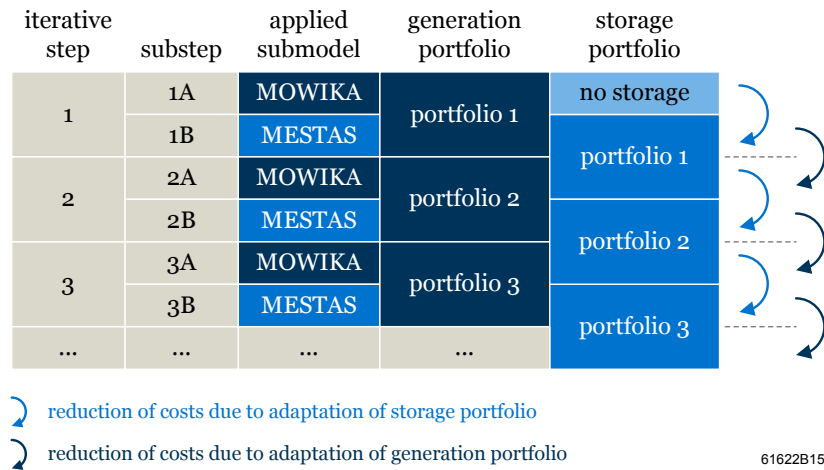


Figure 3.5: Schematic representation of the iterative process and expected cost reductions in the model IMAKUS

In the first substep of each iterative step, the expansion and operation of generation capacity is optimised in MOWIKA based on a residual demand that reflects the benefits of storage according to the previous iterative step. Consequently, the overall costs of the power system are not only composed of the variable and non-variable costs of power plants incurring in MOWIKA but also of the variable and non-variable costs of storage that were determined in MESTAS in the previous iterative step.

In the second substep, both the expansion and operation of storage capacity and the operation of power plants are optimised in MESTAS, assuming a fixed conventional generation portfolio as determined in MOWIKA in the first substep. Thus, the overall

costs of the power system comprise variable and non-variable costs of storage as well as variable costs of power plants from MESTAS and the non-variable costs of power plants that were determined in MOWIKA in the first substep.

As indicated in Figure 3.5, each adaptation of the storage portfolio as well as each adaptation of the generation portfolio is expected to reduce the overall costs of the power system or to be at least cost-neutral (Kuhn & Kühne 2011, Kuhn 2012): Storage capacity will only be further expanded in MESTAS, if a further smoothening of the residual demand reduces the overall costs of the power system. Otherwise, the optimisation will opt for the same – and, as the case may be, none – investments into storage as in the previous iterative step. On the other hand, a smoothened residual demand improves the level of utilisation of base-load power plants and possibly permits to increase the share of installed base-load capacity in the portfolio. Such adjustments to the generation portfolio will always lead to lower costs of electricity generation and consequently will also reduce the overall costs of the power system.

Thus, due to the mutual adaptation of generation and storage portfolios, a successive decrease of overall costs is expected during the iterative process. However, as pointed out in Kuhn & Kühne (2011) and Kuhn (2012), slight cost increases are observed in later stages of the iterative process. The cost increases exclusively occur between the first and the second substep, i. e. when the adaptation of the storage portfolio should usually cause a reduction of costs.

The reason for these deviations from the expected monotonic decrease of costs is the use of discretised annual load duration curves in the submodel MOWIKA (Kuhn & Kühne 2011, Kuhn 2012): By discretising the annual load duration curve, the variable costs of power plants are systematically underestimated. Whereas the methodology preserves the total amount of energy contained in each discretisation interval, the averaging also causes a systematic shift of energy from the higher to the lower ranking technology in the merit order.

By contrast, the variable costs of power plants are determined more accurately in the submodel MESTAS, where dispatch is planned based on time series in hourly resolution. Thus, the cost difference between the first and the second substep is the total of cost reductions due to storage and the seeming increase of variable costs of generation. However, a positive total only occurs in later stages of the iterative process, when a further adaptation of the storage portfolio does not lead to significant cost reductions (Kuhn & Kühne 2011, Kuhn 2012). As it is shown in Kuhn & Kühne (2011) and Kuhn (2012), the deviations from the expected monotonic decrease of costs reduce considerably if the number of discretisation intervals is increased. Thus, the observed cost increases do not disprove the convergence of the iterative process towards lower overall costs but are rather due to more accurate cost estimations in the second substep.

Moreover, it is shown in Kuhn & Kühne (2011) and Kuhn (2012) that a stable generation and storage portfolio can be established after an acceptable number of iterative steps. Figure 3.6 illustrates the iterative adaptation of generation and storage portfolios in an exemplary scenario. Owing to an apparently high initial value of minimum installed capacity, the installed generation capacity decreases considerably during the first iterative steps. This mainly affects gas turbine capacity, which is reduced as the firm capacity of the power system is successively adjusted to the target value.

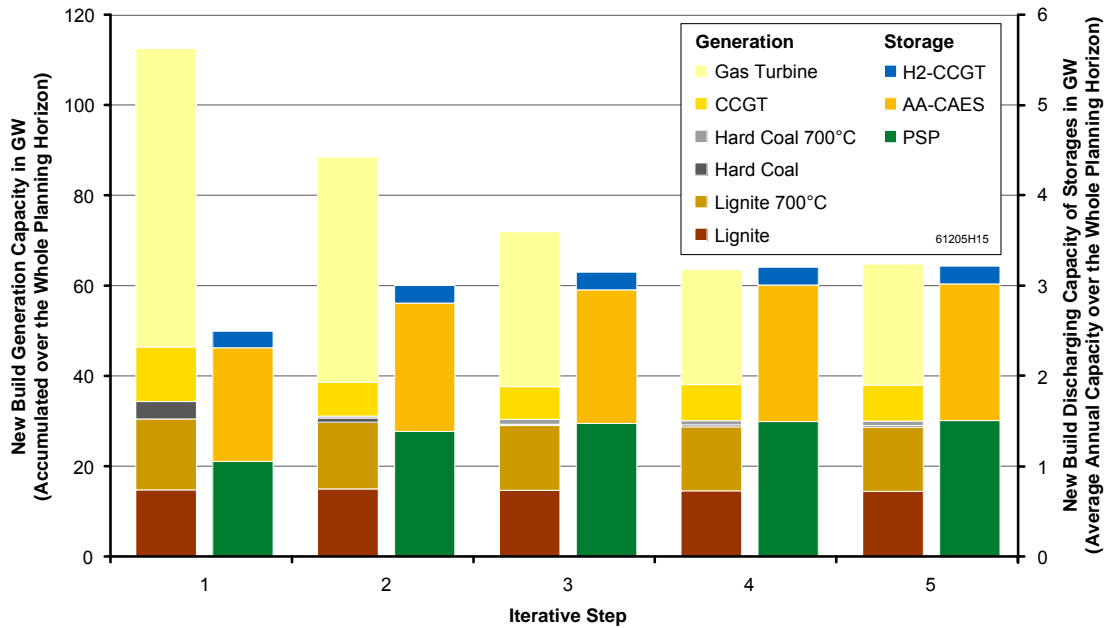


Figure 3.6: Iterative adaptation of conventional generation and storage portfolios in IMAKUS in an exemplary scenario

The figure furthermore shows how the structure of the generation and storage portfolios is adapted iteratively. Installed capacity increases for PSP and AA-CAES during the iterative process. By contrast, the amount of hydrogen capacity remains virtually constant, as the economic feasibility of hydrogen storage is largely determined by the availability of surplus generation from RES and CHP, while the structure of the generation portfolio is of minor importance (Kuhn & Kühne 2011, Kuhn 2012). As it can be observed, in this case, a more or less stable generation and storage portfolio is already established after five iterative steps.

In order to address the final question of how closely the global optimum is approximated by the iterative process, a model is needed which allows to solve the original optimisation problem of generation and storage capacity expansion holistically.

Whereas, due to above considerations, the optimisation of such a problem is not possible for a planning horizon of several decades, the computational burden is actually manageable if the planning horizon only comprises a single year.

The submodel MESTAS was extended by Heilek (2015) to also allow for the endogenous optimisation of generation capacity expansion. Thus, investment decisions into conventional power plants and storages as well as the economic dispatch can be optimised simultaneously for one simulation year. On the other hand, IMAKUS can be used to iteratively determine investment and dispatch decisions for a one-year planning horizon. This, however, requires to use the annuity method for depreciation when calculating the salvage value of power plants in MOWIKA (vide Section 3.3.1).

By comparing results from IMAKUS and MESTAS for a given simulation year, the convergence of the iterative process towards the global optimum can be evaluated. As requirements of security of supply cannot be considered in MESTAS, the conventional generation capacity is merely constrained to a suitable minimum installed capacity in both models. For simulations of the year 2050 according to the three base scenarios defined in Kuhn *et al.* (2012), the comparison shows that, after 16 iterative steps, the objective function value only falls 0.1–2.4 % short of the global optimum.

3.3 Extensions to the model IMAKUS

3.3.1 Calculating the salvage value by using the annuity method for depreciation

As described in Section 3.2.1, the non-variable costs of new build generation capacity are reduced by a salvage value in MOWIKA, which reflects the residual value of an asset that does not reach the end of its lifetime within the planning horizon. By this means, the increase of average annual investment costs is reduced, thus mitigating the so-called end effect, i. e. the tapering off of capacity expansion and the short-sighted preference of less capital-intensive peaking plants during the final years of the planning horizon.

In order to determine the salvage value of new build power plants in MOWIKA, Kuhn (2012) proposed to calculate the undepreciated investment at the end of the planning horizon by means of straight-line depreciation (vide equation (3-15)). While this approach serves the purpose of reducing the increase of average annual investment costs towards the end of the planning horizon to a certain extent, other methods of depreciation might be even more suitable.

As an alternative, the annuity method for depreciation is presented in this section, which not only allows to further mitigate the end effect of generation expansion in

MOWIKA but also establishes the equivalence of the two submodels MOWIKA and MESTAS with regard to the modelling of costs. In order to demonstrate how the salvage value is calculated if the annuity method for depreciation is assumed, first, a recursive definition of the book value of a given asset in a given year of its economic lifetime is derived.

Generally, the book value at the end of a given year yl is the book value at the end of the previous year decreased by depreciation expenses:

$$B_{yl} = B_{yl-1} - D_{yl} \quad (3-54)$$

| | |
|----------------|--|
| where B_{yl} | book value of a given asset at end of year yl |
| B_{yl-1} | book value of a given asset at end of year $yl-1$ |
| D_{yl} | depreciation expense in year yl |
| yl | set of years of the economic lifetime of a given asset |

If the book value at the end of the asset's economic lifetime is assumed to be zero, the total annual expenses can be calculated by multiplying the initial book value of the asset B_o (i. e. investment costs) by the reciprocal of the present value interest factor of an ordinary annuity. According to Graham (2011), these total annual expenses equal each year's sum of depreciation expense D_{yl} and foregone interest I_{yl} :

$$E^a = D_{yl} + I_{yl} = B_o \cdot \frac{i \cdot (1+i)^l}{(1+i)^l - 1} \quad (3-55)$$

$$I_{yl} = i \cdot B_{yl-1} \quad (3-56)$$

| | |
|-------------|---|
| where E^a | total annual expenses |
| D_{yl} | depreciation expense in year yl |
| I_{yl} | foregone interest in year yl |
| B_o | initial book value of a given asset |
| i | real discount rate |
| l | lifetime |
| B_{yl-1} | book value of a given asset at end of year $yl-1$ |

yl set of years of the economic lifetime
of a given asset

Thus, using equations (3-55) and (3-56), the book value B_{yl} of a given asset in a given year yl of its economic lifetime can be specified as follows:

$$B_{yl} = B_{yl-1} \cdot (1+i) - B_o \cdot \frac{i \cdot (1+i)^l}{(1+i)^l - 1} \quad (3-57)$$

where B_{yl} book value of a given asset at
end of year yl
 B_{yl-1} book value of a given asset at
end of year $yl-1$
 B_o initial book value of a given asset
 i real discount rate
 l lifetime
 yl set of years of the economic lifetime
of a given asset

Based on this recursive definition, it is also possible to give a functional notation of the book value:

$$\begin{aligned} B_{yl} &= B_o \cdot \left\{ (1+i)^{yl} - \frac{i \cdot (1+i)^l}{(1+i)^l - 1} \cdot \sum_{n=0}^{yl-1} (1+i)^n \right\} \\ &= B_o \cdot \left\{ (1+i)^{yl} - \frac{i \cdot (1+i)^l}{(1+i)^l - 1} \cdot \frac{(1+i)^{yl} - 1}{i} \right\} \end{aligned} \quad (3-58)$$

where B_{yl} book value of a given asset at
end of year yl
 B_o initial book value of a given asset
 i real discount rate
 l lifetime
 n number of payment periods (years)
 yl set of years of the economic lifetime
of a given asset

For yl equal to one, B_{yl-1} becomes B_0 and it is easily found that equation (3-58) equals equation (3-57). In case of yl equal to l , equation (3-58) yields zero. Thus, as assumed above, the book value is reduced to zero at the end of the asset's economic lifetime. If the annuity method for depreciation is to be used, the book value, determined according to equation (3-58), can be used as an estimate of an asset's salvage value at the end of a given year.

By means of an example, the annuity method for depreciation is compared with the straight-line depreciation approach. In Figure 3.7 the two methods are compared with regard to effective investment costs, i. e. investment costs decreased by the salvage value, and average annual investment costs, i. e. effective investment costs divided by the number of years of utilisation. The example considers investment into an asset with economic lifetime of 20 years and investment costs of 1 million €. Depending on the year of investment, the figure illustrates the impact of the applied depreciation method on costs over a planning horizon of 20 years. The assumed interest rate is 5 %.

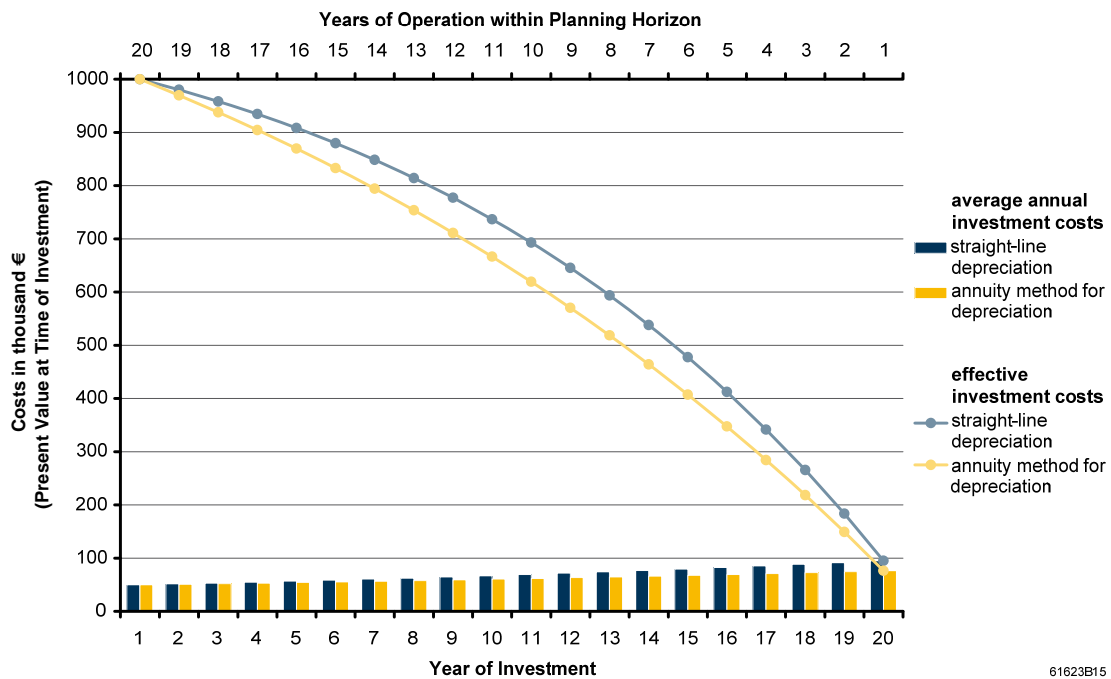


Figure 3.7: Comparison of annuity method for depreciation and straight-line depreciation (assuming a 20-year planning horizon, 1 million € investment, 20 years lifetime and 5 % interest rate)

As it can be observed, the two depreciation methods are equivalent if the whole economic lifetime is covered by the planning horizon, i. e. if investment takes place in the first year and the asset can be utilised for 20 years. By contrast, if the investment is made in the second year of the planning horizon or later, the economic lifetime of the asset is only partly covered by the planning horizon and the book value at the end of the planning horizon has to be taken into account. In this case, the costs resulting from the two approaches differ significantly: Lower effective investment costs are observed for the annuity method for depreciation and, consequently, the increase of average annual investment costs towards the end of the planning horizon is lower than in case of straight-line depreciation.

The average annual investment costs resulting from the annuity method for depreciation are furthermore equivalent to average annual investment costs in case of an annualised costs approach, as it is used, for instance, in MESTAS. Without loss of generality, this equivalence is shown under the assumption that only one year of the asset's economic lifetime is covered by the planning horizon (i. e. yl equal to one). In this case, the average annual investment costs are calculated as follows:

$$\begin{aligned}\tilde{\kappa}_1^{inv,avg} &= \frac{1}{1+i} \cdot \{B_0 \cdot (1+i) - B_1\} \\ &= \frac{1}{1+i} \cdot \left\{ B_0 \cdot (1+i) - B_0 \cdot (1+i) + B_0 \cdot \frac{i \cdot (1+i)^l}{(1+i)^l - 1} \right\} \quad (3-59) \\ &= \frac{1}{1+i} \cdot \frac{i \cdot (1+i)^l}{(1+i)^l - 1} \cdot B_0\end{aligned}$$

| | |
|------------------------------------|--|
| where $\tilde{\kappa}_1^{inv,avg}$ | present value of average annual investment costs for one year of utilisation |
| i | real discount rate |
| B_0 | initial book value of a given asset |
| B_1 | book value of a given asset at end of first year |
| l | lifetime |
| yl | set of years of the economic lifetime of a given asset |

For one year of operation within the planning horizon, the present value at time of investment of average annual investment costs is equivalent to the present value of

effective investment costs (vide Figure 3.7). As it is found, the present value of average annual investment costs equals the initial book value multiplied by the reciprocal of the present value interest factor of an annuity due over the lifetime of the asset (vide Van Horne & Wachowicz 2004). Thus, by applying the annuity method for depreciation in the submodel MOWIKA, average annual investment costs would become equivalent to costs in MESTAS, where the above factor is used to calculate annualised investment costs (vide equations (3-44), (3-45) and (3-46)).

In order to implement the annuity method for depreciation in MOWIKA, equation (3-60) is substituted for equation (3-15):

$$\tilde{\kappa}_{pi}^{sal} = \frac{1}{(1+i)^{y^s - y^{base}}} \cdot \frac{1}{(1+i)^{l_{pi}^{rel}}} \cdot \dots \quad (3-60)$$

$$\kappa_{pi}^{inv} \cdot \left\{ (1+i)^{l_{pi}^{rel}} - \frac{i \cdot (1+i)^{l_{pi}}}{(1+i)^{l_{pi}} - 1} \cdot \frac{(1+i)^{l_{pi}^{rel}} - 1}{i} \right\}$$

| | |
|-----------------------------------|--|
| where $\tilde{\kappa}_{pi}^{sal}$ | present value of salvage value of new build power plant pi |
| i | real discount rate |
| y^{base} | base year |
| l_{pi}^{rel} | relevant lifetime of new build power plant pi |
| κ_{pi}^{inv} | investment costs of new build power plant pi |
| l_{pi} | lifetime of new build power plant pi |
| ys | set of simulation years |
| pi | set of new build power plants available for installation in simulation year ys |

It calculates the salvage value at the end of the relevant lifetime according to equation (3-58). The salvage value is then discounted to the simulation year ys in which the power plant is installed and further discounted to the base year y^{base} .

While the further mitigation of the end effect of generation expansion in MOWIKA is an important improvement in itself, the annuity method for depreciation particularly establishes consistency in the modelling of costs in MOWIKA and MESTAS. Due to the equivalence to the annualised costs approach, MOWIKA and IMAKUS thus also become suitable for one-year planning horizons. The annuity method for depreciation is therefore applied in Section 4.4.2, where IMAKUS is used for snapshot simu-

lations of individual years. Moreover, the annuity method for depreciation is used as the default method to calculate the salvage value throughout Chapters 5 and 6.

3.3.2 Optimisation of initial and final storage levels

As described in Section 3.2.2, the existing submodel MESTAS allows to fix storage levels at the beginning of the simulation year to any value between zero and the respective storage capacity. However, the model does not include a constraint for the storage level at the end of the simulation year. If the initial storage level is set to a value greater than zero, storage units will benefit from discharging the extra energy during the year and will be completely emptied until the last time step. Thus, the annual energy balance of storages is skewed.

As simulation years can only be optimised individually in MESTAS, the introduction of a cyclic constraint is essential to maintain the annual energy balance in each individual year. Cyclic constraints are commonly used in storage modelling (e. g. Schaber 2013, Scholz 2012). In order to avoid the imbalance of energy charged and discharged, the final storage level of a given storage is fixed at the same value as the initial storage level. By this means, the total energy discharged over one year is required to equal the total energy charged over the year minus storage losses.

A cyclic constraint can be easily implemented in MESTAS by complementing equations (3-24), (3-25), (3-26) and (3-27) by the following two equations:

$$S_{se,8760} = \sigma_{se} \cdot C_{se}^{storage} \quad (3-61)$$

$$S_{sn,8760} = \sigma_{sn} \cdot C_{sn}^{storage} \quad (3-62)$$

| | |
|---------------------|---|
| where $S_{se,8760}$ | storage level of existing storage se in last time step |
| $S_{sn,8760}$ | storage level of new build storage sn in last time step |
| σ_{se} | relative storage level of existing storage se at the beginning of the simulation year |
| σ_{sn} | relative storage level of new build storage sn at the beginning of the simulation year |
| $C_{se}^{storage}$ | storage capacity of existing storage se |
| $C_{sn}^{storage}$ | storage capacity of new build storage sn |

| | |
|------|---------------------------|
| se | set of existing storages |
| sn | set of new build storages |

If the above equations are included, initial storage levels greater than zero can also be considered correctly in MESTAS. The impact of different values of exogenously fixed initial storage levels on storage profitability is analysed in Section 4.7.5. However, it should be noted that in case of new build storages, final and initial storage levels of subsequent simulation years have to be assumed completely independent: With storage capacity potentially increasing from one year to another, the same relative storage level still leads to different storage levels in absolute terms.

By exogenously fixing initial storage levels to arbitrary values, storage dispatch is however constrained unnecessarily, which inevitably leads to a suboptimal solution to the optimisation problem. First and foremost, the approach neglects the fact that time series of generation and demand possess seasonal characteristics (vide Section 5.3.1). For instance, electricity generation from wind power usually reaches its peak during winter season in Germany (Kaltschmitt *et al.* 2014). Therefore, particularly in case of long-duration storages, neither 0 % nor 100% are expected to be an optimal choice for the storage level at the turn of the year.

Instead, the model should allow for the optimisation of initial storage levels, so that storages can fully capitalise on the seasonality of renewable electricity generation. For this purpose, equations (3-26) and (3-27) are reformulated as follows:

$$S_{se,1} = (1 - \lambda_{se}) \cdot S_{se,8760} + \dots - \frac{1}{\eta_{se}^{discharge}} \cdot P_{se,1}^{discharge} + \eta_{se}^{charge} \cdot P_{se,1}^{charge} \quad (3-63)$$

$$S_{sn,1} = (1 - \lambda_{sn}) \cdot S_{sn,8760} + \dots - \frac{1}{\eta_{sn}^{discharge}} \cdot P_{sn,1}^{discharge} + \eta_{sn}^{charge} \cdot P_{sn,1}^{charge} \quad (3-64)$$

| | |
|------------------|---|
| where $S_{se,1}$ | storage level of existing storage se in first time step |
| $S_{sn,1}$ | storage level of new build storage sn in first time step |
| λ_{se} | hourly rate of self-discharge of existing storage se |
| λ_{sn} | hourly rate of self-discharge of new build storage sn |

| | |
|-------------------------|---|
| $S_{se,8760}$ | storage level of existing storage se in last time step |
| $S_{sn,8760}$ | storage level of new build storage sn in last time step |
| η_{se}^{charge} | charging efficiency of existing storage se |
| η_{sn}^{charge} | charging efficiency of new build storage sn |
| $P_{se,1}^{charge}$ | mean value of charging power of existing storage se in first time step |
| $P_{sn,1}^{charge}$ | mean value of charging power of new build storage sn in first time step |
| $\eta_{se}^{discharge}$ | discharging efficiency of existing storage se |
| $\eta_{sn}^{discharge}$ | discharging efficiency of new build storage sn |
| $P_{se,1}^{discharge}$ | mean value of discharging power of existing storage se in first time step |
| $P_{sn,1}^{discharge}$ | mean value of discharging power of new build storage sn in first time step |
| se | set of existing storages |
| sn | set of new build storages |

By this means, the storage level again becomes subject to a cyclic constraint: The storage level in the first hour of the simulation year is dependent on the storage level in the last hour of the same simulation year. The latter one, representing both the final and initial storage level, is chosen by the model with respect to the minimum cost solution. The optimal values for relative initial storage levels of existing and new build storages can be calculated after the optimisation problem is solved:

$$\sigma_{se} = \frac{S_{se,8760}}{C_{se}^{storage}} \quad (3-65)$$

$$\sigma_{sn} = \frac{S_{sn,8760}}{C_{sn}^{storage}} \quad (3-66)$$

where σ_{se} relative storage level of existing storage
 se at the beginning of the simulation year
 σ_{sn} relative storage level of new build storage
 sn at the beginning of the simulation year

| | |
|--------------------|--|
| $S_{se,8760}$ | storage level of existing storage se in last time step |
| $S_{sn,8760}$ | storage level of new build storage sn in last time step |
| $c_{se}^{storage}$ | storage capacity of existing storage se |
| $C_{sn}^{storage}$ | storage capacity of new build storage sn |
| se | set of existing storages |
| sn | set of new build storages |

Whereas the complementary implementation of equations (3-61) and (3-62) ensures that the annual energy balance is maintained if exogenously fixed storage levels are used in MESTAS, the alternative reformulation of energy balance equations (3-63) and (3-64) also allows for the optimisation of initial and final storage levels. Again, it should be noted that for both methods final and initial storage levels of subsequent simulation years have to be assumed completely independent.

In Section 4.7.5, the impact of storage level optimisation on storage profitability is analysed. Results on optimal initial storage levels are contrasted with exogenously fixed storage levels. The endogenous optimisation of initial and final storage levels in MESTAS is used as the default method throughout Chapters 5 and 6.

3.3.3 Constraining emissions over the whole planning horizon

While carbon emissions can be implicitly limited in MOWIKA and MESTAS by fixing an exogenous carbon price, the two models alternatively allow to directly constrain emissions by means of annual targets. For this purpose, the pathway of annual emissions reduction has to be defined ex ante for the whole planning horizon. Instead of explicitly limiting annual emissions, the total amount of emissions permitted over the whole planning horizon could be constrained. Thus, the decision when to reduce emissions would be left to the optimisation model.

Due to the time value of money, the model will tend to delay emissions abatement to later years if only the total amount of emissions is constrained. While this approach allows to further minimise whole-systems costs, it should be noted that delaying efforts to reduce emissions in the near future is very likely to hinder the mitigation of climate change, i. e. to prevent a temperature increase of more than 2 °C relative to pre-industrial levels (Edenhofer *et al.* 2014).

In MOWIKA, a constraint on the total amount of emissions can be implemented directly, as the whole planning horizon is optimised intertemporally. For this purpose, equation (3-8) is reformulated to sum up the annual amounts of carbon emissions produced by existing and new build power plants over all simulation years ys . This sum is limited to the exogenously defined maximum amount of emissions permitted over the whole planning horizon:

$$\sum_{ys} \left\{ \sum_{di} \left(\sum_{pe} \varepsilon_{pe}^{electr} \cdot P_{pe,ys,di}^{gen} \cdot \delta_{di} + \dots \right. \right. \quad (3-67)$$

$$\left. \left. \sum_{pn} \varepsilon_{pn}^{electr} \cdot P_{pn,ys,di}^{gen} \cdot \delta_{di} \right) \right\} \leq e^{max,total}$$

| | |
|-----------------------------------|--|
| where $\varepsilon_{pe}^{electr}$ | emissions of existing power plant pe per unit of electricity generated |
| $P_{pe,ys,di}^{gen}$ | mean value of generating power of existing power plant pe in discretisation interval di in simulation year ys |
| δ_{di} | duration of discretisation interval di in hours |
| $\varepsilon_{pn}^{electr}$ | emissions of new build power plant pn per unit of electricity generated |
| $P_{pn,ys,di}^{gen}$ | mean value of generating power of new build power plant pn in discretisation interval di in simulation year ys |
| $e^{max,total}$ | maximum amount of emissions permitted over the whole planning horizon |
| ys | set of simulation years |
| pe | set of existing power plants operational in simulation year ys |
| pn | set of new build power plants operational in simulation year ys |
| di | set of discretisation intervals in simulation year ys |

In MESTAS, the amount of emissions cannot be constrained directly for the whole planning horizon, as each simulation year is optimised individually. If MESTAS is

however used within the iterative process of the superordinate model IMAKUS, the annual amounts of emissions resulting from MOWIKA for the individual years of the planning horizon can be used as the respective annual maximum amounts of emissions e^{max} in equation (3-37) in MESTAS.

Thus, it is also possible to constrain emissions over the whole planning horizon in IMAKUS: The optimal pathway of annual emissions reduction is determined intertemporally in MOWIKA (already considering the impact of storages by means of smoothed annual load duration curves). For each simulation year in MESTAS, the annual amount of emissions is then limited accordingly.

Analogously to the systematic underestimation of variable costs of power plants in MOWIKA (vide Section 3.2.4), the amount of emissions is generally overestimated in MOWIKA, as the use of discretised annual load duration curves causes a systematic shift of energy from the higher – usually less carbon-intensive – to the lower ranking technology in the merit order. Thus, the marginal abatement measure that was necessary in MOWIKA might not be needed in MESTAS to keep to the same maximum amount of emissions.

The carbon emissions price is specified according to results from MESTAS, as the planning of dispatch in hourly resolution allows to determine emissions more accurately. Moreover, annual values of the carbon emissions price can be obtained for the individual simulation years in MESTAS, whereas only a single price results from the overall constraint in MOWIKA (i. e. the costs of the most expensive abatement measure of the whole planning horizon).

In Section 4.6, the described method of constraining emissions over the whole planning horizon is compared with the application of annual emissions targets. In order to enable the model to choose the cost-optimal pathway of annual emissions reduction, emissions are by default constrained over the whole planning horizon in all scenarios presented in Chapters 5 and 6.

4 Qualitative analysis of the influence of methodology and assumptions on modelling results

As the review of studies in Chapter 2 showed, the broad range of results on energy storage demand can only be better understood by further analysing the influence of methodology, assumptions and input parameters on modelling results. In this chapter, it is discussed how assumptions and the choice of methodological approaches affect modelling results on energy storage demand, i. e., in particular, whether they lead to an increase or decrease of storage capacity expansion. For this purpose, an extensive (yet not exhaustive) selection of approaches and assumptions that are commonly encountered in energy systems modelling is analysed qualitatively. Wherever possible, this qualitative analysis is complemented and underpinned by comparing results obtained for different approaches and assumptions with the whole-systems cost minimisation model IMAKUS.

4.1 Resolving space

With regard to the modelling of power systems, the choice of spatial resolution is closely related to the question of how the interconnection of different regions is modelled. Starting from the extreme case of a single-node (or copper plate) model, i. e. modelling the whole geographic scope as a single region where all generation and demand is connected, the considered region can be split up into any number of sub-regions or nodes. Whereas transmission constraints are neglected in case of a single-node model, the transmission of power has to be modelled explicitly if more than one region is considered.

The single-node approach is commonly employed in the modelling of power systems (vide Section 2.1). As the modelling of several interconnected regions increases the computational burden of the optimisation problem, spatial resolution is often abandoned in favour of higher temporal resolution, longer planning horizons or, for instance, a stronger focus on storage modelling.

However, several multi-region models exist that also allow for the optimisation of storage capacity expansion (e. g. Scholz 2012, Strbac *et al.* 2012, Short *et al.* 2011, Schaber 2013). In these models, the transmission of power between different regions is modelled as a simple transport problem, i. e. power flow is only constrained by transmission capacities. While a better approximation of physical power flows can be achieved by applying the DC power flow method (Ahlhaus & Stursberg 2013, Schaber 2013), this method is mostly used in unit commitment and economic dispatch models that do not optimise capacity expansion (e. g. Hand *et al.* 2012, EPRI 2012).

Apart from redispatch of conventional generation and curtailment of RES and CHP generation, the main options to remedy any imbalances of generation and demand in the power system are either spatial or temporal balancing. Which combination of balancing measures is cost-optimal can only be determined by simultaneously optimising the expansion and operation of storage and transmission capacities.

If a single-node model like IMAKUS is used to determine energy storage demand, it is assumed that the potential of spatial balancing of generation and demand can be fully exploited. However, as spatial balancing will always be restricted in a realistic transmission system, the actual potential of temporal balancing of generation and demand is, in any case, underestimated by such models. Therefore, the obtained results represent a lower estimate of storage capacity that is economically feasible in spite of an ideal transmission system (Kuhn & Kühne 2011).

On the contrary, if transmission constraints are modelled, the level of storage capacity expansion will come closer to the actual energy storage demand. Furthermore, multi-region models allow to identify the optimal location of storages, also taking into account possible geographic restrictions of certain technologies.

By simultaneously optimising the expansion of storage capacities as well as transmission and distribution capacities with a multi-region model of the British power system, Strbac *et al.* (2012) show that storage capacity expansion can generate savings both on the transmission and the distribution network level. Thus, storage is not only an option to remedy any remaining imbalances when further grid expansion is not economically feasible but also represents a competitive alternative to spatial balancing. These results disprove accounts that spatial and temporal balancing are mutually exclusive measures, each suitable to resolve only a certain type of imbalance (Agora

Energiewende 2014), and that storages are not an adequate and economically feasible option to reduce the need for grid expansion (dena 2010).

4.2 Resolving time

4.2.1 Representative time slices vs. annual time series

According to Pfenninger *et al.* (2014), approaches to resolve time in energy systems models can generally be classified as either integral, i. e. using load duration curves, semi-dynamic, i. e. using representative time slices, or fully-dynamic, i. e. using chronological time series of generation and demand. Although integral approaches have been occasionally applied in models that optimise storage expansion and operation (e. g. EPRI 2012), this class of approaches is not further discussed in this section, as it completely neglects the interdependence of time steps. It is thus regarded as being unsuitable for storage modelling.

Instead, this section focuses on a comparison of the representative time slices and the annual time series approaches. While, naturally, results based on chronological time series in high temporal resolution will best approximate reality, it is also clear that, depending on other factors like an extended planning horizon or requirements for high spatial resolution, the computational burden of the optimisation problem might not be manageable.

Therefore, representative time slices approaches are quite commonly used in energy systems modelling to reduce model size (e. g. Short *et al.* 2011, Schaber 2013, Nahmmacher *et al.* 2014). Instead of simply reducing the temporal resolution of a given annual time series (vide Section 4.2.2), these approaches consider only a small number of time slices which are identified to be representative of the whole year. Each time slice is weighted according to the number of periods per year it represents.

Despite the common principle, approaches may differ in terms of number and length of time slices, number of consecutive time slices as well as with regard to the methodology of selecting suitable time slices. In Short *et al.* (2011), only 17 time slices are used to represent the whole year: four diurnal time slices for each season, complemented by an additional time slice that characterises summer peak load. A clustering algorithm method is presented by Nahmmacher *et al.* (2014) to determine representative time slices. It is furthermore proposed that a number of six representative days in three-hourly resolution, i. e. 48 time slices, approximates the whole year sufficiently well. By contrast, Schaber (2013) uses exhaustive search to identify six representative weeks in hourly resolution, resulting in 1008 time slices per year.

If a representative time slices approach is used, special care has to be taken in storage modelling to correctly account for storage between time slices of different modelled periods. Energy can be easily shifted between the consecutive time slices of a given contiguous period (e. g. a representative day or week) by means of an ordinary energy balance equation. However, if inter-day, inter-week or inter-seasonal storage is to be considered, any energy that is stored at the end of the modelled period as well as at the end of the non-modelled periods it represents has to be carried over to the next modelled period.

Nahmmacher *et al.* (2014) justify the use of representative days instead of weeks, referring to the lower computational burden and claiming that intra-day storage usually is economically more attractive than inter-day storage. This is, however, contradicted by several studies identifying considerable demand for inter-day and even seasonal storage based on annual time series approaches (e. g. Kuhn 2012, Kuhn *et al.* 2012, Scholz 2012, Strbac *et al.* 2012). By contrast, Schaber (2013) uses representative weeks and presents a method to correctly account for storage between the different weeks, thus allowing to consider seasonal storage with a representative time slices approach.

Provided that storage is modelled as proposed by Schaber (2013), the representative time slices approach would yield the same results on storage expansion and operation as the modelling of the whole year, if the selected time slices were fully representative of the remaining, non-modelled periods. However, this ideal case is never reached for real time series of generation and demand: An inherent problem of reducing annual time series to a small number of selected time slices is that correlations and “system-defining extreme points” are missed (Pfenninger *et al.* 2014).

Thus, although an adequate method to model storage between representative periods is at hand, the accuracy of representative time slices approaches is still limited. The limited representativeness of time slices has to be compensated for by increasing the overall number of time slices as well as the number of consecutive time slices as far as possible. By using longer periods of consecutive time slices (e. g. weeks instead of days), longer-term variations of generation and demand can be explicitly considered in storage planning.

Results on storage demand obtained from representative time slices approaches will consequently differ from results that are based on annual time series, particularly with regard to storage technologies whose storage duration exceeds the length of the modelled periods of consecutive time slices. As representative time slices can either over- or underestimate the variations of generation and demand time series during non-modelled periods, the question whether storage demand will be over- or underestimated by such an approach cannot be answered in general terms.

4.2.2 Hourly resolution of time series

While in the past a coarse temporal resolution was usually sufficient to model power systems that were predominantly based on conventional electricity generation, the increased shares of RES in future power systems necessitate time series in higher resolution in order to comprehensively capture the variability of renewable electricity generation (Pfenninger *et al.* 2014). If the employed resolution is too coarse, time series will not fully reflect the demand for flexibility, thus underestimating the need for temporal and spatial balancing of generation and demand as well as for increased flexibility of conventional power plants.

Whereas time slices approaches often aggregate several hours into one time slice in order to reduce model size (vide Section 4.2.1), models that are based on annual time series usually emphasise temporal detail and thus commonly use time series in at least hourly resolution. For instance, Kuhn (2012), Scholz (2012) and Strbac *et al.* (2012) optimise storage capacity expansion based on time series in hourly resolution. Other studies using mixed methods to analyse storage demand are also often based on time series in hourly resolution (e. g. Adamek *et al.* 2012, Klaus *et al.* 2010, Agora Energiewende 2014).

Due to the increased computational burden, higher resolutions of time series are less commonly employed in storage expansion planning and in energy systems modelling in general. One example is the unit commitment model PLEXOS, which supports time series in resolutions from hourly up to five-minute scale and which was used in EPRI (2012) to optimally allocate storage capacity between providing ancillary services and conducting energy arbitrage.

While the resolution of annual time series is also limited by computational power, time series of generation and demand are often not available in higher resolutions than hourly resolution (vide Janker 2015). However, by using average hourly values, intra-hourly peaks and gradients of electrical load and renewable generation are omitted. The demand for flexibility is therefore neglected to a certain extent by models like IMAKUS that are based on time series in hourly resolution.

If storage demand is determined based on time series in hourly resolution, the obtained results represent a lower estimate of storage capacity. By contrast, a higher temporal resolution would increase the demand for storage and could also reveal the potential of typical short-duration storage technologies like batteries, which are characterised by a high ratio of energy-related costs to power-related costs. If hourly resolution is used, batteries are often not considered at all (e. g. Kuhn 2012, Kuhn *et al.* 2012) or – due to short-term variability of time series being neglected – prove to be less attractive than other storage technologies (e. g. Strbac *et al.* 2012).

4.3 System boundaries

4.3.1 Geographic scope

One of the main challenges of energy systems modelling is to define system boundaries as narrowly as possible to keep the computational burden manageable and as widely as necessary to include all interdependencies that are relevant to the investigated problem. As to the geographic scope of energy systems models and, particularly, power systems models, the main question is whether the investigated area can be assumed isolated from other geographical areas or – if areas are interconnected physically and on the market level – how to account for the energy exchange between the investigated area and other regions. For a general discussion of the geographic scope of energy systems models, vide Mai *et al.* (2013).

As a large number of studies are concerned with the future development of power supply in a certain country, geographic scope is often based on political borders. In other cases, the geographic scope corresponds to the area which is covered by a certain transmission system operator (TSO) (e. g. EPRI 2012). However, power systems that are defined in this manner often cannot be assumed isolated but usually are part of a larger, interconnected system, like, for instance, the synchronous grid of Continental Europe.

Extending the geographic scope to regions that lie outside the area of interest but are however relevant to the investigation may be a viable option if regions can be aggregated. However, an extension of geographic scope often involves the necessity for spatial resolution, thus increasing the computational burden of the investigated problem (vide Section 4.1). In Scholz (2012), Schaber (2013) and Agora Energiewende (2014) different approaches are employed to combine a broad geographic scope such as the European power system with multi-region modelling. This is realised by splitting up the problem, at the expense of temporal resolution or by abandoning endogenous capacity expansion. Apart from limits of computational power, the availability of data might also hinder the extension of geographic scope.

Three general methods can be identified that deal with the incongruity of the investigated geographic scope and the actual extent of power systems: Several studies simply neglect any interconnections between the investigated country and its neighbouring regions (e. g. Adamek *et al.* 2012). Other models use generalised approaches to account for energy exchange, for instance, by allowing energy export at an exogenously fixed price (e. g. Kuhn 2012, Kuhn *et al.* 2012) or by exogenously fixing the annual amount and schedule of energy exchange (e. g. Short *et al.* 2011). Alternatively, interconnections between the investigated country and its neighbouring regions are explicitly modelled (e. g. EPRI 2012, Strbac *et al.* 2012). In order to keep

the computational burden at an acceptable level, the model may include only selected countries or aggregated regions modelled in less detail.

Obviously, the decision on which method is used to model energy exchange also affects results on storage demand: With regard to utilising surplus generation from RES and CHP, the export to other regions represents a competing option to the integration of surplus into the power system through storage. Furthermore, instead of charging storages during times of low demand, base-load generation could also be exported if revenues exceed the benefits of storage. On the other hand, any cheap electricity that is imported during peaking hours could not only substitute conventional generation but also the discharging of storages.

Thus, if interconnections between the investigated country and its neighbouring regions are completely neglected, results on storage demand will always represent an upper estimate of storage capacity that is economically feasible without competition from energy exchange. Kuhn *et al.* (2012) attempted to roughly estimate the impact of electricity export on storage demand with the model IMAKUS.

While the geographic scope of the model IMAKUS is restricted to Germany and energy exchange is, by default, neglected, export can be optionally considered by allowing electricity to be sold at an exogenously fixed, constant price. In this case, export is either unconstrained or assumed to be constrained by a certain maximum capacity. As already mentioned in Section 3.1, this optional approach is described by Kuhn (2012). It is however not considered to be part of the functionality of IMAKUS within the scope of this thesis. As Kuhn (2012) maintains that, regarding the impact on storage, importing electricity from neighbouring countries is equivalent to adding cheap generation capacity to the domestic power plant portfolio, only export is included as a competing option to storage.

Results in Kuhn *et al.* (2012) illustrate that, depending on the assumed export revenues, export can significantly reduce storage demand in Germany compared to the base scenario, where energy exchange with neighbouring countries is neglected. It is shown that, above all, the possibility to export surplus generation represents an alternative to seasonal storage and, therefore, especially reduces the demand for hydrogen storage: Under the optimistic scenario of unconstrained export capacity and export revenues of 25 €/MWh, total installed storage capacity in 2050 is reduced by 52 % and installed hydrogen storage capacity is reduced by 60 % compared to the base scenario. In this scenario, the assumed share of electricity generation from RES amounts to 80 % in 2050.

4.3.2 Sectoral scope

The system boundaries of an energy systems model are also defined with regard to the sectoral scope of the model. However, there are several approaches to subdivide energy systems along sectoral boundaries which are not necessarily consistent but nevertheless often used side by side (e. g. Mai *et al.* 2013, Agora Energiewende 2014, Zucker *et al.* 2013): While the transport sector is a typical end-use sector comprising any form of energy that is associated with transportation (e. g. mechanical, electrical, heating, cooling), the definition of the heating sector is based on the end-use demand for a certain form of energy (usually in buildings). In both cases, sectors are defined irrespective of the form of final energy (e. g. electricity, natural gas, district heating) that is actually used to supply the demand.

By contrast, the power sector is defined based on the demand for a certain form of final energy, i. e. electricity. This obviously leads to overlaps: For instance, electricity is used as an energy carrier in the transport sector (e. g. railway transportation, electric vehicles) as well as in the heating sector (e. g. storage heating, heat pumps).

In its narrow sense, a power systems model is restricted to the power sector. Thus, it commonly considers an exogenously defined electricity demand that comprises the demand for electrical energy in all end-use sectors across the considered geographic scope (e. g. Adamek *et al.* 2012, EPRI 2012). Furthermore, only electricity generation is modelled endogenously.

However, several power systems models also include partial representations of other sectors like transport or heating, for instance, by endogenously modelling the charging of electric vehicles to satisfy mobility requirements or the operation of electric heating systems to cover a certain share of heat demand (e. g. Strbac *et al.* 2012, Short *et al.* 2011). Analogously, the supply side may be extended to other sectors, for instance, by endogenously modelling the cogeneration of heat and power in CHP plants (e. g. Scholz 2012, Agora Energiewende 2014).

As pointed out in Agora Energiewende (2014), the coupling of the power sector and other sectors holds considerable potential to provide the flexibility that is needed to balance generation and demand in power systems with high shares of RES: Flexible loads like electric vehicles and electric heating systems as well as the flexible production of hydrogen or methane compete with energy storage for the integration of surplus generation. Only by endogenously modelling these options, is it possible to assess their impact on storage demand in the power system.

The model IMAKUS, as it is described in Chapter 3, is clearly restricted to the power sector. If such a model is used to determine storage demand in the power system, the obtained results represent an upper estimate of storage capacity that is economically feasible without competition from flexible options in the transport and heating sec-

tors or from power-to-gas applications. However, the model IMAKUS has been extended to also account for some of these flexible options. While these extensions are not considered to be part of the functionality of IMAKUS in this thesis (vide Section 3.1), results from corresponding analyses are reported below to allow for a rough estimate of the impact of sectoral scope on storage demand.

In Kuhn *et al.* (2012), IMAKUS is extended to also include partial representations of the transport and heating sectors. Results show, for instance, that the optimised charging of almost 30 million electric vehicles has a significant impact on the economic feasibility of short- and medium-duration storage technologies in Germany, whereas demand for long-duration storage is hardly affected. Compared to the base scenario – where the charging energy of vehicles is assumed to be part of the exogenously defined electricity demand –, total installed storage capacity in 2050 is reduced by 23 % and installed AA-CAES storage capacity is reduced by 78 % if a fully developed charging infrastructure is assumed. In this scenario, the assumed share of electricity generation from RES amounts to 80 % in 2050.

In a further study, Heilek *et al.* (2016), IMAKUS is extended to the hydrogen sector. Instead of endogenously modelling the hydrogen market, the sale of hydrogen is allowed at an exogenously fixed and constant price. Thus, hydrogen which is electrolytically produced can be optimally allocated between either storage and subsequent generation of electricity or an alternative sale to other areas of application (not considering costs for infrastructure and transport). Results show that the level of hydrogen production for the market strongly depends on the assumed market value. Under a scenario with renewable generation well exceeding demand in 2050, the sale of hydrogen to other areas of application becomes a viable alternative to storage and electricity generation starting from 20 €/MWh_{H₂} and completely replaces storage and electricity generation above 40 €/MWh_{H₂}.

Heilek (2015) presents the extension of the submodel MESTAS to a full model of the power and heating sectors, allowing to simultaneously optimise power and heat generation for individual simulation years. The model considers an exogenously defined heat demand and optimises the expansion and operation of conventional heating systems as well as CHP, electric heating systems and thermal storage in buildings and district heating networks. Results demonstrate that the coupling of sectors offers considerable potential for cost savings and reduced storage demand in the power system: Assuming a share of RES of 86 % in 2050, the demand for PSP, AA-CAES and hydrogen storage amounts to a total installed storage capacity of just over 5 TWh if electric heating systems are not available. By contrast, only 40 GWh of additional PSP storage capacity is needed if electric heating systems are considered.

4.4 Foresight and planning horizons

4.4.1 Planning with perfect foresight

Due to the long-term character of investments in energy systems, the optimality of investment decisions significantly depends on foresight. According to Mai *et al.* (2013), the classification of energy systems models in terms of foresight is based on the question of “how much ‘knowledge’ of the future a model has when it makes decisions”, i. e. how far into the future its knowledge extends. This knowledge may include the annual amounts or hourly values of electricity demand and renewable generation, the development of fuel costs, the decommissioning of power plants, etc.

The two main categories of models identified by Mai *et al.* (2013) are, on the one hand, intertemporal approaches, where the energy systems model has perfect foresight over the whole planning horizon, and, on the other hand, myopic or short-sighted models, where the planning horizon is split up into several shorter periods for which, again, perfect foresight is assumed. While it is clear that results obtained from a myopic model will usually fall short of the optimal solution determined with an intertemporal model, it is nevertheless difficult to estimate the general impact on specific issues, like e. g. storage capacity expansion.

As described in Chapter 3, both methods are used in the model IMAKUS: Whereas the submodel MOWIKA optimises generation capacity expansion intertemporally across the whole planning horizon of several decades, a myopic approach is used in MESTAS, individually optimising storage capacity expansion for each year of the considered planning horizon. Due to the iterative coupling of submodels within the superordinate model IMAKUS, the otherwise limited foresight in MESTAS is at least extended to information obtained from MOWIKA. By using the intertemporally optimised power plant portfolio as an input, the submodel MESTAS implicitly gains knowledge on the whole planning horizon, giving it an advantage over genuinely myopic approaches.

A special case of the myopic approach is the optimisation of snapshot years, where the aim of determining the least-cost pathway over a planning horizon of several decades is abandoned and, instead, only a number of selected years along that pathway or merely the final year is considered (with foresight being limited to the respective snapshot year). As this approach is widely used in energy systems modelling (e. g. Adamek *et al.* 2012, Scholz 2012, Strbac *et al.* 2012, Agora Energiewende 2014), a detailed comparison with the intertemporal approach is presented in Section 4.4.2.

Although not commonly used in capacity expansion planning, the myopic approach can, in principle, also be employed on a smaller time scale to further split up a one-year planning horizon into periods of e. g. 12, 24 or 72 hours. In this case, periods are

often defined to be partially overlapping, resulting in a continuous progress of foresight referred to as “rolling horizon”. While this method is frequently used in unit commitment modelling to keep the computational burden of mixed-integer problems manageable (Palmintier & Webster 2011), it is also a common approach to account for limited forecast horizons and uncertainty of renewable electricity feed-in (e. g. Klaus *et al.* 2010).

Whereas a rolling horizon approach better approximates reality and, thus, is especially suitable for models with an operational focus, the assumption of perfect foresight over the whole year is more appropriate for planning problems, like e. g. capacity expansion planning. In these cases, it is usually the aim to determine the optimal system design from a social planner’s perspective (Pfenninger *et al.* 2014), which is supported by allowing the model to act strategically over the whole planning horizon.

With regard to storage demand, the assumption of perfect foresight over a one-year planning horizon (as e. g. in MESTAS) leads to an upper estimate of storage capacity that is economically feasible. This is particularly true for long-duration storage technologies like hydrogen, which typically balance long-term and seasonal fluctuations and, thus, benefit from extended foresight. By contrast, as there is less uncertainty about demand and renewable feed-in within shorter time horizons, the assumption of perfect foresight over a period of only a few days is much more realistic. Therefore, overestimation of short-duration storage demand should be less significant.

4.4.2 Intertemporal approach vs. snapshot years

When planning the future development of energy systems, it is essential to consider the whole pathway from the system’s status quo to the final year of the investigated period. Generally, this holds true even for studies where merely a certain year is of interest: Not only for analyses with a short- or mid-term perspective but also in case of investigations with a long-term perspective spanning several decades, it has to be assumed that systems evolve continuously and are only seldom altered abruptly by disruptive events.

Thus, intertemporal approaches that allow to simultaneously optimise both short- and long-term decisions across the planning horizon are, in principle, the method of choice for energy systems planning. While intertemporal approaches are desirable, the computational burden of such optimisation problems can however increase dramatically for a planning horizon of several decades, especially if at the same time a high temporal and spatial resolution is required.

Therefore, several studies on the future development of power systems not only abandon the intertemporal approach but also refrain from considering the whole pathway of system development. Instead, a small number of years along that pathway or merely the final year is taken into account. For instance, the optimisation of so-called “snapshot years” is applied by Adamek *et al.* (2012), Scholz (2012), Strbac *et al.* (2012) and in Agora Energiewende (2014).

As foresight is always limited to the respective snapshot year, the power system is optimally adapted to the specific conditions of each snapshot year, while its suitability for past and future years is neglected. Furthermore, snapshot years are usually assumed to be independent of each other, i. e. new build capacities from previous snapshot years are not carried over. However, existing capacities are commonly considered if still expected to be operational in the given snapshot year.

Exemplary analysis: intertemporal approach vs. snapshot years

In order to further analyse the differences between an intertemporal approach to power systems planning and a snapshot year approach, the whole-systems cost minimisation model IMAKUS is used. While the submodel MOWIKA allows to optimise generation capacity expansion intertemporally over a planning horizon of several decades (vide Section 3.2.1), storage capacity expansion is only optimised for individual years with limited foresight in MESTAS (vide Section 3.2.2). However, due to the iterative coupling within the superordinate model IMAKUS, storage capacity expansion is at least planned in consideration of an intertemporally optimised power plant portfolio.

Besides determining the least-cost pathway for a planning horizon of several decades intertemporally, IMAKUS also offers the possibility to optimise snapshot years. In this case, the planning horizon and, consequently, foresight are limited to the considered year. In order to correctly account for costs, the annuity method for depreciation is employed in MOWIKA, which – as pointed out in Section 3.3.1 – establishes equivalence to the annualised costs approach commonly used for one-year planning horizons.

Results obtained from IMAKUS for snapshot year simulations of 2010, 2020, 2030, 2040 and 2050 are compared with results for the respective years that are obtained from the intertemporal optimisation of the whole planning horizon 2010–2050. The analysis is based on the scenario “80/minus15” defined by Kuhn *et al.* (2012). In this scenario, the assumed share of electricity generation from RES in Germany amounts to 80 % in 2050.

For reasons of consistency, the annuity method for depreciation also has to be used in the intertemporal case. Furthermore, when simulating snapshot years, generation capacity expansion cannot be constrained with regard to potential limits of annual

economic productivity, as it has to be ensured that sufficient generation capacity can be installed to satisfy demand. Therefore, generation capacity expansion is also not constrained in the intertemporal optimisation.

In contrast to Kuhn *et al.* (2012), only four basic generation technologies are assumed to be available for expansion, namely hard coal, lignite, combined cycle gas turbines (CCGT) and gas turbines. Thus, in principle, in each snapshot year the same generation portfolio can be achieved as in the intertemporal case. As new build options are usually considered to be at the state of the art in snapshot years, the technical and economic parameters of power plants vary over the period 2010–2050 according to scenario “80/minus15”. The existing power plant portfolio is considered both in the intertemporal case and in snapshot years.

Figure 4.1 illustrates the differences in generation portfolios between the intertemporal and the snapshot year approaches. Over the short-term horizon, only very small differences between generation portfolios can be observed. This is due to the fact that existing power plants still represent the largest part of installed generation capacity in 2010 and 2020, amounting to more than 95 % and almost 60 % respectively.

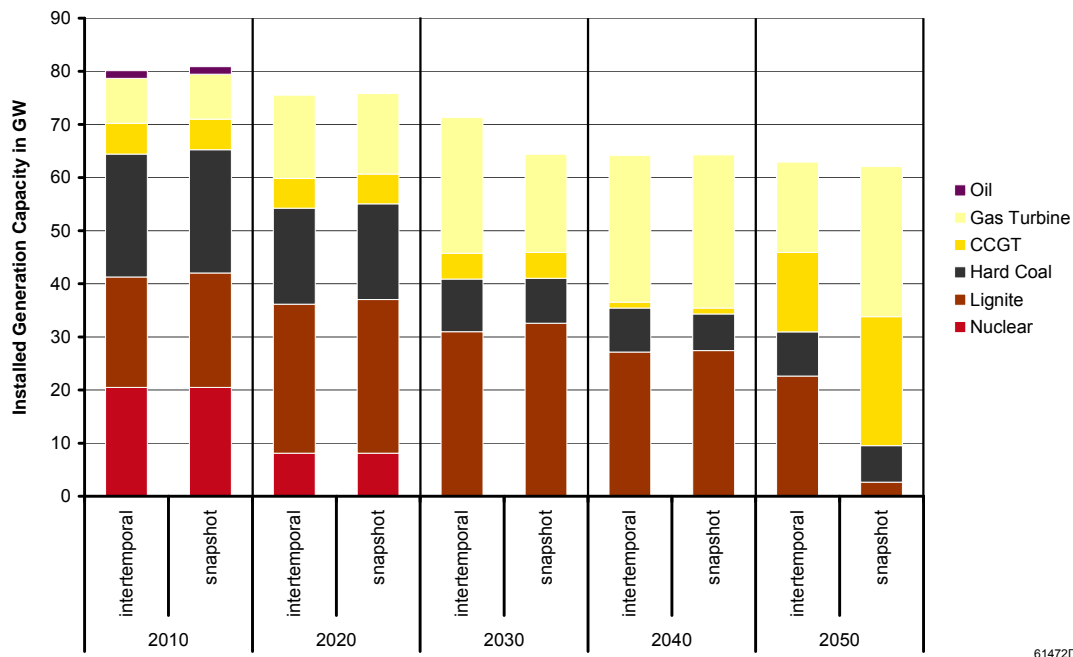


Figure 4.1: Comparison of conventional generation portfolios obtained from intertemporal optimisation and from the optimisation of snapshot years in an exemplary scenario

A significant difference is however observed for the year 2030: While in the intertemporal case surplus capacities are built up in preceding years, the considerably smaller capacity installed in the snapshot simulation corresponds to the actual firm capacity target in 2030. Apart from surplus peaking capacities, only small differences can be observed between generation portfolios in 2030 and 2040, where existing capacity amounts to less than 35 % and less than 20 % respectively.

In the considered scenario, the more crucial changes in the boundary conditions of the power system seem to take place after 2040, with the share of RES increasing from 65 % to 80 % in 2050 (Kuhn *et al.* 2012). This leads to significant differences between results from the two modelling approaches: Whereas in case of the snapshot simulation the generation portfolio can be optimally adapted to the specific boundary conditions in 2050, the generation portfolio is largely determined by power plants installed in previous years if an intertemporal approach is applied.

Due to only small differences between generation portfolios until 2040, the resulting storage portfolios also differ only slightly within this period (vide Figure 4.2).

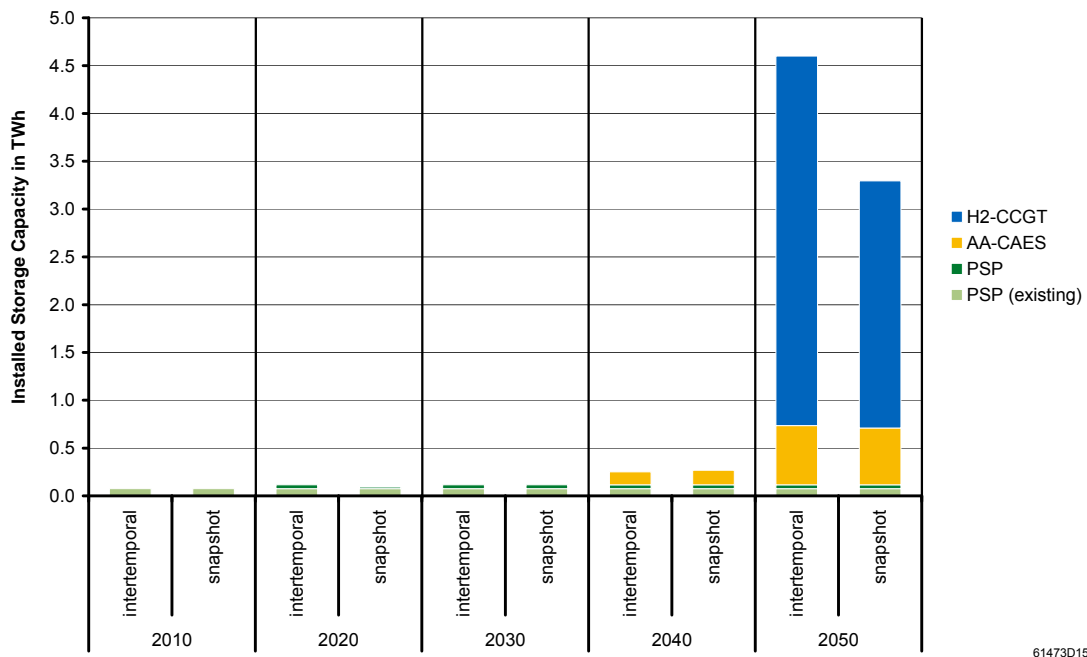


Figure 4.2: Comparison of storage portfolios obtained from intertemporal optimisation and from the optimisation of snapshot years in an exemplary scenario

By contrast, less AA-CAES storage capacity and, particularly, less hydrogen storage capacity is installed in 2050 in the snapshot simulation. At the same time, installed discharging capacities of AA-CAES and hydrogen storage are higher than in the intertemporal case (not shown).

This can be explained by the differences that are observed in the generation portfolio of 2050: Apart from new build CCGT plants, only older and inefficient coal power plants or expensive gas turbines are available in the snapshot simulation. Base-load and mid-merit capacity, i. e. non-gas turbine capacity, is roughly 12 GW smaller than in the intertemporal case. Thus, the utilisation of expensive generation during load peaks can only be avoided if sufficient discharging capacity is installed. The amount of curtailed generation is virtually the same in both cases.

While it becomes apparent that results for snapshot years can differ significantly from intertemporally obtained results (especially with regard to the long-term perspective), it is nevertheless not possible to make a general statement about the impact of the snapshot approach on storage demand.

4.5 Discounting the future

In order to correctly account for costs in energy systems models, the time value of money has to be considered, i. e. costs incurring in the future have to be weighted relative to the present. For this purpose, a discount rate is used to discount all costs to their present values in a given base year. A comprehensive overview of the concept of time value of money as well as related formulae can be found in Van Horne & Wachowicz (2004).

However, as Mai *et al.* (2013) put it, “figuring out what discount rate to use can be highly speculative” and usually depends on the context. An important axis along which models can be distinguished is the dichotomy between using a social discount rate and using a discount rate that reflects the expected rate of return of investors. While the former is usually employed to “estimate social cost and benefit” (Mai *et al.* 2013) in models that adopt a social planner’s perspective, the latter is generally higher and is mostly used in models focusing on individual investors. In order to “properly account for private-sector investment decisions” (Hand *et al.* 2012), the discount rate in such models is commonly defined as the WACC.

Another axis along which models can be differentiated is whether one single discount rate or several different discount rates are used. If the concept of a social discount rate is adopted, usually only a single discount rate is assumed. This also relates to the underlying assumption of a perfect market, which is often encountered in whole-

systems models (vide Roth 2008). More than one discount rate is usually used if investor- or technology-specific discount rates are assumed, like e. g. in Strbac *et al.* (2012). There are, however, exceptions to this rule. For instance, Hand *et al.* (2012) adopt an investor's perspective and propose the use of a WACC (to calculate annualised investment costs) alongside a social discount rate, which is employed to weight costs incurring in different years.

Moreover, discount rates can either be nominal or real rates. If a model is based on inflation-adjusted real values of costs, a real discount rate has to be employed.

By means of the above classification, the type of discount rate to be used in the model IMAKUS can be determined. To begin with, a real discount rate is required, as all costs in IMAKUS are assumed to be inflation-adjusted real values. Furthermore, a social discount rate is required: IMAKUS minimises whole-systems cost and, thus, represents a classic social planner's approach (vide Trutnevyte 2014).

In Kuhn *et al.* (2012), IMAKUS is used to analyse the German power system, assuming a real social discount rate of 3 %. While the discount rate obviously depends on the considered country, its appropriate value is also a constant subject of scientific discussion: For instance, Hand *et al.* (2012) use a real social discount rate of 3 % for the United States; Pearce & Ulph (1995) analyse approaches to determine the real social discount rate and report a credible range of 2–4 % for the United Kingdom. By contrast, Evans & Sezer (2004) estimate real social discount rates of 4.1 %, 4.6 % and 4.2 % for Germany, the United States and the United Kingdom respectively.

Exemplary analysis: variation of the discount rate

Before analysing the impact of specific values of the discount rate on generation and storage capacity expansion with IMAKUS, some general thoughts on how higher discount rates will affect investment decisions are offered. In principle, a higher discount rate results in future cash flows – i. e. usually the earnings from a given investment – being devalued more strongly compared to the expenses that incur at the time of investment. Thus, the net present value (NPV) of a given investment decreases and, consequently, the competing option of a financial investment with identical risk becomes more attractive.

Therefore, higher discount rates can generally be regarded as a disincentive to investments into new build capacity. This becomes obvious when investment costs are annualised, using, for instance, the present value interest factor of an annuity due as in MESTAS (vide Section 3.2.2): For higher discount rates, annual investment costs increase and, thus, the attractiveness of investment is reduced.

Moreover, if a high discount rate is assumed, future expenditures are comparatively cheap. Due to this fact, two general effects are expected: First, future expenditures

associated with a given investment become less important (e. g. a rise in gas prices) and, secondly, as much investments as possible will be shifted to later years.

The impact of the discount rate on generation and storage capacity expansion is further analysed with the whole-systems cost minimisation model IMAKUS. The analysis is based on the scenario “80/minus15” defined by Kuhn *et al.* (2012). In this scenario, the assumed share of electricity generation from RES in Germany amounts to 80 % in 2050.

While in Kuhn *et al.* (2012) a real social discount rate of 3 % is used, below, modelling results are presented for discount rates of 0.1 % and 7 %. These values do not necessarily represent adequate values of real social discount rates but are rather chosen to allow for the observation of significant changes in the development of generation and storage portfolios.

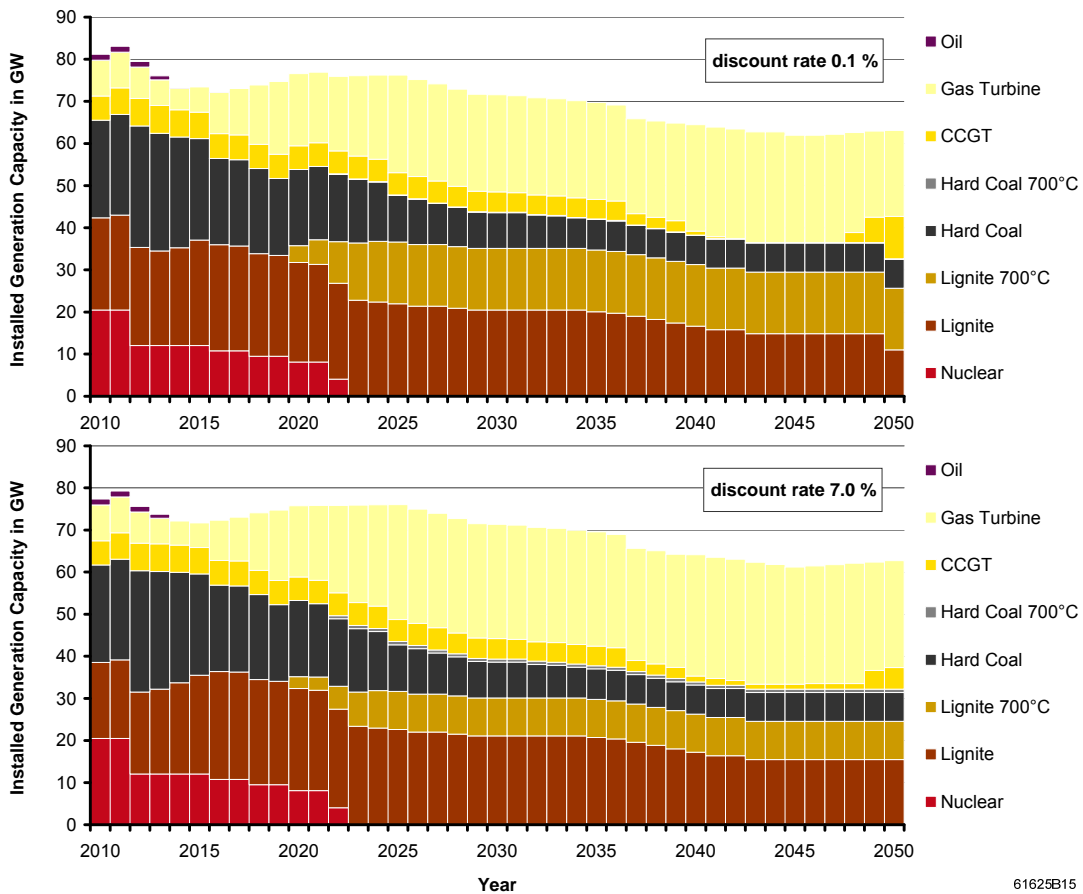


Figure 4.3: Comparison of conventional generation portfolios assuming different real social discount rates in an exemplary scenario

For a very low discount rate of 0.1 %, present and future expenditures are almost weighted equally. Therefore, already from the beginning of the period, considerable investment into coal-fired power plants is observed, as, by this means, savings in operational expenditures can be achieved across the whole planning horizon (vide Figure 4.3, top). By contrast, in case of a 7 % discount rate, future expenditures are comparatively cheap. Thus, investments tend to be shifted to later years and, although involving higher operating costs, the expansion of gas-fired power plants increases towards the end of the planning horizon (vide Figure 4.3, bottom).

As claimed above, higher discount rates generally represent a disincentive to investments into new build capacity. However, due to the requirements of security of supply, the total installed conventional generation capacity does not decrease as dramatically as expected if a higher discount rate is assumed. Differences in total installed capacity are hardly noticeable in Figure 4.3: In case of a 7 % discount rate, capacity is 660 MW smaller on average.

The negative impact of higher discount rates on investment activity is, however, still evident: The overall new build generation capacity decreases by more than 4 GW if a discount rate of 7 % is assumed. Throughout the planning horizon, the share of less capital-intensive gas-fired power plants is considerably larger than in case of a 0.1 % discount rate. This is also reflected by total non-variable costs of new build capacity, which decrease by 28 % (undiscounted) compared to the low discount rate case. The preference of less capital-intensive peaking plants is further supported towards the end of the planning horizon, as the end effect, i. e. the deformation of non-variable costs caused by the salvage value method (vide Section 3.2.1), is much more pronounced for higher discount rates.

Figure 4.4 illustrates the impact of higher discount rates on storage capacity expansion in the submodel MESTAS, where investment costs are annualised. As expected, in case of a 7 % discount rate, storage capacity expansion is delayed by two or more years as compared to the low discount rate case. However, it becomes apparent that, whereas investment into other storage technologies decreases as expected, the expansion of hydrogen storage capacity increases. This even leads to an increase of total installed storage capacity during the last years of the planning horizon.

While the share of hydrogen storage technology also increases in terms of charging and discharging capacity, the total installed charging and discharging capacities decrease as compared to the low discount rate case. Thus, all in all, a negative impact of higher discount rates on investment activity can also be observed for storage expansion. The contrarian effect on storage capacity of hydrogen storage is due to the low energy-related investment costs that are assumed for this technology. However, it should be noted that a detailed understanding of all effects observed for storage ca-

capacity expansion would require the consideration of interdependencies between storage and generation portfolios.

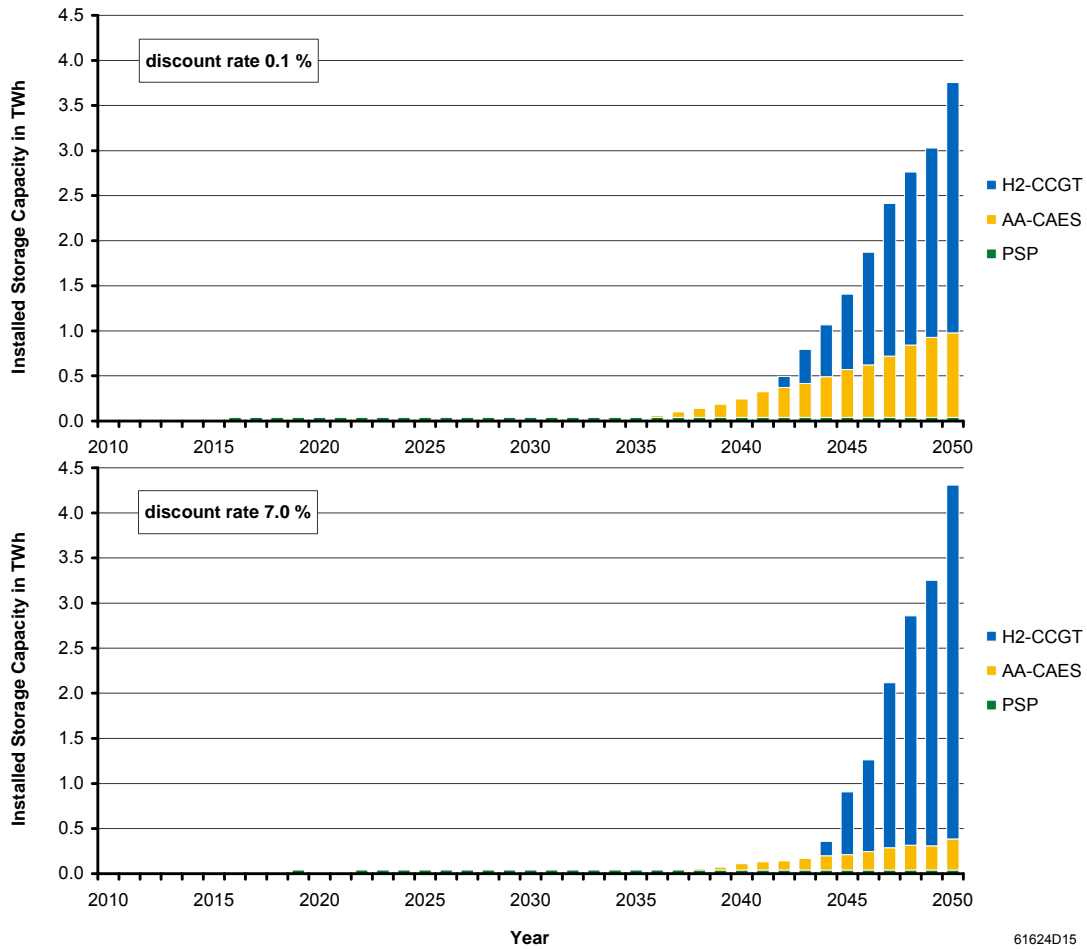


Figure 4.4: Comparison of storage capacity expansion assuming different real social discount rates in an exemplary scenario

4.6 Carbon prices vs. carbon emissions targets

In order to facilitate carbon emissions abatement, two general instruments are available (Kuhn 2012, Voß & Flinkerbusch 2013): price regulation, e. g. the implementation of a carbon tax, and quantity regulation, e. g. the implementation of a cap-and-trade scheme like the European Union emissions trading system (EU ETS) (EC 2003). Given that the costs of available abatement measures – usually represented by a marginal abatement cost (MAC) curve – are well-known, both methods are, in principle, equivalent. However, this is usually not the case. Thus, the implementation

of price regulation leads to uncertainty about the quantity of emissions, whereas the implementation of quantity regulation leads to uncertainty about the carbon price.

Both of the above mentioned instruments of carbon emissions abatement can be easily implemented in power system models: By exogenously limiting the quantity of emissions, a cap-and-trade scheme like the EU ETS can be modelled. In this case, the carbon price is determined endogenously. By contrast, a carbon tax can be modelled by exogenously fixing the carbon price. In this case, the amount of emissions is the result of cost optimisation.

The instrument which is used in reality (either quantity regulation or price regulation) does not necessarily determine the approach which is chosen to account for emissions abatement in a model (either constraining emissions or setting a carbon price). For instance, if the implemented emissions trading scheme does not only cover the power sector but also extends to other industries, it might make sense to exogenously fix the carbon price, e. g. to a value obtained from a coarse-scale, multi-sector model. By this means, abatement measures that are available in other industries and compete with abatement measures in electricity generation can be considered implicitly in the model.

Although the MAC curve is well-known within the limited scope of a power system model, approaches with fixed carbon price and approaches with fixed emissions targets are not completely equivalent. This is due to the discrete character of the MAC-curve: The abatement costs of electricity generation are determined by costs and emission intensities of fuels as well as by efficiencies of each pair of power plants switching in the merit order (Roth 2008, Delarue *et al.* 2008). As the size of generating units is not infinitesimal, the MAC curve is discrete and discontinuous at each switching point of different pairs of power plants.

Between switching points, the merit order of power plants does not change (vide Figure 4.5, left). Therefore, in certain intervals, an increase in carbon price does not lead to a further reduction of emissions. In fact, exogenously fixing the carbon price at a certain level of abatement costs will already cause the complete switching of the marginal pair of power plants (vide Figure 4.5, right).

By contrast, exogenously fixed emissions targets allow for the continuous reduction of emissions, as the marginal pair of power plants does not switch completely in the merit order. Instead, production is only shifted to the extent necessary to reach the respective emissions target (vide Figure 4.5, middle). Thus, although there is a corresponding carbon price to each emissions target (i. e. the abatement cost of the marginal pair of power plants), exogenously fixing the carbon price will always result in lower emissions and, consequently, higher costs.

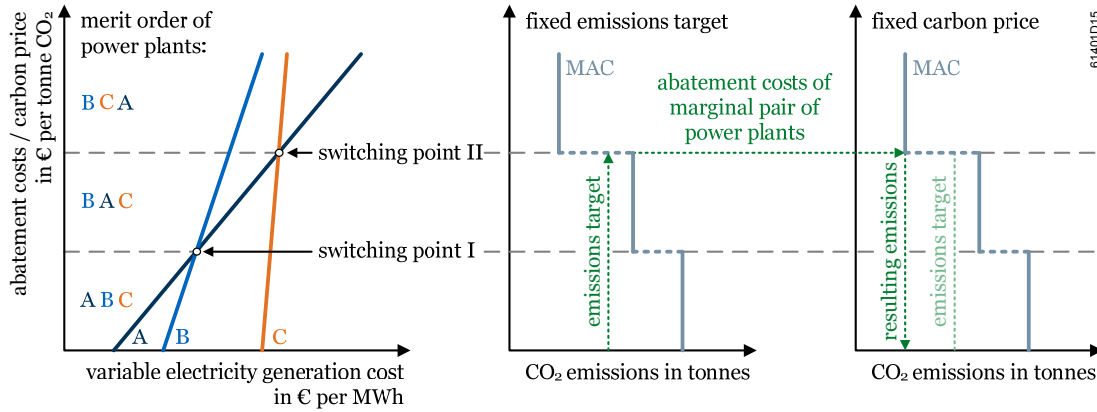


Figure 4.5: Discrete MAC curve and its effect on emissions when exogenously fixing the carbon price

Exogenously fixed carbon prices are commonly used in power systems modelling (e. g. Kuhn 2012, Kuhn *et al.* 2012, Adamek *et al.* 2012, Agora Energiewende 2014). An obvious advantage over fixing emissions targets is the reduced computational burden, as additional constraints on the amount of emissions are not required in the model. A more fundamental reason for choosing the fixed carbon price approach could be its relevance for emissions abatement in reality: According to Voß & Flinkerbusch (2013), implementing a carbon tax is more efficient under uncertainty, even though the tax has to be adjusted on a regular basis to meet emissions targets.

However, if the fixed carbon price approach is not used to model a carbon tax (which, in principle, could be defined arbitrarily) but instead serves to represent the carbon price formed in a cap-and-trade system, the crucial question is how this carbon price can be determined adequately. As above mentioned, the assumed carbon price has to reflect abatement options in all sectors under the emissions trading scheme.

Several factors have an impact on the carbon price, including, most importantly, fuel costs (Fezzi & Bunn 2009, Hintermann 2010). Thus, if a fixed carbon price approach is used, assumptions on the development of carbon price, fuel costs, etc. should be mutually consistent. Nevertheless, carbon price and fuel costs are often based on very different assumptions (e. g. Kuhn 2012, Agora Energiewende 2014).

Whereas it cannot be guaranteed that emissions targets are met when applying a fixed carbon price approach, exogenously fixed emissions targets form binding constraints of the optimisation problem. Thus, from an abatement perspective, the comparability of different scenarios is enhanced if the quantity – and not the price – of carbon emissions is exogenously fixed.

However, in order to determine adequate emissions targets, the degree to which the scope of the real cap-and-trade scheme is matched by the geographic and sectoral scope of the model has to be taken into account. Alternatively, national policies on carbon emissions reduction can be consulted. For instance, for a model of the German power system like IMAKUS, emissions targets for the power sector could be defined in proportion to German overall reduction targets (vide Section 5.2.10). It should be noted that, in this case, trading of emissions allowances with other regions or sectors of the trading scheme is neglected. Consequently, the resulting carbon price only applies to the power sector of the considered region.

With regard to modelling results, general statements about the impact of exogenously fixing either the quantity or the price of emissions are rather difficult to make. However, two distinctions are apparent: As the marginal pair of power plants switches completely in case of a fixed carbon price approach (vide supra), slightly more production is shifted from carbon-intensive to less carbon-intensive technologies than in case of exogenously fixed emissions targets. Furthermore, any use of storages that leads to an increase in emissions (i. e. if cheap but carbon-intensive generation is stored to substitute expensive but less carbon-intensive generation) is directly limited by exogenously fixed emissions targets. Thus, investment into storage typically starts later than in case of a fixed carbon price (given that renewable electricity generation increases over the planning horizon).

Exemplary analysis: constraining emissions over the whole planning horizon

If a planning horizon of several years is considered, the quantity of carbon emissions either can be explicitly limited for each year or can be constrained by the total amount of emissions permitted over the whole planning horizon. In the latter case, the decision when to reduce emissions is left to the optimisation model: Due to the time value of money, the model will tend to delay emissions abatement to later years, in order to further minimise whole-systems costs.

As described in Section 3.3.3, both annual emissions targets and the limitation of emissions over the whole planning horizon can be modelled with the whole-systems cost minimisation model IMAKUS. The model is therefore used to analyse the impact of the two different approaches to constraining emissions. This analysis is based on the scenario “80/minus15” defined by Kuhn *et al.* (2012), which assumes a share of renewable electricity generation of 80 % in Germany in 2050.

Annual emissions targets for the German power sector are defined in proportion to national overall reduction targets: In BMWi & BMU (2010), the German government committed to the reduction of GHG emissions by 40 % until 2020 and by 80 % until 2050 (on 1990 levels). Starting from 357 million tonnes carbon dioxide (CO₂) emis-

sions in the power sector in 1990 (Icha 2014), the pathway of annual emissions reduction between 2010 and 2050 is determined by linear interpolation.

The annual emissions budget to be spent by the model is reduced ex ante, first, by emissions of exogenously defined electricity generation from fossil CHP and, secondly, by an estimated 2 % to account for emissions related to start-up losses that are not modelled endogenously. Figure 4.6 shows the assumed pathway of annual emissions reduction.

The overall emissions target for the whole planning horizon is calculated as the total of annual emissions targets. Figure 4.6 also presents the annual emissions which result from the optimisation of the considered scenario when assuming the calculated overall emissions target.

As expected, emissions abatement is delayed to later years if emissions are only constrained over the whole planning horizon. Annual emissions exceed the original annual targets during the first half of the planning horizon. In order to meet the overall emissions target for the planning horizon, emissions are then reduced considerably during the second half of the period.

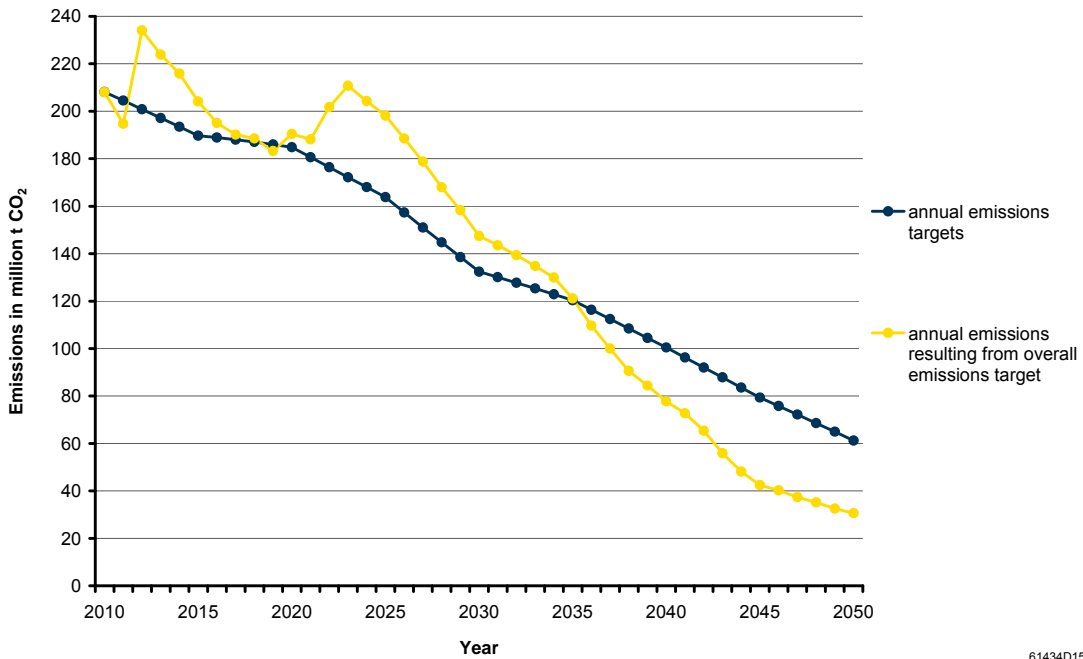


Figure 4.6: Annual emissions targets and annual emissions resulting from an overall emissions target in an exemplary scenario

61434D15

The impact of an overall emissions target on the structure of electricity generation corresponds to the observed cost-optimal pathway of emissions reduction: Compared to the scenario with annual emissions targets, generation from gas-fired power plants – which offers low carbon intensity at the expense of high variable costs – is reduced during the first half of the period. Due to the time value of money, the shift from a largely coal-based to an almost completely gas-based electricity generation – and, thus, emissions abatement – is delayed to later years.

While the described impact on electricity generation can be considered to be generally valid, it is rather difficult to assess the general impact of an overall emissions target on storage. Although emissions are not limited to specific annual targets, additional emissions caused by conventional peak shaving at the beginning of the planning horizon are only acceptable to the extent that further emissions abatement is economically feasible in later years. Therefore, the attractiveness of storage improves only slightly as compared to the case of annual emissions targets.

4.7 Modelling of power plants and energy storage

4.7.1 Simplified modelling of unit commitment

In unit commitment planning, generating units and storages are represented in detail: Models usually include start-up costs, a minimum generation constraint, minimum up and down time constraints and ramping constraints (Hobbs 1995, Pandžić *et al.* 2013). As most of these aspects cannot be modelled with a basic linear programming approach, the use of more complex approaches is required. A method which is commonly used to solve unit commitment problems is mixed-integer linear programming (Pandžić *et al.* 2013).

However, considering these additional constraints in a mixed-integer model significantly increases the computational burden as compared to the simpler linear programming approach. The application of most unit commitment models is thus restricted to very short planning horizons (Palmintier & Webster 2011). Therefore, the above mentioned details of unit commitment are usually neglected in expansion planning models (e. g. Kuhn 2012, Scholz 2012, Short *et al.* 2012, EPRI 2012). At least in the past, this was generally considered an acceptable simplification, as load patterns were characterised by “highly predictable and fairly slow time dynamics” (Palmintier & Webster 2011).

However, examples of expansion planning models that include unit commitment constraints exist: Strbac *et al.* (2012) optimise generation and storage capacity expansion using mixed-integer linear programming and considering start-up costs,

minimum generation, minimum up and down time as well as ramping constraints. By combining generation expansion planning and unit commitment constraints in a mixed-integer model, Palmintier & Webster (2011) demonstrate that neglecting these constraints during planning leads to a suboptimal generation portfolio, involving a significant increase in operating costs and emissions.

As pointed out in Chapter 3, the economic dispatch of power plants and storages is modelled in a very simplified manner in IMAKUS: While in the submodel MOWIKA dispatch of conventional power plants is only based on annual load duration curves, power plant and storage dispatch is modelled chronologically in MESTAS, but start-up costs, minimum generation, minimum up and down time as well as ramping constraints are nevertheless ignored. Thus, a unit's generating power can be varied continuously between zero and the maximum output power and is not dependent on power plant dispatch in adjacent hours.

If unit commitment is modelled as simplified as in IMAKUS, the flexibility of power plants – and, in particular, the flexibility of base-load power plants – is overestimated. As a consequence, investment into peaking plants is reduced in favour of higher investment into base-load power plants. Moreover, results on storage demand which are obtained from such a model represent a lower estimate of storage capacity: In reality, the lower flexibility of conventional power plants leads to a higher level of surplus generation from RES and CHP and, thus, to a higher demand for flexible technologies like storage.

4.7.2 Curtailment of generation from RES and CHP

With growing shares of renewable electricity generation, surplus generation, i. e. the amount of energy that cannot be directly utilised to supply demand, increases. Quite obviously, the level of energy storage demand crucially depends on the question whether the curtailment of generation from RES and CHP is accepted or not.

If curtailment is allowed, surplus energy is only integrated to the extent that storage expansion is economically feasible. As the capacity which is required to integrate the marginal MWh of surplus generation will already be rarely utilised, it is usually cost optimal to not further expand storages and instead pass up a certain amount of surplus energy. By contrast, if curtailment is not allowed, storage has to be expanded – in terms of storage capacity, charging and discharging capacity – until every MWh of surplus generation from RES and CHP can be utilised.

Whereas most studies assume the economic integration of surplus generation, there are also cases where curtailment is restricted: In Adamek *et al.* (2012), storage new

builds are initially rated to enable the balancing of all fluctuations of residual demand. Thus, generation from RES and CHP can be completely integrated into the power system. In Klaus *et al.* (2010), curtailment is allowed but limited to 1 % of surplus generation.

Exemplary analysis: economic integration vs. no curtailment

While, by default, the economic integration of surplus generation from RES and CHP is assumed in the whole-systems cost minimisation model IMAKUS, curtailment can also optionally be restricted (vide Section 3.2.2). The model is thus used to compare storage capacity expansion in case of economic integration and in case of curtailment being not allowed. The analysis is based on the scenario “80/minus15” defined by Kuhn *et al.* (2012). In this scenario, the assumed share of electricity generation from RES in Germany amounts to 80 % in 2050.

Figure 4.7 shows results on new build storage capacity and new build charging capacity for selected years of the considered planning horizon 2010–2050. Existing PSP capacities are not represented.

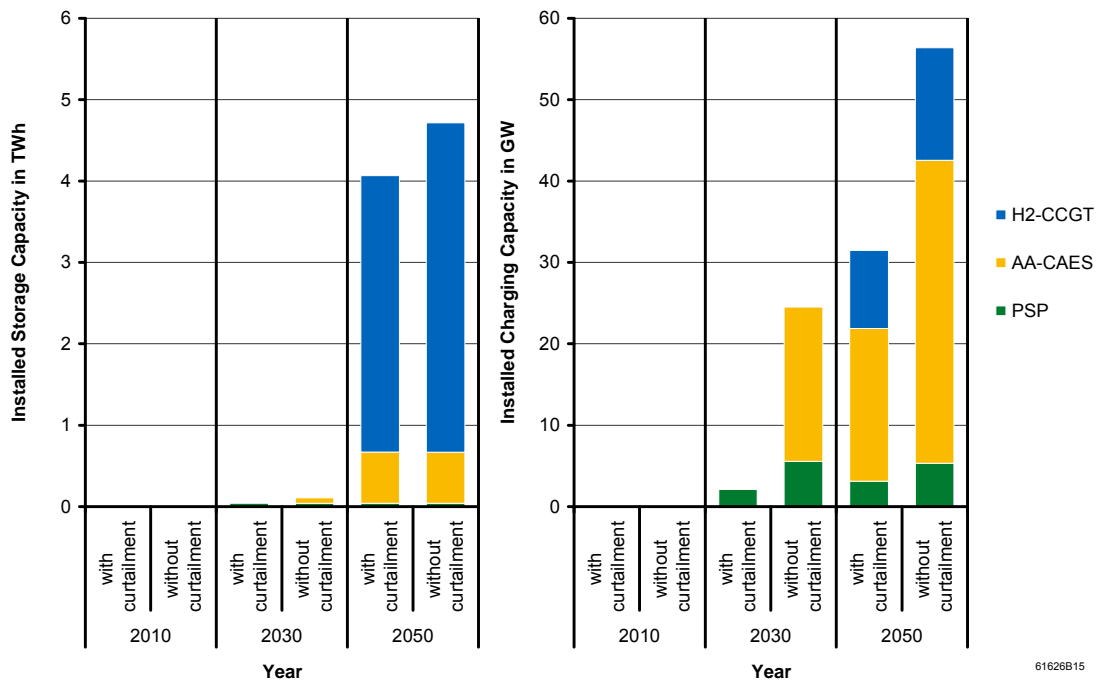


Figure 4.7: Comparison of storage capacity expansion with and without curtailment of surplus generation in an exemplary scenario

If curtailment is not allowed, the expansion of AA-CAES starts much earlier, as storage capacity expansion is exogenously limited to 40 GWh for PSP. Installed storage capacity increases considerably compared to the case of economic integration, particularly for hydrogen storage.

In principle, the same differences can be observed for charging capacity (and discharging capacity, which is not shown). However, the increase of charging capacity is much more significant: If curtailment of generation from RES and CHP is not allowed, investment into additional PSP charging capacity becomes economically feasible (despite the constraint on storage capacity). In 2050, the total installed charging capacity increases by almost 80 % compared to the economic integration case, whereas total installed storage capacity increases by just over 15 %.

Although predominantly hydrogen storage is expanded with regard to storage capacity, the more radical increase of installed charging capacity is observed for AA-CAES. As AA-CAES offer the lowest power-related investment costs, this technology is used to initially absorb the high power peaks of surplus generation. However, due to the much lower energy-related investment costs of hydrogen storage, it is apparently not cost-optimal to also expand AA-CAES storage capacity to the same degree. Instead, surplus energy is discharged promptly and afterwards stored over longer periods in hydrogen storage capacities.

4.7.3 *Must-run of conventional generation*

Another axis along which power systems models can be differentiated is whether or not a certain amount of conventional generation is assumed to be in operation at all times for system stability reasons. In today's power system, the purpose of conventional power plants is not restricted to electricity generation, i. e. the supply of active power. Beyond that, conventional power plants also supply reactive power, provide reserve capacity and black-start capability and participate in load frequency control and voltage control (Kuhn 2012).

In some models the provision of capacity for such ancillary services is explicitly considered (e. g. Short *et al.* 2012, Strbac *et al.* 2012). If this is not the case, a lower bound can be imposed on conventional generating power to implicitly consider the need for the permanent availability of conventional power plants for system stability reasons.

However, the question of how much conventional must-run capacity is actually required for these purposes is not well studied. One of the few studies concerning conventional must-run capacity in the German power system, FGH *et al.* (2012), reports

3 GW due to $n-1$ contingency requirements, a broad range of 4–20 GW necessary for voltage stability as well as a broad range of 8–25 GW necessary for load frequency control. While all values are strongly dependent on consumer demand and renewable electricity feed-in, it is also noted that the determined capacities are not necessarily mutually exclusive.

While assuming a need for conventional must-run capacity to guarantee system stability reflects the status quo, a contrary view is that, in the future, renewable generation units will very well be capable of ensuring stability and, thus, conventional power plants will not be required to stay online at all times. Kuhn (2012) even argues that only if renewable energy technologies were capable of providing ancillary services, would power systems with high shares of RES become conceivable. Under this assumption, the constraint of conventional must-run generation could be neglected in power systems modelling.

A quite obvious effect of neglecting must-run of conventional generation is that the level of surplus energy from RES and CHP is lower than in case of considering a conventional must-run capacity (Kuhn 2012): Whereas without conventional must-run generation surplus only occurs when RES and CHP generation exceeds demand, in the must-run case surplus already occurs when RES and CHP generation exceeds the actual demand less the amount of must-run capacity. Thus, as energy storage demand is largely driven by the amount of surplus energy from RES and CHP, it can be generally stated that neglecting must-run of conventional generation will lead to less storage capacity expansion.

Exemplary analysis: impact of conventional must-run capacity

The whole-systems cost minimisation model IMAKUS is used to further analyse the impact of different levels of conventional must-run capacity on storage demand. Whereas the default assumption in IMAKUS is that must-run of conventional generation can be neglected (Kuhn 2012), it is also possible to constrain total conventional generation to a lower bound in each hour (vide Chapter 3).

The analysis is based on the scenario “80/minus15” defined by Kuhn *et al.* (2012), which assumes a share of renewable electricity generation of 80 % in Germany in 2050. Besides the reference case (which neglects conventional must-run generation), storage demand is optimised for values of conventional must-run capacity of 5 GW and 10 GW. As pointed out above, the amount of surplus energy from RES and CHP is significantly higher if must-run of conventional generation is considered: For instance, the surplus of 44 TWh reached in 2050 in the reference case without must-run increases to 61 TWh and 82 TWh in case of conventional must-run capacities of 5 GW and 10 GW respectively.

Due to the higher availability of surplus energy in case of conventional must-run generation, the expansion of storage increases (vide Figure 4.8). In 2050, the total installed storage capacity triples compared to the reference case without must-run if a 10 GW conventional must-run capacity is assumed.

With regard to all three dimensions – storage capacity, charging capacity and discharging capacity –, the assumption of conventional must-run generation mainly leads to the further expansion of hydrogen storage. Due to the constant feed-in of electricity from conventional power plants, not only the amount of surplus energy but also the duration of surplus periods increases. Therefore, for each additional unit of surplus energy, the possibility to be balanced within a short-term horizon becomes less likely. Apparently, the demand for long-duration storage increases.

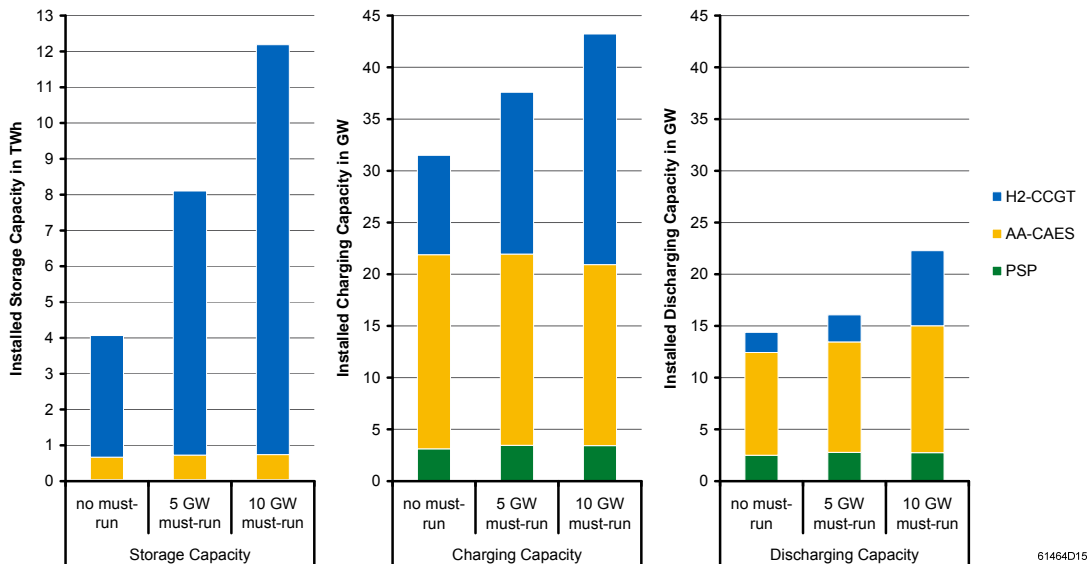


Figure 4.8: Comparison of storage capacity expansion with and without must-run of conventional generation in an exemplary scenario in 2050

4.7.4 Independent rating of storage dimensions

With regard to storage capacity expansion, the number of degrees of freedom differs significantly between power systems models: Either the three dimensions of new build storages – i. e. storage capacity, charging capacity and discharging capacity – are rated completely independently or some or even all of their ratios are exogenously fixed. For instance, the proportion of storage capacity to discharging capacity, the so-called storage duration, is often fixed to a certain value.

More precisely, storage duration is calculated as the ratio of effective storage capacity (i. e. the installed storage capacity weighted by the discharging efficiency) to the installed discharging capacity. It thus specifies the time it takes to completely empty a fully charged storage at its rated discharging power and allows for the classification of storages into short-duration and long-duration storages.

For the majority of existing PSP in Germany, storage duration ranges from 3 h to 8 h (vide Appendix C.1). As the rating of existing PSP might be owing to local geological or topographical constraints and to a business case that assumed operation in a hydro-thermal power system, the optimal storage duration of future new build PSP is not necessarily restricted to this range. From a technical perspective, there are no general restrictions to the ratio of storage capacity to discharging capacity – neither for PSP nor for AA-CAES and hydrogen storage.

However, in various studies, storage durations of all or some of the considered technologies are fixed to generic values: In Scholz (2012), dimensions of new build storages are rated independently except for PSP, which are fixed to 8 h storage duration. In Hand *et al.* (2012), storage duration of PSP and high-energy batteries is fixed to 8 h, while storage duration of CAES is fixed to 15 h.

Moreover, studies that only consider generic types of storages (like short-duration and long-duration storage) commonly define these types by fixing storage duration to generic values: For instance, Adamek *et al.* (2012) define a storage duration of 5 h for short-duration storage. In Strbac *et al.* (2012), storage duration is varied between generic values of 6 h, 24 h and 48 h.

It is quite clear that by – unnecessarily – fixing the ratios of storage dimensions to generic values, only suboptimal storage portfolios can be obtained from the optimisation of power systems. Nevertheless, the impact of an independent rating of storage dimensions on storage demand cannot be generalised.

In fact, at least the amount of energy that is economically feasible to be stored with a suboptimally rated storage portfolio will also be stored with storages that are optimally adapted to the power system. As usually only one of the three storage dimensions represents the bottleneck in the fixed-ratio case, an optimally rated storage unit would exhibit less expansion of the other two dimensions. Consequently, if storage dimensions are optimised independently, total system costs would decrease.

However, it is quite possible that the freedom to independently rate storage dimensions leads to additional opportunities to profitably store energy. In this case, storage expansion could increase compared to the fixed-ratio case and, consequently, total system costs would be further reduced. Thus, by independently rating storage dimensions and allowing new build storages to optimally adapt to the power system, the estimated storage demand likely – but not necessarily – increases.

Exemplary analysis: fixed vs. optimised storage duration

In order to illustrate the impact of independently rated storage dimensions as compared to using exogenously fixed ratios, the case of storage duration is further analysed with the whole-systems cost minimisation model IMAKUS. Whereas, by default, storage rating is optimised in IMAKUS, the ratios between the three storage dimensions can optionally also be fixed or limited to a certain range.

The analysis is based on the scenario “80/minus15” defined by Kuhn *et al.* (2012), which assumes a share of renewable electricity generation of 80 % in Germany in 2050. In the fixed-ratio case, storage duration is exogenously fixed to 8 h for PSP and 15 h for AA-CAES, while hydrogen storage can be rated independently. For comparison, storage capacity expansion is also determined assuming the optimisation of storage duration for all storage technologies. In both cases, the ratio of discharging to charging capacity of PSP is limited to a range from 0.8 to 1.2 (vide Section 3.2.2).

If storage duration is optimised, total system costs (undiscounted) are reduced by 0.2 % and curtailment of RES and CHP decreases by 5 % over the planning horizon 2010–2050. Also, the impact on storage demand is considerable. Figure 4.9 illustrates the differences in the optimal storage portfolio in 2050: Most notably, the level of installed discharging capacity reduces if storage duration is optimised. In case of AA-CAES, this even involves an increase of storage capacity. Thus, storage durations of 14 h for PSP and 53 h for AA-CAES prove optimal in the considered scenario.

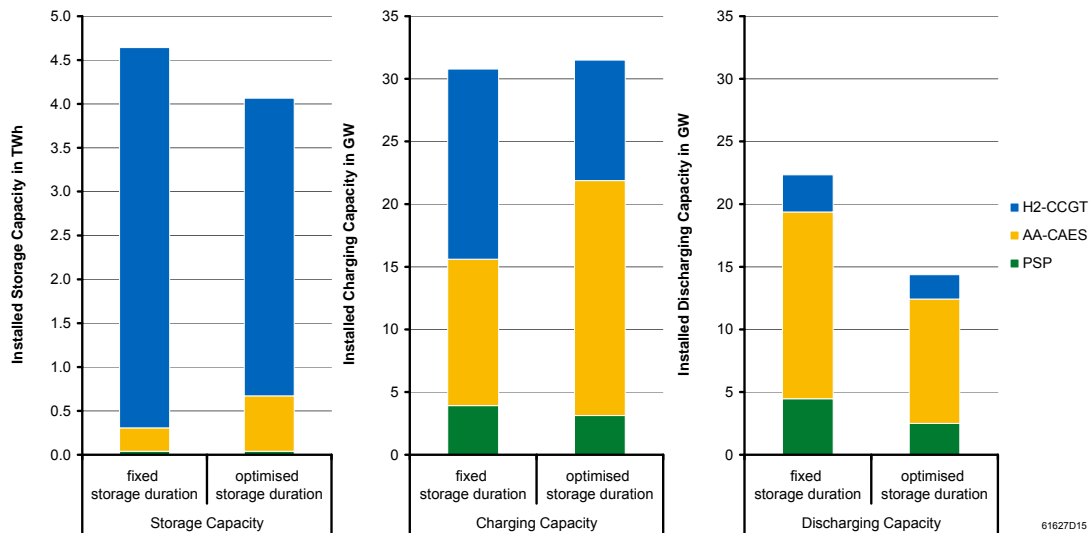


Figure 4.9: Comparison of storage capacity expansion with fixed storage duration and with optimised storage duration in an exemplary scenario in 2050

4.7.5 Optimising vs. exogenously fixing initial storage levels

A very specific question of storage modelling is how to handle the initial and final storage levels of the considered planning horizon. For power systems models that only optimise individual years, suitable values have to be determined for the storage levels at the beginning and at the end of the considered years.

Usually, each year is considered independent of adjacent years and annual time series of generation and demand are assumed to recur cyclically. Based on this assumption, a cyclic constraint is commonly imposed on the storage level of each storage unit (e. g. Schaber 2013, Scholz 2012): In order to maintain the annual energy balance, the final storage level of a given storage is fixed at the same value as the initial storage level. Thus, the total energy discharged over one year is required to equal the total energy charged over the year minus storage losses.

If the initial (and at the same time final) storage level is however exogenously fixed to an arbitrary value, storage dispatch will be constrained unnecessarily. Most probably, the chosen storage level will not fit the requirements arising from the seasonal characteristics of generation and demand, thus leading to a suboptimal solution to the optimisation problem.

Therefore, the preferred approach is to let the optimisation model determine initial storage levels endogenously. By this means, storages can fully capitalise on the seasonality of renewable electricity generation.

In most cases, an increase in the number of degrees of freedom of storage dispatch will supposedly benefit the expansion of storages. However, – as illustrated by the following analysis of an exemplary scenario – the effect of optimised initial storage levels on the estimated storage demand cannot be generalised.

Exemplary analysis: optimised vs. fixed initial storage levels

The analysis is based on the scenario “80/minus15” defined by Kuhn *et al.* (2012). In this scenario, the assumed share of electricity generation from RES in Germany amounts to 80 % in 2050. First, the model IMAKUS is used to optimise storage capacity expansion for exogenously fixed initial storage levels: In each year of the planning horizon 2010–2050, the initial (and final) storage levels of existing and new build storage units are fixed to 0 %, 50 % and 100 % of the respective installed storage capacity. Moreover, storage capacity expansion is also determined assuming the endogenous optimisation of initial storage levels.

Results on storage capacity expansion for the year 2050 are compared in Figure 4.10. While the expansion of hydrogen storage capacity varies significantly, only small differences are observed for storage capacity of PSP and AA-CAES.

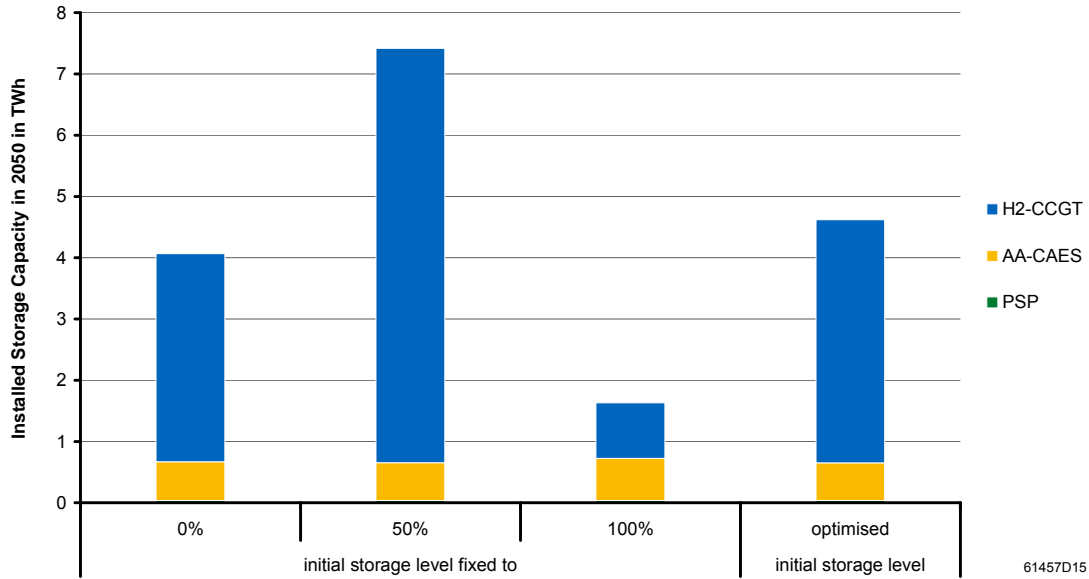


Figure 4.10: Comparison of storage capacity expansion with fixed and with optimised initial storage levels in an exemplary scenario in 2050

It thus becomes clear that the choice of the initial storage level mainly affects the ability of long-duration storages (like H₂-CCGT) to balance seasonal fluctuations of residual demand. In the considered scenario, the share of wind power in total renewable electricity generation amounts to 63 % in 2050. As surplus wind generation primarily accumulates during winter, a fixed initial storage level of 100 % significantly reduces the profitability of hydrogen storage. Consequently, the amount of surplus generation that has to be curtailed is comparably high in this case.

The relatively small difference in installed H₂-CCGT storage capacity between a fixed initial storage level of 0 % and the optimised case suggests that the optimal storage level at the beginning of the year is rather close to zero. In fact, the optimal initial (and final) storage level for hydrogen storage is found to be 7 % in 2050. Starting from this level, the hydrogen storage is charged more or less continuously to reach 100 % after the first 1800 hours of the year (vide Figure 4.11). However, it should be noted that the optimal initial storage level is strongly dependent both on the assumed structure of RES and the assumed time series.

Although the installed hydrogen storage capacity practically doubles compared to the 0 % case if the initial storage level is exogenously fixed to 50 %, curtailment of RES and CHP does not decrease significantly. As Figure 4.11 illustrates, this can be explained by the resulting dispatch of hydrogen storage, which basically exhibits the

same characteristics as the dispatch in case of an optimised initial storage level (and in case of a 0 % fixed initial storage level). In order to allow for this optimal storage dispatch pattern, hydrogen storage capacity is rated larger than actually necessary. Due to the low energy-related investment costs of hydrogen storage, this installation of surplus capacity is still economically feasible.

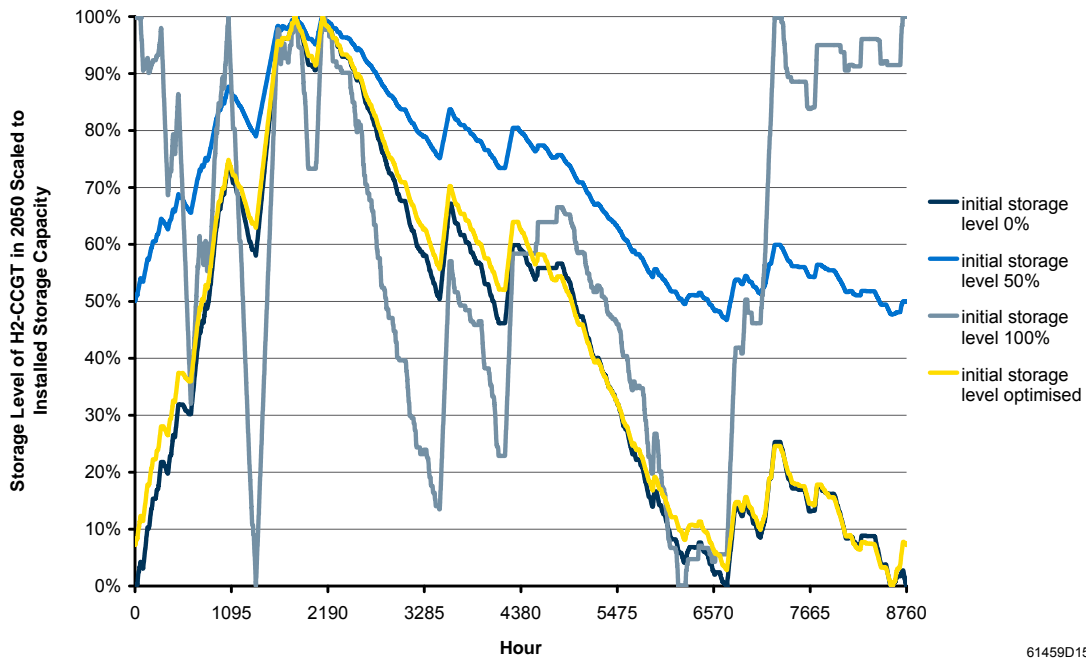


Figure 4.11: Comparison of the storage level of H₂-CCGT with fixed and with optimised initial storage levels in an exemplary scenario in 2050

4.8 Discussion and conclusion

In this chapter, methodological approaches and assumptions that are commonly encountered in energy systems modelling are analysed with regard to their qualitative influence on estimated storage demand. While the question whether a certain methodological choice leads to an increase or decrease of storage capacity expansion is answered for the majority of the considered approaches, a few cases are identified where the impact on storage demand cannot be determined definitely.

For some of the considered methodological approaches, a complementary analysis of modelling results indicates significant effects on both the scale and the structure of storage capacity expansion. It is also shown that several approaches mainly influence

the estimated demand for long-duration storage like H₂-CCGT. These are namely: neglecting energy exchange with neighbouring countries; planning with perfect foresight; neglecting must-run of conventional generation; and the optimisation of initial and final storage levels.

Table 4.1 summarises the findings of this analysis. It is meant as a brief overview that could serve to better evaluate and compare modelling results on energy storage demand with regard to the choice of methodological approaches and assumptions.

Table 4.1: Overview of analysed methodological approaches and an indication of whether they lead to an increase (+) or decrease (-) of estimated storage capacity expansion

| section | approach | impact |
|----------------|---|---------------|
| 4.1 | neglecting transmission constraints | - |
| 4.2.1 | only representative time slices | +/- |
| 4.2.2 | only hourly resolution | - |
| 4.3.1 | neglecting energy exchange with other countries | + |
| 4.3.2 | neglecting the coupling with other sectors | + |
| 4.4.1 | planning with perfect foresight | + |
| 4.4.2 | only considering snapshot years | +/- |
| 4.5 | using higher discount rates | - |
| 4.6 | exogenously fixing emissions targets | - |
| 4.7.1 | simplified modelling of unit commitment | - |
| 4.7.2 | not allowing curtailment | + |
| 4.7.3 | neglecting must-run of conventional generation | - |
| 4.7.4 | independent rating of storage dimensions | +/- |
| 4.7.5 | optimising initial storage levels | +/- |

While the analysis in this chapter comprises a selection of commonly encountered approaches and assumptions, it of course does not represent an exhaustive investigation of available methods in energy systems modelling. Several other methodological choices can be suspected to affect results on energy storage demand and should thus be subject to further analysis.

For instance, the question of how uncertainty is addressed reveals a number of criteria along which energy systems models can be differentiated: first and foremost, if and how security of supply is ensured and whether the provision of operating reserve is considered. More fundamentally, the uncertainty about input parameters like elec-

tricity demand or renewable electricity generation is either neglected in deterministic models or is explicitly accounted for with stochastic approaches (e. g. Strbac *et al.* 2012, Epe 2011). As Strbac *et al.* (2012) demonstrate, the possibility to optimally allocate storage resources between providing reserve and conducting energy arbitrage using a stochastic scheduling approach increases the value of storage by up to 75 % compared to the deterministic case.

While stochastic programming represents a formal approach to address uncertainty by considering different realisations of input parameters and their probability distributions, it is also possible to examine the impact of varying inputs by repeatedly applying a deterministic model (Pfenninger *et al.* 2014). By conducting such a sensitivity analysis in the next chapter, the question is addressed of how strongly dependent modelling results on storage demand are on selected input parameters.

5 Sensitivity analysis of energy storage demand in the German power system

As the review of studies in Chapter 2 showed, the broad range of results on energy storage demand is not only due to different methodological approaches and assumptions but is obviously caused to a large extent by differing input parameters. Whereas the impact of methodological choices on estimated storage demand was discussed in the previous chapter, this chapter addresses the question of how strongly dependent modelling results are on input parameters. By analysing the sensitivity of results to changes in selected input parameters with the whole-systems cost minimisation model IMAKUS, the drivers of energy storage demand in Germany are identified.

In the first section of this chapter, the general framework for this sensitivity analysis is introduced. Subsequently, a reference scenario is defined and an overview of corresponding optimisation results is presented. Afterwards, selected input parameters are varied. Results from this variation are analysed with regard to the impact on total storage capacity expansion as well as on technology-specific storage demand.

5.1 Scenario framework for sensitivity analysis

In order to improve the understanding of the broad range of results on energy storage demand, the whole-systems cost minimisation model IMAKUS is used in this chapter to analyse the sensitivity of modelling results to the variation of input parameters. For this purpose, a scenario framework is established that comprises a suitable reference scenario and defines which input parameters are subject to variation and which are not.

As models can only provide helpful insight if assumptions and input data are transparent, all input parameters required by the model IMAKUS are presented in detail.

Input parameters are either valid for the whole planning horizon (e. g. the level of security of supply) or have to be defined for each year (e. g. annual amounts of electricity consumption) or in hourly resolution (e. g. annual time series of electricity demand). While this section describes the general concept of the scenario framework, Section 5.2 provides a detailed presentation of the input parameters that are assumed in the reference scenario.

The main rationale behind the definition of the scenario framework in this thesis is to avoid non-linearities in modelling results and thus allow for their unambiguous interpretation. Therefore, in the reference scenario as well as in the variation scenarios, all input parameters that are defined on an annual basis are subject to a linear development: Technical and economic parameters of new build power plants and storages are considered constant over the planning horizon. While the annual amount of electricity consumption is also assumed to remain constant over the planning horizon, the share of RES is assumed to increase linearly. Furthermore, fuel costs are held constant over the planning horizon.

While these assumptions certainly do not reflect reality, it is also difficult to determine a more realistic development of e. g. electricity consumption or fuel costs. For instance, Nitsch *et al.* (2012) use scenarios of low, moderate and significant price rises to represent a broad range of possible futures: In these scenarios, the increase of natural gas price ranges from 14 % to as much as 81 % until 2030 and from 40 % to as much as 157 % until 2050 (on 2010 levels).

As it is not the focus of this thesis to determine the most realistic scenario and the corresponding pathway of storage capacity expansion, the – albeit simple – assumption of a linear development of input parameters is preferred over defining detailed scenarios of the development of fuel costs, electricity consumption, etc. Nevertheless, the uncertainty about the level of selected input parameters is addressed in the variation scenarios.

Although the reference scenario defined in Section 5.2 does not lay claim to being representative in all aspects, input parameters are for the most part based on data which are commonly used in literature or fixed by national and international policies.

As storage demand is largely influenced by the chronological characteristics of renewable electricity generation and electricity demand, the reference scenario should particularly represent the typical characteristics of demand and generation time series. Thus, a set of annual time series has to be determined which is consistent, i. e. which reflects the relevant correlations between demand and different types of renewable generation, and which can be considered representative of several years. For this purpose, a meteorological reference year is selected in Section 5.3.

While the annual time series corresponding to the selected meteorological reference year are employed in the reference scenario, other consistent sets of annual time series are used to test the sensitivity of storage demand in the variation scenarios (vide Section 5.5.1). Also, the total share as well as the structure of renewable electricity generation is varied to analyse sensitivity (vide Section 5.5.2 and Section 5.5.3 respectively). Moreover, fuel costs, storage investment costs and the bonus on storage costs are all subject to variation (vide Sections 5.5.4, 5.5.5 and 5.5.6).

5.2 Defining the reference scenario

5.2.1 General assumptions

The following general assumptions are valid for the reference scenario and throughout the variation scenarios. The considered planning horizon covers the period from 2010 to 2050. The expansion of generation and storage capacity is however not allowed before 2014. Carbon emissions are constrained over the whole planning horizon (vide Section 5.2.10).

All costs are measured in real prices in €_{2010} (denoted as € for convenience). The assumed real social discount rate is 3 % (vide Section 4.5). As pointed out in Section 3.2, the first year of the planning horizon – i. e. 2010 – is defined as the base year to which costs are discounted.

The desired level of security of supply is assumed at 99.5 %. As a precaution, the target value of firm capacity is defined as the annual peak load augmented by 4 % (vide Section 3.2.3).

5.2.2 Electricity demand

In IMAKUS, electricity demand is exogenously fixed. The required annual time series of demand are determined by scaling normalised time series (vide Section 5.2.4) by annual electricity consumption. As explained in Section 3.2, all generation capacities in IMAKUS are already decreased by the auxiliary consumption of power plants. Thus, the net electricity consumption has to be considered.

As mentioned above, the annual amount of electricity consumption is assumed to remain constant over the whole planning horizon 2010–2050. Its value is fixed at 536 TWh, which is the net electricity consumption in Germany in 2010 according to

scenario “2011 A” defined by Nitsch *et al.* (2012). The corresponding gross electricity consumption amounts to 604 TWh (Nitsch *et al.* 2012). In contrast to Kuhn (2012) and Kuhn *et al.* (2012), transmission losses are not accounted for. These assumptions are valid for the reference scenario as well as for all variation scenarios.

5.2.3 Share and structure of RES

Electricity generation from RES (as well as from fossil CHP) is exogenously fixed in IMAKUS. Analogously to electricity demand, the required annual time series of generation are determined by scaling normalised time series (vide Section 5.2.4) by the annual amounts of electricity generation.

Table 5.1 shows the amounts of electricity generation in Germany that are assumed for 2010 and 2050 in the reference scenario. All values for the year 2010 are based on scenario “2011 A” defined by Nitsch *et al.* (2012).

As mentioned above, the underlying rationale for scenarios considered in this thesis is a linear development over the planning horizon 2010–2050. In the reference scenario, total electricity generation from RES is assumed to increase linearly from 103.5 TWh in 2010 to 483.2 TWh in 2050. Thus, the total share of RES amounts to 80 % of gross electricity consumption in 2050, a goal set by the German government in BMWi & BMU (2010). The shares of electricity generation from RES are presented in Table 5.2.

Table 5.1: Electricity generation from RES and CHP in Germany in 2010 and 2050 as assumed in the reference scenario

| <i>in TWh/a</i> | 2010 | 2050 |
|----------------------|-------------|-------------|
| fossil CHP | 72.0 | 43.0 |
| biomass | 33.3 | 62.4 |
| total CHP | 105.3 | 105.3 |
| hydropower | 20.6 | 20.6 |
| geothermal | 0.0 | 20.2 |
| onshore wind | 37.6 | 155.0 |
| offshore wind | 0.2 | 150.2 |
| solar | 11.7 | 74.9 |
| total RES | 103.5 | 483.2 |

Sources: Nitsch *et al.* (2012); own assumptions.

Table 5.2: Shares of electricity generation from RES in Germany in 2010 and 2050 as assumed in the reference scenario

| <i>in % of gross electricity consumption</i> | 2010 | 2050 |
|--|-------------|-------------|
| biomass | 5.5 | 10.3 |
| hydropower | 3.4 | 3.4 |
| geothermal | 0.0 | 3.3 |
| <i>RES other than wind and solar</i> | 8.9 | 17.1 |
| onshore wind | 6.2 | 25.7 |
| offshore wind | 0.0 | 24.9 |
| solar | 1.9 | 12.4 |
| <i>total RES</i> | 17.1 | 80.0 |

Sources: Nitsch *et al.* (2012); BMWi & BMU (2010); own assumptions.

Annual total CHP generation from fossil- and biomass-fired units is assumed constant until 2050. However, the proportions of fossil- and biomass-fired CHP change considerably over the planning horizon: The annual biomass generation is assumed to increase linearly to a share of 10.3 % of gross electricity consumption, which is equivalent to the share of biomass in 2050 defined by Nitsch *et al.* (2012) in scenario “2011 A”. Correspondingly, the annual generation from fossil CHP decreases linearly over the planning horizon.

Annual hydro generation is considered constant over the whole planning horizon. It is fixed to 20.6 TWh, which, according to scenario “2011 A” by Nitsch *et al.* (2012), is the amount of electricity generated in Germany in 2010.

The annual amount of electricity generation from geothermal energy is assumed to increase linearly to a share of 3.3 % of gross electricity consumption, which is equivalent to the share of geothermal generation in 2050 defined by Nitsch *et al.* (2012) in scenario “2011 A”.

In total, electricity generation from biomass, hydro and geothermal plants amounts to 103.2 TWh or 17.1 % of gross electricity consumption in 2050. In order to reach a total share of RES of 80 %, the remaining renewable generation, i. e. 380 TWh, is assumed to come from wind and solar power. The ratio of electricity generation from onshore wind, offshore wind and solar PV in 2050 – roughly 2:2:1 – is based on scenario “2011 A” defined by Nitsch *et al.* (2012). Again, the annual amounts of generation are assumed to increase linearly, starting from 2010 levels.

Figure 5.1 illustrates the assumed development of generation from RES and CHP until 2050. While these assumptions are valid for the reference scenario, the total

share as well as the structure of renewable electricity generation is varied in Sections 5.5.2 and 5.5.3 respectively.

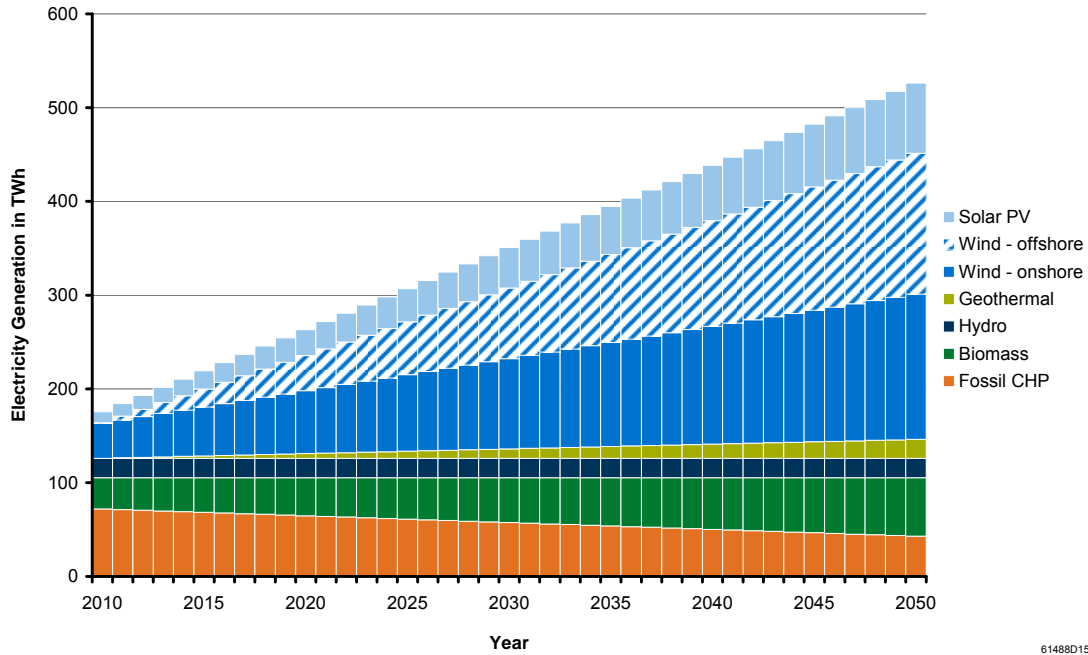


Figure 5.1: Electricity generation from RES and CHP over the planning horizon 2010–2050 as assumed in the reference scenario

5.2.4 Time series of demand and generation

A database presented by Janker (2015) provides a consistent set of annual time series of global electricity generation from wind and solar power for the period 1979–2012, both as high resolution raster data and aggregated on a regional or country level. Besides annual time series of wind and solar generation in hourly resolution, the database also provides annual time series of temperature in hourly resolution, which can be used to model electricity demand and CHP generation. This section describes how, based on these data, a consistent set of normalised annual time series is established for Germany for each year of the period 2003–2012, characterising electricity generation from wind and solar power and CHP as well as electricity demand.

This section furthermore describes how annual time series of hydro and geothermal generation are modelled for the period 2003–2012. Unlike demand, wind, solar or

CHP, hydro and geothermal generation are however assumed to be unaffected by annual weather variations.

As the length of years is fixed to a default value of 8760 h in IMAKUS, the number of hours of annual time series is reduced to 8760 h in all leap years occurring within the ten-year period by cutting off the last 24 h. An average year is selected from the period 2003–2012 (vide Section 5.3), which is used as the meteorological reference year in the reference scenario.

Time series of wind and solar generation

Annual time series of electricity generation from onshore and offshore wind power as well as from solar PV are taken from the database presented by Janker (2015). The time series are in hourly resolution and represent the hourly capacity factor, i. e. the mean power output in each hour per MW of capacity installed. In order to determine aggregated time series of onshore wind and solar generation for Germany, it was assumed that within German federal states installed capacity is uniformly distributed.

Table 5.3: Relative distribution of installed onshore wind and solar PV capacity across German federal states in 2011 (total installed capacity = 100 %)

| German federal state | onshore wind | solar PV |
|-----------------------------|---------------------|-----------------|
| Baden-Württemberg | 1.8 % | 14.9 % |
| Bayern | 2.1 % | 33.1 % |
| Berlin | 0.0 % | 0.2 % |
| Brandenburg | 15.9 % | 6.3 % |
| Bremen | 0.6 % | 0.1 % |
| Hamburg | 0.2 % | 0.1 % |
| Hessen | 2.3 % | 4.9 % |
| Mecklenburg-Vorpommern | 5.8 % | 2.0 % |
| Niedersachsen | 24.4 % | 8.6 % |
| Nordrhein-Westfalen | 10.4 % | 10.9 % |
| Rheinland-Pfalz | 5.6 % | 4.7 % |
| Saarland | 0.5 % | 0.9 % |
| Sachsen-Anhalt | 13.0 % | 3.4 % |
| Sachsen | 3.5 % | 3.6 % |
| Schleswig-Holstein | 11.1 % | 4.1 % |
| Thüringen | 2.9 % | 2.1 % |

Source: own calculations based on BDEW (2013).

The relative distribution of total installed capacity across the 16 German federal states was assumed according to Table 5.3, which shows the relative distribution of installed onshore wind and solar PV capacity in Germany in 2011.

With regard to aggregated time series of offshore wind generation, a linear distribution of installed capacity across Germany's offshore regions was assumed, preferring good offshore sites over sites with less favourable wind conditions. The aggregated time series of wind and solar generation for Germany are extracted from the database for the period 2003–2012.

Time series of temperature

The annual time series of temperature provided by Janker (2015) can be used to model electricity demand and CHP generation consistently with wind and solar generation. Due to its location close to the geographical centre of Germany, the city of Würzburg is assumed to be representative for Germany with regard to temperature. The time series of temperature for Würzburg are extracted from the database for the period 2003–2012.

Table 5.4 shows the number of heating degree days (HDD) for each of the ten years, which is calculated as the sum of differences between an indoor comfort temperature of 20 °C and the daily average outside temperature, however only considering days with an average outside temperature below 15 °C.

Table 5.4: Annual HDD for the period 2003–2012

| <i>in Kd</i> | 2003 | 2004 | 2005 | 2006 | 2007 | 2008 | 2009 | 2010 | 2011 | 2012 |
|--------------|-------------|-------------|-------------|-------------|-------------|-------------|-------------|-------------|-------------|-------------|
| HDD | 3882 | 3893 | 3819 | 3747 | 3506 | 3700 | 3677 | 4385 | 3492 | 3747 |

Source: own calculations based on Janker (2015).

Time series of electricity demand

Based on the extracted time series of temperature, time series of electricity demand and time series of electricity generation both from fossil-fired and biomass-fired CHP are modelled. To generate time series of electricity demand in hourly resolution, a model developed by Heilek (2006) is used. The model synthesises the electrical load from a set of 25 load profiles representing characteristic days with regard to the season and the type of day (weekday, weekend or public holiday), also considering the correlation of electricity demand and three-day average temperature.

The sequence of weekdays and the occurrence of holidays are assumed as in the calendar year 2005, as in this year neither a very large nor a very small number of pub-

lic holidays coincided with weekends (Gobmaier 2013). Like the time series of wind and solar generation, the generated time series of demand are normalised time series, which are scaled to the annual maximum load.

Time series of fossil CHP generation

The time series of electricity generation from fossil-fired CHP are modelled applying a method presented in Kuhn (2012), which uses load profiles of Germany's natural gas supply to approximate the chronological characteristics of electricity feed-in from CHP, assuming a strong correlation between CHP heat production, heat consumption in district heating systems and natural gas consumption. As the power to heat ratio is assumed to be constant, electricity feed-in and heat production from CHP are directly proportional.

The characteristics of heat production are determined by the structure of heat demand, i. e. the shares of heat demand consumed by private households, the trade, commerce and services (TCS) sector and the industry sector. While the demand for space and water heating in private households is usually mainly dependent on outside temperature, it is also strongly influenced by the type of day in the TCS sector.

As the demand for space and water heating dominates heat demand with 92.5 % in private households and with 86.4 % in the TCS sector (Heilek 2015), the impact of process heat demand on the characteristics of total heat demand in these sectors is neglected. Both the dependency of daily heat demand on the three-day average temperature and the characteristics of heat demand based on load profiles of natural gas supply are assumed as specified by Kuhn (2012) to model electricity feed-in from CHP in private households and the TCS sector.

On the contrary, with a share of 88 % (Heilek 2015), heat demand in the industry sector is largely dominated by the demand for process heat and, thus, can be considered mostly independent of outside temperature. The electricity feed-in from CHP in the industry sector is assumed to be 100 % on weekdays and 75 % on weekends, public holidays as well as between 24 December and 6 January.

Although neither all CHP generation is connected to district heating systems nor all generators in district heating systems are necessarily CHP units, historical data on the sectoral structure of heat demand in district heating systems are used to determine the shares of private households, the TCS sector and the industry sector in total electricity feed-in from CHP. Table 5.5 shows the sectoral structure of heat demand in district heating systems in Germany for the period 2003–2012.

Whereas in the years 2003–2006 heat demand is highest in the TCS sector and lowest in the industry sector, from 2007 on a structural change is observed and heat demand of private households usually exceeds heat demand in the industry sector,

which in turn usually exceeds heat demand in the TCS sector. This sectoral structure is assumed to be valid for the future.

In order to synthesise a comparable set of annual time series of fossil CHP generation for the years 2003–2012, it is also assumed that this structure is valid for the whole period 2003–2012. By calculating the gradients of heat demand increase and decrease in TWh per Kd relative to the average values of heat demand and annual HDD in the period 2007–2012, typical values of heat demand are determined for private households and the TCS sector for each year of the period 2003–2012. Thus, the heat demand of private households and the TCS sector is considered to be only dependent on temperature and any impact of economic development is neglected.

With regard to typical values of heat demand in the industry sector, it is assumed that there is no dependency on temperature. The average annual heat demand for the period 2007–2012 is assumed as a typical value of heat demand, thus neglecting any impact of economic development.

Table 5.6 shows the resulting typical values of heat demand of private households, the TCS sector and the industry sector in district heating systems. The relative shares of sectoral heat demand are used to synthesise characteristic annual time series of fossil CHP generation for the years 2003–2012.

Table 5.5: Sectoral structure of heat demand in district heating systems in Germany for the period 2003–2012

| <i>in TWh</i> | 2003 | 2004 | 2005 | 2006 | 2007 | 2008 | 2009 | 2010 | 2011 | 2012 |
|-------------------|-------------|-------------|-------------|-------------|-------------|-------------|-------------|-------------|-------------|-------------|
| households | 43.4 | 45.7 | 42.7 | 42.0 | 43.1 | 45.6 | 49.0 | 52.6 | 45.7 | 48.0 |
| industry | 29.7 | 29.3 | 31.5 | 38.3 | 42.0 | 36.2 | 42.2 | 40.5 | 47.1 | 47.1 |
| TCS | 45.9 | 49.7 | 50.9 | 44.6 | 33.5 | 39.3 | 27.6 | 38.0 | 24.0 | 27.0 |

Source: own calculations based on BMWi (2013).

Table 5.6: Sectoral structure of heat demand in district heating systems in Germany for the period 2003–2012 (typical values, based on own assumptions)

| <i>in TWh</i> | 2003 | 2004 | 2005 | 2006 | 2007 | 2008 | 2009 | 2010 | 2011 | 2012 |
|-------------------|-------------|-------------|-------------|-------------|-------------|-------------|-------------|-------------|-------------|-------------|
| households | 48.4 | 48.5 | 47.9 | 47.3 | 43.4 | 46.5 | 46.1 | 52.6 | 43.1 | 47.3 |
| industry | 42.5 | 42.5 | 42.5 | 42.5 | 42.5 | 42.5 | 42.5 | 42.5 | 42.5 | 42.5 |
| TCS | 33.2 | 33.2 | 32.4 | 31.4 | 24.4 | 30.1 | 29.4 | 39.3 | 24.0 | 31.4 |

Another input needed to synthesise time series of fossil CHP generation is the total annual CHP generation, which should reflect a dependency on temperature, i. e. on annual HDD, while the impact of economic development again is being neglected. The historical values of annual CHP generation in Germany are shown in Table 5.7.

While the highest total CHP generation is actually observed for the coldest year of the period (according to Table 5.4, the maximum of HDD was reached in 2010), total CHP generation in 2011 exceeded total CHP generation in 2007 despite similar levels of HDD. This could be due to both economic reasons and changes in installed CHP capacity.

As historical data for the year 2012 was not available, the gradients of generation increase and decrease in TWh per Kd relative to the average values of generation and annual HDD are calculated for the period 2007–2011 and are used to determine typical values of total CHP generation, which are only dependent on temperature. Table 5.8 shows the calculated values, which are used to synthesise characteristic annual time series of fossil CHP generation for the years 2003–2012.

In order to obtain normalised time series of fossil CHP generation, the synthesised time series are scaled to the maximum power output observed throughout the years 2003–2012, which is assumed to equal the installed fossil-fired CHP capacity. Thus, the coldest year of the period 2003–2012 corresponds with the time series that show the highest number of full load hours (FLH) and will consequently lead to the highest annual CHP generation.

Table 5.7: Annual CHP generation by public utilities and industry in Germany for the period 2003–2012

| <i>in TWh</i> | 2003 | 2004 | 2005 | 2006 | 2007 | 2008 | 2009 | 2010 | 2011 | 2012 |
|-----------------|-------------|-------------|-------------|-------------|-------------|-------------|-------------|-------------|-------------|-------------|
| public | n/a | n/a | 52.3 | 54.0 | 51.9 | 53.8 | 50.5 | 53.4 | 51.1 | n/a |
| industry | 23.5 | 22.9 | 25.6 | 25.8 | 25.8 | 25.7 | 26.6 | 29.8 | 28.4 | n/a |
| total | n/a | n/a | 77.9 | 79.8 | 77.6 | 79.5 | 77.0 | 83.2 | 79.6 | n/a |

Source: own calculations based on VIK (2013).

Table 5.8: Total annual CHP generation in Germany for the period 2003–2012 (typical values, based on own assumptions)

| <i>in TWh</i> | 2003 | 2004 | 2005 | 2006 | 2007 | 2008 | 2009 | 2010 | 2011 | 2012 |
|---------------|-------------|-------------|-------------|-------------|-------------|-------------|-------------|-------------|-------------|-------------|
| total | 80.2 | 80.2 | 79.8 | 79.3 | 77.2 | 78.9 | 78.7 | 83.2 | 77.0 | 79.3 |

Time series of biomass generation

Like for fossil-fired CHP, the method presented in Kuhn (2012) is also applied to model the time series of electricity generation from biomass-fired CHP. In order to obtain time series exhibiting the characteristically high level of FLH (according to BDEW (2013) FLH of electricity generation from biomass ranged from 3181 h to 6981 h in Germany in 2011), a share of 76 % of constant base-load generation is assumed, while 16 % of biomass generation are modelled according to the characteristics of heat demand in private households and 8 % are modelled according to the characteristics of heat demand in the TCS sector.

Time series of biomass generation are synthesised for the years 2003–2012, using the typical values of total annual CHP generation presented in Table 5.8 to reflect the temperature-dependency of annual generation. The synthesised time series are then scaled to the maximum power output observed throughout the years 2003–2012 to obtain normalised time series.

Time series of hydro and geothermal generation

Both hydro and geothermal generation are assumed to be independent of temperature. Time series of hydro generation are taken from Kuhn (2012), where hydro generation is assumed to be constant on a monthly basis. Kuhn (2012) analysed the seasonality of hydropower generation in Germany by calculating the average share of total annual energy produced per month for the period 2000–2009. The time series are modelled by distributing average monthly production to constant hourly values of power output.

Furthermore, as in Kuhn (2012), geothermal generation is assumed to be constant throughout the year. The time series are modelled by distributing the annual production to constant hourly values of power output.

5.2.5 Existing power plant portfolio

For the reference scenario as well as for all variation scenarios, the portfolio of existing conventional power plants is assumed as in Kuhn *et al.* (2012). It comprises generation capacities of both public utilities and industry existing in Germany in 2010 as well as additional capacities expected to start operations until 2013. The main generation technologies represented in the portfolio are nuclear, lignite, hard coal, CCGT and gas turbines. A very small fraction of existing power plants is oil-fired. As electricity generation from CHP is fixed exogenously in IMAKUS (vide Section 3.2), only the dispatchable portion of cogeneration capacity is included in the portfolio.

The phase out of nuclear power plants in Germany is assumed according to current legislation (BGBL 2011). Hence, the last three nuclear power plants are shut down at the end of the year 2022. With regard to the other generation technologies, the remaining lifetime of power plants is estimated: Whereas a general lifetime of 30 years is assumed for gas-fired power plants, 40 years is a common estimate for lignite and hard coal (Kuhn *et al.* 2012).

Given these assumptions, Figure 5.2 illustrates the gradual reduction of existing conventional generation capacity in Germany over the planning horizon 2010–2050. Although generation capacity is modelled at plant level, an aggregated representation of generation technologies is used in the figure.

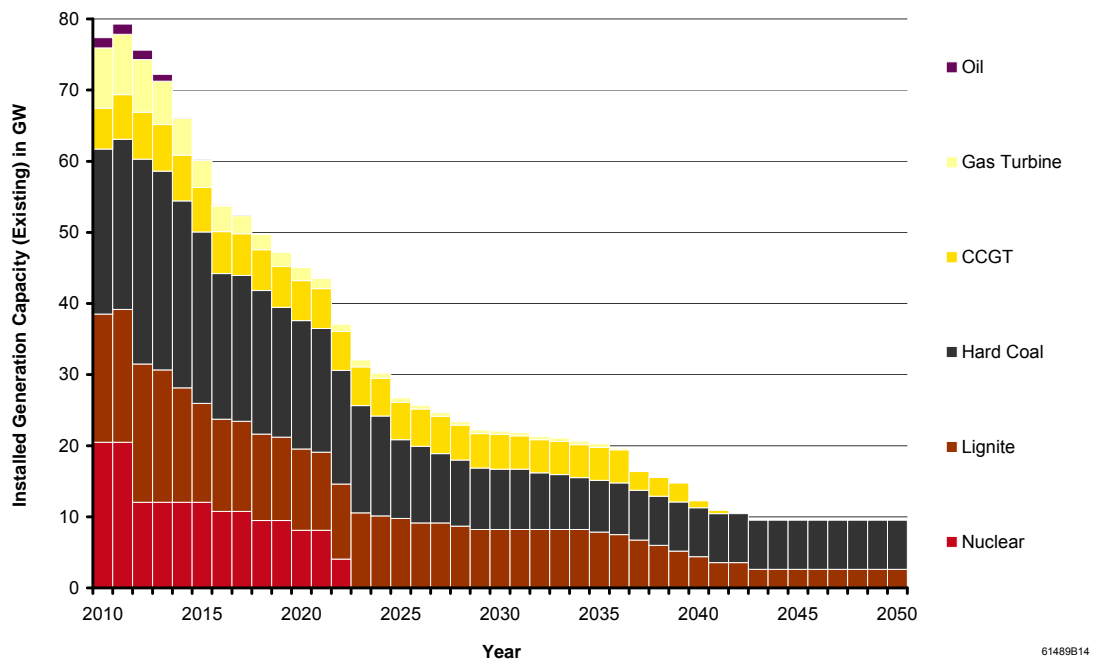


Figure 5.2: Development of existing conventional generation capacity in Germany over the planning horizon 2010–2050

As described in Section 3.2, the installed net generation capacity of power plants is weighted by a reduction coefficient to implicitly account for both planned and unplanned unavailability of generation capacity. Table 5.9 presents historical data by VGB (2010) on the average availability and unavailability of power plants in Germany over the period 2000–2009. The technology-specific values of energy availability are used as reduction coefficients for existing power plants in IMAKUS.

Furthermore, based on these data, technology-specific values of technical reliability can be calculated by applying equations (3-1) and (3-50). The calculated values given in Table 5.9 are used to determine the probability distributions of available generation capacity from existing power plants (vide Section 3.2.3).

The variable O&M costs of a power plant are assumed to depend on the respective generation technology. Table 5.10 shows technology-specific costs for existing power plants, which are taken from Kuhn *et al.* (2012).

Table 5.9: Energy availability, planned and unplanned energy unavailability and technical reliability of existing power plants by generation technology

| <i>in %</i> | gas turbine | CCGT | hard coal | lignite | nuclear | oil |
|----------------------------|--------------------|-------------|------------------|----------------|----------------|------------|
| energy availability | 86.6 | 86.8 | 84.4 | 86.2 | 85.5 | 90.3 |
| planned unavail. | 8.7 | 8.2 | 8.4 | 6.5 | 9.2 | 5.8 |
| unplanned unavail. | 4.7 | 5.0 | 7.2 | 7.3 | 5.3 | 3.9 |
| tech. reliability | 94.9 | 94.6 | 92.1 | 92.2 | 94.2 | 95.9 |

Source: VGB (2010); own calculations.

Table 5.10: Variable O&M costs of existing power plants by generation technology

| <i>in €/MWh_{el}</i> | gas turbine | CCGT | hard coal | lignite | nuclear | oil |
|-------------------------------|--------------------|-------------|------------------|----------------|----------------|------------|
| variable O&M costs | 2.17 | 2.08 | 4.17 | 4.17 | 0.52 | 5.21 |

Source: Kuhn *et al.* (2012).

5.2.6 Existing storage portfolio

The portfolio of existing storages in Germany – which is valid for the reference scenario as well as for all variation scenarios – is assumed as in Kuhn *et al.* (2012). It comprises 25 PSP plants with a total storage capacity of 77 GWh, a total charging capacity of 6.2 GW and a total discharging capacity of 6.5 GW.

Another storage plant that has been in operation since 1978 is the 290 MW CAES plant in Huntorf, northern Germany (Höflich *et al.* 2010). However, due to the necessary co-firing of natural gas during the discharging process, diabatic CAES are not considered a genuine storage technology. The mentioned CAES plant is thus not assumed to be part of the existing storage portfolio.

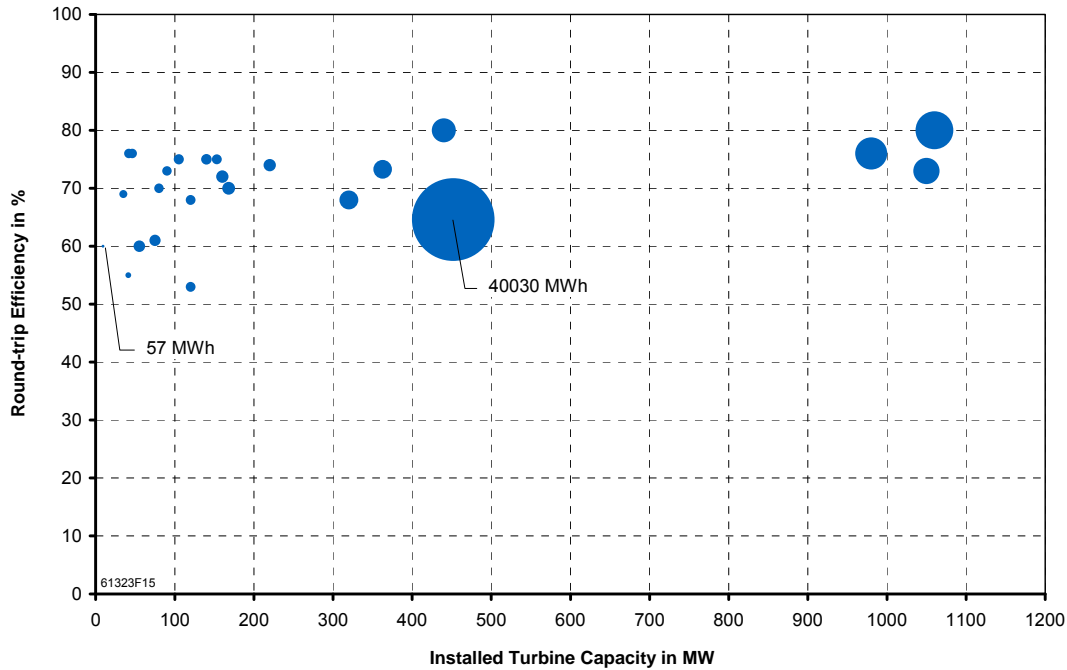


Figure 5.3: Characteristics of existing PSP in Germany

Figure 5.3 illustrates the diversity of existing PSP in Germany with regard to round-trip efficiency, turbine capacity and storage capacity (indicated by dot size). The majority of PSP plants have an installed turbine capacity of less than 200 MW and storage capacity of less than 1000 MWh. While for older plants efficiencies of as low as 53 % are observed, more recently built plants reach efficiencies of up to 80 %.

Appendix C.1 provides the parameters of existing PSP plants that are considered in the reference scenario and throughout the variation scenarios. The lifetimes of all existing PSP are assumed to exceed the planning horizon. Any losses due to self-discharge are neglected.

Analogously to power plants, storages are subject to planned and unplanned unavailability. As described in Section 3.2.2, this unavailability is considered implicitly by means of a reduction coefficient, which is multiplied with installed charging and discharging capacities. Furthermore, the technical reliability of storage units is taken into account when their capacity credit is determined (vide Section 3.2.3). Based on Kuhn *et al.* (2012), a technical reliability of 95 % and two weeks of maintenance, i. e. a planned unavailability of 3.8 %, are assumed for existing PSP. Correspondingly, the reduction coefficient of existing PSP – which is equivalent to energy availability – amounts to 91.4 % (vide Table 5.11).

As the considered storage technologies neither require fuel nor involve direct emissions, the variable costs of charging and discharging storages only consist of O&M costs (vide equation (3-40)). For existing PSP, variable O&M costs are assumed as in Kuhn *et al.* (2012) (vide Table 5.12).

Table 5.11: Energy availability, planned and unplanned energy unavailability and technical reliability of existing storages by storage technology

| <i>in %</i> | PSP |
|---------------------------------|------------|
| energy availability | 91.4 |
| planned unavailability | 3.8 |
| unplanned unavailability | 4.8 |
| technical reliability | 95.0 |

Source: Kuhn *et al.* (2012); own calculations.

Table 5.12: Variable O&M costs of existing storages by storage technology

| <i>in €/MWh_{el}</i> | PSP |
|--|------------|
| variable O&M costs: charging | 0.28 |
| variable O&M costs: discharging | 0.28 |

Source: Kuhn *et al.* (2012).

5.2.7 Fuels

For all endogenously modelled generation technologies, assumptions on costs and emission intensity of the respectively burned fuel have to be made. The fuels which are utilised by the different types of existing and new build power plants comprise natural gas, lignite, hard coal, oil and nuclear fuel.

As mentioned in Section 5.1, in the reference scenario as well as in the variation scenarios, fuel costs are held constant over the whole planning horizon 2010–2050. As fuels usually have to be transported from extraction sites via transfer sites (e. g. harbours) to the power plant site, the fuel costs assumed in IMAKUS should also account for transport costs.

For the reference scenario, assumptions on costs of natural gas, hard coal and oil are based on historical prices in Germany. For this purpose, five-year average prices are calculated for the period 2008–2012, using cross-border prices reported in BAFA

(2013a), BAFA (2013b) and SKW (2014). As all costs shall be measured in real prices in €₂₀₁₀, the cross-border prices are converted to €₂₀₁₀, using historical inflation rates according to Destatis (2014). In order to account for transport costs, the resulting costs of natural gas, hard coal and oil are augmented by an estimated 3 €/MWh_{th}.

For lignite and nuclear fuel, the 2010 level of fuel costs reported in Kuhn (2012) is assumed. Table 5.13 presents all fuel costs as assumed for the planning horizon 2010–2050 in the reference scenario. Whereas costs for fossil fuels are specified per unit of thermal energy, costs are specified per unit of electricity generated in case of nuclear power plants. Correspondingly, nuclear power plants are modelled with a net efficiency of 100 % in IMAKUS.

Table 5.13: Fuel costs as assumed in the reference scenario

| fuel | unit | fuel costs |
|-------------|---------------------|-------------------|
| natural gas | €/MWh _{th} | 27.38 |
| hard coal | €/MWh _{th} | 14.62 |
| oil | €/MWh _{th} | 50.12 |
| lignite | €/MWh _{th} | 5.50 |
| nuclear | €/MWh _{el} | 8.00 |

Sources: own calculations based on BAFA (2013a), BAFA (2013b), SKW (2014) and Destatis (2014); Kuhn (2012).

Compared to the broad range of fuel costs described by the scenarios of low, moderate and significant price rises in Nitsch *et al.* (2012), costs assumed for natural gas and hard coal in the reference scenario are considerably higher in 2010 but close to the lower end of the range in 2030 and 2050. However, it should be noted that fuel costs in Nitsch *et al.* (2012) reflect cross-border prices. The uncertainty about the level of fuel costs is addressed in variation scenarios in Section 5.5.4.

In the reference scenario as well as in the variation scenarios, the emission intensity of fossil fuels is assumed as in Kuhn *et al.* (2012) (vide Table 5.14). Nuclear fuel is considered emission-free.

Whereas most fuels are traded globally, lignite-fired power plants are generally located close to where lignite is mined (Kuhn *et al.* 2012). As, due to low public acceptance, a further increase of lignite extraction in Germany seems unlikely, Kuhn *et al.* (2012) propose to limit the annual consumption of lignite when modelling the German power system. Accordingly, annual lignite consumption is constrained in the

reference scenario and all variation scenarios to today's level of extraction of approximately 163 million tonnes or 407 TWh_{th} (Kuhn *et al.* 2012).

Table 5.14: Carbon emission intensity of fossil fuels

| fuel | unit | emission intensity |
|-------------|------------------------|---------------------------|
| natural gas | t CO ₂ /MWh | 0.20160 |
| hard coal | t CO ₂ /MWh | 0.33975 |
| oil | t CO ₂ /MWh | 0.27000 |
| lignite | t CO ₂ /MWh | 0.39816 |

Source: Kuhn *et al.* (2012).

5.2.8 Technical and economic parameters of new build power plants

All assumptions on technical and economic parameters of new build power plants are valid for the reference scenario and throughout the variation scenarios. As already mentioned, the endogenous expansion of generation capacity is not allowed before 2014, as power plants which are expected to start operations until 2013 are already included in the existing generation portfolio.

The following generation technologies are considered for expansion: New gas turbines and CCGT plants can be installed from 2014 on. Whereas conventional hard coal and lignite capacities can be expanded from 2014 to 2019, only 700 °C technology is assumed to be available for hard coal and lignite new builds from 2020 on. For each technology, capacity expansion is constrained to a maximum capacity of 4 GW available for installation per year.

Corresponding to the main rationale for scenarios in this thesis, all technical and economic parameters of new build power plants are assumed constant over the planning horizon 2010–2050. Parameters for gas turbines and CCGT as well as for conventional hard coal and lignite power plants are based on assumptions for 2020 according to Kuhn *et al.* (2012). For hard coal and lignite plants employing 700 °C technology, technical and economic parameters estimated by Kuhn *et al.* (2012) for the year 2030 are used.

Table 5.15 shows the assumed technical parameters of new build generation technologies, namely net efficiency as well as minimum and maximum sizes of generating units. The latter are used in the submodel MOGLIE to break down new build capacities obtained in MOWIKA – which are only classified with regard to technology and the year of installation – to plant level (vide Section 3.2.3).

Table 5.15: Technical parameters of new build power plants by generation technology

| | | gas turbine | CCGT | hard coal | hard coal 700 °C | lignite | lignite 700 °C |
|-----------------------|--------------|-------------|------|-----------|------------------|---------|----------------|
| net efficiency | <i>in %</i> | 39 | 61 | 46 | 51 | 45 | 50 |
| minimum size | <i>in MW</i> | 10 | 500 | 400 | 400 | 525 | 800 |
| maximum size | <i>in MW</i> | 250 | 1000 | 800 | 800 | 1050 | 1600 |

Source: Kuhn *et al.* (2012).**Table 5.16: Economic parameters of new build power plants by generation technology**

| | | gas turbine | CCGT | hard coal | hard coal 700 °C | lignite | lignite 700 °C |
|---------------------------|-------------------------------|-------------|--------|-----------|------------------|---------|----------------|
| invest. costs | <i>in €/kW_{el}</i> | 338.47 | 729.00 | 1353.87 | 1489.25 | 1562.15 | 1718.37 |
| fixed costs | <i>in €/kW_{el}·a</i> | 12.17 | 20.12 | 36.00 | 39.57 | 40.23 | 44.78 |
| var. O&M costs | <i>in €/MWh_{el}</i> | 2.17 | 2.08 | 4.17 | 4.17 | 4.17 | 4.17 |
| decomm. costs | <i>in €/kW_{el}</i> | 2.08 | 8.33 | 10.41 | 10.41 | 12.50 | 12.50 |

Source: Kuhn *et al.* (2012).**Table 5.17: Energy availability, planned and unplanned energy unavailability and technical reliability of new build power plants by generation technology**

| <i>in %</i> | gas turbine | CCGT | hard coal | hard coal 700 °C | lignite | lignite 700 °C |
|----------------------------|-------------|------|-----------|------------------|---------|----------------|
| energy availability | 86.6 | 86.8 | 84.4 | 84.4 | 86.2 | 86.2 |
| planned unavail. | 8.7 | 8.2 | 8.4 | 8.4 | 6.5 | 6.5 |
| unplanned unavail. | 4.7 | 5.0 | 7.2 | 7.2 | 7.3 | 7.3 |
| tech. reliability | 94.9 | 94.6 | 92.1 | 92.1 | 92.2 | 92.2 |

Source: VGB (2010); own calculations and assumptions.

Table 5.16 presents the assumed economic parameters of new build power plants, namely investment costs, annual fixed costs, variable O&M costs and decommissioning costs. Assumptions on the lifetime of new build power plants are also based on Kuhn *et al.* (2012): While for gas-fired power plants a lifetime of 30 years is assumed, 40 years is assumed for hard coal and lignite power plants.

Assumptions on energy availability and unavailability of new build power plants are specified in Table 5.17. The same technology-specific values are used as for the exist-

ing generation portfolio (vide Table 5.9). In particular, the values assumed for conventional hard coal and lignite power plants are also considered to be valid for power plants employing 700 °C technology.

5.2.9 Technical and economic parameters of new build storage

In the reference scenario as well as in all variation scenarios, three storage technologies are considered for expansion: PSP, AA-CAES and H₂-CCGT, i. e. a power-to-power hydrogen storage technology that comprises an electrolyser for charging, a cavern for storage and a CCGT unit for discharging. As in case of power plants, the endogenous expansion of storage capacity is not allowed before 2014. Moreover, it is assumed that AA-CAES technology is not available before 2020 and H₂-CCGT can only be installed from 2025 on.

All technical and economic parameters of new build storages are assumed constant over the planning horizon 2010–2050. The technical parameters – which are valid in the reference scenario as well as in all variation scenarios – are presented in Table 5.18. All values are taken from Kuhn *et al.* (2012). As for existing PSP, losses due to self-discharge are neglected for all three new build technologies.

The minimum and maximum values specified in Table 5.18 refer to the size of discharging units of storages. They are used in the submodel MOGLIE to break down new build capacities obtained in MESTAS to plant level (vide Section 3.2.3).

As charging, discharging and storage capacities are rated independently in MESTAS, the economic parameters of new build storages are specified separately for the relevant storage dimensions (vide Table 5.19). Whereas investment costs of new build storages are varied in Section 5.5.6, the values given for annual fixed costs, variable O&M costs and decommissioning costs are valid in all scenarios.

Table 5.18: Technical parameters of new build storages by storage technology

| | | PSP | AA-CAES | H₂-CCGT |
|------------------------------|--------------|------------|----------------|---------------------------|
| round-trip efficiency | <i>in %</i> | 80 | 70 | 40 |
| minimum size | <i>in MW</i> | 50 | 10 | 200 |
| maximum size | <i>in MW</i> | 1000 | 300 | 800 |

Source: Kuhn *et al.* (2012).

Table 5.19: Economic parameters of new build storages by storage technology as assumed in the reference scenario

| | | PSP | AA-CAES | H₂-CCGT |
|--|-------------------------------|------------|----------------|---------------------------|
| invest. costs: charging | <i>in €/kW_{el}</i> | 450.97 | 421.63 | 1000.00 |
| invest. costs: discharging | <i>in €/kW_{el}</i> | 450.97 | 421.63 | 729.00 |
| invest. costs: storage | <i>in €/kWh_{el}</i> | 6.34 | 30.65 | 0.09 |
| fixed costs: charging | <i>in €/kW_{el}-a</i> | 5.59 | 4.47 | 10.06 |
| fixed costs: discharging | <i>in €/kW_{el}-a</i> | 5.59 | 4.47 | 10.06 |
| var. O&M costs: charging | <i>in €/MWh_{el}</i> | 0.28 | 1.40 | 1.51 |
| var. O&M costs: discharging | <i>in €/MWh_{el}</i> | 0.28 | 1.40 | 1.51 |
| decomm. costs: charging | <i>in €/kW_{el}</i> | 4.17 | 1.04 | 4.17 |
| decomm. costs: discharging | <i>in €/kW_{el}</i> | 4.17 | 1.04 | 4.17 |

Source: Kuhn *et al.* (2012).

As described in Section 3.2.2, the non-variable costs of charging, discharging and storage capacity can optionally be reduced by a bonus to account for potential contribution margins earned on markets that are not endogenously modelled in MESTAS. In the reference scenario, a bonus of 50 %, which is suggested by Kuhn *et al.* (2012), is assumed. It is valid for all new build storage technologies.

With regard to the lifetime of new build storages, 70 years are assumed for PSP, while 30 years are assumed both for AA-CAES and hydrogen storage plants (Kuhn *et al.* 2012). These assumptions are valid for all scenarios.

Whereas expansion is not constrained in case of AA-CAES and H₂-CCGT, the additional storage capacity of PSP is limited to 40 GWh (about half of the existing capacity) in the reference scenario as well as in all variation scenarios. This estimate of the remaining potential of PSP in Germany is based on Kuhn *et al.* (2012) and reflects both limited topographic potential and low public acceptance. Moreover, as discharging and charging units of modern PSP are usually combined in one pump-turbine, the ratio of discharging to charging capacity of new build PSP is limited to a range from 0.8 to 1.2 (vide Kuhn *et al.* 2012).

Assumptions on energy availability and unavailability of new build storages are valid for the reference scenario and throughout the variation scenarios. In case of PSP, the same parameters are used as for existing storage plants (vide Table 5.11). For AA-CAES and H₂-CCGT, a technical reliability of 90 % and a planned unavailability of 3.8 % (two weeks of maintenance) are assumed as in Kuhn *et al.* (2012). The corresponding energy availability amounts to 86.6 % (vide Table 5.20).

Table 5.20: Energy availability, planned and unplanned energy unavailability and technical reliability of new build storages by storage technology

| <i>in %</i> | PSP | AA-CAES | H₂-CCGT |
|---------------------------------|------------|----------------|---------------------------|
| energy availability | 91.4 | 86.6 | 86.6 |
| planned unavailability | 3.8 | 3.8 | 3.8 |
| unplanned unavailability | 4.8 | 9.6 | 9.6 |
| technical reliability | 95.0 | 90.0 | 90.0 |

Source: Kuhn *et al.* (2012); own calculations.

5.2.10 Overall emissions target

As already stated in Section 5.2.1, carbon emissions are constrained over the whole planning horizon. In order to define an overall emissions target for the German power sector, national policies on emissions reduction are consulted. In BMWi & BMU (2010), the German government committed to the reduction of GHG emissions by 40 % until 2020 and by 80 % until 2050 (on 1990 levels). If carbon emissions targets for the German power sector are defined in proportion to national GHG reduction targets, emissions will have to be reduced from 357 million tonnes CO₂ in 1990 (Icha 2014) to 214 million tonnes in 2020 and 71 million tonnes in 2050.

By assuming linear reduction paths between 1990 and 2020 as well as between 2020 and 2050, the total carbon emissions budget over the planning horizon 2010–2050 can be estimated for the German power sector: The annual emissions targets add up to 6831 million tonnes CO₂. This total carbon emissions budget is valid for the reference scenario as well as for the variation scenarios.

However, not the whole budget can be spent endogenously by the model. The annual emissions targets actually have to be reduced: first, by an estimated 2 % to account for emissions related to start-up losses (which are not modelled endogenously); and, secondly, by emissions of exogenously defined electricity generation from fossil CHP.

In order to determine the latter, the average emission intensity of electricity generation from fossil CHP is calculated using the so-called “Finnish method” (Mauch *et al.* 2010). While the average CHP coefficient, i. e. the ratio of electrical power to heat, is assumed to increase linearly from 0.46 in 2010 to 0.72 in 2050 (Nitsch *et al.* 2012), the overall efficiency is assumed to remain constant at 90 % for all types of cogeneration units. The development of the structure of electricity generation from fossil CHP outlined in Nitsch *et al.* (2012) is adopted and supplemented by linear interpolation (vide Table 5.21). It should be noted that only the relative amounts of electricity generation are relevant for determining the average emission intensity of fossil CHP.

The method furthermore requires the definition of conventional reference technologies of heat and electricity generation: Corresponding with parameters of new build generation technologies defined in Section 5.2.8, an efficiency of 61 % is assumed for gas-fired power plants. While before 2020 45 % and 46 % are assumed for lignite- and hard coal-fired power plants respectively, 50 % and 51 % are assumed from 2020 on. The efficiency of conventional heat generation is estimated at 80 %.

The resulting average emission intensity of electricity generation from fossil CHP amounts to 0.3382 tonnes CO₂ per MWh of electricity produced in 2010. Until 2050, intensity decreases to 0.2936 tonnes CO₂ per MWh of electricity produced. The average emission intensities are then used to determine the annual emissions associated with the annual amounts of electricity generation from fossil CHP.

For the reference scenario, the reduced annual emissions targets add up to a total carbon emissions budget of 5973 million tonnes CO₂ that can be spent by the model over the whole planning horizon 2010–2050.

As fossil CHP generation and, thus, related emissions are dependent on temperature, the amount of emissions that can be spent by the model has to be adjusted when annual time series are varied in Section 5.5.1. Table 5.22 presents the overall emissions targets resulting for the different sets of annual time series that were established in Section 5.2.4. As the year 2012 is selected as the meteorological reference year for the reference scenario (vide Section 5.3.3), the overall emissions target for the reference scenario can be found in the respective column in Table 5.22.

Table 5.21: Development of annual electricity generation from fossil CHP in Germany by fuel

| <i>in TWh/a</i> | 2010 | 2015 | 2020 | 2025 | 2030 | 2040 | 2050 |
|--------------------|-------------|-------------|-------------|-------------|-------------|-------------|-------------|
| lignite | 4.9 | 3.3 | 1.8 | 1.4 | 1.4 | 1.1 | 0.5 |
| hard coal | 13.3 | 14.3 | 15.1 | 13.5 | 12.3 | 7.8 | 7.2 |
| natural gas | 56.9 | 61.6 | 86.1 | 84.8 | 73.9 | 58.6 | 43.5 |

Source: Nitsch *et al.* (2012).

Table 5.22: Overall CO₂ emissions target for the planning horizon 2010–2050 (assuming different annual time series of fossil CHP generation)

| <i>in million t</i> | 2003 | 2004 | 2005 | 2006 | 2007 | 2008 | 2009 | 2010 | 2011 | 2012 |
|---------------------|-------------|-------------|-------------|-------------|-------------|-------------|-------------|-------------|-------------|-------------|
| emissions | 5965 | 5965 | 5969 | 5973 | 5986 | 5975 | 5977 | 5938 | 5987 | 5973 |

5.3 Selecting a meteorological reference year

5.3.1 Characterising annual time series of demand and generation

In order to select a certain year from the period 2003–2012 that is deemed representative and thus can be used as a meteorological reference year, the annual time series of demand and generation need to be characterised with regard to relevant properties. A quantity that is commonly used to characterise time series of renewable electricity generation is either the capacity factor or the corresponding FLH (Giebel 2000, Jarass *et al.* 2009, Janker 2015). Definitions of capacity factor and FLH are given by Kaltschmitt *et al.* (2014). Both quantities can be used analogously to characterise time series of electricity demand.

When annual time series of generation or demand are considered, the capacity factor specifies the ratio of the energy actually produced (or consumed) over one year to the potential energy that would be produced (or consumed) if the generating unit was operating at rated power for 8760 h (or if power was consumed at rated power for 8760 h). Correspondingly, FLH specify the number of hours it would take to produce (or consume) the energy actually produced (or consumed) over one year at rated power. FLH are easily obtained by multiplying the capacity factor by 8760 h.

Table 5.23 shows FLH of demand and generation from wind, solar and CHP for the period 2003–2012 in Germany, based on the set of annual time series that was established in Section 5.2.4. While FLH of generation time series refer to the installed generation capacity, FLH of demand time series are scaled to the annual maximum load. This maximum load is constant for each year, as according to Heilek (2006) the electrical load already peaks at an outside temperature of 2 °C, a temperature level that is undercut regularly in Germany even in relatively warm winters.

Table 5.23: FLH of demand and generation time series for the period 2003–2012 in Germany

| <i>in h</i> | 2003 | 2004 | 2005 | 2006 | 2007 | 2008 | 2009 | 2010 | 2011 | 2012 |
|-------------------|-------------|-------------|-------------|-------------|-------------|-------------|-------------|-------------|-------------|-------------|
| on. wind | 1375 | 1609 | 1490 | 1493 | 1811 | 1699 | 1465 | 1379 | 1660 | 1558 |
| off. wind | 2955 | 3414 | 3425 | 3230 | 3619 | 3600 | 3306 | 3109 | 3575 | 3470 |
| solar | 973 | 900 | 936 | 874 | 911 | 864 | 907 | 870 | 955 | 898 |
| fossil CHP | 3354 | 3356 | 3338 | 3319 | 3259 | 3308 | 3302 | 3481 | 3255 | 3320 |
| biomass | 5547 | 5552 | 5521 | 5491 | 5390 | 5471 | 5462 | 5757 | 5385 | 5491 |
| demand | 6706 | 6704 | 6698 | 6692 | 6688 | 6702 | 6692 | 6711 | 6688 | 6695 |

Source: own calculations based on Janker (2015).

As hydropower and geothermal generation are assumed to be unaffected by annual weather variations, respective FLH were not included in the table. For the time series of hydro generation described in Section 5.2.4, FLH amount to 4926 h, while FLH amount to 8760 h for geothermal generation, which is assumed constant throughout the year.

As intended, a dependence on temperature is observed for both electricity demand and generation from fossil CHP and biomass generation. FLH – and thus the amount of energy either consumed or generated annually – reach their highest level in the coldest year of the considered period, 2010, whereas the lowest number of FLH is observed in 2011, which is the warmest year of the period (vide Table 5.4). The annual time series of the year 2007 offer the highest number of FLH for onshore and offshore wind, while the highest level of solar generation is observed in 2003.

For validation purposes, FLH calculated from the annual time series of onshore wind generation were compared with historical values of onshore wind generation in Germany presented in Czakainski *et al.* (2013). As Figure 5.4 shows, there is a good concordance between FLH calculated from the annual time series and the historical data in terms of both absolute values and relative variation between years.

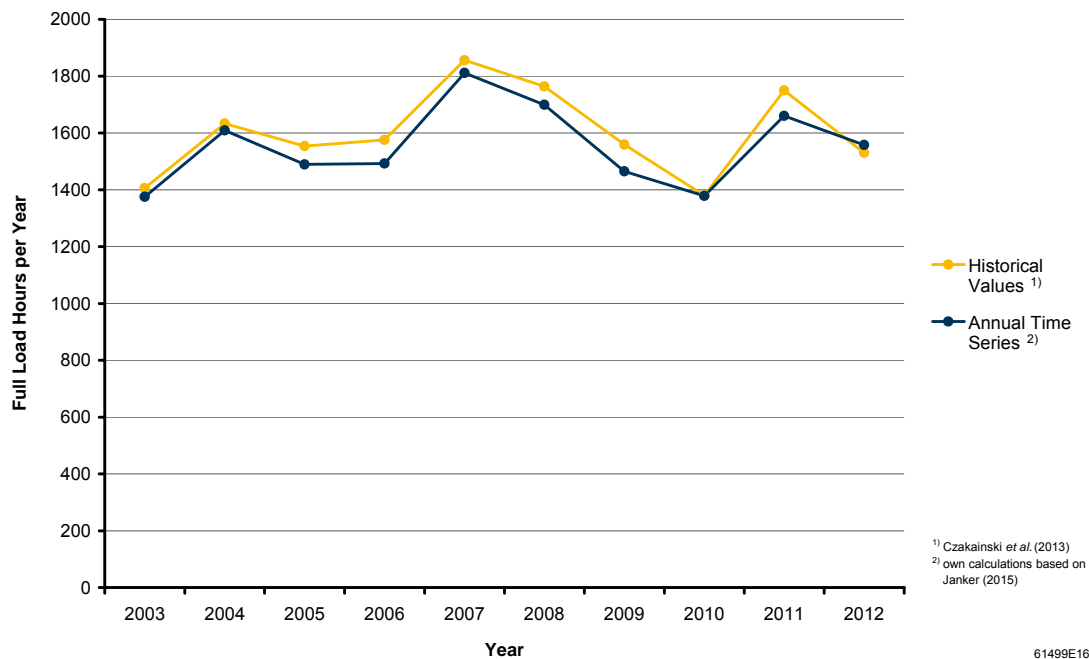


Figure 5.4: Comparison of FLH of onshore wind generation based on annual time series and historical values for the period 2003–2012 in Germany

While FLH and capacity factor indicate the level of utilisation of installed capacity, they generally do not give any information on the distribution of energy over time, i. e. whether energy is spread very evenly over the considered period or whether generation (or consumption) is fluctuating, intermittent or even occurring only in a single, contiguous, but short period of time. However, very high numbers of FLH usually indicate a more even distribution of energy and a capacity factor of 1 is only possible if generation (or consumption) is constantly at the level of rated power.

In addition to FLH, Giebel (2000) uses the minimum and maximum power output and the standard deviation to characterise time series of wind generation. Whereas minimum, maximum and standard deviation are appropriate for measuring the smoothing effect of dispersed generation as in the analysis presented by Giebel (2000), they are less significant with regard to inter-annual variations.

Table 5.24 and Table 5.25 show the minimum and maximum power of demand and generation from wind, solar and CHP for the period 2003–2012 in Germany, based on the set of annual time series that was established in Section 5.2.4. Both quantities are apparently subject to only very little variation between years. This holds for time series of generation as well as for time series of demand.

As aforementioned, the annual maximum load reaches the same level in each year, as temperature regularly drops below the threshold of 2 °C. For offshore wind generation a maximum power output of 90 % of installed capacity is observed for all years. It is determined by the performance factor of 0.9 estimated in Janker (2015), which considers the technical availability of wind turbines as well as the wake effect of wind farms.

Table 5.24: Minimum power of demand and generation time series for the period 2003–2012 in Germany (scaled to annual maximum load and installed capacity respectively)

| | 2003 | 2004 | 2005 | 2006 | 2007 | 2008 | 2009 | 2010 | 2011 | 2012 |
|-------------------|------|------|------|------|------|------|------|------|------|------|
| on. wind | 0.00 | 0.00 | 0.00 | 0.00 | 0.00 | 0.00 | 0.00 | 0.00 | 0.00 | 0.00 |
| off. wind | 0.00 | 0.00 | 0.00 | 0.00 | 0.00 | 0.00 | 0.00 | 0.00 | 0.00 | 0.00 |
| solar | 0.00 | 0.00 | 0.00 | 0.00 | 0.00 | 0.00 | 0.00 | 0.00 | 0.00 | 0.00 |
| fossil CHP | 0.12 | 0.13 | 0.12 | 0.13 | 0.13 | 0.13 | 0.13 | 0.12 | 0.14 | 0.13 |
| biomass | 0.49 | 0.49 | 0.49 | 0.49 | 0.48 | 0.49 | 0.48 | 0.51 | 0.48 | 0.49 |
| demand | 0.45 | 0.44 | 0.44 | 0.43 | 0.43 | 0.43 | 0.43 | 0.45 | 0.43 | 0.44 |

Source: own calculations based on Janker (2015).

Table 5.25: Maximum power of demand and generation time series for the period 2003–2012 in Germany (scaled to annual maximum load and installed capacity respectively)

| | 2003 | 2004 | 2005 | 2006 | 2007 | 2008 | 2009 | 2010 | 2011 | 2012 |
|-------------------|------|------|------|------|------|------|------|------|------|------|
| on. wind | 0.86 | 0.90 | 0.89 | 0.89 | 0.90 | 0.90 | 0.83 | 0.88 | 0.88 | 0.90 |
| off. wind | 0.90 | 0.90 | 0.90 | 0.90 | 0.90 | 0.90 | 0.90 | 0.90 | 0.90 | 0.90 |
| solar | 0.69 | 0.70 | 0.68 | 0.70 | 0.70 | 0.69 | 0.71 | 0.69 | 0.69 | 0.70 |
| fossil CHP | 0.96 | 0.91 | 0.94 | 0.99 | 0.92 | 0.82 | 0.98 | 0.96 | 0.92 | 1.00 |
| biomass | 0.98 | 0.95 | 0.97 | 0.99 | 0.96 | 0.91 | 0.99 | 0.98 | 0.98 | 1.00 |
| demand | 1.00 | 1.00 | 1.00 | 1.00 | 1.00 | 1.00 | 1.00 | 1.00 | 1.00 | 1.00 |

Source: own calculations based on Janker (2015).

Table 5.26: Standard deviation of demand and generation time series for the period 2003–2012 in Germany (scaled to annual maximum load and installed capacity respectively)

| | 2003 | 2004 | 2005 | 2006 | 2007 | 2008 | 2009 | 2010 | 2011 | 2012 |
|-------------------|------|------|------|------|------|------|------|------|------|------|
| on. wind | 0.17 | 0.19 | 0.18 | 0.17 | 0.20 | 0.20 | 0.16 | 0.16 | 0.19 | 0.17 |
| off. wind | 0.27 | 0.28 | 0.27 | 0.27 | 0.29 | 0.28 | 0.26 | 0.26 | 0.28 | 0.26 |
| solar | 0.17 | 0.17 | 0.17 | 0.16 | 0.17 | 0.16 | 0.17 | 0.16 | 0.17 | 0.16 |
| fossil CHP | 0.20 | 0.19 | 0.19 | 0.20 | 0.17 | 0.17 | 0.19 | 0.21 | 0.18 | 0.19 |
| biomass | 0.12 | 0.11 | 0.12 | 0.12 | 0.11 | 0.11 | 0.12 | 0.12 | 0.11 | 0.12 |
| demand | 0.14 | 0.14 | 0.14 | 0.14 | 0.14 | 0.14 | 0.14 | 0.14 | 0.14 | 0.14 |

Source: own calculations based on Janker (2015).

The standard deviation of demand and generation time series is presented in Table 5.26. The level of standard deviation differs considerably for the different types of time series, but again inter-annual variations are not significant.

Minimum and maximum power as well as standard deviation only indicate the level of variation of time series, i. e. whether generation (or consumption) is constant or varying and, in the latter case, how large and how frequent deviations from the mean are. They do not characterise the distribution of energy over time. However, the information whether generation (or consumption) is subject to intra-day variability or whether it is dominated by intra-annual (i. e. seasonal) fluctuations can be very useful and is apparently essential when time series are used as an input to analyses of energy storage demand.

Kuhn (2012) observed a high sensitivity of storage capacity expansion, particularly for long-duration storage technologies, to different input time series of wind genera-

tion and found a correlation between the seasonality of wind time series and the economic feasibility of long-duration storages capable of balancing seasonal fluctuations. The seasonality of time series is analysed in Kuhn (2012) by cumulating the hourly values of wind generation time series that are scaled to the annual energy production. Figure 5.5 shows the resulting curves for onshore wind generation for the years 2005, 2009 and 2012 in Germany, based on the set of annual time series that was established in Section 5.2.4. As a reference, an additional line is included that indicates a constant hourly power output throughout the whole year.

By examining the depicted curves, it is possible to distinguish the annual time series of onshore wind generation with regard to the seasonal occurrence of generation. While in case of the year 2005 already more than 50 % of the total annual energy is generated within the first 3285 hours of the year, 50 % of the total annual energy is reached only after approximately 3700 h in 2012. By contrast, the generation from onshore wind stays relatively close to the line of constant hourly power output during the first half of the year 2009 and more or less reaches 50 % of the total annual energy after 4380 h. Whereas by this means the seasonality of time series can be evaluated qualitatively, a general method to also quantitatively characterise the occurrence of generation (or consumption) over time would be desirable.

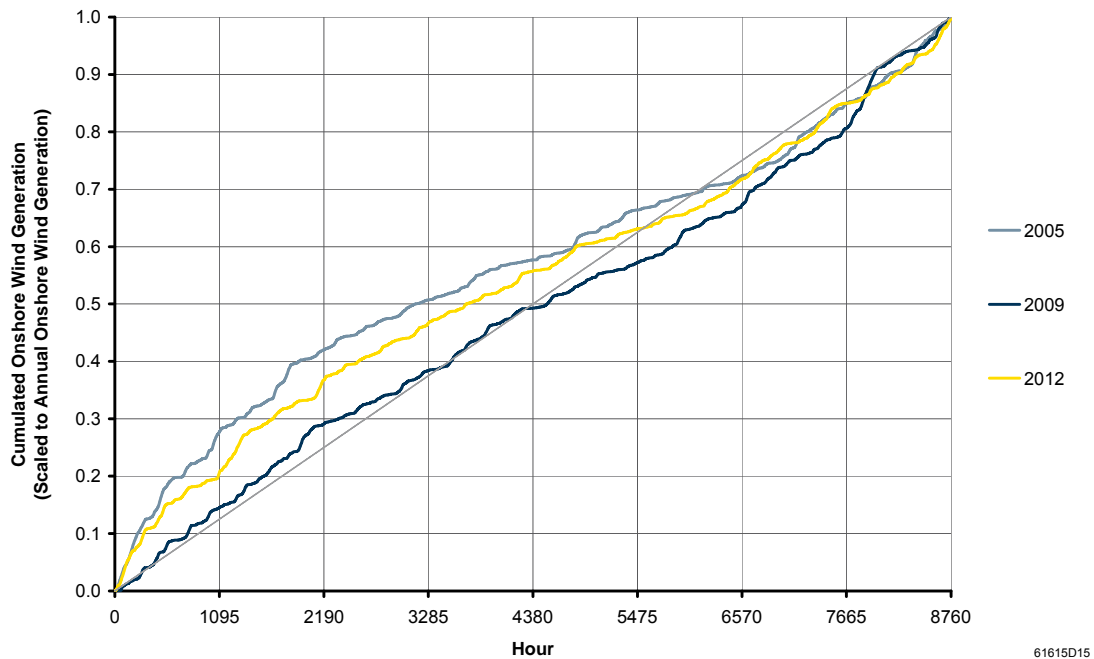


Figure 5.5: Cumulated hourly values of onshore wind generation for the years 2005, 2009 and 2012 in Germany (scaled to annual onshore wind generation)

Janker (2015) developed a quantitative method to measure the temporal distribution of energy by introducing so-called variability indices for the high-, mid- and low-frequency components of generation and demand time series. While the high-frequency variability index $V_{high-freq}$ measures the intra-day variability of the considered time series, the intra-annual variability or seasonality of the time series is characterised by the low-frequency variability index $V_{low-freq}$. Fluctuations with period T of more than one day but less than one month are captured by the mid-frequency variability index $V_{mid-freq}$.

In order to obtain the variability indices, the theoretical storage capacities $C_{theoretical}$ necessary to balance all fluctuations of generation (or consumption) within the respective frequency ranges fr are determined. These capacities are scaled to the corresponding worst-case storage capacities $C_{worst-case}$ that would be necessary if generation (or consumption) occurred with maximum power over a contiguous period of time. The resulting variability indices are normalised values and are adjusted for energy. A variability index of zero indicates that the time series is not composed of fluctuations within the respective frequency range, while values greater than zero indicate the relative size of storage capacity theoretically necessary to balance all fluctuations. For a detailed description of the method used in this thesis to calculate variability indices of generation and demand time series, vide Appendix B.1.

Table 5.27 shows the low-frequency variability of demand and generation from wind, solar and CHP for the period 2003–2012 in Germany, based on the set of annual time series that was established in Section 5.2.4. The mid- and high-frequency variability indices are presented in Table 5.28 and Table 5.29 respectively.

Table 5.27: Low-frequency variability index of demand and generation time series for the period 2003–2012 in Germany

| | 2003 | 2004 | 2005 | 2006 | 2007 | 2008 | 2009 | 2010 | 2011 | 2012 |
|-------------------|------|------|------|------|------|------|------|------|------|------|
| on. wind | 0.80 | 0.82 | 0.96 | 0.72 | 0.93 | 0.91 | 0.74 | 0.91 | 0.90 | 0.84 |
| off. wind | 0.80 | 0.87 | 0.96 | 0.78 | 0.80 | 0.91 | 0.84 | 0.99 | 0.76 | 0.88 |
| solar | 1.00 | 1.00 | 1.00 | 1.00 | 1.00 | 1.00 | 1.00 | 1.00 | 1.00 | 1.00 |
| fossil CHP | 1.00 | 1.00 | 1.00 | 1.00 | 1.00 | 1.00 | 1.00 | 0.99 | 1.00 | 1.00 |
| biomass | 1.00 | 1.00 | 1.00 | 1.00 | 1.00 | 1.00 | 1.00 | 0.99 | 1.00 | 1.00 |
| demand | 1.00 | 1.00 | 1.00 | 1.00 | 1.00 | 1.00 | 1.00 | 1.00 | 1.00 | 0.99 |

Source: own calculations based on Janker (2015).

Table 5.28: Mid-frequency variability index of demand and generation time series for the period 2003–2012 in Germany

| | 2003 | 2004 | 2005 | 2006 | 2007 | 2008 | 2009 | 2010 | 2011 | 2012 |
|-------------------|------|------|------|------|------|------|------|------|------|------|
| on. wind | 0.52 | 0.55 | 0.53 | 0.53 | 0.60 | 0.49 | 0.53 | 0.46 | 0.69 | 0.46 |
| off. wind | 0.56 | 0.53 | 0.48 | 0.63 | 0.55 | 0.62 | 0.44 | 0.46 | 0.58 | 0.48 |
| solar | 0.42 | 0.40 | 0.37 | 0.33 | 0.36 | 0.26 | 0.26 | 0.36 | 0.30 | 0.31 |
| fossil CHP | 0.62 | 0.62 | 0.56 | 0.62 | 0.67 | 0.62 | 0.70 | 0.63 | 0.72 | 0.60 |
| biomass | 0.61 | 0.58 | 0.54 | 0.64 | 0.70 | 0.63 | 0.68 | 0.64 | 0.70 | 0.57 |
| demand | 0.53 | 0.53 | 0.54 | 0.53 | 0.52 | 0.53 | 0.52 | 0.53 | 0.55 | 0.55 |

Source: own calculations based on Jancker (2015).

Table 5.29: High-frequency variability index of demand and generation time series for the period 2003–2012 in Germany

| | 2003 | 2004 | 2005 | 2006 | 2007 | 2008 | 2009 | 2010 | 2011 | 2012 |
|-------------------|------|------|------|------|------|------|------|------|------|------|
| on. wind | 0.70 | 0.66 | 0.80 | 0.74 | 0.88 | 0.63 | 0.63 | 0.71 | 0.68 | 0.75 |
| off. wind | 0.72 | 0.73 | 0.70 | 0.84 | 0.85 | 0.65 | 0.67 | 0.69 | 0.86 | 0.63 |
| solar | 1.02 | 1.00 | 1.00 | 1.03 | 1.02 | 1.02 | 0.99 | 1.02 | 1.00 | 0.97 |
| fossil CHP | 0.97 | 1.00 | 1.02 | 0.96 | 0.93 | 1.01 | 1.00 | 0.98 | 1.00 | 0.99 |
| biomass | 0.99 | 1.02 | 1.04 | 0.97 | 0.97 | 1.03 | 1.00 | 0.98 | 1.00 | 0.99 |
| demand | 0.95 | 0.95 | 0.94 | 0.95 | 0.95 | 0.95 | 0.95 | 0.95 | 0.95 | 0.95 |

Source: own calculations based on Jancker (2015).

The low-frequency variability of onshore and offshore wind generation varies considerably between years, but with a minimum variability index of 0.72 and 0.76 respectively both onshore and offshore wind are generally subject to significant seasonal fluctuation. The impression received from the qualitative analysis of seasonality of onshore wind generation in Figure 5.5 is confirmed by the calculated low-frequency variability indices: With a value of 0.96 the annual time series of 2005 shows more seasonal characteristics than the time series of 2012 (0.84) or 2009 (0.74). Due to the pronounced seasonal variation of solar radiation and outside temperature, time series of solar and CHP generation as well as demand exhibit the maximum value of low-frequency variability in almost every year.

Mid-frequency variability is observed to be lower than low-frequency variability for all types of generation as well as for demand. Apparently, solar generation is less dominated by mid-frequency fluctuations than wind generation. By contrast, the high-frequency variability of wind is considerably lower than for solar. While over a relatively large area like Germany wind conditions change rather slowly, solar radia-

tion is naturally governed by the day-night cycle and thus time series of solar generation exhibit high-frequency variability indices close to 1. As expected, intra-day fluctuations of electricity and heat demand furthermore lead to a very high level of high-frequency variability for time series of electricity demand and CHP generation.

While the observation of high-frequency variability indices greater than 1 is probably unexpected, it is still plausible. Whereas the whole high-frequency component of a time series is zero-mean, the individual 24 h-intervals do not necessarily have to be. As the theoretical storage capacity $C_{theoretical, high-freq}$ is defined to balance all intra-day fluctuations over one year, it can actually become larger than the worst-case storage capacity $C_{worst-case, high-freq}$, which is determined based on only one 24 h-interval. Analogously, a variability index greater than 1 is also possible for the mid-frequency range, while the low-frequency variability index is limited to 1, as in this case the worst-case storage capacity $C_{worst-case, low-freq}$ is determined based on the whole year (vide Appendix B.1).

Janker (2015) showed that the theoretical storage capacity $C_{theoretical, low-freq}$ necessary to balance all low-frequency fluctuations of a wind generation time series is already a good indicator of the long-duration storage capacity installed by a cost minimisation model to balance seasonal fluctuations of wind generation. This theoretical storage capacity is dependent on both FLH and the low-frequency variability of the time series. Hence, when time series of generation or demand are characterised in the context of energy storage demand, not only FLH but also the low-frequency variability index of time series should be consulted.

Whereas the variability indices for the mid- and high-frequency components are helpful to characterise the distribution of energy over smaller time horizons, they are less significant with regard to storage demand, as the defined ranges of period T do not necessarily coincide with the duration of storage cycles observed for mid- and short-duration storages. For instance, PSP are usually described as short-duration storage, but often a full storage cycle is completed within a few days to one week rather than within 24 h. On this account, only the low-frequency variability index is used in this thesis to characterise time series of generation and demand with regard to the distribution of energy over time.

5.3.2 Characterising annual time series of residual demand

The separate analysis of annual time series of generation and demand will not always allow the unambiguous identification of the most representative year, as the characteristics of different time series may point to different years. Furthermore, if a power

system comprises must-run generation from several sources, it is the residual demand that crucially affects decisions concerning the design and operation of the conventional generation and storage portfolio.

Thus, in order to select a meteorological reference year from the period 2003–2012, also the annual time series of residual demand have to be characterised with regard to relevant properties. However, as the residual demand depends on the individual shares of RES and CHP generation, an analysis is only possible if the respective shares are given.

Whereas for non-negative time series like generation and demand time series FLH can be used to measure the amount of energy generated (or consumed), it is not possible to calculate FLH for time series of residual demand, which can generally take both positive and negative values. Instead, two quantities have to be consulted to characterise such time series: the residual energy demand, i. e. the sum of all positive hourly values, and the surplus energy, i. e. the sum of all negative hourly values.

While residual energy demand and surplus energy can be used directly to characterise time series of residual demand, it is also possible to scale these amounts of energy to the annual maximum load of the original demand time series. In the latter case, a representation very similar to FLH is obtained, as residual energy demand and surplus energy are measured in MWh per MW maximum load.

As aforementioned, the low-frequency variability of a time series is a good indicator of long-duration storage capacity. Hence, it is furthermore desirable to also characterise time series of residual demand in terms of low-frequency variability. The method applied in Section 5.3.1 to determine variability indices for time series of generation and demand is therefore adapted such that it is also applicable for time series of residual demand. For a detailed description of the method used in this thesis, vide Appendix B.2.

Again, the resulting variability indices are normalised values and are adjusted for energy. The indices indicate the relative size of storage capacity theoretically necessary to balance all fluctuations of residual demand within the respective frequency ranges. The method was first presented in Kühne *et al.* (2014), where it was also shown that the analysis of low-frequency variability of residual demand time series improves the understanding of results for long-duration storage demand obtained with the whole-systems cost minimisation model IMAKUS.

It was furthermore shown that the low-frequency variability index $V_{low-freq}$ and the corresponding theoretical storage capacity $C_{theoretical,low-freq}$ are even better indicators of long-duration storage demand if the full integration of surplus generation is required, i. e. if curtailment is not allowed. As for time series of generation and de-

mand, only the low-frequency variability index is used in this thesis to characterise time series of residual demand with regard to the distribution of energy over time.

5.3.3 *Approach to selecting a reference year*

As storage demand is largely influenced by the chronological characteristics of generation and demand, it is necessary to base the reference scenario on a meteorological reference year that represents the typical characteristics of annual time series of generation, demand and residual demand. A set of quantities was identified in the previous sections that shall be used to characterise these time series: FLH, residual energy demand and surplus energy as well as the low-frequency variability index.

While for time series of generation or demand FLH indicate the level of utilisation of installed capacity, the amount of energy contained in a residual demand time series has to be measured separately in terms of residual energy demand (positive) and surplus energy (negative). The low-frequency variability index measures the seasonal distribution of energy and thus is an indicator of long-duration storage demand.

In order to be selected as the meteorological reference year, the year in question should exhibit annual time series of generation and demand that are average both in terms of FLH and in terms of low-frequency variability. Furthermore, and, as capacity expansion and dispatch are ultimately determined by residual demand, even more importantly, the corresponding time series of residual demand should be average in terms of residual energy demand, surplus energy and low-frequency variability.

To begin with, the annual time series of generation and demand are analysed. FLH and low-frequency variability were already presented in Table 5.23 and Table 5.27 respectively. A graphical representation of these quantities can be used to identify the year which is closest to the respective mean values for the period 2003–2012. As the two quantities cannot be prioritised with respect to their impact on storage demand, the Euclidean metric is used to evaluate the distance between two points in the FLH-variability plane.

For each year of the considered period, Figure 5.6 shows FLH and the low-frequency variability index of onshore wind generation in Germany, based on the set of annual time series that was established in Section 5.2.4. Analogously, Figure 5.7 shows the annual values of FLH and low-frequency variability of offshore wind generation in Germany. As a reference, the figures also indicate the mean values of FLH and low-frequency variability calculated for the period 2003–2012 as well as the corresponding standard deviations.

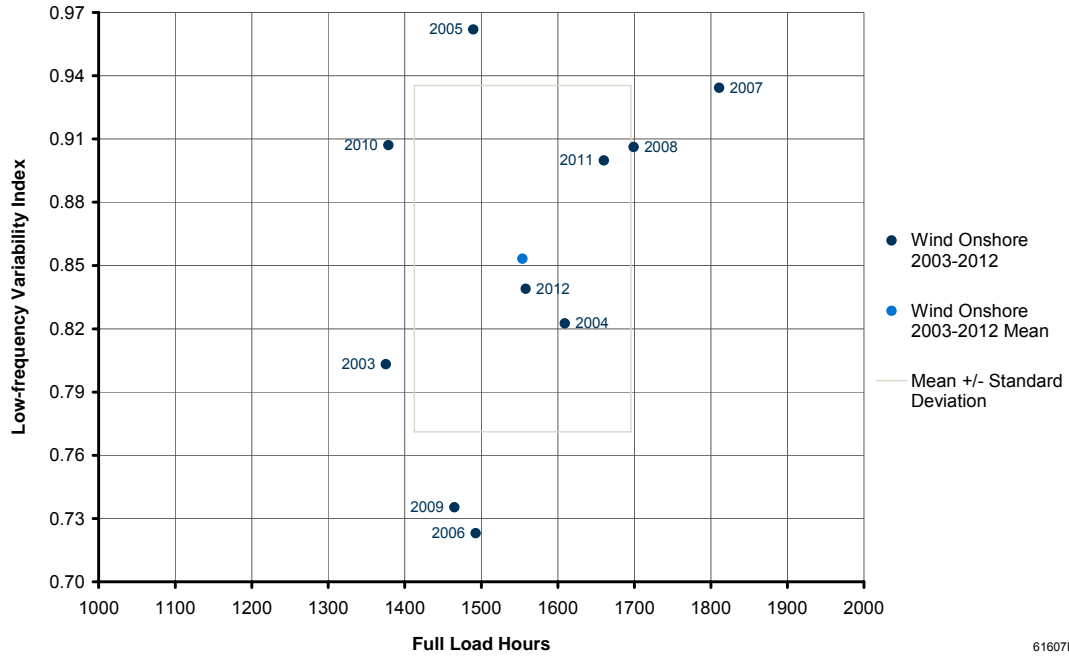


Figure 5.6: FLH and low-frequency variability of annual time series of onshore wind generation

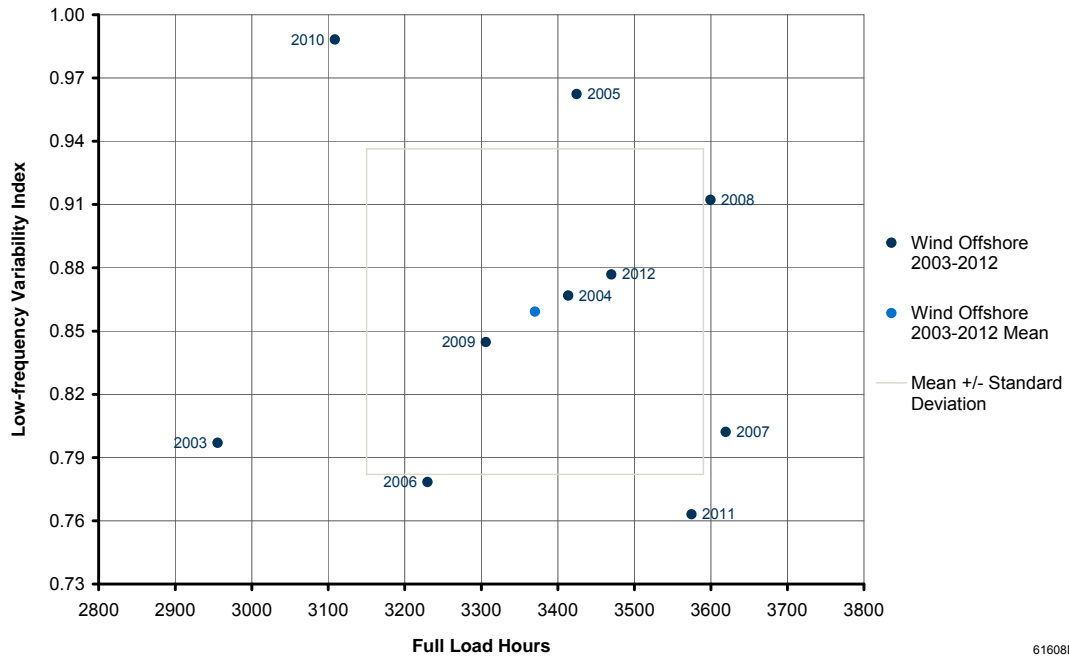


Figure 5.7: FLH and low-frequency variability of annual time series of offshore wind generation

For onshore wind generation the three years 2004, 2011 and 2012 are within the limits of standard deviation from the mean values of FLH and low-frequency variability. For offshore wind generation the three years 2004, 2009 and 2012 are found within the limits of standard deviation. Whereas with regard to onshore wind 2012 is the year that clearly comes closest to the ten-year average values of FLH and low-frequency variability, 2004 and 2009 are observed to be more typical with regard to the characteristics of offshore wind generation.

Figure 5.8 shows FLH and the low-frequency variability index of solar generation in Germany for each year of the period 2003–2012.

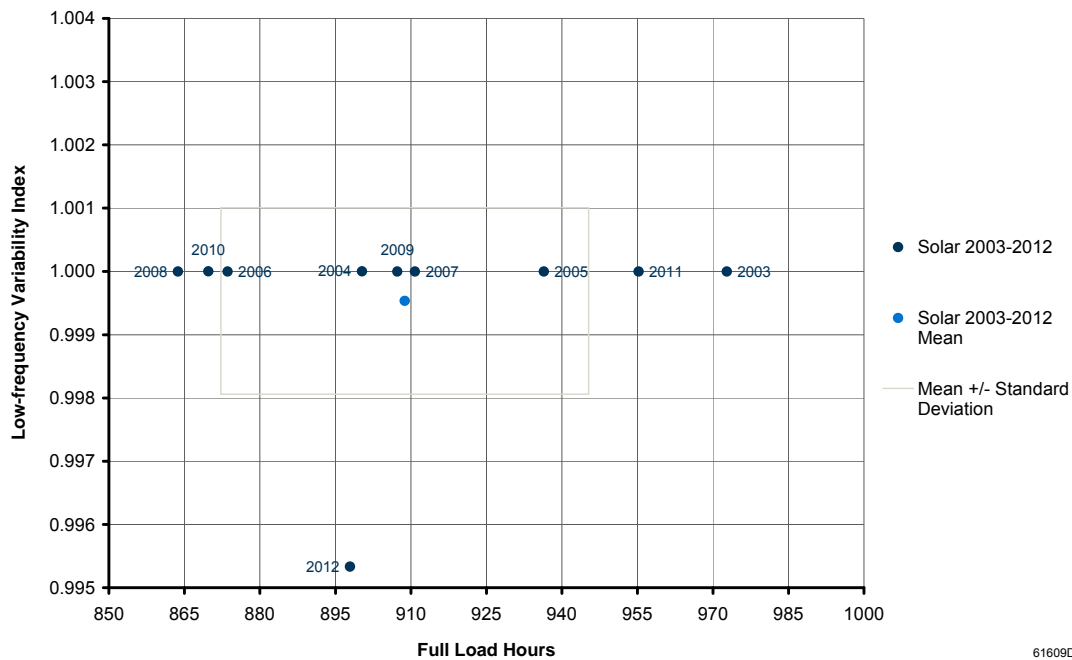


Figure 5.8: FLH and low-frequency variability of annual time series of solar generation

As it could already be observed from Table 5.27, due to the pronounced seasonal variation of solar radiation, solar generation reaches the maximum value of low-frequency variability practically every year. Given the scale of the axis, the deviation from the maximum index for the year 2012 is apparently negligible. With regard to FLH the years 2004, 2007, 2009 and 2012 all come very close to the ten-year average.

Similar to solar generation, time series of generation from fossil CHP and biomass exhibit the maximum value of low-frequency variability in almost every year, which in this case is due to the pronounced seasonal variation of outside temperature. For both sources of generation the largest deviation from the maximum index that could be observed in Table 5.27 amounted to a low-frequency variability index of 0.99 in 2010. With regard to FLH the mean value for the period 2003–2012 amounts to 3329 h in case of fossil CHP generation and, according to Table 5.23, the annual FLH of 2005 and 2012 come very close to this value. The ten-year average value of FLH for biomass generation amounts to 5507 h, which is also best approximated by time series of the years 2005 and 2012.

Figure 5.9 shows FLH and the low-frequency variability index of electricity demand in Germany for each year of the period 2003–2012. As for CHP generation, the pronounced seasonal variation of outside temperature also leads to very high levels of low-frequency variability for demand. The largest, but apparently still negligible deviation from the maximum index amounts to a low-frequency variability index of approximately 0.99 in 2012. While in terms of FLH several years are well within the limits of standard deviation, annual FLH of the years 2005 and 2012 come closest to the ten-year average.

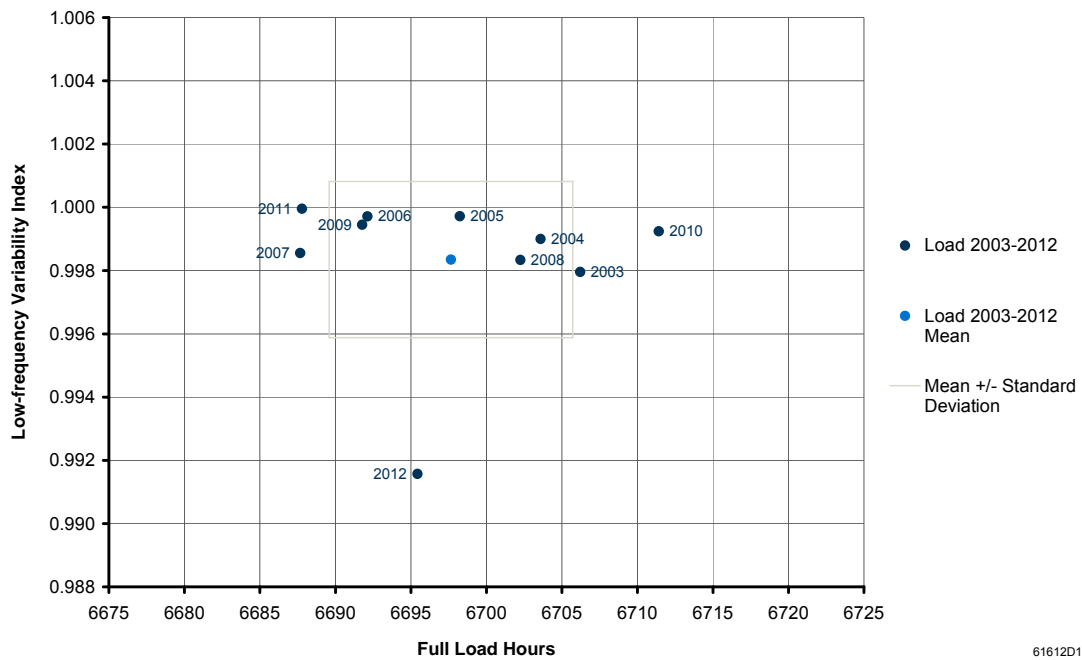


Figure 5.9: FLH and low-frequency variability of annual time series of electricity demand

Despite this analysis of annual time series of generation and demand, the identification of the most representative year remains difficult if not impossible. Whereas, for instance, the analysis of onshore wind generation time series clearly points to 2012 as being the most typical in terms of FLH and low-frequency variability, the analysis of offshore wind generation time series rather identifies 2004 as the best approximation of the ten-year average values. Considering all aspects, one would probably chose either 2004, 2005 or 2012, as the different annual time series of these years come closest to the respective mean values of the period 2003–2012.

However, it has to be verified whether the year in question is also average with regard to the residual demand. As the residual demand depends on the individual shares of RES and CHP generation, the analysis has to be conducted for a particular scenario. For this purpose, the residual demand is determined assuming the values of annual electricity consumption and annual generation from RES and CHP as specified for the reference scenario in Sections 5.2.2 and 5.2.3 respectively. As the pursued share of RES generation of 80 % is only reached in the last year of the planning horizon, the residual demand is determined based on the structure of RES and CHP generation in 2050.

In order to obtain a comparable set of annual time series of residual demand for the period 2003–2012, it has to be assumed that the installed generation capacities as well as the annual maximum load are constant. On this account, one year from the period is selected, which is used to calculate the installed capacity for each source of generation based on the annual energy production as defined in the reference scenario and the FLH of the generation time series for this year. Analogously, the annual maximum load is calculated based on the annual energy consumption as defined in the reference scenario and the FLH of demand time series for the selected year.

Assuming that a year which is average in terms of annual generation and demand will most probably also be average with regard to the residual demand, one of the more representative years 2004, 2005 and 2012 should be selected for this purpose. With a share of 25.7 % of gross electricity consumption, onshore wind represents the largest share of RES generation in 2050 and consequently will also strongly influence the characteristics of residual demand time series. Therefore, the year 2012 is selected, which proved to be typical with regard to onshore wind and was also observed to be close to the respective ten-year average values for the other generation and demand time series. Table 5.30 shows the calculated installed capacities of all sources of must-run generation for the year 2050.

Furthermore, based on the annual electricity consumption of 536 TWh in 2050 and 6695 FLH for the demand time series of the year 2012 (vide Table 5.23), an annual

maximum load of 80055 MW is determined. As already mentioned in Section 5.3.1, the annual maximum load is constant for each year of the period 2003–2012.

The calculated generation capacities and the calculated annual maximum load are used to scale annual time series of generation and demand for the remaining years of the period 2003–2012. Table 5.31 shows the resulting total annual electricity generation and total annual electricity consumption in 2050.

While, due to varying FLH, total electricity consumption as well as total electricity production from wind, solar, fossil CHP and biomass vary on an annual basis, total electricity production from hydro and geothermal (not included in Table 5.31) is constant at 20.6 TWh and 20.2 TWh respectively, as these sources are assumed to be unaffected by annual weather variations.

Table 5.30: Installed generation capacities in 2050 (assuming annual energy production as defined in the reference scenario and FLH according to the meteorological reference year 2012)

| source of generation | installed capacity in MW |
|----------------------|--------------------------|
| onshore wind | 99462 |
| offshore wind | 43279 |
| solar | 83400 |
| fossil CHP | 12941 |
| biomass | 11359 |
| hydropower | 4188 |
| geothermal | 2303 |

Source: own calculations.

Table 5.31: Total annual electricity generation and total annual electricity consumption in 2050 (assuming different annual time series of generation and demand)

| <i>in TWh</i> | 2003 | 2004 | 2005 | 2006 | 2007 | 2008 | 2009 | 2010 | 2011 | 2012 |
|-------------------|-------|-------|-------|-------|-------|-------|-------|-------|-------|-------|
| on. wind | 136.8 | 160.0 | 148.2 | 148.5 | 180.1 | 169.0 | 145.7 | 137.1 | 165.1 | 155.0 |
| off. wind | 127.9 | 147.7 | 148.2 | 139.8 | 156.6 | 155.8 | 143.1 | 134.5 | 154.7 | 150.2 |
| solar | 81.1 | 75.1 | 78.1 | 72.9 | 76.0 | 72.0 | 75.7 | 72.5 | 79.7 | 74.9 |
| fossil CHP | 43.4 | 43.4 | 43.2 | 43.0 | 42.2 | 42.8 | 42.7 | 45.0 | 42.1 | 43.0 |
| biomass | 63.0 | 63.1 | 62.7 | 62.4 | 61.2 | 62.1 | 62.0 | 65.4 | 61.2 | 62.4 |
| demand | 536.9 | 536.7 | 536.2 | 535.7 | 535.4 | 536.5 | 535.7 | 537.3 | 535.4 | 536.0 |

Source: own calculations.

Based on the annual time series of generation and demand for the period 2003–2012, the annual time series of residual demand are determined. The time series are compared with regard to residual energy demand and surplus energy as well as low-frequency variability. Before determining variability indices according to the method described in Appendix B.2, residual demand time series are scaled to the annual maximum load of the original demand time series.

The amounts of residual energy demand and surplus energy in 2050 under varying time series of residual demand are presented in Table 5.32, assuming the installed generation capacities according to Table 5.30 as well as an annual maximum load of 80055 MW. Considering the relatively wide range of both residual energy demand and surplus energy, it already becomes clear that different meteorological conditions can have a considerable impact on the characteristics of residual demand.

Table 5.32: Residual energy demand and surplus energy in 2050 (assuming different annual time series of residual demand)

| <i>in TWh</i> | 2003 | 2004 | 2005 | 2006 | 2007 | 2008 | 2009 | 2010 | 2011 | 2012 |
|----------------|-------------|-------------|-------------|-------------|-------------|-------------|-------------|-------------|-------------|-------------|
| demand | 125.0 | 110.4 | 105.7 | 117.6 | 99.8 | 103.3 | 114.6 | 119.6 | 104.0 | 106.3 |
| surplus | 81.1 | 103.9 | 90.6 | 89.1 | 121.4 | 109.4 | 88.9 | 77.8 | 112.2 | 96.4 |

Source: own calculations.

Table 5.33: Low-, mid- and high-frequency variability of residual demand in 2050 (assuming different annual time series of residual demand)

| | 2003 | 2004 | 2005 | 2006 | 2007 | 2008 | 2009 | 2010 | 2011 | 2012 |
|------------------------------------|-------------|-------------|-------------|-------------|-------------|-------------|-------------|-------------|-------------|-------------|
| <i>V_{low-frq}</i> | 0.53 | 0.46 | 0.87 | 0.60 | 0.78 | 0.78 | 0.33 | 0.71 | 0.64 | 0.66 |
| <i>V_{mid-frq}</i> | 0.54 | 0.53 | 0.47 | 0.55 | 0.60 | 0.52 | 0.52 | 0.43 | 0.61 | 0.46 |
| <i>V_{high-frq}</i> | 0.80 | 0.86 | 0.90 | 0.90 | 1.07 | 0.80 | 0.82 | 0.80 | 0.88 | 0.80 |

Source: own calculations.

Table 5.33 shows the low-frequency variability of residual demand in 2050, assuming different meteorological conditions represented by the time series for the period 2003–2012. Although not being used as criteria to select typical time series in this thesis, the mid- and high-frequency variability indices calculated for the time series of residual demand are also included in this table.

The low-frequency variability of residual demand ranges from time series that exhibit a very low level of seasonality (i. e. a minimum index of 0.33 for time series of 2009)

to extremely seasonal time series (i. e. a maximum index of 0.87 for time series of 2005). As it is assumed that onshore and offshore wind generation together amount to more than half of the gross electricity consumption in 2050, it is plausible that the relatively low level of seasonality in wind time series of 2009 also leads to minimum seasonality for residual demand, while the high level of wind seasonality for time series of 2005 correlates with the maximum low-frequency variability index of residual demand (vide Table 5.27).

Whereas the overall level of intra-day variability is relatively high, significant differences can be observed for the different annual time series of residual demand. Apparently, intra-day fluctuations of electricity demand, solar and CHP generation do not always cancel each other out to the same degree.

As for time series of generation and demand, a graphical representation of the characteristic quantities is used to identify the most representative annual time series of residual demand. Figure 5.10 shows residual energy demand and low-frequency variability of the residual demand time series that were determined for different meteorological conditions in 2050. In addition, the low-frequency variability index is also plotted against surplus energy in Figure 5.11.

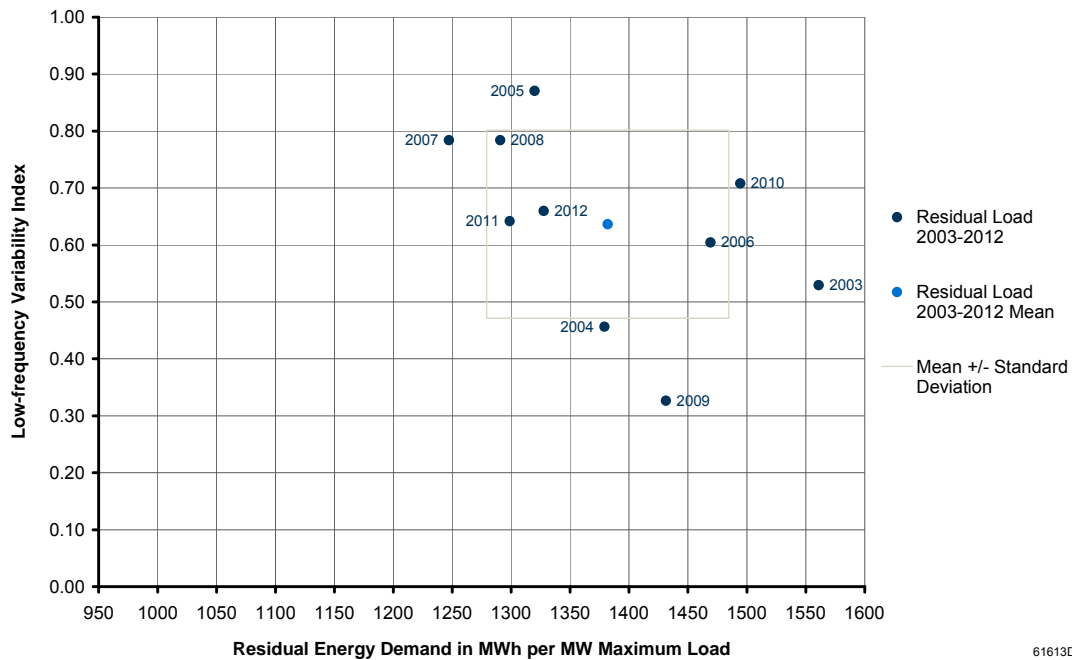


Figure 5.10: Residual energy demand and low-frequency variability of annual time series of residual demand

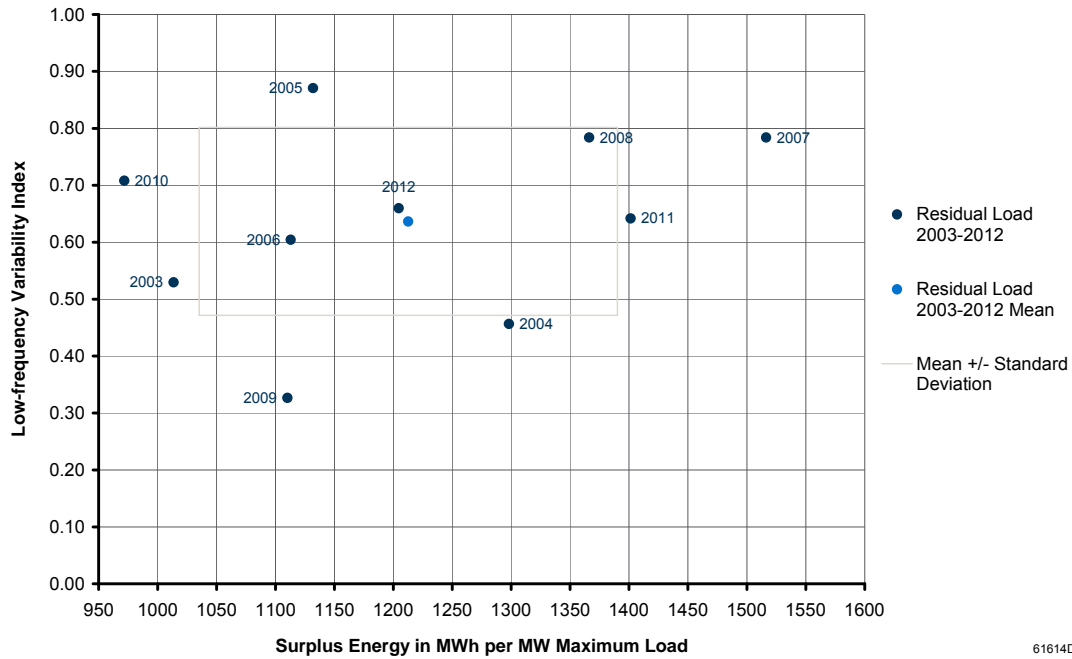


Figure 5.11: Surplus energy and low-frequency variability of annual time series of residual demand

Whereas residual energy demand and surplus energy are presented in absolute numbers in Table 5.32, the relative quantities measured in MWh per MW maximum load are used in these figures. Again, the figures also indicate the mean values of total annual energy and low-frequency variability and the corresponding standard deviation.

While with regard to low-frequency variability only the residual demand time series of 2011 comes closer to the mean value than the 2012 time series, 2012 is clearly the most typical with regard to residual energy demand and surplus energy. Thus, assuming the share and structure of RES and CHP generation in 2050 according to the reference scenario, the meteorological conditions described by the set of annual time series for the year 2012 prove to be the most representative of the period 2003–2012.

The year 2012 is therefore selected as the meteorological reference year. The reference scenario as well as all other scenarios (except for variations of annual time series, vide Section 5.5.1) are based on this meteorological reference year, i. e. the 2012 set of annual time series is used to model generation and demand in each year of the considered planning horizon. The installed generation capacities specified for 2050 in Table 5.30 apply for all scenarios.

5.4 Results from the reference scenario

5.4.1 Economic savings of storage expansion

The economic savings of storage expansion in the reference scenario are determined in comparison to a simulation of the reference scenario without the possibility of endogenous storage expansion. The savings that are generated by new build storages can be measured as either the gross system benefit or the net system benefit (vide Strbac *et al.* 2012).

The gross system benefit comprises savings in capital expenditures (CAPEX) of generation, i. e. non-variable costs of new build power plants according to equation (3-10), and savings in operating expenditures (OPEX) of both existing and new build power plants (vide equations (3-16) and (3-17)) as well as of existing storages (vide equation (3-40)). By contrast, the net system benefit reflects the reduction of overall system costs. It is calculated as the gross system benefit decreased by capital and operating expenditures for new build storages.

Figure 5.12 illustrates the economic savings of storage expansion in the reference scenario. The gross system benefit of storage expansion amounts to 7.24 billion € over the whole planning horizon (discounted to the present value in the base year 2010). It is mostly comprised of savings in generation CAPEX and OPEX, while accumulated savings in existing storage OPEX are insignificant. As capital and operating expenditures for new build storages amount to 4.08 billion €, a net system benefit of storage expansion of 3.16 billion € remains.

Whereas the accumulated net system benefit over the planning horizon will always be greater than or equal to zero if storage capacity expansion is optimised, the annually calculated net system benefit may also take negative values: Any negative impact on the overall system costs of a certain year is due to the intertemporal optimisation of the generation portfolio and only occurs, if it is compensated by savings in other years of the planning horizon.

Already during the first half of the planning horizon, the generation portfolio in the reference scenario is adapted to the later expansion of storage. Therefore, although storage expansion is mostly restricted to the second half of the planning horizon, a considerable portion of generation CAPEX savings already occur before 2030. By contrast, generation OPEX savings are primarily generated during the second half of the planning horizon and, in later years, are mostly due to the increased integration of surplus generation from RES and CHP (vide Section 5.4.2).

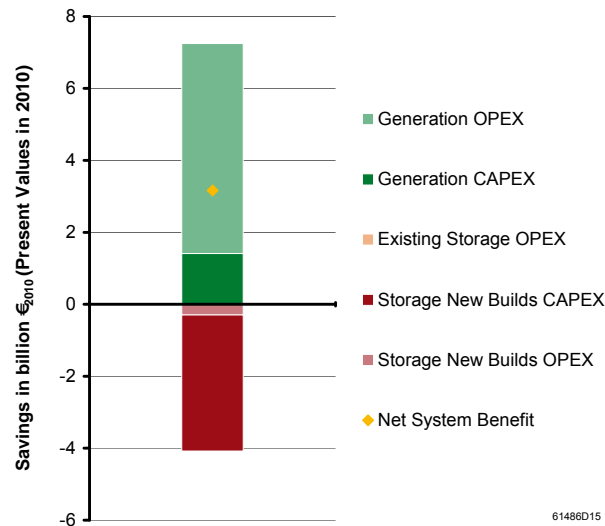


Figure 5.12: Economic savings of storage expansion in the reference scenario accumulated over the planning horizon 2010–2050

5.4.2 Curtailment of generation from RES and CHP

In this section, the amount of surplus generation from RES and CHP that is curtailed in the reference scenario is analysed. The amount of surplus energy which can be neither directly utilised nor economically integrated through storage expansion is compared with the original amount of surplus energy in the reference scenario (i. e. if storage is not available) as well as with the amount of curtailed energy if only existing storages are available.

In the reference scenario, the portion of electricity generation from RES and CHP that cannot be directly utilised accumulates to 1063 TWh over the planning horizon 2010–2050. If existing PSP are considered, this surplus can be reduced to 934 TWh. If the optimisation model is also allowed to expand storage capacity, the amount of curtailed energy is further reduced to 549 TWh. Thus, over the whole planning horizon, almost half of the original amount of surplus energy can be economically integrated into the power system.

Figure 5.13 illustrates the curtailment of generation from RES and CHP for selected years. While small amounts of generation from RES and CHP that cannot be directly utilised without storages occur as early as 2014, surplus generation is still at an insignificant level of 0.5 TWh in 2020. By 2030, surplus generation that cannot be directly utilised reaches 12.2 TWh and, by 2050, this curtailed energy amounts to 18 % of the total annual electricity generation from RES and CHP, i. e. 96.4 TWh.

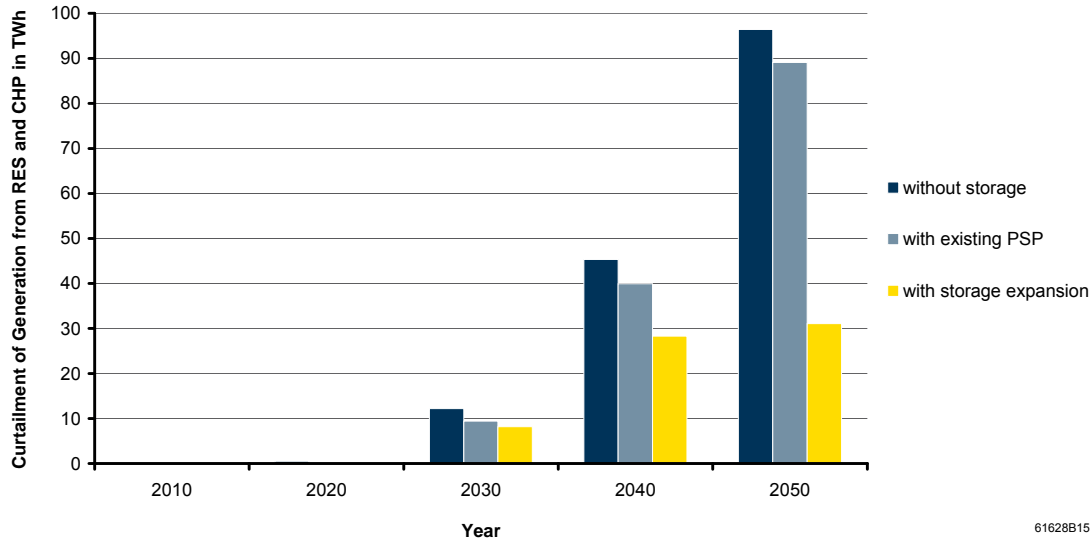


Figure 5.13: Curtailment of generation from RES and CHP in the reference scenario in comparison to cases without storage expansion and without storage

The existing storage portfolio can only reduce the curtailment of must-run generation to a minor degree: In 2050, curtailment with existing PSP amounts to 89.1 TWh or 17 % of the total annual electricity generation from RES & CHP. The additionally integrated surplus generation of 7.3 TWh already makes up more than 90 % of the total energy charged by existing PSP units over the year.

If storage capacity expansion is allowed in the reference scenario, curtailment is reduced significantly compared to the amounts of surplus energy observed without storage or with existing storages. As storage expansion increases dramatically after 2034 (vide Section 5.4.3), the amount of surplus generation that is additionally integrated into the power system also grows considerably during the last years of the planning horizon. In 2050, the remaining surplus energy reaches a level of 31.1 TWh or 6 % of the total annual electricity generation from RES & CHP.

5.4.3 Storage expansion and operation

This section analyses storage capacity expansion as well as the operation of existing and new build storages in the reference scenario. The expansion of storage capacity over the whole planning horizon is presented in Figure 5.14. Whereas the expansion

of PSP is first observed at an RES share of 31 % in 2019, investment into PSP turns out to be uneconomical again in 2023, when the assumed nuclear phase out is completed. Expansion of PSP re-starts in 2024, at an RES share of 39 %.

It should be noted that the observed decrease of installed PSP capacity in subsequent years is due to the green-field approach, which is applied in the submodel MESTAS (vide Section 3.2.2). While these results do not represent a realistic pathway of storage expansion, they nevertheless illustrate how the nuclear phase out leads to a temporary loss of profitability for PSP new builds.

As Figure 5.14 furthermore shows, the expansion of AA-CAES starts in 2034, at an RES share of 55 %. By contrast, the expansion of hydrogen storage first begins in 2040, when RES have reached a share of 64 %. In 2050, the demand for new build storage capacity amounts to 5.2 TWh. The installed storage capacity is then dominated by H₂-CCGT with 4.7 TWh. For comparative purposes, the total storage capacity of existing PSP (77 GWh) is also included in the figure.

The expansion of charging and discharging capacity is presented for selected years of the planning horizon in Figure 5.15. Again, total charging and discharging capacities of existing PSP are included for comparison (6.2 GW and 6.5 GW respectively).

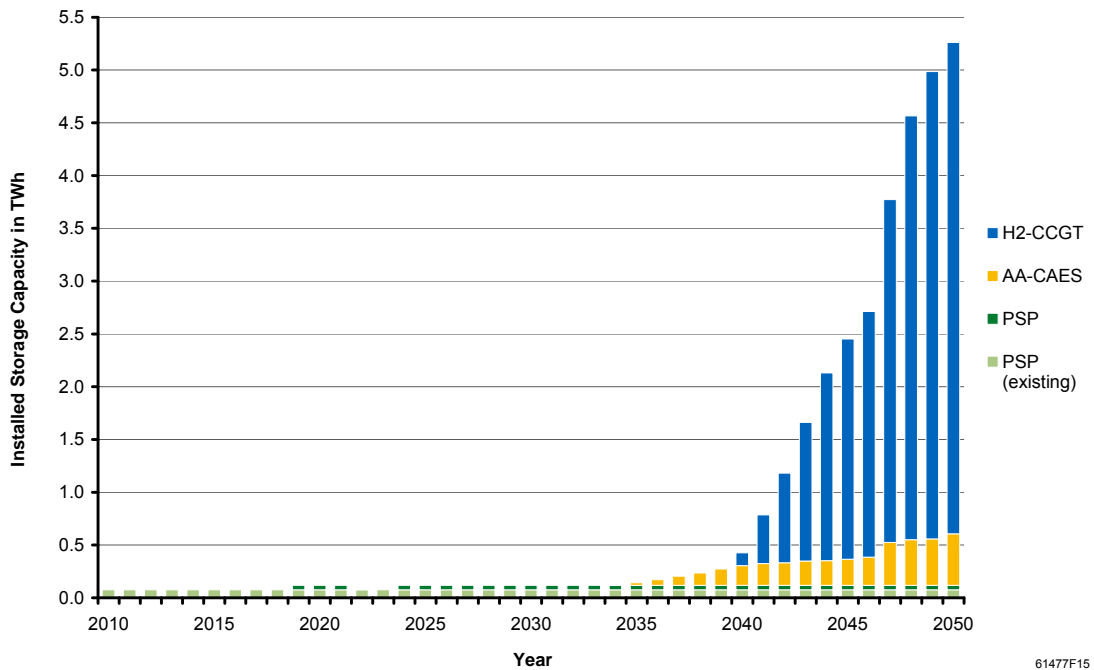


Figure 5.14: Expansion of storage capacity over the planning horizon 2010–2050 in the reference scenario

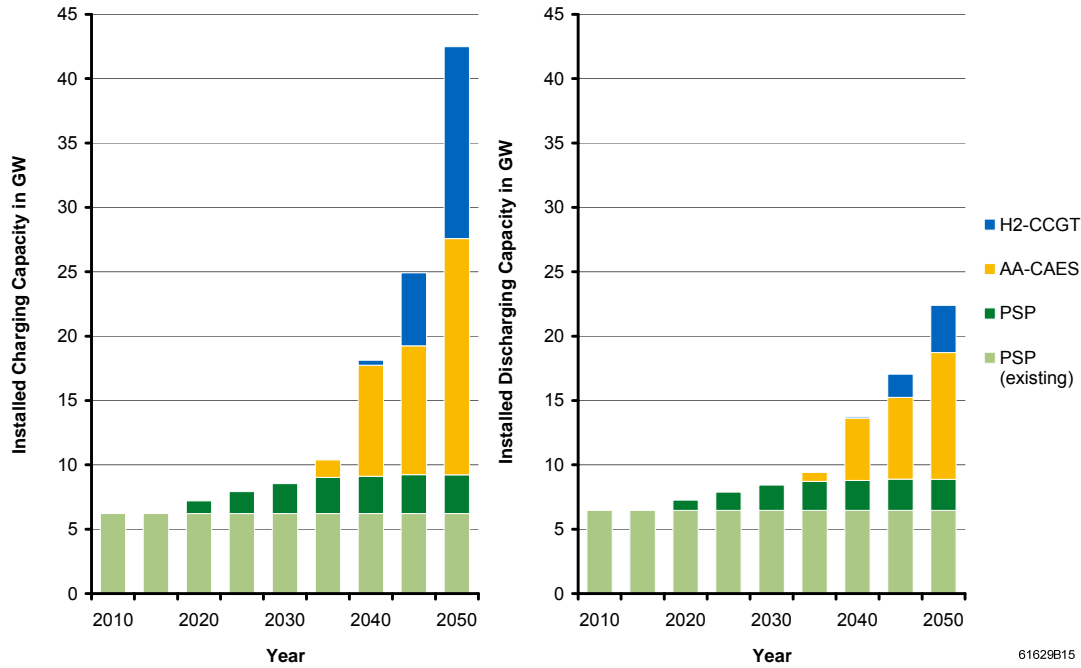


Figure 5.15: Expansion of charging and discharging capacity over the planning horizon 2010–2050 in the reference scenario

In 2050, the installed charging capacity of new build storages amounts to 36.3 GW and the installed discharging capacity reaches 15.9 GW. Whereas the total installed pump capacity of existing PSP is slightly smaller than the total installed turbine capacity, charging capacity exceeds discharging capacity for all new build technologies. The highest ratio – approximately 4:1 in 2050 – is observed for H₂-CCGT.

The reason for this significant difference between installed charging and installed discharging capacity is quite obvious: In case of high shares of RES, large charging capacities are necessary to integrate surplus generation, which typically occurs in the form of short-term power peaks. By contrast, the discharging of storages can usually be spread over several – equally profitable – hours. The general tendency of installed charging capacity exceeding installed discharging capacity is further intensified by low round-trip efficiencies, as, for instance, in case of hydrogen storage.

With regard to storage operation, equivalent full cycles are analysed. The equivalent full cycles of a given storage unit are calculated as the ratio of total energy stored over one year to installed storage capacity. The total energy stored over one year can be determined by multiplying the total energy discharged over the year by the reciprocal of the unit’s discharging efficiency. Equivalent full cycles thus measure how often a

given storage unit would have to be fully charged and discharged to achieve the actual annual energy throughput.

While equivalent full cycles allow to characterise how different storages are typically operated – with smaller numbers indicating long-duration storage and higher numbers indicating short-duration storage –, they are not necessarily a suitable quantity to describe the level of utilisation: Considering a pair of different storages, the storage unit with the smaller number of equivalent full cycles can still store more energy over the year if it possesses the larger storage capacity. However, if a single storage unit is examined in different years, a smaller number of equivalent full cycles clearly points to less energy stored and, hence, a lower level of utilisation.

Figure 5.16 presents the development of equivalent full cycles of existing and new build storages over the whole planning horizon in the reference scenario.

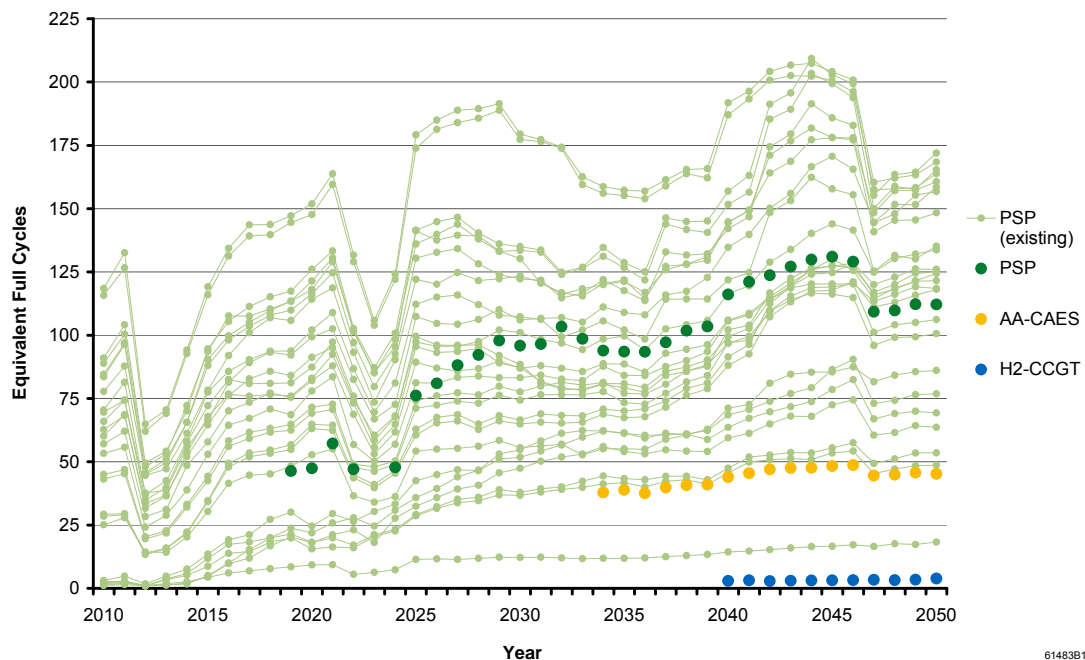


Figure 5.16: Development of equivalent full cycles of existing and new build storages over the planning horizon 2010–2050 in the reference scenario

For new build PSP, a relatively broad range of 50–125 equivalent full cycles per year is observed. However, in most years, new build PSP conduct between 75 and 115 full cycles. As efficiencies of existing PSP are usually lower than 80 % and storage dimensions deviate from optimal storage ratings for the respective simulation years, the

range of equivalent full cycles is much larger for the existing PSP portfolio: While for some units more than 200 full cycles per year are observed, a very long storage duration of 71 h of one existing PSP (vide Appendix C.1) leads to less than 20 full cycles per year, which is already close to the typical level for long-duration storages.

According to the results from the reference scenario, AA-CAES are optimally operated at approximately 40–50 equivalent full cycles per year. Hydrogen storages conduct approximately 3–4 full cycles per year, thus balancing long-term and seasonal fluctuations of residual demand.

Both the shut down of large parts of nuclear capacity in 2012 and the completed nuclear phase out in 2023 significantly affect equivalent full cycles of existing PSP (and new build PSP). Moreover, a discontinuity is observed after the year 2046, particularly for PSP and AA-CAES: Both storage technologies are operated at significantly less full cycles and, thus, are increasingly used to balance longer-term fluctuations. This discontinuity – which can also be observed in the development of capacity expansion of AA-CAES and H₂-CCGT (vide Figure 5.14 and Figure 5.15) – is caused by certain emissions abatement measures that suddenly become economically feasible after 2046 due to the time value of money (vide Section 5.4.4).

5.4.4 Generation expansion and operation

In the reference scenario, the optimised expansion of generation capacity only comprises lignite- and gas-fired power plants. After endogenous expansion is allowed in 2014, the model installs 10.3 GW of conventional lignite capacity over the next three years. As Figure 5.17 illustrates, these capacities compensate for the shutdown of one nuclear power plant by the end of 2015 as well as for the shutdown of lignite capacities in 2014, 2015 and 2016 (vide Section 5.2.5). Furthermore, 9.3 GW of lignite-fired power plants are installed immediately after 700 °C technology becomes available in 2020. Again, these capacities apparently compensate for the loss of base-load capacity due to the nuclear phase out.

An additional 5.8 GW of CCGT capacity is installed over the planning horizon. However, the largest portion of new build generation capacity is made up by gas turbines (29.8 GW or almost 54 %). While gas turbines are also used on a small scale to generate electricity during peak load hours, they are – being the least capital-intensive technology – mainly installed as backup capacity to achieve the desired level of security of supply in the German power system.

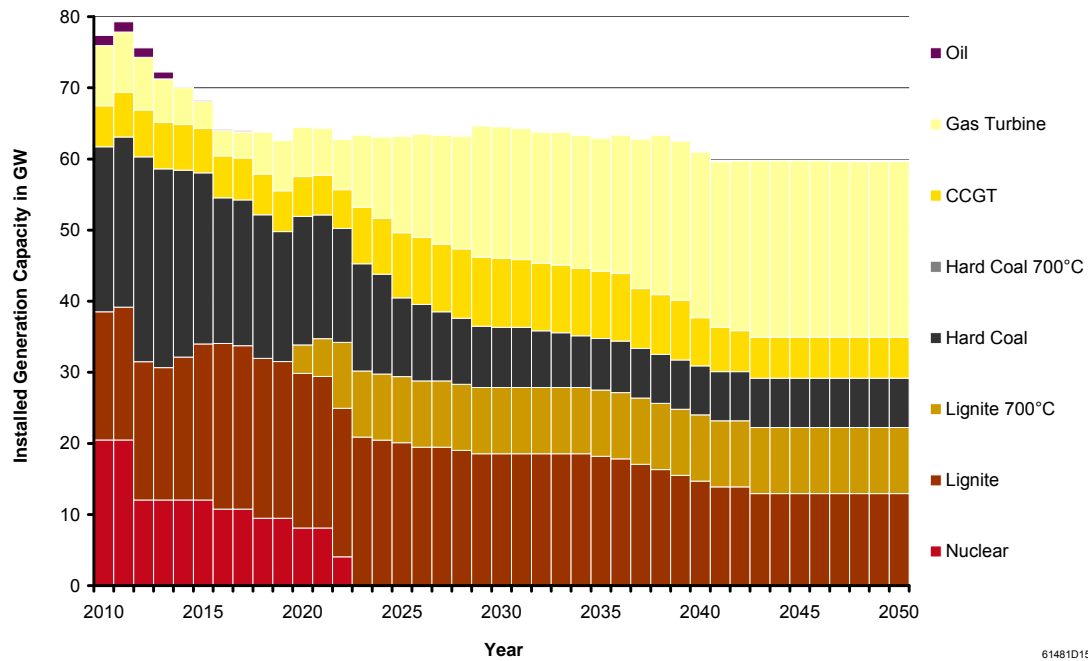


Figure 5.17: Development of the conventional generation portfolio over the planning horizon 2010–2050 in the reference scenario

Although the share of RES is still increasing with each year, the power plant portfolio stabilises after 2043 (vide Figure 5.17): From then on until 2050, no power plants reach the end of their lifetime except for gas turbines. However, shut down gas turbine capacity is reinstated at more or less equal levels, as the marginal contribution of additional variable renewable generation capacity to the system's firm capacity is rather low when added to a system with high shares of RES (vide Brückl 2005).

It should be noted that surplus capacities in the conventional generation portfolio are not reduced until 2041, when the system's firm capacity does not exceed the target value of firm capacity – i. e. the peak load plus 4 % (vide Section 3.2.3) – by more than 0.2 %.

The structure of electricity generation in the reference scenario is presented in Figure 5.18 for the whole planning horizon. The figure includes both the exogenously fixed generation from RES and CHP (vide Section 5.2.3) and the generation from conventional power plants and storages, which results from optimisation. Furthermore, the curtailment of surplus generation from RES and CHP is illustrated in the figure. However, surplus energy from RES and CHP is only represented in aggregated form, i. e. the total electricity generation from these sources that cannot be integrated.

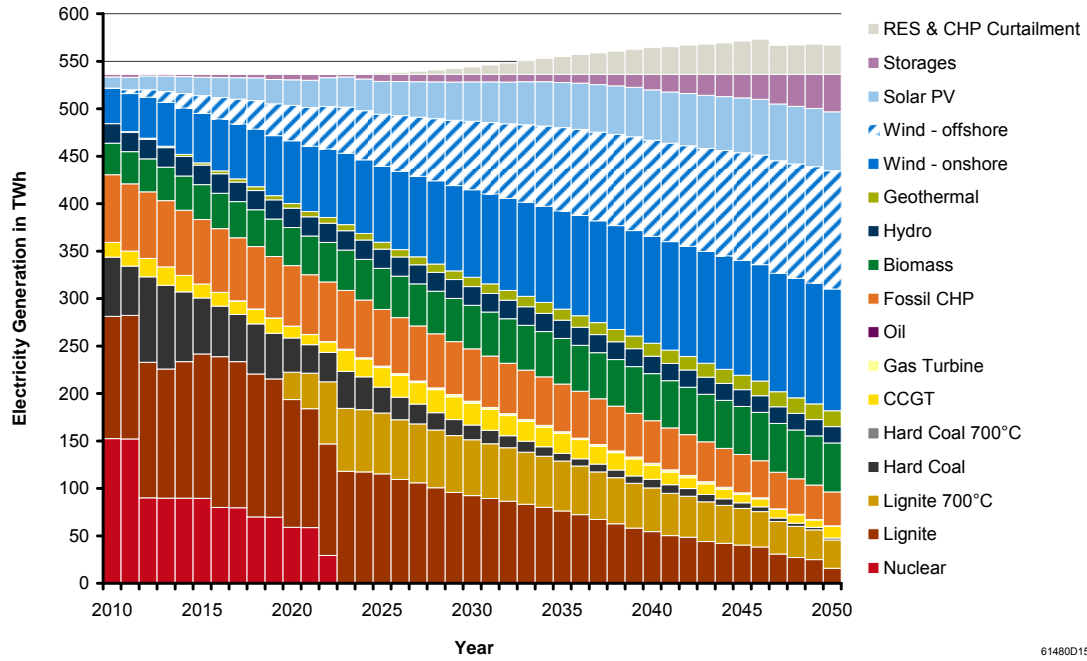


Figure 5.18: Electricity generation over the planning horizon 2010–2050 in the reference scenario

In each year of the planning horizon, the annual total of electricity generation (excluding curtailed energy) equals the exogenously fixed net electricity consumption of 536 TWh (vide Section 5.2.2). It should be noted that, when electricity generation from storages is taken account of, electricity generation from all other sources has to be reduced by the amount of energy that serves for charging storages. By this means, any double counting of energy is avoided and storage losses are considered.

As it is not possible to definitely determine to what extent each generation technology is actually utilised for charging, it is assumed for illustrative purposes that the total energy charged by storages is distributed among the different generation technologies in proportion to their respective shares in total electricity generation. This assumption will certainly be the least appropriate during the last years of the planning horizon, when storages are predominantly used to integrate renewable generation rather than for peak-shaving purposes.

Probably the most striking aspect concerning electricity generation in the reference scenario is that such large shares of lignite are apparently consistent with the assumed carbon emissions target (vide Section 5.2.10): From 2023 on, between 75 % and 84 % of annual conventional electricity generation is coming from lignite-fired power plants. The exogenously fixed constraint on annual lignite consumption (vide

Section 5.2.7) is only reached in the years 2022, 2023 and 2024. However, as argued in Section 4.7.1, the preference of base-load technologies may to a certain extent result from overestimating the flexibility of power plants with a simplified unit commitment approach as it is used in IMAKUS.

Analogously to the discontinuities detected for storage expansion and operation in the previous section, discontinuities can also be observed for electricity generation after 2046 in Figure 5.18: First, the level of RES and CHP curtailment is significantly lower than in earlier years. Correspondingly, electricity generation from storages increases. Secondly, whereas generation from conventional and 700 °C lignite power plants decreases gradually over most of the simulation period, generation from conventional lignite plants is reduced at disproportionately high rates after 2046.

Moreover, if annual carbon emissions and carbon prices are examined, the same discontinuities can be observed after 2046 (vide Figure 5.19). After a gradual increase until 2036, the carbon price subsequently declines due to the possibility to integrate large amounts of surplus energy through the expansion of AA-CAES and H₂-CCGT. In five consecutive years, from 2042 to 2046, marginal abatement costs are obviously determined by the same abatement measure: The (undiscounted) carbon price remains constant.

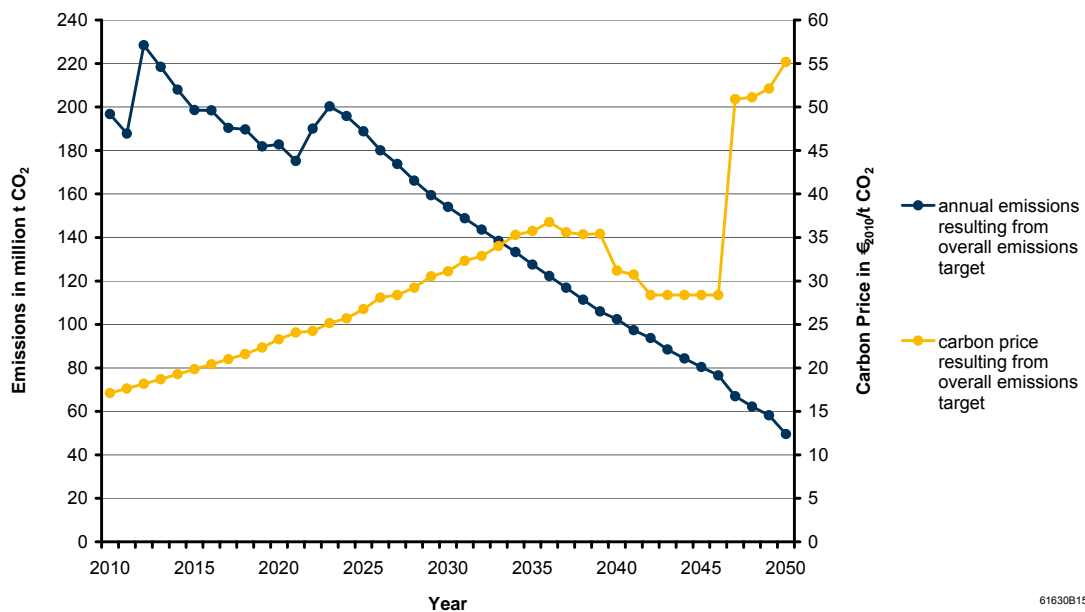


Figure 5.19: Annual carbon emissions and carbon prices over the planning horizon 2010–2050 in the reference scenario

As the generation portfolio does not change after 2043 and all costs are assumed constant, the sudden increase of the carbon price after 2046 can only be explained by certain abatement measures becoming economically feasible due to the time value of money. The implementation of these measures apparently changes the structure of electricity generation – i. e., above all, the increasing elimination of generation from conventional lignite plants – and causes the observed discontinuities. Consequently, annual carbon emissions also decline at much higher rates after 2046.

As emissions are only subject to an overall emissions target over the whole planning horizon, the decision when to reduce emissions is left to the optimisation model. Apparently, emission abatement is generally postponed to later years due to the time value of money. However, before the phase out is completed in 2022, nuclear power plants are utilised to contribute considerably to the overall emissions target.

5.5 Defining the variation scenarios

5.5.1 Variation of annual time series

In Section 5.2.4, consistent sets of annual time series of generation and demand were established for each year of the period 2003–2012. The set of annual time series corresponding to the year 2012 – the meteorological reference year – was identified in Section 5.3 as the most representative from this ten-year period and, thus, was employed in the reference scenario. In order to test the sensitivity of storage demand to the chronological characteristics of renewable electricity generation and electricity demand, nine additional variation scenarios are examined which employ the other sets of annual time series.

The installed capacity for each year of the planning horizon and for each source of must-run generation is calculated based on annual energy production as defined in the reference scenario (vide Section 5.2.3) and FLH of the corresponding time series in the meteorological reference year (vide Table 5.23, Section 5.3.1). Analogously, the annual maximum load is calculated based on annual energy consumption as defined in the reference scenario (vide Section 5.2.2) and FLH of demand time series in the meteorological reference year (vide Table 5.23, Section 5.3.1).

The calculated values of installed must-run generation capacity are reported in Appendix C.2 for the whole planning horizon 2010–2050. As the annual amount of electricity generation from hydro is assumed to remain constant over the planning horizon, a constant installed hydropower capacity of 4188 MW is specified. Analo-

gously, due to the assumption of a constant annual amount of electricity consumption, the annual maximum load is also constant at 80055 MW.

The calculated installed generation capacities as well as the calculated annual maximum load are considered valid throughout the variation scenarios and are used to scale annual time series of generation and demand for the remaining years of the period 2003–2012. By this means, a comparable set of ten scenarios representing different meteorological conditions is obtained (including the reference scenario).

Due to varying FLH, total electricity consumption and total electricity production from wind, solar, fossil CHP and biomass vary across scenarios. By contrast, total electricity production from hydro and geothermal is constant, as these sources are assumed to be unaffected by annual weather variations (vide Section 5.2.4).

Based on the different sets of annual time series of generation and demand, the annual time series of residual demand are determined. For the ten variation scenarios representing meteorological conditions in the period 2003–2012, Figure 5.20 shows the integrated share of electricity generation from RES and CHP in 2050, the surplus energy which would have to be curtailed without storage as well as the residual energy demand which would have to be covered by conventional generation. While differences are small for total annual electricity consumption – which is equivalent to total annual electricity production decreased by curtailment –, the variation of residual energy demand and surplus energy is considerable.

As installed capacities are fixed and FLH vary, the structure of RES generation also changes across the variation scenarios. Whereas, in the reference scenario, wind and solar generation originally makes up 62.9 % of gross electricity consumption in 2050 (vide Table 5.2, Section 5.2.3), this share increases to as much as 68.3 % if meteorological conditions of 2007 are assumed and decreases to only 57 % in case of 2010 conditions. The ratio of generation from onshore wind, offshore wind and solar PV can also deviate quite significantly from the reference scenario: For instance, a ratio of 1.7:1.6:1 is observed in 2050 under the 2003 scenario as compared to roughly 2:2:1 under the reference scenario 2012.

Considering the relatively wide range of residual energy demand and surplus energy as well as the varying structure of RES generation, it already becomes clear that different meteorological conditions can have a considerable impact on the characteristics of residual demand and, thus, affect results on storage demand. Furthermore, residual demand time series that are similar in terms of surplus energy – e. g. variation scenarios 2005, 2006 and 2009 – can still differ significantly in terms of low-frequency variability (vide Figure 5.11, Section 5.3.3). Results from the variation of annual time series are presented and discussed in Sections 5.6 and 5.7.1.

It should be noted that, as fossil CHP generation and, thus, related emissions are dependent on temperature, the amount of emissions that can be spent by the model has to be adjusted when annual time series are varied. For overall emissions targets resulting for the different sets of annual time series, vide Table 5.22, Section 5.2.10.

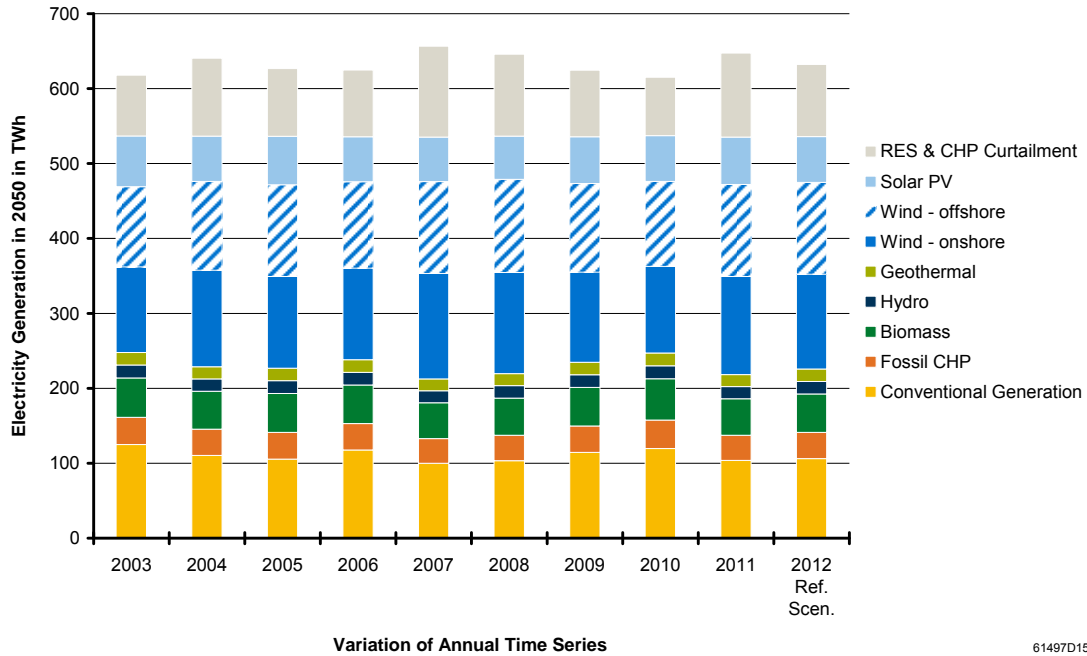


Figure 5.20: Electricity generation from RES and CHP, surplus energy and residual energy demand in 2050 under varying time series of generation and demand

5.5.2 Variation of RES share

In the reference scenario, total electricity generation from RES is assumed to increase linearly to 483.2 TWh in 2050, which is equivalent to 80 % of gross electricity consumption. In order to analyse the sensitivity of storage demand to renewable penetration levels, the total share of RES in 2050 is varied between 40 % and 100 % in six additional scenarios.

As in the reference scenario, all values for 2010 are based on scenario “2011 A” defined by Nitsch *et al.* (2012) (vide Table 5.1, Section 5.2.3). Throughout variation scenarios, both the development of fossil CHP generation and the development of hydro, geothermal and biomass generation are assumed as in the reference scenario. In 2050, the latter add up to a share of 17.1 % of gross electricity consumption.

Table 5.34: Shares of electricity generation from RES in 2050 for scenarios varying RES share

| <i>in % of gross electricity consumption</i> | 40 % RES | 50 % RES | 60 % RES | 70 % RES | 80 % RES | 90 % RES | 100 % RES |
|--|-----------------|-----------------|-----------------|-----------------|-----------------|-----------------|------------------|
| RES other than wind and solar | 17.1 | 17.1 | 17.1 | 17.1 | 17.1 | 17.1 | 17.1 |
| onshore wind | 9.3 | 13.4 | 17.5 | 21.6 | 25.7 | 29.7 | 33.8 |
| offshore wind | 9.1 | 13.0 | 17.0 | 20.9 | 24.9 | 28.8 | 32.8 |
| solar | 4.5 | 6.5 | 8.5 | 10.4 | 12.4 | 14.4 | 16.3 |
| total RES | 40.0 | 50.0 | 60.0 | 70.0 | 80.0 | 90.0 | 100.0 |

Source: own assumptions.

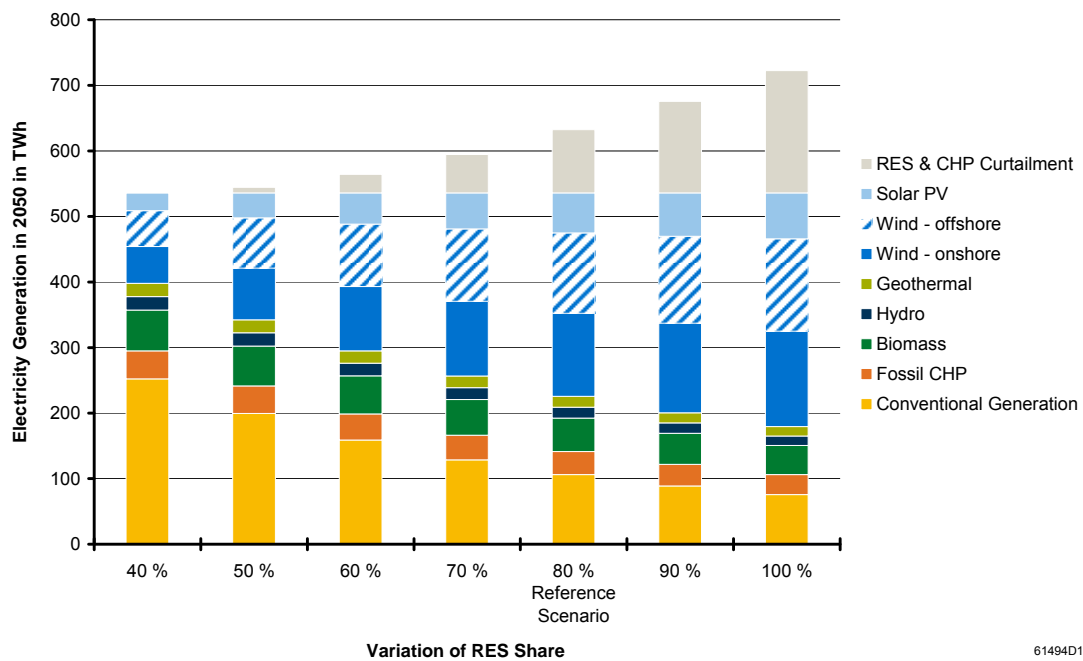


Figure 5.21: Electricity generation from RES and CHP, surplus energy and residual energy demand in 2050 under varying RES shares

In order to reach the respective total share of RES, wind and solar generation is assumed to increase linearly until 2050. The ratio of electricity generation from onshore wind, offshore wind and solar PV in 2050 is assumed as in the reference scenario, i. e. roughly 2:2:1. Table 5.34 presents the shares of electricity generation from RES in 2050 (including the 80 % reference scenario).

For the seven scenarios of varying RES share, Figure 5.21 shows the integrated share of electricity generation from RES and CHP in 2050, the surplus energy which would have to be curtailed without storage as well as the residual energy demand which would have to be covered by conventional generation. Although all variation scenarios are based on the set of time series of generation and demand from the meteorological reference year, the different shares of RES naturally affect the characteristics of the residual demand time series.

As expected, the deviation of residual energy demand and surplus energy is considerable: The amount of surplus energy in 2050 ranges from virtually zero in the 40 % case to 186.5 TWh in the 100 % case. Compared to the reference scenario (96.4 TWh surplus), approximately 3 TWh have to be curtailed for each additional terawatt hour of demand covered by RES and CHP generation in the 100 % scenario. Moreover, the variation of RES share will obviously also affect residual demand time series in terms of variability. Results from the variation of RES share are presented and discussed in Sections 5.6 and 5.7.2.

5.5.3 Variation of RES structure

In the reference scenario, the ratio of electricity generation from onshore wind, offshore wind and solar PV in 2050 – roughly 2:2:1 – is based on scenario “2011 A” defined by Nitsch *et al.* (2012). In order to analyse the impact of RES structure on storage demand, 15 additional scenarios are analysed that vary the ratio of generation from onshore wind, offshore wind and solar PV.

As in the reference scenario, the total share of RES in 2050 is fixed to 80 % of gross electricity consumption and the same development of hydro, geothermal and biomass generation is assumed (reaching 17.1 % in 2050). Also, the development of fossil CHP generation is assumed according to the reference scenario. The 15 variation scenarios are defined by the structure of the remaining 62.9 % of renewable generation in 2050, i. e. 380 TWh. The structure is specified by three percentages – the relative shares of generation from onshore wind, offshore wind and solar PV – that add up to 100 % (vide Figure 5.22).

As in the reference scenario, all values for 2010 are based on scenario “2011 A” defined by Nitsch *et al.* (2012) (vide Table 5.1, Section 5.2.3). Starting from 2010 levels, onshore wind, offshore wind and solar generation are assumed to develop linearly until 2050. However, as in several scenarios only one or two of these technologies contribute to the electricity generation mix in 2050, the annual amount of generation can either increase or decrease linearly.

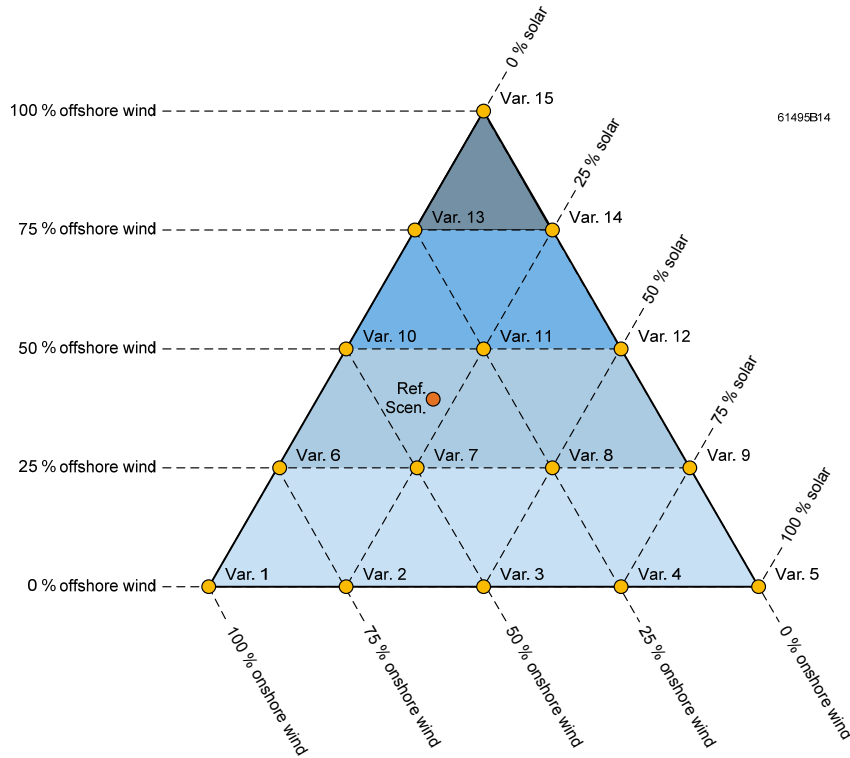


Figure 5.22: Graphical representation of relative shares of onshore wind, offshore wind and solar generation as assumed in scenarios varying RES structure

Only three variations – numbers 7, 8 and 11 – represent scenarios where onshore wind, offshore wind and solar PV contribute to the generation mix in 2050. In each of these scenarios, one of the three major RES dominates electricity generation with a relative share of 50 %, i. e. 190 TWh or a share of 31.5 % of gross electricity consumption. By contrast, variations located on the edges of the triangle represent scenarios with no contribution from one of the three major RES. Variations located in the corners of the triangle represent extreme scenarios that assume that 380 TWh (or 62.9 % of gross electricity consumption) are exclusively covered by one technology: onshore wind (number 1), offshore wind (number 15) or solar PV (number 5).

While most of the defined variations of RES structure might not represent realistic scenarios, the analysis of more extreme cases with low diversification is expected to indicate very clearly how a predominant expansion of one or two of the major RES affects storage demand in Germany. For comparative purposes, the reference scenario is also included in Figure 5.22: The relative shares of onshore wind, offshore wind and solar generation amount to 40.8 %, 39.5 % and 19.7 % respectively (equivalent to a ratio of roughly 2:2:1).

For six selected variations of RES structure and the reference scenario, Figure 5.23 shows the integrated share of electricity generation from RES and CHP in 2050, the surplus energy which would have to be curtailed without storage as well as the residual energy demand which would have to be covered by conventional generation. It should be noted that, although fossil CHP, hydro, geothermal and biomass generation is not varied, integrated shares can differ significantly between the variation scenarios. For illustrative purposes, it is assumed that all sources of must-run generation are integrated to the same degree.

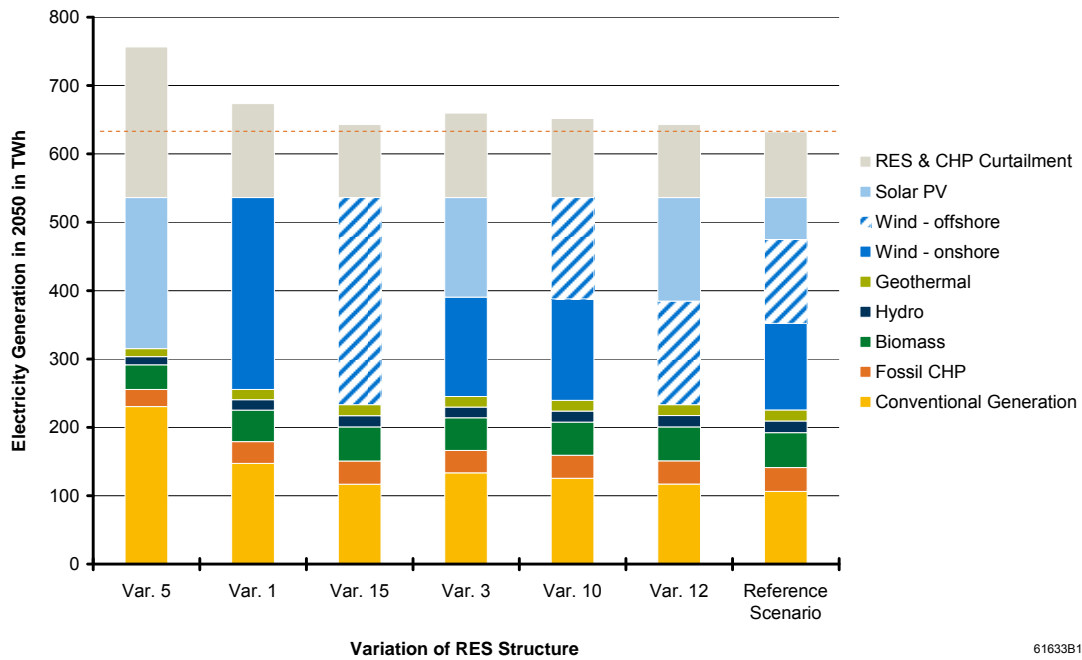


Figure 5.23: Electricity generation from RES and CHP, surplus energy and residual energy demand in 2050 under scenarios varying RES structure

Apparently, the amount of surplus energy is mainly determined by the degree of seasonal correlation of generation and demand: The largest amount of surplus energy is observed for the 100 % solar case (variation number 5), a scenario where generation and demand time series exhibit high correlation in terms of intra-day variability but low correlation in terms of seasonality (i. e. low-frequency variability).

While the intra-day variability of wind generation is strongly dependent on elevation and topography and is not necessarily correlated with the day-night cycle of demand (Kaltschmitt *et al.* 2014), wind generation exhibits quite high levels of low-frequency

variability (vide Table 5.27, Section 5.3.1) and – like electricity demand – usually reaches its peak during winter season in Germany (Kaltschmitt *et al.* 2014).

For the meteorological reference year 2012, the level of low-frequency variability – and, thus, the seasonal correlation with demand – is even higher for offshore wind compared to onshore wind (vide Table 5.27, Section 5.3.1). Moreover, with offshore FLH exceeding onshore FLH by more than twofold (vide Table 5.23, Section 5.3.1), offshore wind generation is also better suited to supply base load. This leads to less surplus energy in the 100 % offshore wind case (variation number 15).

As Figure 5.23 furthermore illustrates, diversification can have very different effects on energy surplus: As onshore wind and solar generation are not as well correlated with demand as offshore wind generation, the partial substitution of offshore generation with one of the two technologies (variation numbers 10 and 12) leads to an increase of surplus energy compared to the 100 % offshore wind case. By contrast, in a scenario of 50 % onshore wind and 50 % solar generation (number 3), surplus energy decreases compared to the respective 100 % cases. Due to counter-cyclical characteristics, seasonal fluctuations are balanced to a certain extent.

Compared to the six variation scenarios presented in Figure 5.23, an even smaller amount of surplus energy is observed for the reference scenario (96.4 TWh), where all three major RES contribute to the generation mix in 2050. Similar amounts are observed for variation scenarios 7 and 11 (100.1 TWh and 91.5 TWh respectively), whose RES structures come closest to the structure in the reference scenario (vide Figure 5.22). However, not all combinations of onshore wind, offshore wind and solar generation are necessarily advantageous in terms of surplus energy: In variation scenario 8, a relative share of 50 % from solar leads to 113.6 TWh of surplus energy, which, for instance, exceeds the level in the less diversified scenarios 12 and 15.

Results from the variation of RES structure are presented and discussed in Sections 5.6 and 5.7.3.

5.5.4 Variation of fuel costs

The uncertainty about the level of fuel costs is addressed in four variation scenarios. As in the reference scenario, fuel costs are again held constant over the whole planning horizon 2010–2050. Table 5.35 presents the assumptions on fuel costs in the variation scenarios. For comparative purposes, the table also includes fuel costs as assumed in the reference scenario.

Table 5.35: Fuel costs as assumed in variation scenarios (in comparison to fuel costs in the reference scenario)

| fuel | unit | reference scenario | minus 10 % | plus 10 % | expensive gas & oil I | expensive gas & oil II |
|-------------|---------------------|---------------------------|-------------------|------------------|----------------------------------|-----------------------------------|
| natural gas | €/MWh _{th} | 27.38 | 24.64 | 30.12 | 34.27 | 41.16 |
| hard coal | €/MWh _{th} | 14.62 | 13.16 | 16.09 | 14.62 | 14.62 |
| oil | €/MWh _{th} | 50.12 | 45.11 | 55.14 | 58.96 | 67.80 |
| lignite | €/MWh _{th} | 5.50 | 4.95 | 6.05 | 5.50 | 5.50 |
| nuclear | €/MWh _{el} | 8.00 | 7.20 | 8.80 | 8.00 | 8.00 |

Source: own calculations based on BAFA (2013a), BAFA (2013b), SKW (2014) and Destatis (2014); Nitsch *et al.* (2012); Kuhn (2012).

Two scenarios represent variations of the general price level: In the first variation scenario, the costs assumed in the reference scenario are reduced by 10 % for all five fuel types. In another variation scenario, all fuel costs are raised by 10 %. By this means, the weight of fuel costs compared to non-variable costs decreases or increases for all types of conventional power plants. However, the absolute variation of fuel costs is more pronounced in case of expensive fuels like gas and oil.

As the assumed gas price level in the reference scenario is rather low relative to costs for hard coal, two more scenarios are defined to consider higher spreads between gas and coal price: In scenario “expensive gas & oil II”, fuel costs for gas and oil are assumed as in 2050 in the moderate price scenario “Pfad B mäßig” by Nitsch *et al.* (2012). As Nitsch *et al.* (2012) specify cross-border prices in €₂₀₀₉, fuel costs are first converted to €₂₀₁₀, using the historical inflation rate according to Destatis (2014), and then augmented by an estimated 3 €/MWh_{th} to account for transport costs. Fuel costs for hard coal, lignite and nuclear are assumed as in the reference scenario.

In scenario “expensive gas & oil I”, fuel costs for gas and oil are defined as the respective mean values of costs in the reference scenario and costs in scenario “expensive gas & oil II”. Again, fuel costs for hard coal, lignite and nuclear remain unchanged. Results from the variation of fuel costs are presented and discussed in Section 5.6.

5.5.5 Variation of the bonus on storage costs

In the reference scenario, the non-variable costs of charging, discharging and storage capacity are reduced by a bonus of 50 %, which is suggested in Kuhn *et al.* (2012) and Kuhn (2012) to account for potential contribution margins earned on markets that

are not endogenously modelled, like the ancillary services market. The same bonus is valid for all new build storage technologies.

While assuming 50 % of contribution margins to come from other sources than energy arbitrage might be considered a very optimistic estimate, there are accounts that indicate that storages will have to earn even higher portions of their revenues on the ancillary services market. According to Conrad *et al.* (2014), the revenues of providing operating reserve currently outstrip the revenues that could be earned by PSP in Germany through energy arbitrage. Their analysis furthermore shows that, over the next 30 years, PSP new builds only become economically feasible if contribution margins are earned to a considerable extent on the operating reserve market.

Results in Witzenhausen *et al.* (2013) even suggest that until 2020 storages in Germany would have to earn more than 90 % of their revenues through the provision of operating reserve. The considered storage technologies are, namely, PSP, AA-CAES and batteries.

In order to address the uncertainty about the potential level of contribution margins that are not endogenously modelled, the bonus on storage costs is varied. While even higher portions might be possible (or necessary) in the future, it is assumed that a bonus of 50 % is already a quite optimistic estimate of contribution margins earned on the ancillary services market. Therefore, five more pessimistic scenarios are defined, which assume 40 %, 30 %, 20 %, 10 % and 0 % bonus on storage costs.

For lower bonuses, investment into storage becomes more expensive. In contrast to the variation of storage investment costs (vide next section), the cost proportions of different storage technologies however remain the same. Results from the variation of the bonus on storage costs are presented and discussed in Section 5.6.

5.5.6 Variation of storage investment costs

As the comparison of storage costs in literature shows, the costs assumed for emerging technologies like AA-CAES and hydrogen as well as for well-established PSP span a wide range of values. In order to address this uncertainty about storage costs, the most important cost factor, i. e. investment costs, is varied in additional scenarios. Annual fixed costs, variable O&M costs as well as decommissioning costs are assumed as in the reference scenario (vide Table 5.19, Section 5.2.9).

Some of the studies reviewed in Chapter 2 suggest significantly lower power-related and higher energy-related investment costs for PSP than assumed in the reference scenario (vide Table 5.36). For instance, Adamek *et al.* (2012) specify 300 €/kW for

charging capacity, 250 €/kW for discharging capacity and 10 €/kWh for storage capacity in 2025. Costs for charging and discharging capacity are assumed to decline further until 2050, reaching 250 €/kW and 200 €/kW respectively. In Scholz (2012), investment costs of 640 €/kW for the installation of pump-turbines and 10 €/kWh for storage capacity are specified for 2050. Although costs in Adamek *et al.* (2012) and Scholz (2012) are specified in €₂₀₀₇ and €₂₀₀₉ respectively, if converted to €₂₀₁₀, cost levels still differ considerably from investment costs in the reference scenario.

Table 5.36: Investment costs of new build storages by storage technology as assumed in variation scenarios (in comparison to investment costs in the reference scenario)

| | | reference scenario | lower power- / higher energy-related costs I | lower power- / higher energy-related costs II |
|--|------------------------------|---------------------------|---|--|
| PSP: charging | <i>in €/kW_{el}</i> | 450.97 | 290.00 | 230.00 |
| PSP: discharging | <i>in €/kW_{el}</i> | 450.97 | 290.00 | 230.00 |
| PSP: storage | <i>in €/kWh_{el}</i> | 6.34 | 10.00 | 10.00 |
| AA-CAES: charging | <i>in €/kW_{el}</i> | 421.63 | 421.63 | 330.00 |
| AA-CAES: discharging | <i>in €/kW_{el}</i> | 421.63 | 421.63 | 260.00 |
| AA-CAES: storage | <i>in €/kWh_{el}</i> | 30.65 | 43.00 | 49.00 |
| H₂-CCGT: charging | <i>in €/kW_{el}</i> | 1000.00 | 830.00 | 370.00 |
| H₂-CCGT: discharging | <i>in €/kW_{el}</i> | 729.00 | 729.00 | 729.00 |
| H₂-CCGT: storage | <i>in €/kWh_{el}</i> | 0.09 | 0.62 | 0.73 |

Sources: Kuhn *et al.* (2012); own calculations based on Adamek *et al.* (2012).

The two studies also suggest lower power-related investment costs for AA-CAES in 2050: Adamek *et al.* (2012) specify 320 €/kW and 250 €/kW for charging and discharging capacity respectively; Scholz (2012) assumes combined costs of 650 €/kW for the installation of both compressor and turbine. While in Scholz (2012) energy-related costs of AA-CAES are at a similar level to the reference scenario, Adamek *et al.* (2012) report higher costs for storage capacity, namely 41 €/kWh in 2025 and 47 €/kWh in 2050.

In case of hydrogen storage, Adamek *et al.* (2012) also assume a CCGT unit for discharging and specify investment costs at a similar level to the reference scenario. The study however suggests lower investment costs for charging capacity: Electrolyser costs of 800 €/kW in 2025 and 350 €/kW in 2050 are given. Both Adamek *et al.* (2012) and Scholz (2012) suggest higher energy-related costs for hydrogen storage than assumed in the reference scenario, ranging from 0.2 €/kWh to 0.7 €/kWh.

Considering these accounts, two variation scenarios are defined that assume lower power-related and higher energy-related investment costs for all three storage technologies. Table 5.36 presents the assumed costs, which are specified in €₂₀₁₀. In general, the assumed values in scenario “lower power- / higher energy-related costs I” approximate costs reported by Adamek *et al.* (2012) for 2025 (if converted to €₂₀₁₀), whereas values in scenario “lower power- / higher energy-related costs II” are based on costs reported for 2050.

As, in case of PSP, charging and discharging units are combined in one pump-turbine, investment costs for charging and discharging capacity are assumed to be equal, while adding up to approximately the same values as in Adamek *et al.* (2012). In the scenario “lower power- / higher energy-related costs I”, power-related costs of AA-CAES are assumed as in the reference scenario. Investment costs for the discharging capacity of H₂-CCGT remain unchanged throughout the scenarios.

Like all other technical and economic parameters of new build storages, the specified investment costs are assumed constant over the planning horizon 2010–2050. Results from the variation of storage investment costs are presented and discussed in Section 5.6.

5.6 Overview of results from the variation scenarios

5.6.1 Sensitivity of total storage expansion

All in all, this thesis analyses results on storage expansion from 42 scenarios with varying input parameters (including the reference scenario). While all scenarios explore the pathway from 2010 to 2050, the overview in this section only highlights results for the final year of the planning horizon, i. e. 2050. A more detailed analysis of selected variation scenarios is presented in Section 5.7.

As the overview of results on total new build storage capacity in Figure 5.24 illustrates, significant sensitivity of storage demand is observed for all input parameters. Storage expansion is however only completely abandoned under one of the considered variation scenarios (in case of 40 % RES share). The range of relative deviations between variation scenarios and the reference scenario is presented in Figure 5.25.

It should be noted that extreme deviations from the reference scenario may also be owing to extreme scenarios. For instance, in case of the variation of RES structure, relative deviations of total new build storage capacity in 2050 range from -59 % to +150 % compared to the reference scenario. However, as pointed out in Section 5.5.3, most of these scenarios represent extreme cases with low diversification.

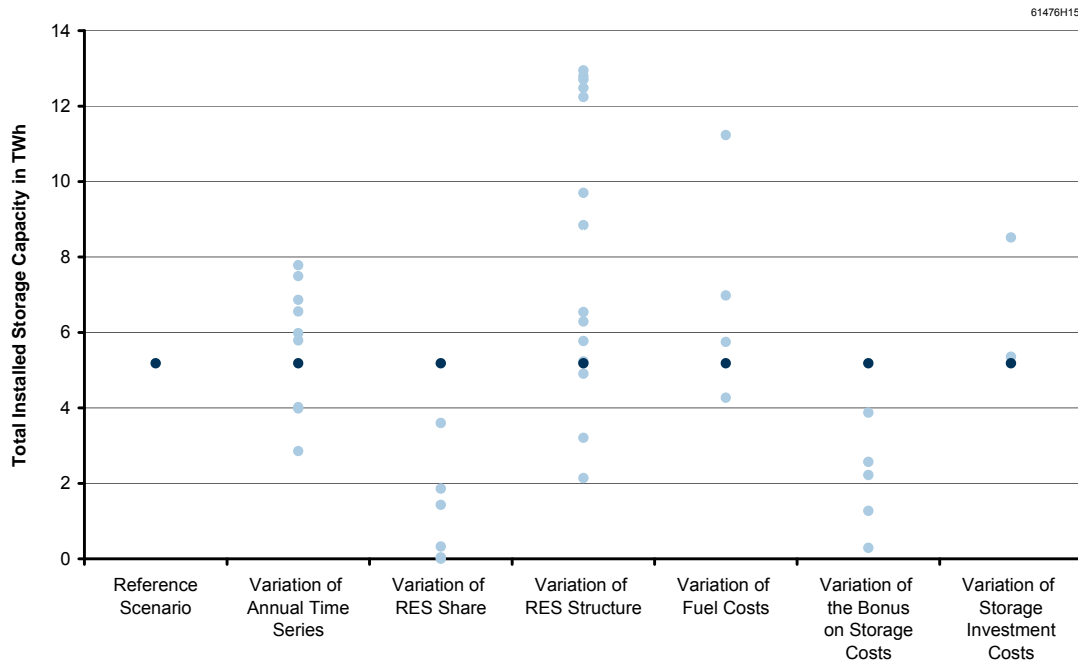


Figure 5.24: Total new build storage capacity in 2050 in the variation scenarios as compared to the reference scenario

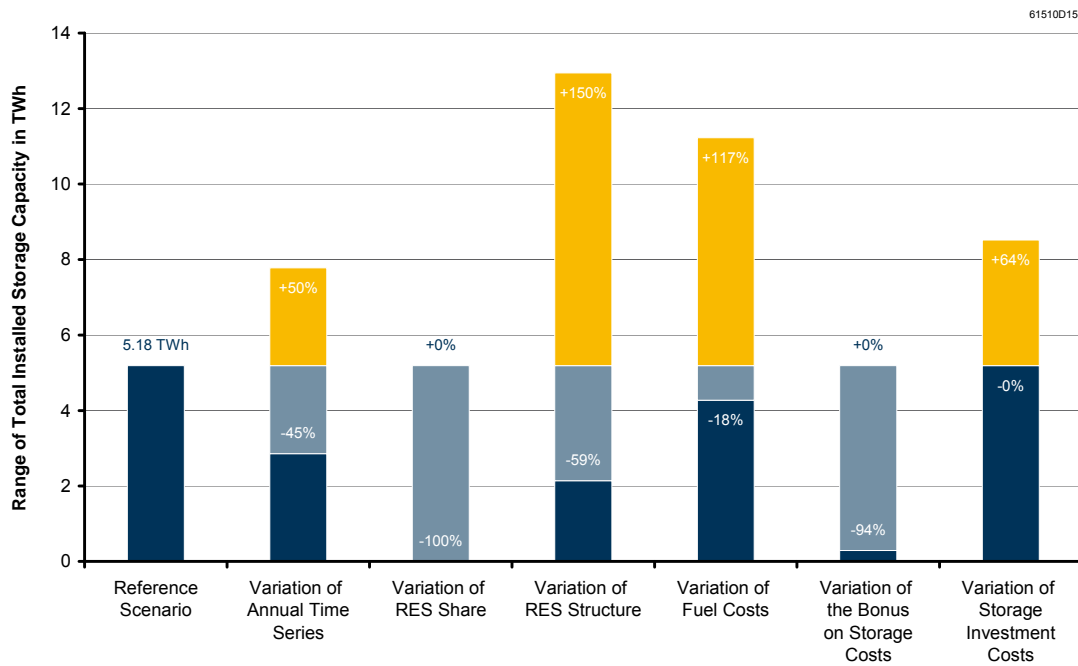


Figure 5.25: Range of relative deviations between variation scenarios and the reference scenario – total new build storage capacity in 2050

If only the three more realistic variation scenarios are considered where all three major RES – onshore wind, offshore wind and solar PV – contribute to the generation mix in 2050, the sensitivity of total storage capacity to RES structure is comparably low: A minimum capacity of 3.21 TWh (-38 % compared to the reference scenario) in variation scenario 11 and a maximum capacity of 5.23 TWh (+1 %) in variation scenario 8 are observed.

Besides RES structure, the variations of annual time series and fuel costs also lead to both lower and higher levels of total new build storage capacity in 2050. For scenarios varying annual time series, relative deviations of total new build storage capacity range from -45 % to +50 % compared to the reference scenario. Whereas the general increase (or decrease) of fuel costs by 10 % leads to a comparably small increase (or decrease) of total new build storage capacity, installed capacity increases by as much as 117 % compared to the reference scenario for scenarios that assume significantly higher costs for gas and oil.

For scenarios varying the share of RES, total new build storage capacity is always smaller than in the reference scenario, even in case of 90 % and 100 % shares. As expected, lower levels of storage capacity are also observed for scenarios that assume a lower bonus on storage costs: If no bonus is granted, total new build storage capacity decreases by as much as 94 % compared to the reference scenario.

Although higher energy-related costs are assumed in both scenarios that vary storage investment costs, total new build storage capacity apparently increases: namely by 3 % in scenario “lower power- / higher energy-related costs I” and by 64 % in scenario “lower power- / higher energy-related costs II”. Even more surprising, the total charging and discharging capacities of new build storages decrease in case of scenario “lower power- / higher energy-related costs I”: charging capacity drops by 5 % and discharging capacity drops by 7 % compared to the reference scenario (vide Figure 5.26 and Figure 5.27).

While, at first glance, these observations are counterintuitive, results become plausible when analysed for each individual storage technology (vide Sections 5.6.2, 5.6.3 and 5.6.4). On a technology-specific level, cost variations lead to the expected results, i. e. lower (higher) investment costs generally lead to more (less) capacity expansion. However, as investment costs are not varied to the same degree for all technologies (vide Table 5.36, Section 5.5.6), the total capacities of the optimal storage portfolio do not necessarily stick to the same rule.

Except for the variation of storage investment costs, the relative deviations between variation scenarios and the reference scenario are comparable for storage capacity and charging and discharging capacity. The relative deviations of total discharging capacity are similar to total charging capacity but generally tend to be smaller.

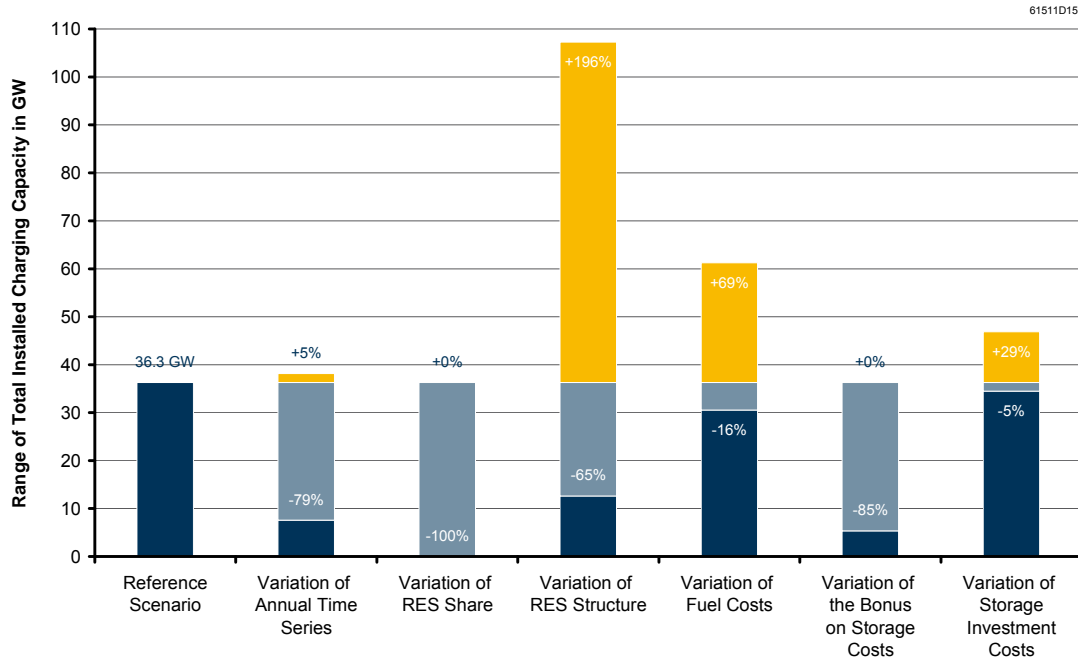


Figure 5.26: Range of relative deviations between variation scenarios and the reference scenario – total new build charging capacity in 2050

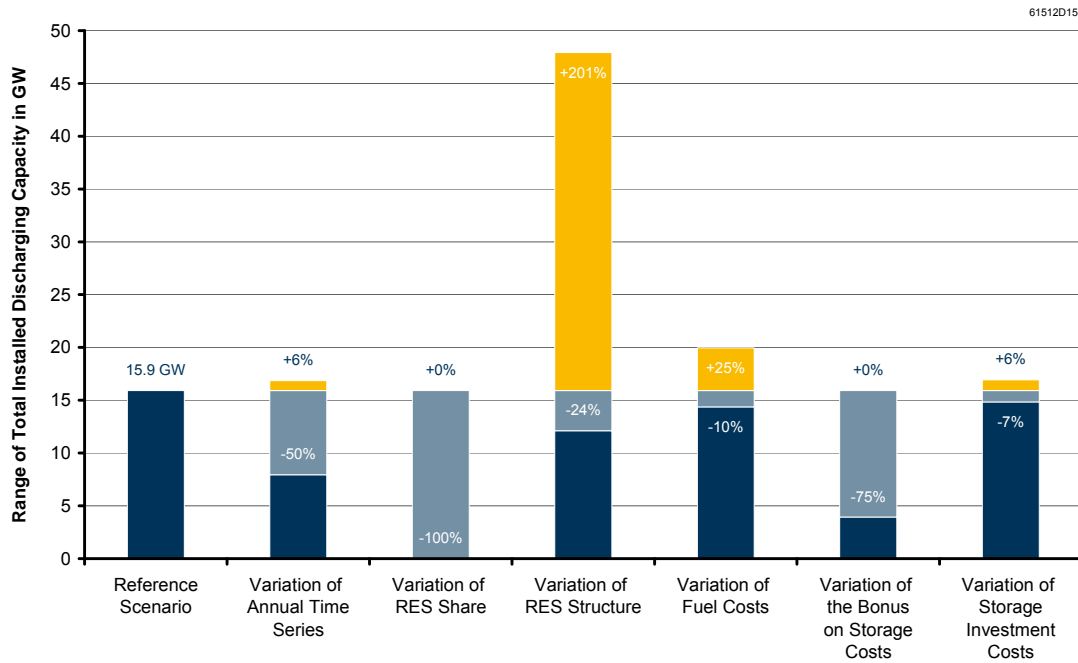


Figure 5.27: Range of relative deviations between variation scenarios and the reference scenario – total new build discharging capacity in 2050

5.6.2 Sensitivity of PSP expansion

While the overview of results on total storage expansion in the previous section already gives an idea of the high sensitivity of storage demand to the selected input parameters, the actual impact of varying input parameters is not always easily understood on such an aggregated level. Therefore, results from the 42 scenarios are also analysed for each individual storage technology.

With regard to PSP, results are comparably robust: The installed storage capacity in 2050 is virtually not affected by varying input parameters. With the exception of the 40 % RES scenario – when storage expansion is completely abandoned –, storage capacity of new build PSP reaches the exogenously defined limit of 40 GWh throughout all variation scenarios.

A stronger influence of varying input parameters is observed for the installed charging and discharging capacities of PSP in 2050. The ranges of the respective relative deviations between variation scenarios and the reference scenario are presented in Figure 5.28 and Figure 5.29.

As compared to the sensitivity of total charging capacity – which represents an average over all storage technologies –, the sensitivity of PSP charging capacity to varying input parameters is usually lower: For instance, PSP charging capacity decreases by at most 27 % if annual time series are varied (compared to an 79 % decline of total new build charging capacity). In case of a 0 % bonus on storage costs, PSP charging capacity only decreases by 9 % (compared to 85 %). Also, due to the high round-trip efficiency, the sensitivity to different levels of fuel costs is considerably lower.

As the ratio of discharging to charging capacity of PSP is anyway limited to a certain range, the relative deviations of discharging capacity are equivalent to the relative deviations of charging capacity under most variation scenarios. However, there are a few exceptions: Under scenarios varying annual time series as well as under scenarios varying the share of RES, discharging capacity increases by up to 10 % compared to the reference scenario, whereas charging capacity does not exhibit this tendency. For variations of annual time series and variations of RES structure, also the minimum deviation of discharging capacity differs from charging capacity. This indicates that, for certain variations of annual time series, RES share and RES structure, the optimal ratio of discharging to charging capacity of PSP changes (*vide infra*).

With regard to the variation of storage investment costs, both charging and discharging capacities of PSP increase as compared to the reference scenario. This is mainly due to the significant reduction of power-related investment costs for PSP – by almost 50 % as compared to an average 30 % for AA-CAES or 36 % for H₂-CCGT. The slightly lower increase of energy-related investment costs compared to AA-CAES or hydrogen storage adds to the attractiveness of PSP in these two variation scenarios.

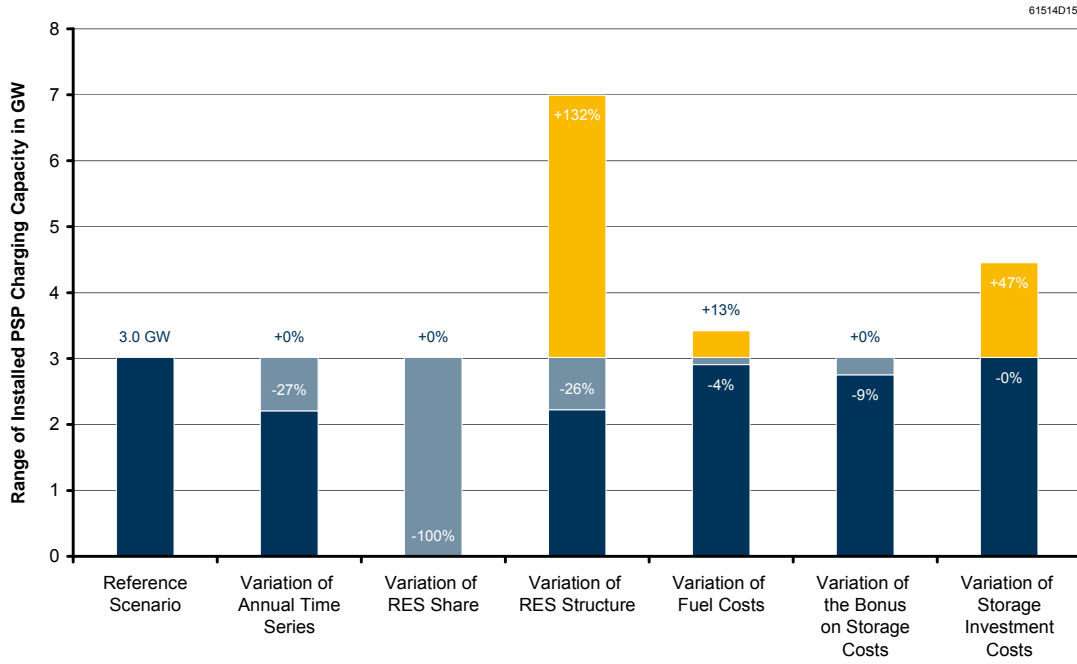


Figure 5.28: Range of relative deviations between variation scenarios and the reference scenario – charging capacity of new build PSP in 2050

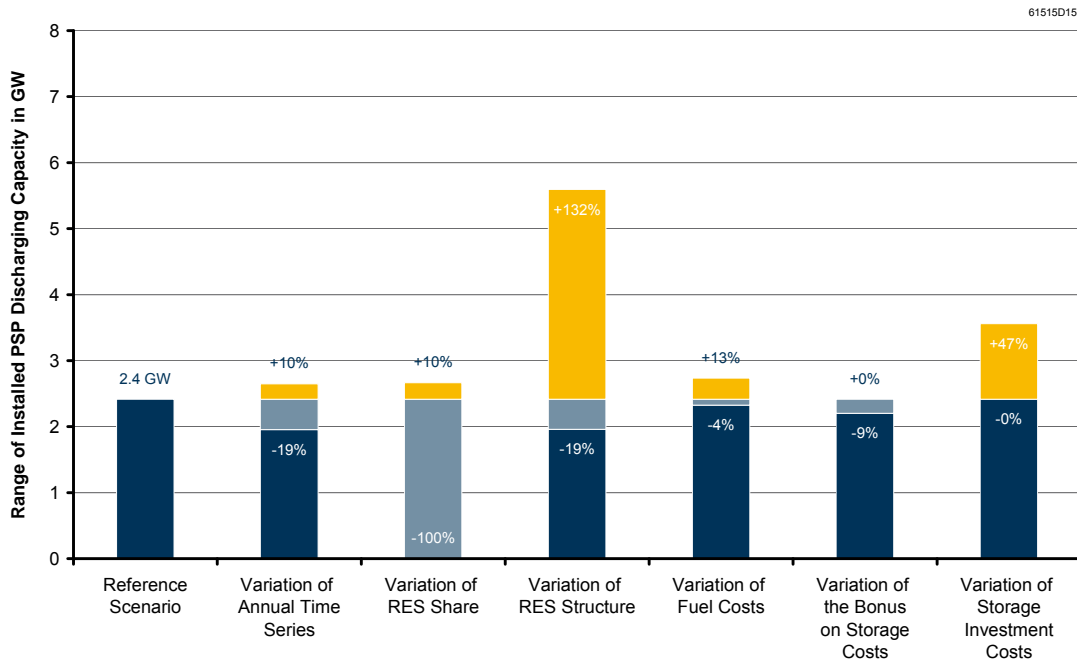


Figure 5.29: Range of relative deviations between variation scenarios and the reference scenario – discharging capacity of new build PSP in 2050

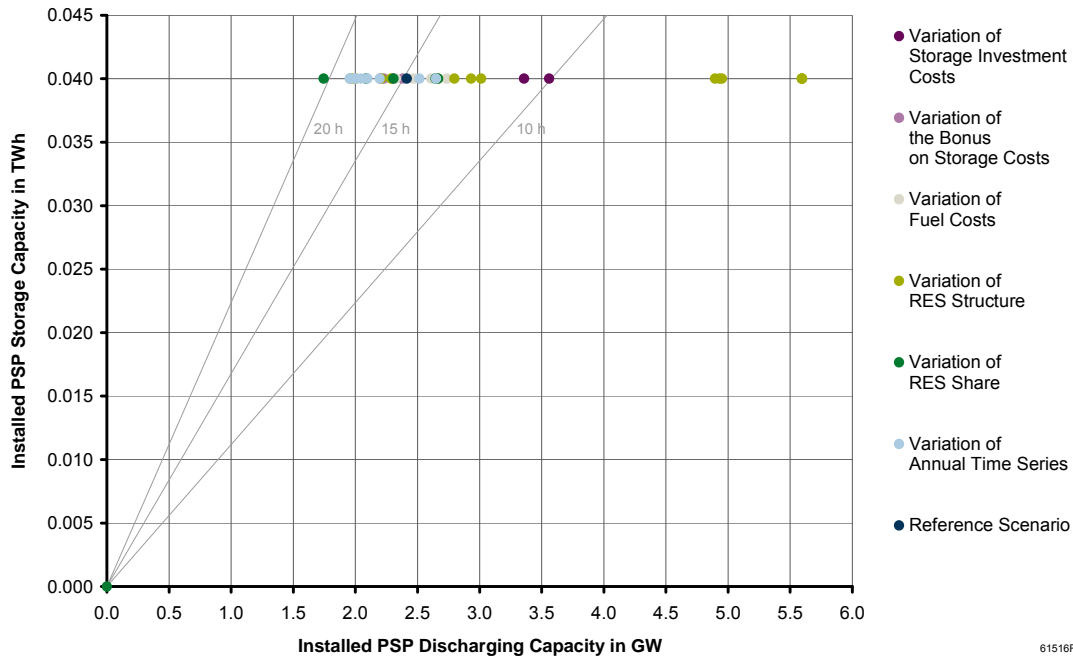


Figure 5.30: Storage duration of new build PSP in 2050 in the variation scenarios as compared to the reference scenario

Optimal storage duration of PSP

In order to better understand the impact of varying input parameters on optimal storage rating, the storage duration of PSP is compared across the different scenarios in Figure 5.30. In the reference scenario, the resulting optimal storage duration of new build PSP in 2050 is approximately 15 h, which is considerably higher than the usual range of 3 h to 8 h for existing PSP in Germany (vide Appendix C.1).

Under the majority of variation scenarios, the optimal storage duration of new build PSP is above 10 h and below 20 h. Extreme deviations from this range of storage duration are only observed for the six variations of RES structure with a relative share of solar generation of 50 % or more. In these cases, storage duration decreases to approximately 6–7 h (while installed discharging capacity increases) to meet the requirements of residual demand time series that are governed by the solar day-night cycle. However, it should be noted that higher storage durations could possibly be optimal if PSP storage capacity was not exogenously limited.

Optimal ratio of charging to discharging capacity of PSP

Another quantity to characterise storage rating – the ratio of charging to discharging capacity – is compared across the 42 scenarios. Figure 5.31 shows installed charging

and discharging capacities of PSP in 2050 for the reference scenario and the variation scenarios. The included isolines indicate the range of the ratio of charging to discharging capacity, namely 0.83–1.25, to which new build PSP are exogenously limited in all scenarios. The range of the reciprocal ratio, i. e. the ratio of discharging to charging capacity, was fixed to 0.8–1.2 in Section 5.2.9.

As in case of high shares of RES usually large charging capacities are necessary to integrate surplus generation, the ratio of charging to discharging power is 1.25:1 under most scenarios. However, lower ratios are observed for some variations of annual time series, RES share and RES structure. For extremely high shares of RES, i. e. 90 % and 100 %, a larger discharging capacity is optimal (ratio of 0.83:1), as only a small number of profitable peaking hours is left to discharge storages.

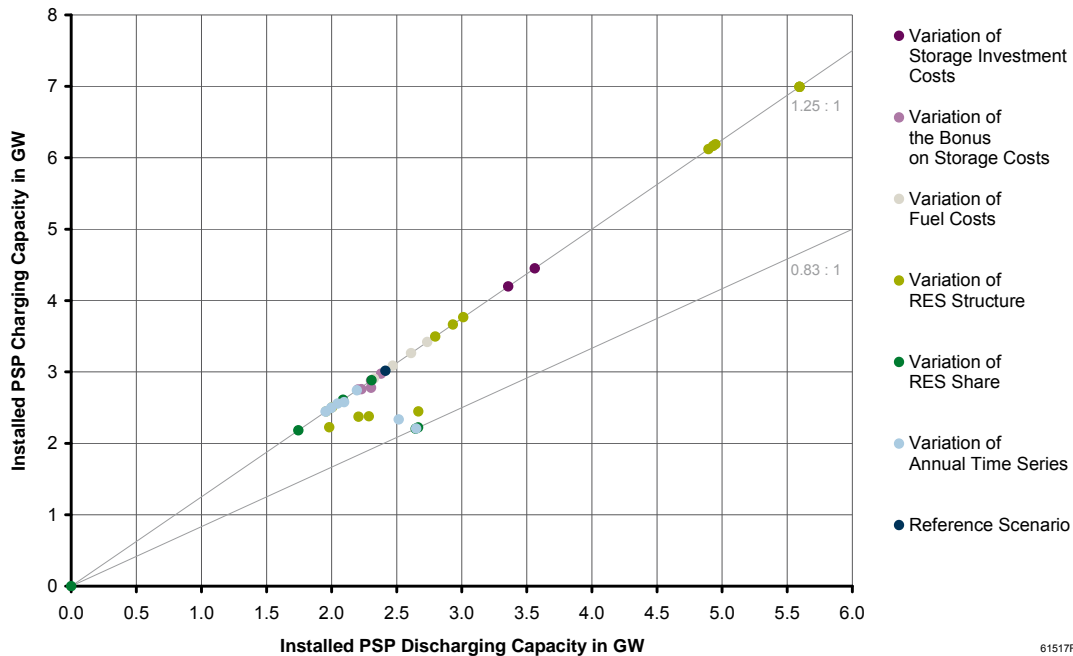


Figure 5.31: Ratio of charging to discharging capacity of new build PSP in 2050 in the variation scenarios as compared to the reference scenario

5.6.3 Sensitivity of AA-CAES expansion

Several of the analysed input parameters show significantly different effects on AA-CAES expansion as compared to the overall impact on storage expansion (vide Section 5.6.1). Figure 5.32 presents an overview of results on storage capacity of new

build AA-CAES in 2050. The range of relative deviations between variation scenarios and the reference scenario is presented in Figure 5.33.

Notably, the sensitivity of storage capacity to different annual time series is comparably high in case of AA-CAES. While eight out of nine variations of annual time series lead to relative deviations of storage capacity in a range from -90 % to +45 % compared to the reference scenario, the expansion of AA-CAES is even completely abandoned when meteorological conditions of 2007 are assumed. Possible causes for this high sensitivity of AA-CAES storage capacity to varying annual time series are discussed in Section 5.7.1.

With regard to the variation of RES structure, the sensitivity of AA-CAES storage capacity is much lower than the sensitivity of total storage capacity. Not considering the most extreme case (variation number 14), relative deviations of storage capacity are limited to a relatively small range from -22 % to +23 % compared to the reference scenario.

In contrast to PSP, the expansion of AA-CAES is not only abandoned in case of a 40 % share of RES but already under the 50 % RES scenario. For variations of fuel costs as well as the bonus on storage costs, the sensitivity of AA-CAES storage capacity is similar to the average over all storage technologies.

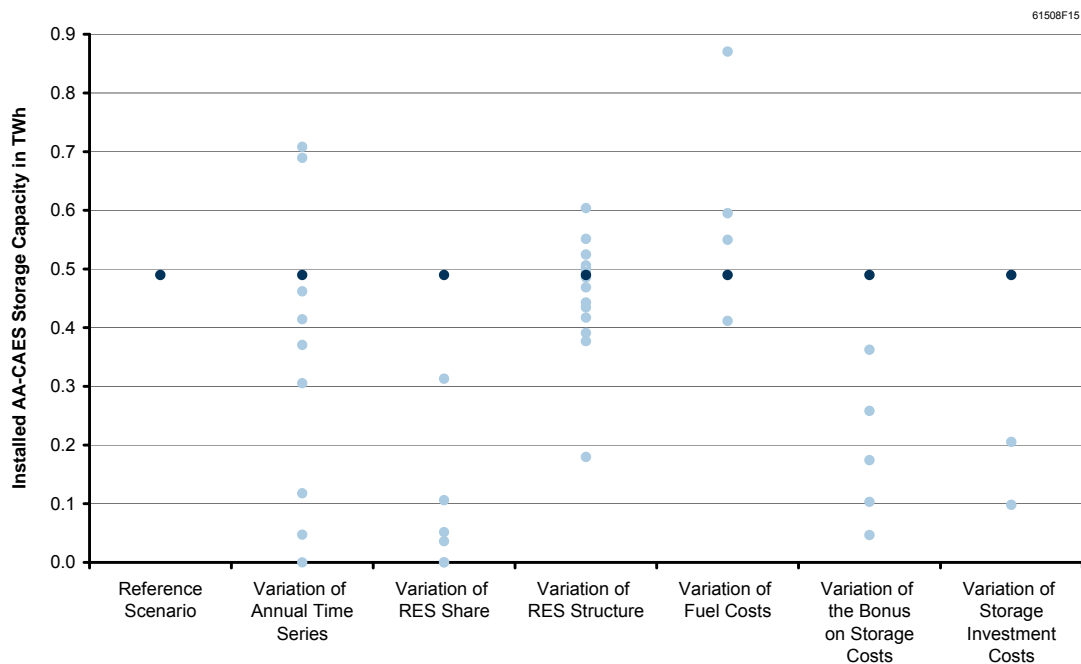


Figure 5.32: Storage capacity of new build AA-CAES in 2050 in the variation scenarios as compared to the reference scenario

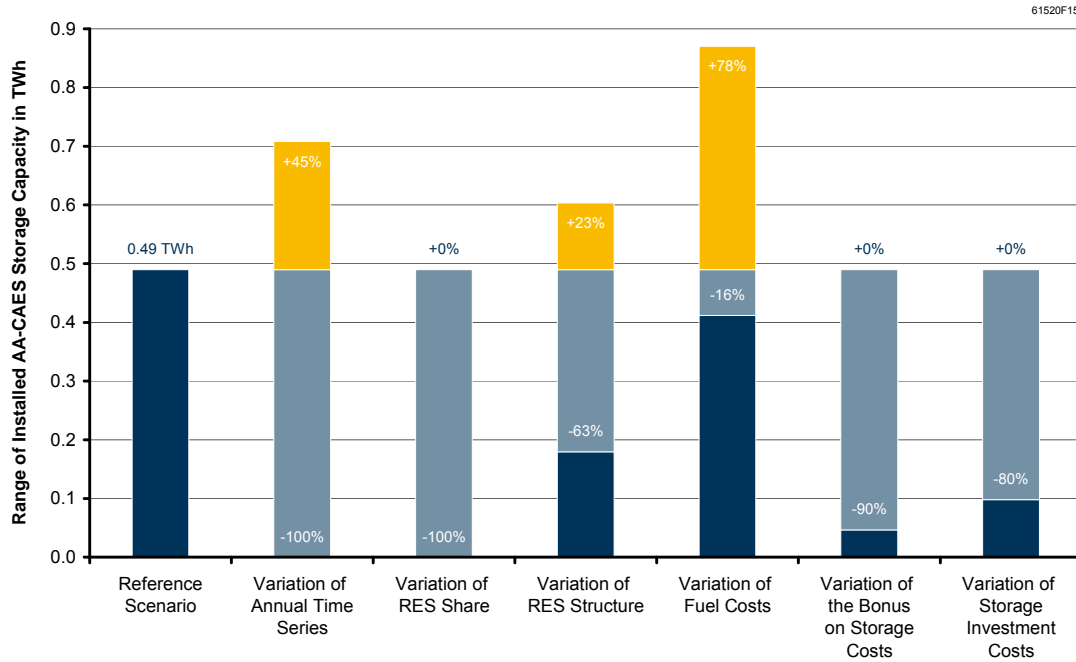


Figure 5.33: Range of relative deviations between variation scenarios and the reference scenario – storage capacity of new build AA-CAES in 2050

The variation of storage investment costs leads to lower levels of AA-CAES storage capacity in 2050 (up to -80 % compared to the reference scenario). Analogously, charging and discharging capacities of AA-CAES decline by 69 % and 60 % respectively. Apparently, the cost assumptions in these two scenarios reduce the relative attractiveness of AA-CAES as compared to PSP and H₂-CCGT: While energy-related investment costs of AA-CAES are subject to a slightly greater increase than PSP costs, the least reduction of power-related investment costs is assumed for AA-CAES.

For most variations, relative deviations of AA-CAES charging and discharging capacities are similar to relative deviations of AA-CAES storage capacity (with deviations of discharging capacity tending to be slightly smaller). The variation of RES structure is a striking exception: In contrast to a rather moderate increase of storage capacity (at most 23 %), AA-CAES charging and discharging capacities are observed to increase by up to 378 % and 305 % respectively under these scenarios.

However, the three scenarios with an increase of charging capacity of more than 250 % represent variations of RES structure with a relative share of solar generation of 75 % or more (numbers 4, 5 and 9). If three more scenarios – numbers 3, 8 and 12 with relative shares of 50 % solar – are excluded, a maximum increase of only 29 % compared to the reference scenario is observed for AA-CAES charging capacity.

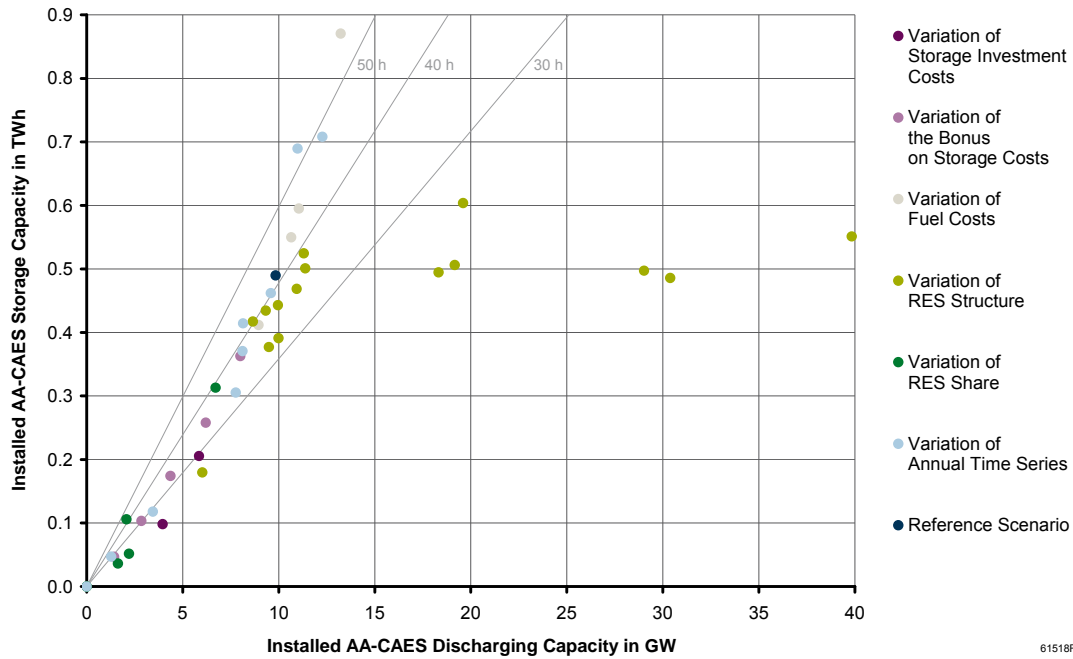


Figure 5.34: Storage duration of new build AA-CAES in 2050 in the variation scenarios as compared to the reference scenario

Optimal storage duration of AA-CAES

Figure 5.34 compares the storage duration of AA-CAES in 2050 across the 42 scenarios. In the reference scenario, the resulting optimal storage duration of new build AA-CAES is approximately 42 h. Under the majority of variation scenarios, storage durations between 30 h and 50 h are observed. Thus, AA-CAES tend to be rated at considerably higher storage durations than PSP. However, while power-related costs are similar, energy-related investment costs of AA-CAES are significantly higher than costs of PSP (vide Table 5.19, Section 5.2.9). Therefore, high storage durations are not a generally valid characteristic of the optimal rating of AA-CAES but are rather owing to the limited storage capacity of new build PSP.

As for PSP, extreme deviations from this range of storage duration are only observed for variations of RES structure: In the three scenarios with a relative share of solar generation of 75 % or more, storage duration decreases to approximately 12–14 h.

Optimal ratio of charging to discharging capacity of AA-CAES

In Figure 5.35, the installed charging and discharging capacities of AA-CAES in 2050 are presented for the reference scenario and the variation scenarios. The included isolines indicate certain ratios of charging to discharging capacity. Under most sce-

narios, the optimal ratio is observed to be above 1.50 and below 2.25. In the reference scenario, the optimal ratio of charging to discharging capacity of AA-CAES is approximately 1.9:1. Analogously to PSP, larger discharging capacities become optimal for RES shares of 90 % and 100 % (ratios of 0.72:1 and 0.65:1 respectively).

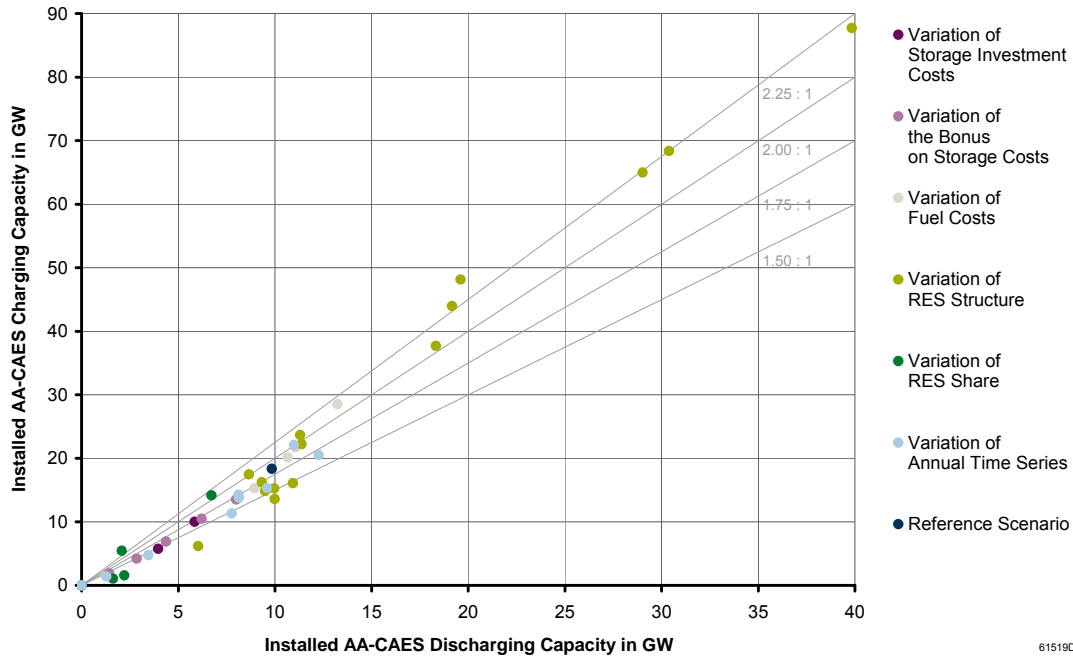


Figure 5.35: Ratio of charging to discharging capacity of new build AA-CAES in 2050 in the variation scenarios as compared to the reference scenario

5.6.4 Sensitivity of H_2 -CCGT expansion

As total new build storage capacity is dominated by hydrogen in 2050, the sensitivity of H_2 -CCGT storage capacity to varying input parameters is very similar to the sensitivity of total storage capacity presented in Figure 5.24, Section 5.6.1. However, as in case of AA-CAES, the expansion of hydrogen storage is abandoned under variation scenarios that assume RES shares of 40 % and 50 % in 2050.

The range of relative deviations of H_2 -CCGT storage capacity between variation scenarios and the reference scenario is presented in Figure 5.36. As compared to the average sensitivity of storage capacity (i. e. relative deviations of total storage capacity presented in Figure 5.25, Section 5.6.1), the relative deviations of H_2 -CCGT storage capacity are similar but tend to be slightly higher: Smaller deviations of PSP and

AA-CAES storage capacities or a contrary impact of input parameters on the expansion of these storage technologies lower the average deviation of storage capacity. For instance, the assumptions in scenario “lower power- / higher energy-related costs II” cause an 80 % drop of AA-CAES storage capacity and an 80 % increase of hydrogen storage capacity compared to the reference scenario (PSP storage capacity is not affected), thus leading to an average increase of storage capacity of 64 %.

While for scenarios varying annual time series relative deviations of H₂-CCGT storage capacity in 2050 range from -55 % to +57 % compared to the reference scenario, more extreme deviations are observed for variations of fuel costs (ranging from -18 % to +122 %) and, particularly, for variations of RES structure (ranging from -59 % to +167 %). As in case of total storage capacity (vide Section 5.6.1), deviations are usually smaller for more realistic variations of RES structure. The high sensitivity of H₂-CCGT storage capacity results from the very low level of energy-related investment costs of hydrogen storage.

The assumption of a lower bonus on storage costs affects the expansion of hydrogen storage capacity to a similar extent as it affects AA-CAES expansion: In case of a 0 % bonus on storage costs, H₂-CCGT storage capacity decreases by 96 %.

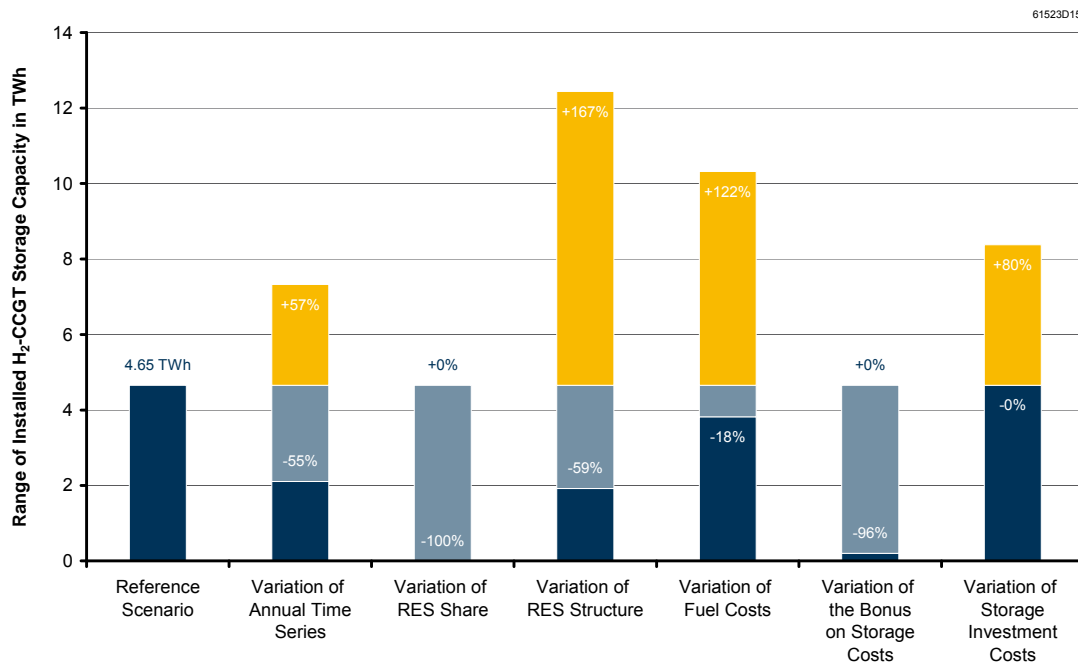


Figure 5.36: Range of relative deviations between variation scenarios and the reference scenario – storage capacity of new build H₂-CCGT in 2050

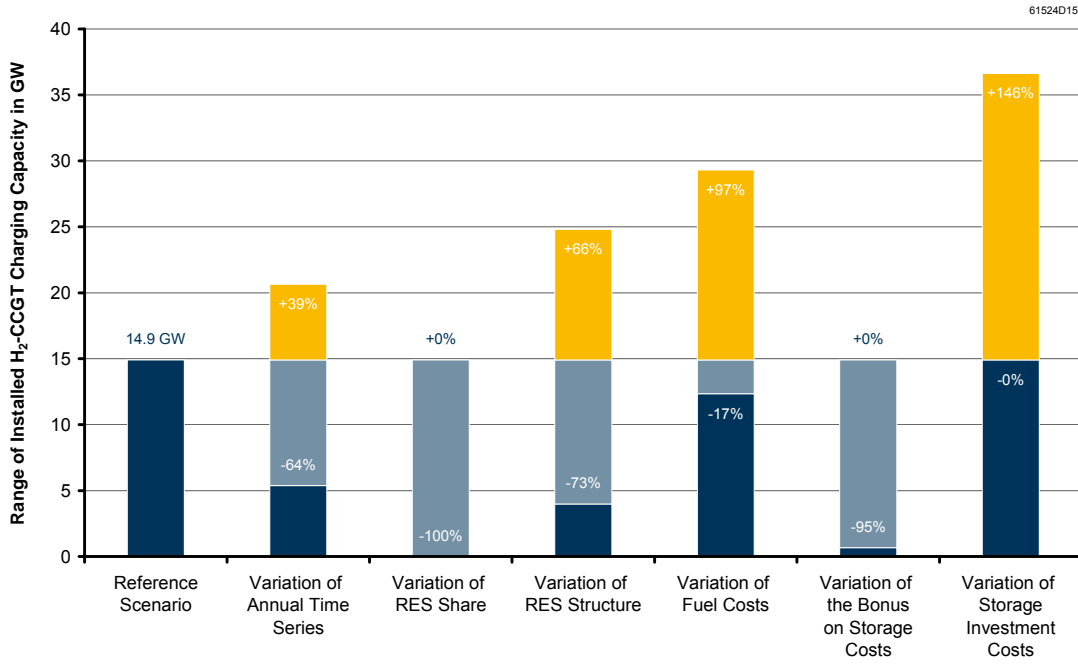


Figure 5.37: Range of relative deviations between variation scenarios and the reference scenario – charging capacity of new build H₂-CCGT in 2050

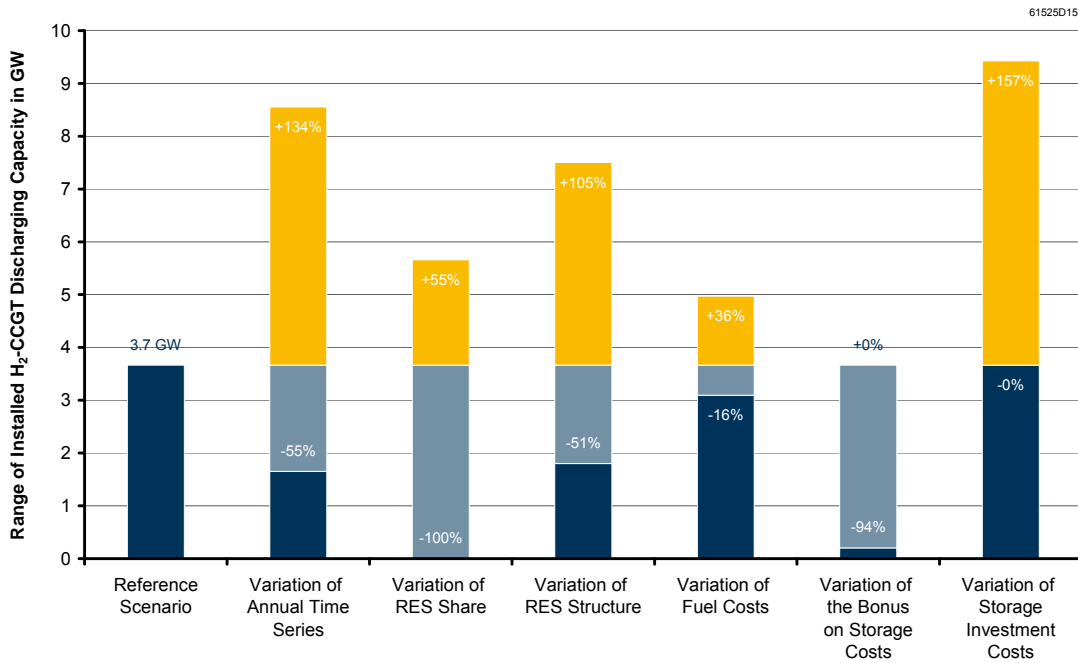


Figure 5.38: Range of relative deviations between variation scenarios and the reference scenario – discharging capacity of new build H₂-CCGT in 2050

The ranges of relative deviations of charging and discharging capacities of hydrogen storage are presented in Figure 5.37 and Figure 5.38 respectively. Under most variation scenarios, relative deviations of H₂-CCGT charging capacity are on a similar, if slightly lower level than relative deviations of H₂-CCGT storage capacity. In contrast to PSP and AA-CAES – where most input parameters have similar effects on charging and discharging capacities –, relative deviations of H₂-CCGT discharging capacity exhibit a significantly different pattern.

By comparing Figure 5.37 and Figure 5.38, it becomes apparent that relative deviations of hydrogen discharging capacity considerably exceed the sensitivity of charging capacity for variations of annual time series, RES share as well as RES structure.

By contrast, varying fuel costs have a much smaller impact on discharging capacity than on charging capacity or storage capacity of H₂-CCGT: As higher prices during peaking hours offer an incentive to integrate more surplus energy, the further expansion of charging capacity and, particularly, storage capacity becomes economically feasible. However, both the low round-trip efficiency of H₂-CCGT and the possibility to spread discharging over an even higher number of profitable hours reduce the impact of fuel costs on installed discharging capacity. Different levels of investment costs for charging and discharging capacity might add to this effect.

A significant increase of charging capacity is observed in case of varying storage investment costs: In scenario “lower power- / higher energy-related costs II”, the assumed reduction of electrolyser costs to almost one third results in a 146 % increase of installed charging capacity compared to the reference scenario. Despite assuming constant investment costs for CCGT plants, this also spurs a considerable increase of discharging capacity (+157 %), as hydrogen storage capacity increases only by 80 %.

Optimal storage duration of H₂-CCGT

Due to the very low level of energy-related investment costs, the optimal rating of hydrogen storages shows a much higher sensitivity to the examined input parameters than the rating of PSP or AA-CAES. As Figure 5.39 illustrates, only in roughly half of the 42 scenarios does optimal storage duration of H₂-CCGT in 2050 lie within the relatively broad range from 600 h to 1200 h. In the reference scenario, the optimal storage duration amounts to approximately 800 h.

Whereas in case of PSP and AA-CAES extreme deviations of storage duration are exclusively observed for variations of RES structure, storage duration of hydrogen storage also deviates significantly under scenarios varying annual time series, RES share and fuel costs: For annual time series of 2011 and 2007 – i. e. under meteorological conditions that lead to a 90 % decrease of AA-CAES storage capacity or even the abandoning of AA-CAES expansion (vide Section 5.6.3) –, the optimal storage duration of H₂-CCGT drops to roughly 420 h and 470 h respectively.

For extremely high shares of RES (90 % and 100 %), the optimal storage duration of H₂-CCGT even decreases to approximately 200 h, as larger discharging capacities are necessary to take advantage of the remaining number of profitable peaking hours. While storage durations of 600–1200 h are actually only optimal in four scenarios that vary RES structure, the most extreme deviations from the reference scenario, i. e. storage durations above 2500 h, are again observed for the three variations with a relative share of solar generation of 75 % or more (numbers 4, 5 and 9).

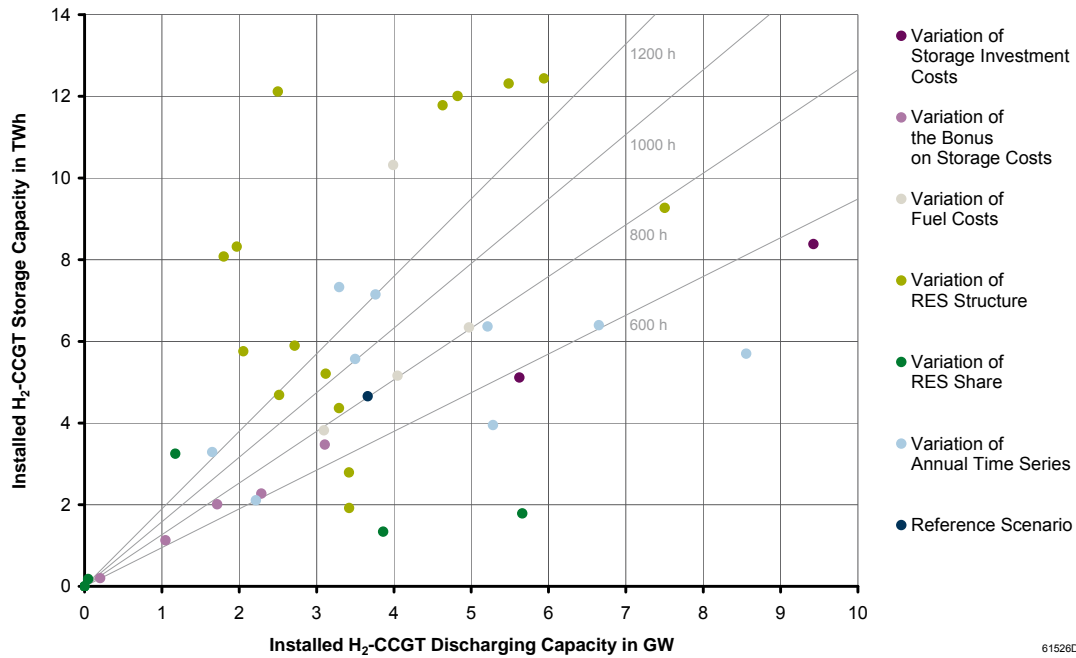


Figure 5.39: Storage duration of new build H₂-CCGT in 2050 in the variation scenarios as compared to the reference scenario

Optimal ratio of charging to discharging capacity of H₂-CCGT

The installed charging and discharging capacities of H₂-CCGT in 2050 are presented in Figure 5.40 for the 42 scenarios. With an installed charging capacity of 14.9 GW and discharging capacity of 3.7 GW, the optimal ratio of charging to discharging capacity amounts to 4:1 in the reference scenario. As explained in Section 5.4.3, the ratio is considerably higher than in case of PSP and AA-CAES due to the low round-trip efficiency of hydrogen storage.

Under the majority of variation scenarios, the optimal ratio of charging to discharging capacity of H₂-CCGT is above 3 and below 5. However, as for storage duration,

extreme deviations from this range are observed for several input parameters. As larger discharging capacities are necessary in case of 90 % and 100 % RES scenarios, very low ratios are reached (0.78:1 and 0.66:1 respectively). Comparably low ratios, which come close to the typical range of PSP or AA-CAES, are also observed for some variations of annual time series and RES structure.

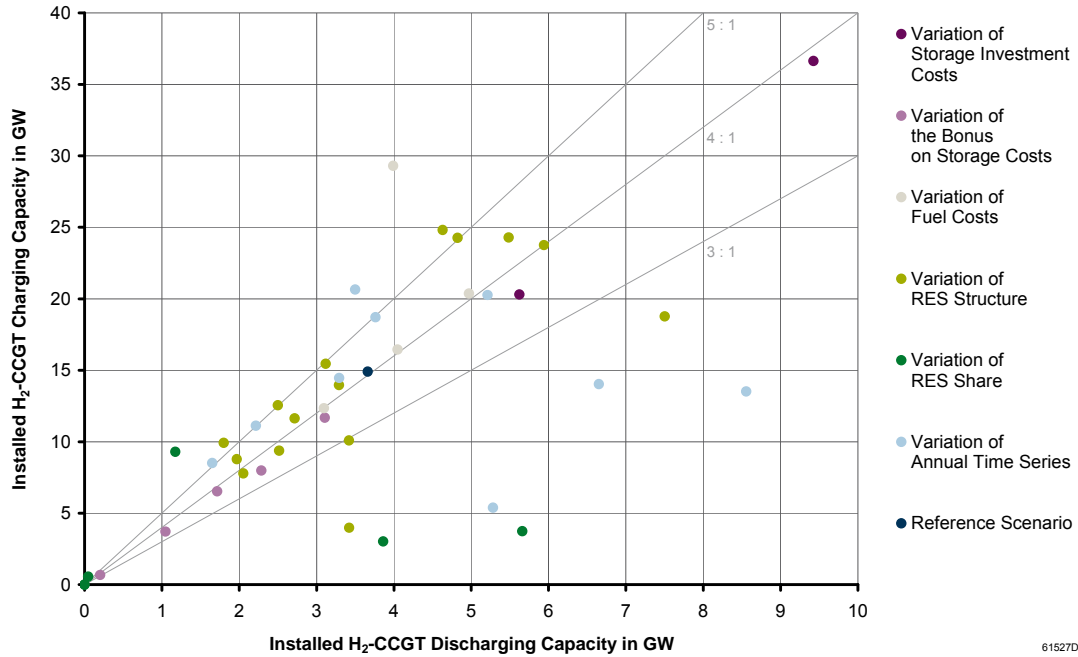


Figure 5.40: Ratio of charging to discharging capacity of new build H₂-CCGT in 2050 in the variation scenarios as compared to the reference scenario

5.7 Detailed discussion of results from the variation scenarios

5.7.1 Variation of annual time series

This section analyses storage demand under scenarios of varying annual time series with regard to the characteristics of the employed residual demand time series, namely surplus energy, residual energy demand and low-frequency variability (vide Sections 5.3.2 and 5.3.3). As the impact of varying meteorological conditions on PSP expansion is rather small (vide Section 5.6.2), the analysis focuses on the demand for AA-CAES and, particularly, H₂-CCGT. Figure 5.41 presents new build storage capacities in 2050 in the variation scenarios as compared to the reference scenario.

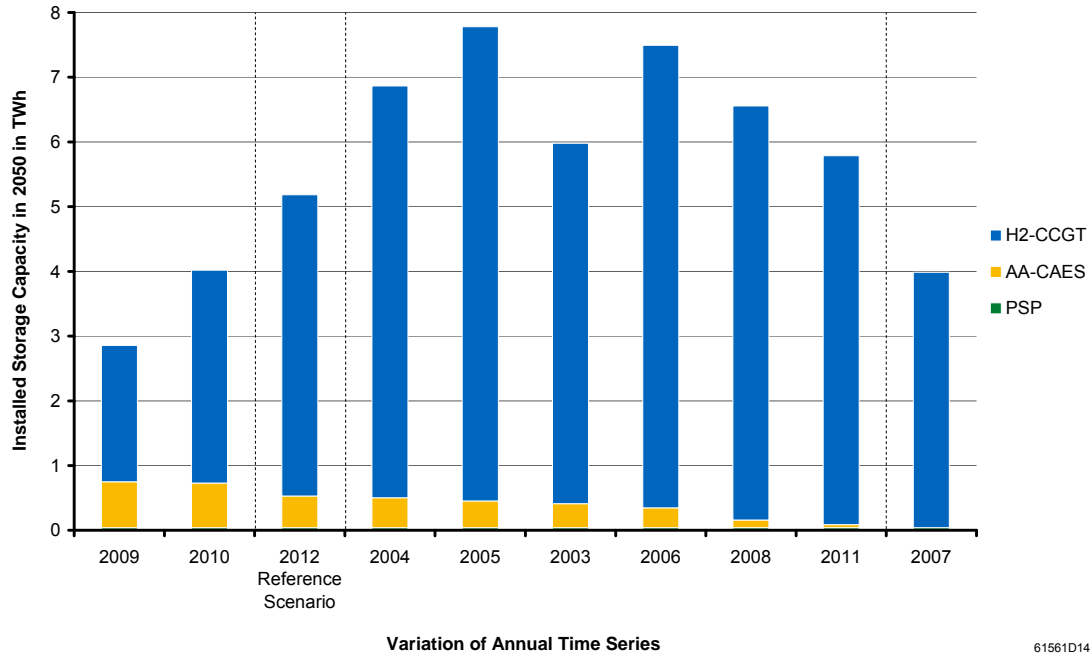


Figure 5.41: New build storage capacity in 2050 for variations of annual time series and the reference scenario

The figure sorts results in descending order of AA-CAES capacity. By this means, three groups of variation scenarios can be distinguished: two scenarios with larger AA-CAES storage capacity and smaller hydrogen storage capacity as compared to the reference scenario (variation scenarios 2009 and 2010); a majority of six scenarios with smaller AA-CAES storage capacity and larger hydrogen storage capacity; as well as one scenario with both smaller AA-CAES storage capacity (actually none) and smaller hydrogen storage capacity (variation scenario 2007).

Thus, in most cases, the impact of annual time series on AA-CAES storage capacity is contrary to the impact on H₂-CCGT storage capacity. For instance, under scenarios 2009 and 2010, hydrogen storage expansion is apparently less profitable than in the reference scenario and AA-CAES capacity is increased to partly take over the balancing of longer-term fluctuations. Compared to the reference scenario, considerably higher values of AA-CAES storage duration (48 h and 53 h respectively) and smaller numbers of equivalent full cycles (38–39) are observed in the two scenarios.

In the six scenarios with smaller AA-CAES and larger hydrogen storage capacity, the rating of AA-CAES tends towards shorter storage durations. The absence of AA-CAES expansion under meteorological conditions of 2007 is due to the lowest residual energy demand among all variations of annual time series (vide Table 5.32, Sec-

tion 5.3.3). Whereas demand decreases for all storage technologies when opportunities to profitably discharge are scarce, the reduction of AA-CAES capacity takes precedence: While PSP offer lower costs and higher efficiency, the lower energy-related costs of H₂-CCGT permit investment into much larger storage capacities, thus allowing to bridge gaps between discharging opportunities.

For the ten scenarios representing the meteorological conditions of the period 2003–2012, Figure 5.42 examines the correlation between surplus energy, residual energy demand and new build hydrogen storage capacity in 2050. It should be noted that the annual amount of generation from RES and CHP varies significantly across the ten scenarios, while there are only very small differences in total annual electricity consumption (vide Figure 5.20, Section 5.5.1).

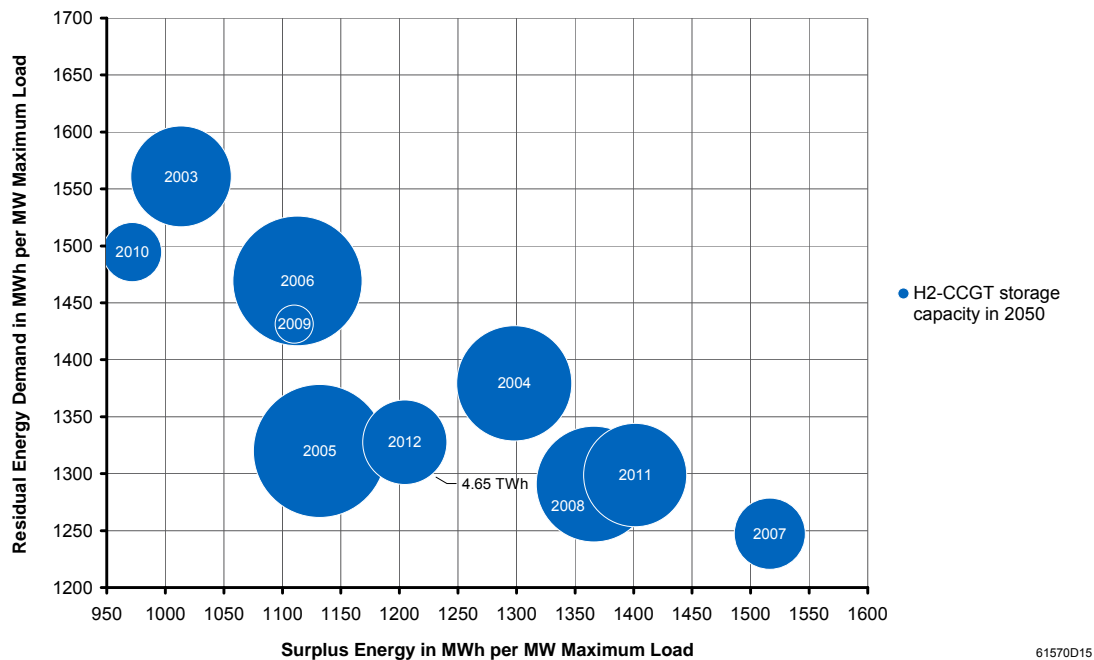


Figure 5.42: Surplus energy, residual energy demand and H₂-CCGT storage capacity in 2050 for variations of annual time series and the reference scenario

According to Figure 5.42, residual energy demand tends to be lower under scenarios with larger amounts of surplus energy. Also, the amounts of surplus energy and residual energy demand are strongly positively and negatively correlated with the total amount of RES and CHP generation. Thus, the highest level of surplus energy and the lowest level of residual energy demand are observed for scenario 2007, which

exhibits the largest amount of total annual must-run generation (556.9 TWh in 2050 as compared to 526.2 TWh in the reference scenario).

However, the share of must-run generation that can be directly integrated usually declines with higher amounts of must-run generation: In the 2007 scenario, only 78.2 % can be directly utilised in 2050 as compared to 81.6 % in the reference scenario. As the extent to which generation from RES and CHP can be integrated is also strongly dependent on the correlation of generation and demand time series, exceptions to this rule are, of course, possible. For instance, despite a considerably higher amount of must-run generation in scenario 2005, the same share – roughly 82.5 % – is integrated as in variations 2006 and 2009.

While storage demand is expected to increase for higher levels of surplus energy as well as for higher levels of residual energy demand (which entail more opportunities to discharge profitably), Figure 5.42 shows that the variation of H₂-CCGT capacity is not adequately described by the amounts of surplus energy and residual energy demand. For instance, despite a larger amount of surplus energy in scenario 2012 as compared to scenario 2005, a lower level of storage capacity is observed (residual energy demands being virtually equal under both scenarios). Furthermore, at a similar level of surplus energy and an only slightly lower residual energy demand, storage capacity in scenario 2009 is significantly smaller than under scenario 2006.

As pointed out in Section 5.3, the distribution of energy over time is another important characteristic of time series that could help to explain the observed results. In particular, low-frequency variability can be considered an indicator for long-duration storage demand such as H₂-CCGT (vide Kühne *et al.* 2014).

For the ten scenarios representing the meteorological conditions of the period 2003–2012, Figure 5.43 shows the theoretical long-duration storage capacity that would be necessary in 2050 to balance all low-frequency fluctuations of residual demand (i. e. fluctuations with period T of more than one month). The theoretical long-duration storage demand increases both for higher values of low-frequency variability and for larger amounts of surplus energy. However, within the considered ranges, the sensitivity to the low-frequency variability index is much more significant.

It should be noted that, whereas the specified surplus represents the total surplus energy of the considered residual demand time series, the theoretical long-duration storage capacity is actually only dependent on the amount of surplus energy that is contained within the low-frequency component of the time series. While, usually, total surplus and low-frequency surplus are fairly well correlated, the 2006 case forms an exception to this rule: Despite lower levels of low-frequency variability and total surplus energy than under scenario 2012, a larger theoretical long-duration storage capacity is reported due to a higher low-frequency surplus.

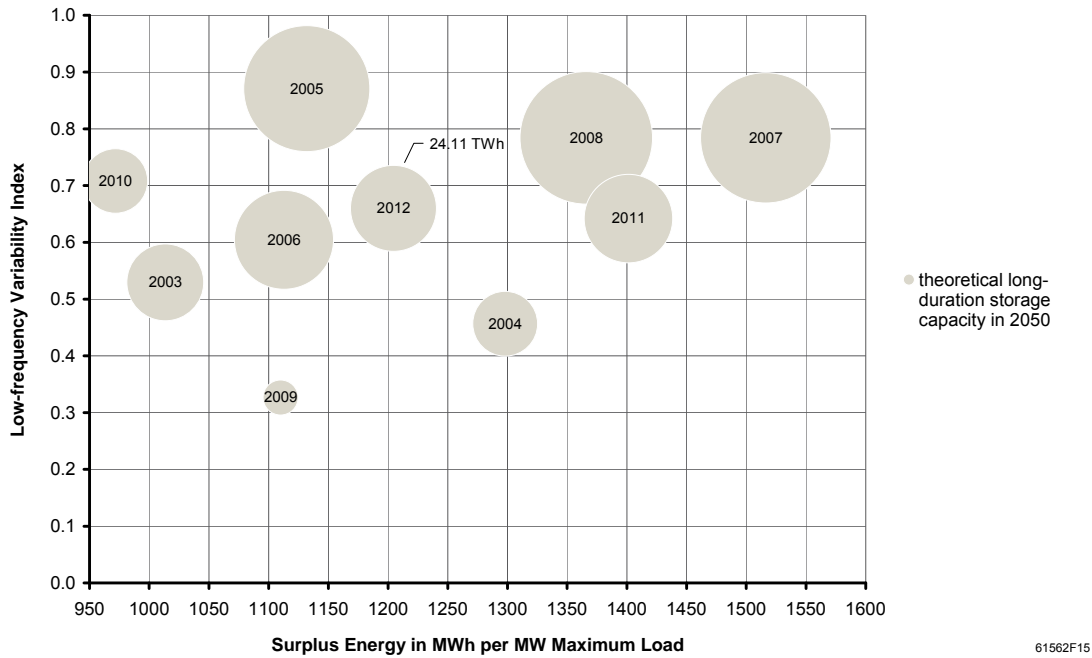


Figure 5.43: Surplus energy, low-frequency variability and theoretical long-duration storage capacity in 2050 for variations of annual time series and the reference scenario

In Figure 5.44, the H₂-CCGT storage capacities resulting for varying annual time series in 2050 are compared to the corresponding theoretical long-duration storage capacities. As the complete balancing of fluctuations, i. e. the complete integration of surplus energy, is not economically feasible, the overall level of installed H₂-CCGT storage capacity is significantly lower than the level of theoretical long-duration storage capacity (4.65 TWh as compared to 24.11 TWh for meteorological conditions of 2012). Theoretical long-duration storage capacities are therefore not represented true to scale but relative to H₂-CCGT storage capacity in the reference scenario.

Thus, the grey dots in Figure 5.44 indicate the theoretically expected size of hydrogen storage capacities in the variation scenarios as compared to the reference scenario. As the figure illustrates, optimised H₂-CCGT storage capacities correspond quite well with theoretically expected capacities for most variations of annual time series.

By also consulting the low-frequency variability index of residual demand time series, a better understanding of the variation of H₂-CCGT storage capacity is achieved: In the above discussed case of scenarios 2005 and 2012, a significantly higher value of low-frequency variability – 0.87 as compared to 0.66 – leads to a larger installed hydrogen storage capacity under scenario 2005 (despite a higher level of surplus energy in the 2012 scenario).

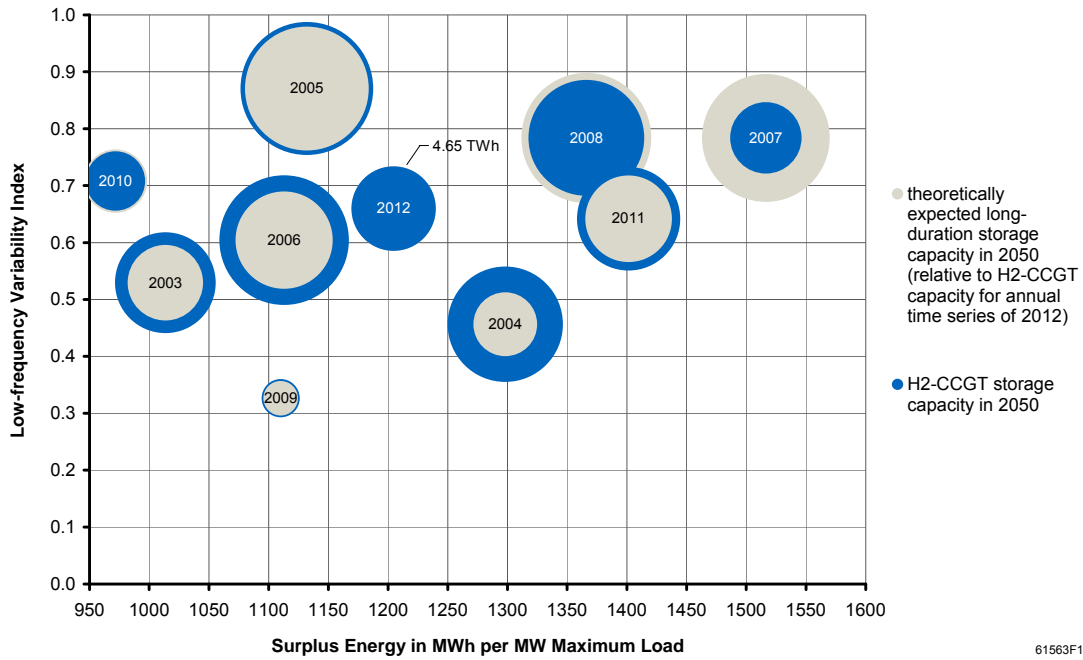


Figure 5.44: H₂-CCGT storage capacity in 2050 as compared to theoretically expected long-duration storage capacity for variations of annual time series and the reference scenario

Furthermore, the very small storage capacity under scenario 2009 as compared to scenario 2006 is supposedly mainly due to low-frequency variability indices differing by almost twofold (0.33 and 0.60 respectively) rather than by the slightly lower residual energy demand in the 2009 case (vide Figure 5.42).

However, in order to explain deviations of optimised H₂-CCGT storage capacity from theoretically expected values, it is sometimes helpful to take residual energy demand into account: Under variation scenario 2004, the storage capacity resulting from optimisation exceeds theoretically expected capacity by 80 %. As Figure 5.42 illustrates, the amount of residual energy demand in scenario 2004 is considerably larger than in the reference scenario, thus adding to the profitability of hydrogen storage.

By contrast, if annual time series of 2007 are assumed, optimised storage capacity undercuts the theoretically expected capacity by 44 %. In this case, a considerably smaller amount of residual energy demand than in the reference scenario is observed (i. e. less opportunities to discharge profitably). Thus, storage expansion is less attractive than expected based on the theoretical analysis of long-duration storage demand. It should be noted that other factors, like e. g. achievable FLH of charging and discharging capacities, may also significantly affect the economic feasibility of storage capacity expansion.

5.7.2 Variation of RES share

As expected, the assumed share of electricity generation from RES has a strong impact on results on storage demand. As the overview of results from variation scenarios in Section 5.6 already showed, storage expansion is completely abandoned if an RES share of only 40 % in 2050 is assumed. The analysis furthermore showed that even in case of an RES share of 50 % only PSP capacity is expanded, while new build AA-CAES and H₂-CCGT are not economically feasible.

For the seven scenarios of varying RES share, Figure 5.45 presents new build storage capacities in 2050 by storage technology. Up to an RES share of 80 %, installed storage capacity in 2050 increases with growing shares of RES. Whereas storage capacity is to a large extent made up by hydrogen storage, AA-CAES constitutes more than half of the installed charging and discharging capacities (not shown) under scenarios of 60 %, 70 % and 80 % RES share.

In case of RES shares of 90 % and 100 % in 2050, significantly lower levels of storage capacity than in the reference scenario are observed. Apparently, such high shares of RES affect AA-CAES expansion even more than H₂-CCGT expansion (both in terms of storage capacity and in terms of charging and discharging capacity).

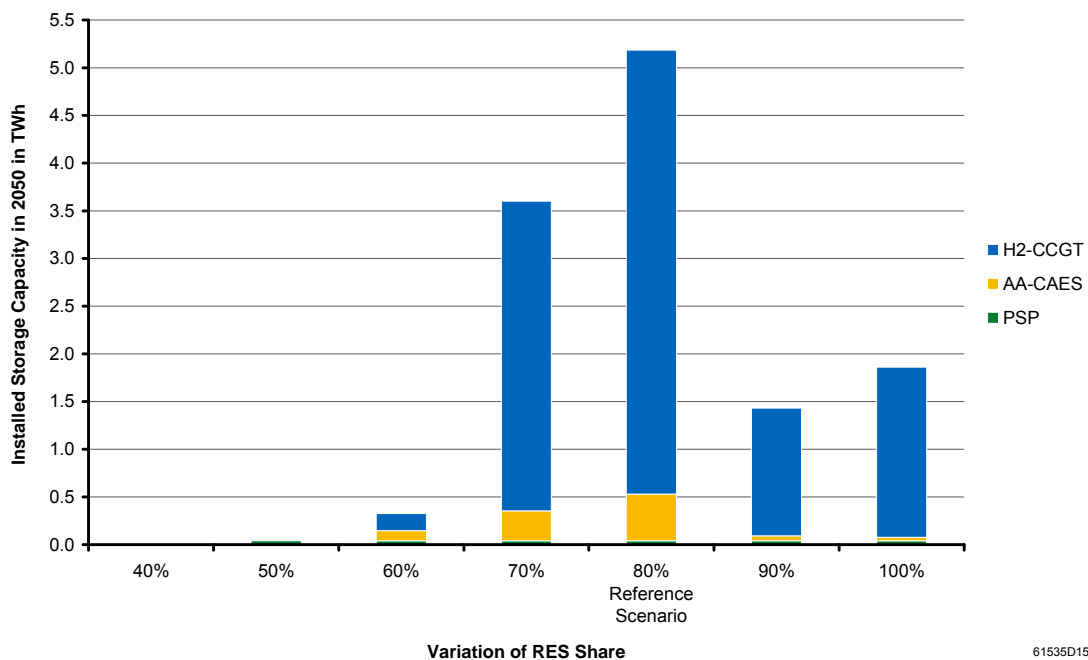


Figure 5.45: New build storage capacity in 2050 for variations of RES share and the reference scenario

While under scenarios with extremely high shares of RES storage demand is obviously subject to completely different effects that need to be analysed separately (vide infra), the – seemingly continuous – increase of storage capacity across scenarios up to an RES share of 80 % leads to the question of whether there are typical thresholds that trigger the expansion of certain storage technologies.

The expansion of storage capacity over the planning horizon is therefore compared across scenarios with regard to the share of RES, surplus energy and residual energy demand. By way of example, Figure 5.46 and Figure 5.47 present these three quantities as well as the expansion of storage capacity over the planning horizon 2010–2050 for the 60 % and the 80 % case respectively.

It should be noted that – despite similar shares of RES – simulation years from different scenarios are never fully comparable: First, the structure of RES usually differs slightly. For instance, with hydro, geothermal and biomass generation adding up to 17.1 % in 2050, 42.9 % come from wind and solar in the 60 % scenario (vide Table 5.34, Section 5.5.2). By contrast, although approximately 60 % (59.6 %) RES generation is reached in 2037 in the reference scenario, hydro, geothermal and biomass generation only add up to 14.4 %, while 45.2 % come from wind and solar. Secondly, depending on the assumed extent of RES expansion, the need to further reduce emissions varies and the conventional generation portfolio might develop very differently.

As Figure 5.46 illustrates, expansion of PSP starts in 2032 if electricity generation from RES is assumed to increase linearly to a share of 60 % in 2050. In 2032, RES reach a share of 40.7 % and surplus energy amounts to roughly 3 TWh. By contrast, the expansion of AA-CAES starts in 2046, at an RES share of 55.7 % and 20 TWh surplus, and hydrogen storage does not become economically feasible before 2050, i. e. at 60 % RES and 28 TWh of surplus energy.

By comparison, under the 80 % reference scenario, the expansion of PSP first starts in 2019 but is interrupted due to the nuclear phase out in 2023 (vide Figure 5.47). For a non-nuclear generation portfolio, expansion of PSP is first observed in 2024, at a 39.1 % RES share and 3 TWh surplus. Expansion of AA-CAES starts in 2034, at a comparable RES share of 54.9 %. Hydrogen storage becomes economically feasible in 2040, at considerably higher values of RES share (64.3 %) and surplus energy (45 TWh) than in the 60 % case.

Despite considerable differences in boundary conditions, more or less narrow ranges of RES share can be specified that typically trigger storage expansion under scenarios varying RES share up to 80 %. Considering a non-nuclear generation portfolio, PSP expansion is usually triggered at 38–44 % RES and only 2–4 TWh of surplus energy. While new build AA-CAES become economically feasible at RES shares of 55–56 %, hydrogen storage expansion is observed to start at 60–64 % RES.

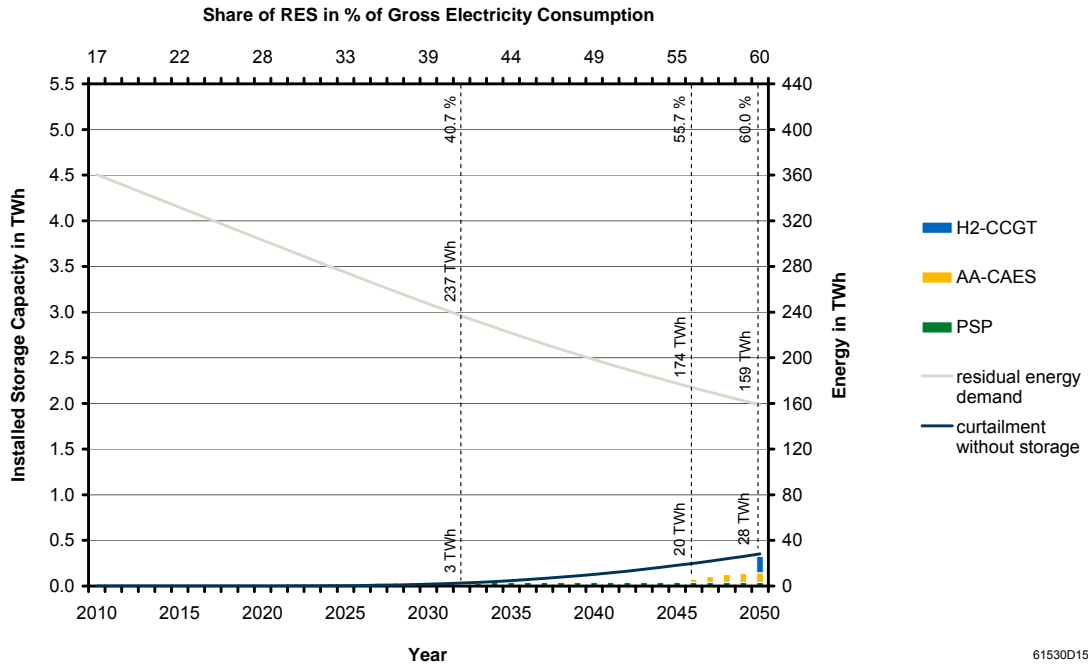


Figure 5.46: Expansion of storage capacity over the planning horizon 2010–2050 in case of an RES share of 60 % in 2050

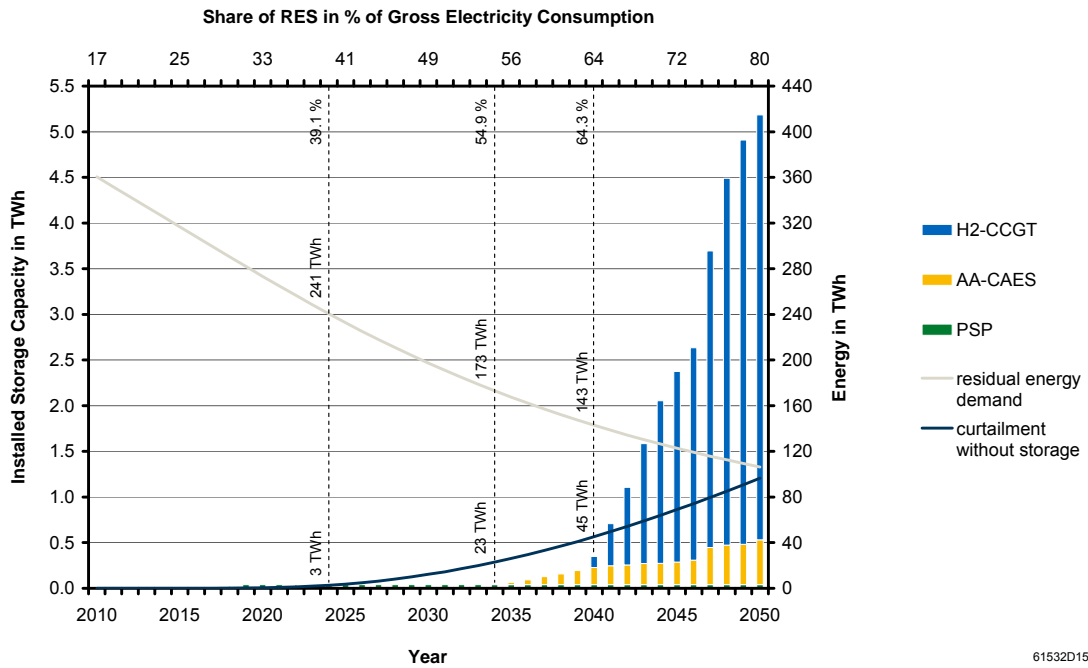


Figure 5.47: Expansion of storage capacity over the planning horizon 2010–2050 in case of an RES share of 80 % in 2050 (reference scenario)

As the scenarios with RES shares of 90 % and 100 % in 2050 show, storage expansion is not only driven by the amount of available surplus energy. The share of RES already exceeds 80 % in 2045 under the 90 % scenario and in 2041 under the 100 % scenario. However, the share of must-run generation (i. e. RES and CHP) that can be directly integrated declines for each additional TWh of must-run generation: Only roughly 71.2 % of the total 647.0 TWh of RES and CHP generation are directly utilised in 2050 under the 100 % scenario, as compared to 81.6 % of 526.2 TWh under the 80 % reference scenario. Thus, in 2050, curtailment in the 100 % case increases almost twofold compared to the 80 % case (vide Figure 5.48).

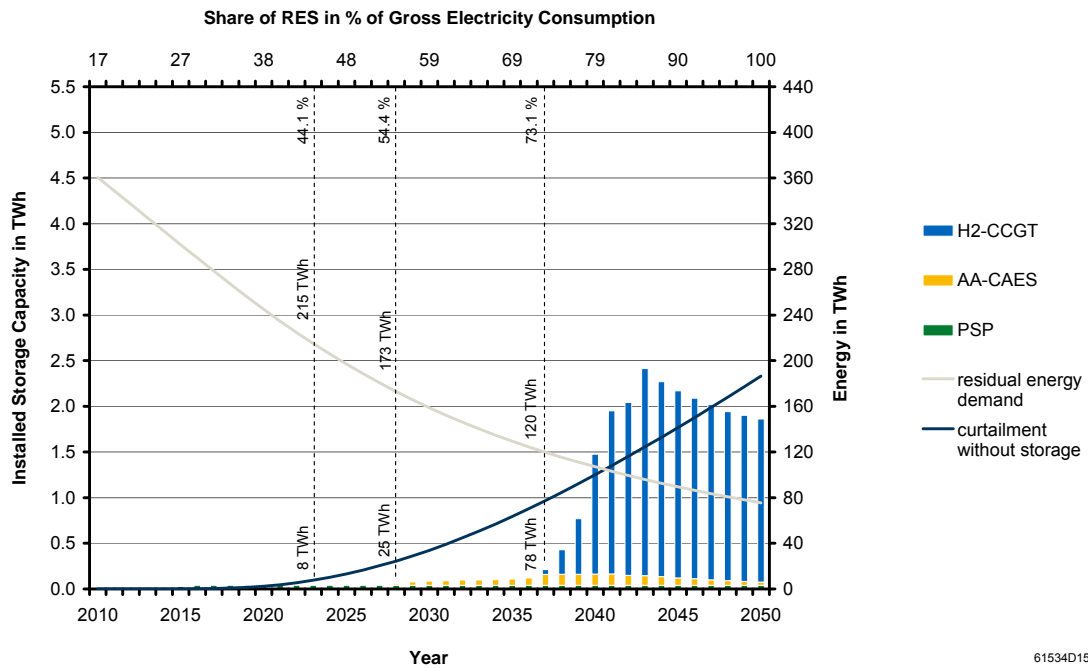


Figure 5.48: Expansion of storage capacity over the planning horizon 2010–2050 in case of an RES share of 100 % in 2050

While surplus energy increases, the amount of residual energy demand further declines for RES shares beyond 80 %: The minimum residual energy demand from the reference scenario (106 TWh in 2050) is already undercut in 2045 under the 90 % scenario and in 2041 under the 100 % scenario. As opportunities to profitably discharge storages become scarcer for lower levels of residual energy demand, the economic feasibility of storage expansion decreases. This explains the low levels of storage demand resulting for RES shares of 90 % and 100 % in 2050 (vide Figure 5.45).

However, storage expansion in earlier years in the 90 % and 100 % scenarios does also not come near to the level observed in the reference scenario in 2050. As Figure 5.48 illustrates, storage demand reaches its peak in 2043 under the 100 % scenario: At an RES share of 85.5 %, total new build storage capacity amounts to only 2.4 TWh (as compared to 5.2 TWh in the reference scenario).

The significantly lower profitability of storage expansion in scenarios with extremely high shares of RES is due to a reduced need for energy storage as an emissions abatement measure. While for all variations of RES share a constant total carbon emissions budget of 5973 million tonnes CO₂ is assumed for the planning horizon 2010–2050, only 98.3 % of the budget is used under the 90 % scenario and only 89.6 % is used under the 100 % scenario. By contrast, the entire budget of 5973 million tonnes CO₂ is spent in the reference scenario (and all other variations of RES share).

Considering the even smaller amount of residual energy demand in case of a 100 % RES share in 2050, the higher level of storage capacity (and, actually, charging and discharging capacity) as compared to the 90 % case might seem implausible. However, due to a lower number of FLH, the portion of gas turbine capacity in the conventional generation portfolio in 2050 is considerably larger under the 100 % scenario, which, in turn, improves the arbitrage opportunities for energy storage.

5.7.3 Variation of RES structure

This section analyses storage demand under scenarios of varying RES structure. As the majority of the examined variations of RES structure represent extreme cases where only one or two of the three major RES contribute to the generation mix in 2050, it is not surprising that – among all variations of input parameters – the largest relative deviations of total storage capacity (as well as total charging and discharging capacity) from the reference scenario are reported for variations of RES structure (vide Section 5.6.1).

However, as shown in Sections 5.6.2, 5.6.3 and 5.6.4, the sensitivity of the considered storage technologies to RES structure differs quite significantly. While in case of PSP the exogenously fixed limit of 40 GWh storage capacity is reached in 2050 for all RES structures (PSP charging and discharging capacities actually vary considerably), a comparably low sensitivity of AA-CAES storage capacity goes along with extreme deviations of AA-CAES charging and discharging capacities. For H₂-CCGT, a significant sensitivity of storage capacity – ranging from -59 % to +167 % – as well as relatively large deviations of charging and discharging capacity are observed.

Figure 5.49 presents new build storage capacity in 2050 by storage technology.

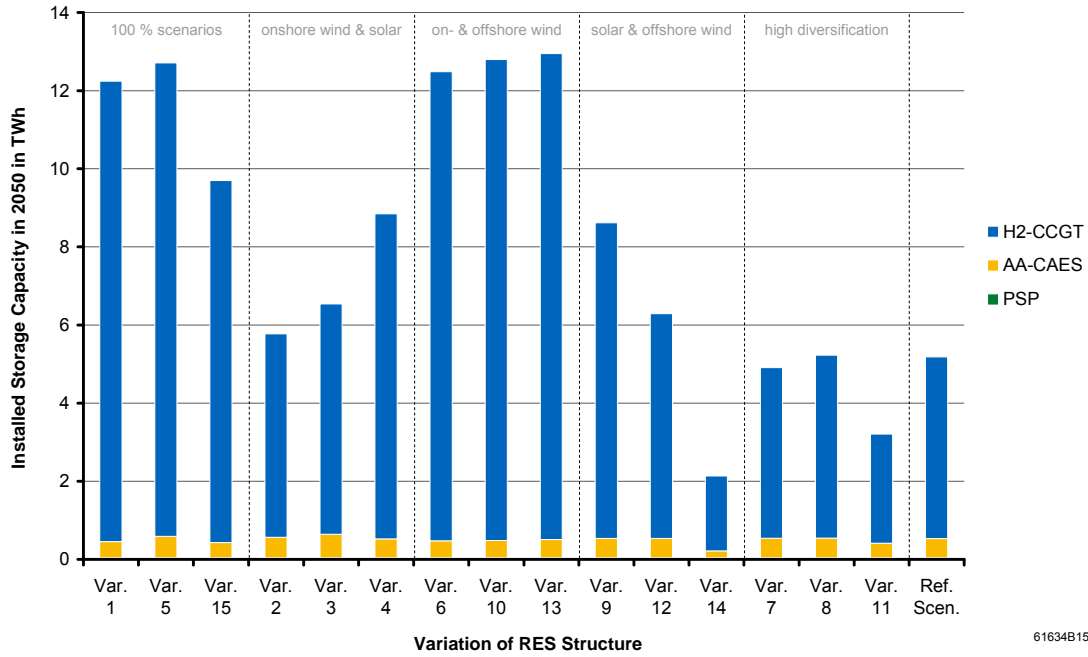


Figure 5.49: New build storage capacity in 2050 for variations of RES structure and the reference scenario

Results are sorted according to the degree of diversification. As already mentioned in Section 5.6.4, total storage capacity in 2050 is dominated by hydrogen. Thus, variations of total storage capacity are mainly determined by the sensitivity of H₂-CCGT.

As expected, high levels of total storage capacity can be observed for extremely low degrees of diversification, namely for variations 1, 5 and 15, where only one of the three major RES contributes to the generation mix in 2050. Among these 100 % scenarios, the lowest level of total storage capacity is observed if only offshore wind is assumed to be part of the generation mix (variation number 15). The reason for this is a considerably smaller amount of surplus energy than for 100 % onshore wind or 100 % solar scenarios (vide Figure 5.23, Section 5.5.3).

High levels of total storage capacity are also observed for variations of RES structure with generation from both onshore and offshore wind but without contribution of solar PV. As in 100 % onshore wind and 100 % offshore wind scenarios, surplus energy mainly occurs during winter season if both onshore and offshore wind contribute to the generation mix. Thus, the demand for the balancing of long-term fluctuations reaches a comparably high level.

By contrast, the levels of hydrogen storage capacity – and, thus, total storage capacity – are significantly lower under scenarios where solar PV and either onshore or off-

shore wind contribute to the generation mix in 2050. In spite of similar or even larger amounts of surplus energy than in pure wind scenarios, there is a reduced potential for long-duration storage, as surplus energy is more evenly distributed over the year. Storage capacity decreases considerably for lower shares of solar generation.

The smallest total storage capacity is observed for variation scenario 14, which assumes relative shares of 25 % solar and 75 % offshore wind generation in 2050 and exhibits the smallest amount of surplus energy (86 TWh). Besides this scenario, the lowest levels of total storage capacity are found for scenarios that assume higher diversification, i. e. contributions from all three major RES (variations 7, 8, 11 as well as the reference scenario). Again, a larger portion of offshore wind – namely a relative share of 50 % in variation scenario 11 – reduces the demand for storage.

The installed storage capacities of AA-CAES and H₂-CCGT in 2050 are illustrated in Figure 5.50 and Figure 5.51 respectively. As it can be observed, AA-CAES storage capacity tends to reach higher levels for low shares of offshore wind and high shares of solar PV. Due to their investment cost structure and comparably high efficiency, AA-CAES represent the best technology to balance short-term fluctuations of solar generation if the expansion of PSP is limited.

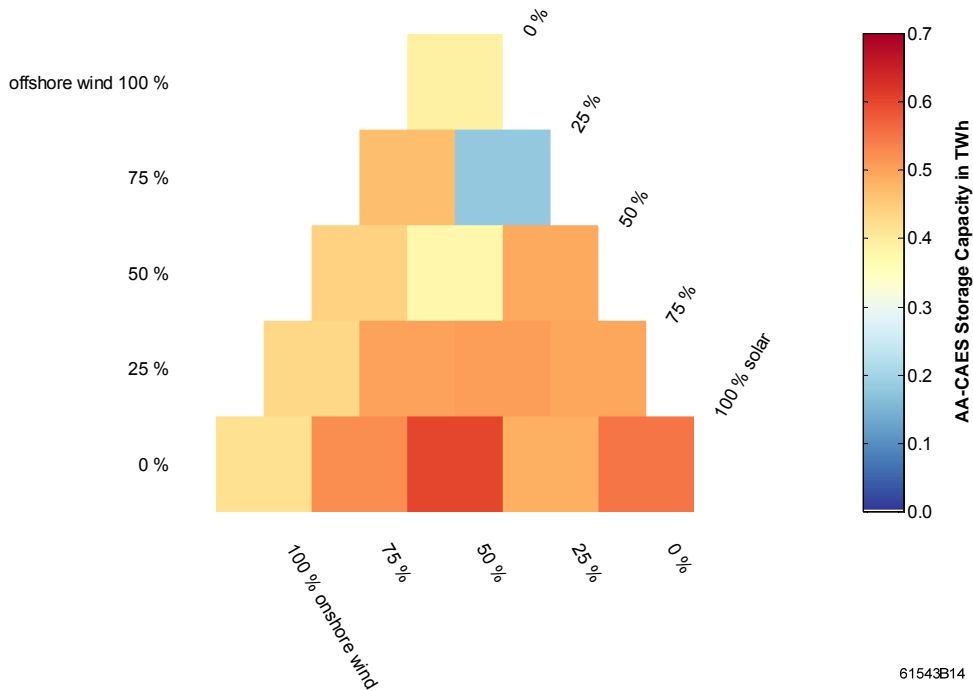


Figure 5.50: Storage capacity of new build AA-CAES in 2050 for variations of RES structure

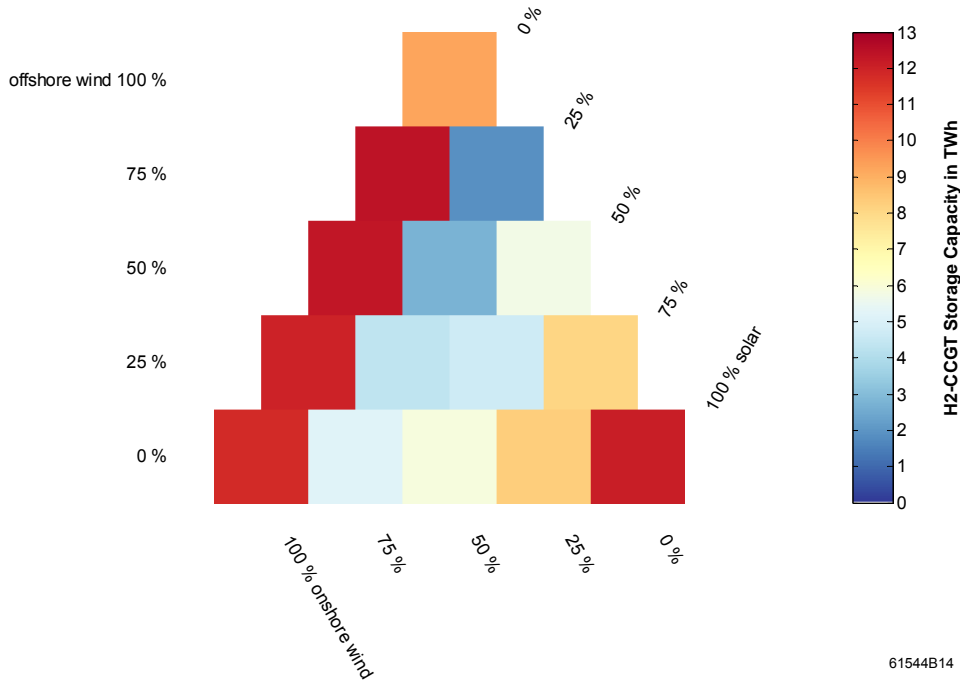


Figure 5.51: Storage capacity of new build H₂-CCGT in 2050 for variations of RES structure

Figure 5.51 again illustrates the comparably low level of hydrogen storage capacity under scenarios with contributions from solar PV and either onshore or offshore wind (variations 2, 3, 4 and 9, 12, 14), which is due to the counter-cyclical seasonal characteristics of wind and solar generation and the more even distribution of surplus energy over the year. By contrast, due to positively correlated onshore and offshore wind generation, extremely large hydrogen storage capacities are installed on the 0 % solar isoline.

Figure 5.51 also visualises the significantly lower level of hydrogen storage capacity in the 100 % offshore wind case (variation number 15) as compared to the 100 % onshore wind and the 100 % solar scenarios. As pointed out in Section 5.5.3, a high number of FLH as well as the strong seasonal correlation of offshore wind generation and demand leads to considerably less surplus energy and, thus, less demand for long-duration storage. Low to moderate levels of hydrogen storage capacity are observed for variation scenarios on isolines of 25 % and 50 % solar generation.

As already mentioned, the variation of RES structure also has considerable impact on the installed charging and discharging capacity. In case of PSP, the relative sensitivity of charging and discharging capacity is usually similar, as the ratio of discharging to charging capacity is limited exogenously (vide Section 5.6.2).

Figure 5.52 presents the installed charging capacity of PSP in 2050. Both PSP charging and discharging capacity increase for higher solar shares: Due to their investment cost structure and high efficiency, PSP are best suited for the balancing of short-term fluctuations of solar generation. Moreover, only very little variation of charging and discharging capacity is observed along solar isolines. Thus, the rating of PSP charging and discharging capacity is primarily determined by the share of solar PV and virtually unaffected by the specific portions of onshore and offshore wind.

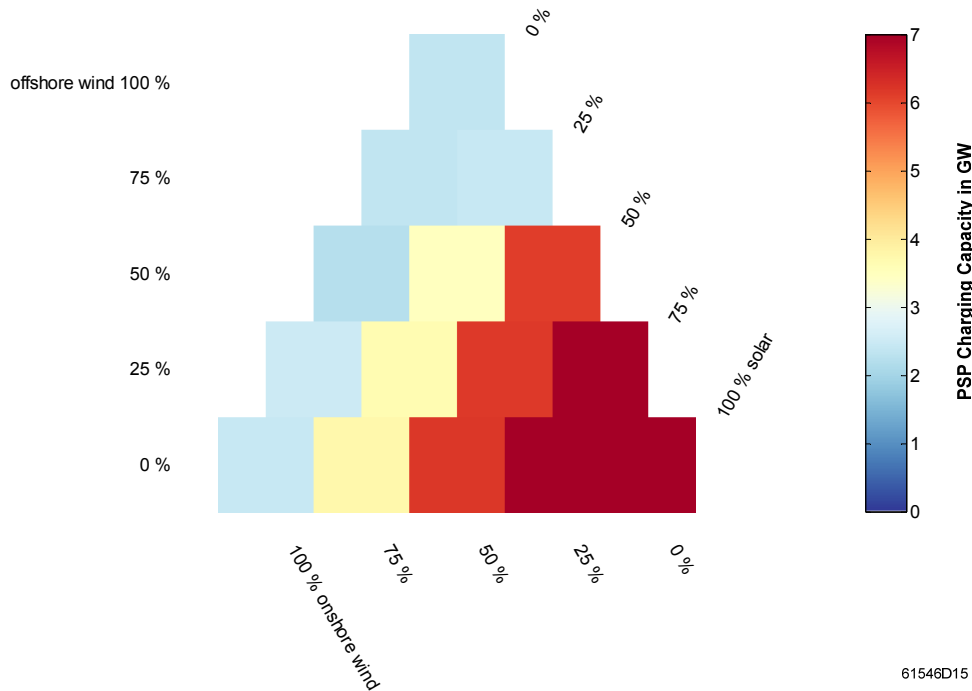


Figure 5.52: Charging capacity of new build PSP in 2050 for variations of RES structure

As in case of PSP, both AA-CAES charging and discharging capacity increase for higher solar shares. However, more variation of charging and discharging capacity is observed along solar isolines than for PSP. The relative sensitivity of charging and discharging capacity of AA-CAES is very similar, although capacities are not constrained to a certain ratio. The correlation with high shares of solar PV is much stronger for AA-CAES charging and discharging capacity than for storage capacity.

In case of H₂-CCGT, the relative sensitivity of charging and discharging capacity to variations of RES structure is generally quite different: As Figure 5.40 in Section

5.6.4 already showed, the optimal ratio of H₂-CCGT charging to discharging capacity varies considerably for different structures of RES.

Figure 5.53 presents the installed charging capacity of H₂-CCGT in 2050. As in case of storage capacity, the highest levels of H₂-CCGT charging and discharging capacity are observed on the 0 % solar isoline, i. e. for scenarios where solar PV does not contribute to the generation mix in 2050. In contrast to storage capacity, where a comparably high level of expansion is also reached under the 100 % solar scenario (vide Figure 5.51), the level of H₂-CCGT charging and discharging capacity is significantly lower in the 100 % solar scenario than in pure wind scenarios.

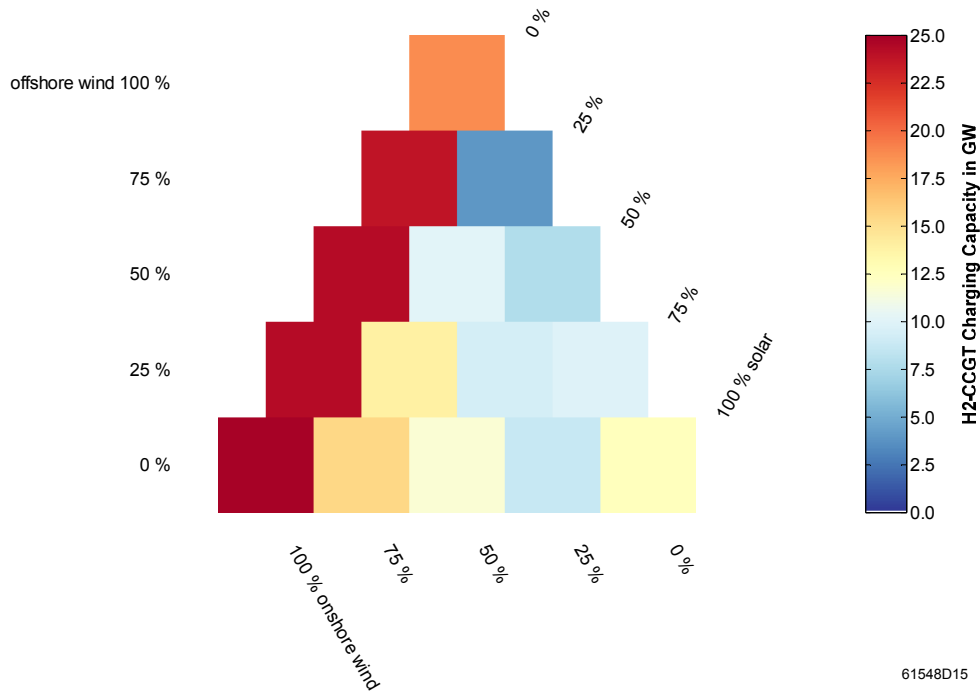


Figure 5.53: Charging capacity of new build H₂-CCGT in 2050 for variations of RES structure

In order to explain the unexpectedly low level of H₂-CCGT charging and discharging capacity in the 100 % solar case, Figure 5.54 compares the patterns of optimised storage dispatch of H₂-CCGT in scenarios with relative shares of 100 % solar and 100 % offshore wind generation in 2050.

Due to the even more pronounced seasonality of solar generation – for the meteorological reference year, a low-frequency variability index of 1 is found in Section 5.3.1 as compared to 0.88 in case of offshore wind generation –, the dispatch of long-

duration storage under a 100 % solar scenario rarely deviates from steadily charging during summer and steadily discharging during winter. Therefore, comparably small charging and discharging capacities are installed. While long-duration storage also clearly balances the seasonal fluctuation of offshore wind generation, the additional balancing of mid-frequency fluctuations requires higher installed charging and discharging capacities.

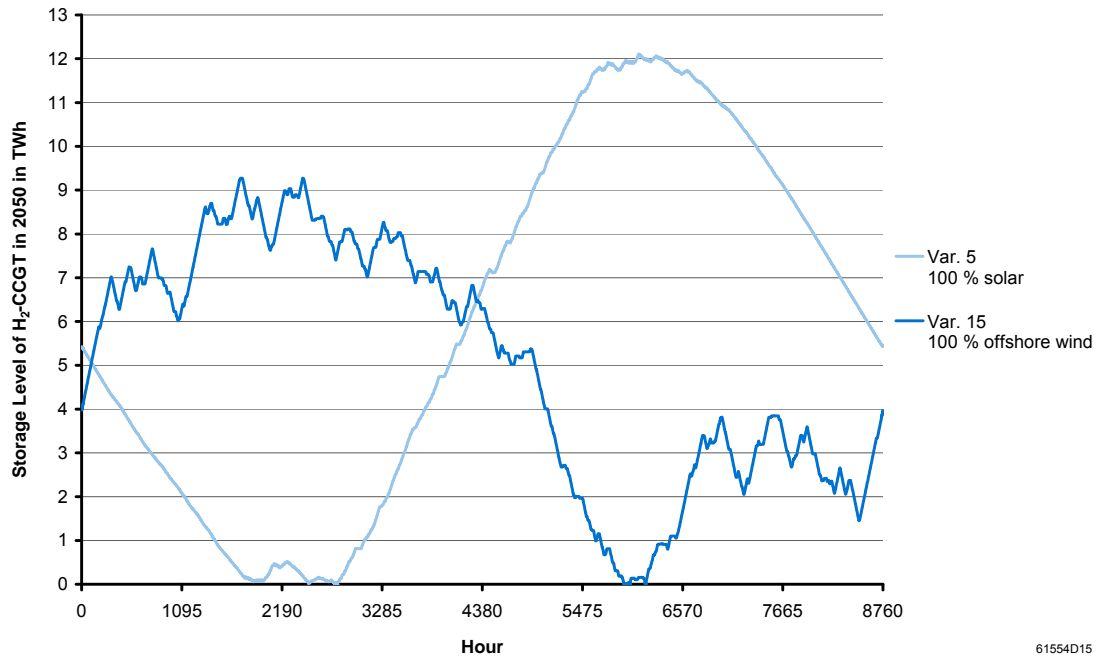


Figure 5.54: Comparison of the storage level of H₂-CCGT in 2050 in scenarios with relative shares of 100 % solar and 100 % offshore wind generation

5.8 Discussion and conclusion

In this chapter, the sensitivity of storage demand to changes in selected input parameters is analysed with the whole-systems cost minimisation model IMAKUS. For this purpose, a scenario framework is established which comprises 42 scenarios, including a suitable reference scenario.

As storage demand is largely influenced by the chronological characteristics of renewable electricity generation and electricity demand, the reference scenario is based on a consistent set of annual time series that is representative of meteorological conditions in Germany. This meteorological reference year is selected from annual time

series of generation and demand for the period 2003–2012, which are evaluated by means of FLH, residual energy demand and surplus energy as well as low-frequency variability.

The sensitivity of storage demand is examined with regard to variations of annual time series, RES share, RES structure, fuel costs, the bonus on storage costs and storage investment costs. The analysis demonstrates a significant sensitivity of storage demand to all of the tested input parameters. However, extreme deviations from the reference scenario are, in part, also owing to extreme scenarios, as, for instance, in case of low shares of RES or low levels of diversification.

With regard to individual technologies, the demand for PSP is observed to be comparably robust to varying input parameters. This is particularly true for variations of annual time series and fuel costs as well as for a varying bonus on storage costs. Under the majority of scenarios, the optimal storage duration of PSP lies within the range of 10–20 h, which is considerably higher than the usual range of 3–8 h for existing PSP in Germany. As PSP storage capacity expansion was exogenously limited to 40 GWh, the sensitivity of the actual economic potential could be higher.

Except for scenarios with RES shares less than 60 % in 2050, total new build storage capacity is dominated by hydrogen in 2050. Due to the very low level of energy-related investment costs, the sensitivity of hydrogen storage capacity to input parameters is generally very high. Therefore, the optimal storage duration of H₂-CCGT is only found within the relatively broad range of 600–1200 h in roughly half of the scenarios. The optimal storage duration of AA-CAES lies within the range of 30–50 h under the majority of scenarios.

As results show, installed charging capacity usually exceeds discharging capacity for all storage technologies, as large charging units are necessary to integrate surplus generation which typically occurs in the form of short-term power peaks. However, for extremely high shares of 90 % and 100 % RES in 2050, larger discharging capacities are optimal: As the amount of residual energy demand declines, opportunities to profitably discharge storages become scarce. Storage expansion is generally observed to decrease for smaller amounts of residual energy demand, but the reduction of AA-CAES takes precedence, as PSP offer higher efficiency at lower costs and H₂-CCGT offer significantly lower energy-related costs.

As expected, RES share has a very strong impact on storage demand: Storage expansion is completely abandoned if an RES share of 40 % in 2050 is assumed. Even in case of 50 % RES in 2050, only new build PSP are economically feasible. Up to an RES share of 80 % installed storage capacity increases with growing shares of RES. Due to the smaller amount of residual energy demand and the reduced need for energy storage as an emissions abatement measure, storage demand decreases again for RES shares of 90 % and 100 %.

More or less narrow ranges of RES share can be specified that typically trigger storage expansion: In a non-nuclear generation portfolio, PSP expansion is triggered at RES shares of 38–44 %. AA-CAES and H₂-CCGT become economically feasible at RES shares of 55–56 % and 60–64 % respectively.

For variations of annual time series, the highest sensitivity is observed for AA-CAES, both in terms of storage capacity and charging and discharging capacity. In most cases, the impact of annual time series on AA-CAES storage capacity is contrary to the impact on H₂-CCGT storage capacity: Whereas AA-CAES partly take over the balancing of long-term fluctuations if meteorological conditions prove less attractive to hydrogen storage, the rating of AA-CAES tends towards shorter storage durations if large hydrogen storage capacities are installed.

Moreover, it is shown that the impact of varying annual time series on hydrogen storage capacity can be better explained if – in addition to the amounts of surplus energy and residual energy demand – the low-frequency variability index of residual demand time series is consulted.

The high sensitivity of storage demand to meteorological conditions that differ from “average conditions” represented by the selected meteorological reference year 2012 demonstrates that – while possibly being average – storage demand in the reference scenario cannot be considered representative, not even for meteorological conditions of the period 2003–2012. In order to find out whether varying meteorological conditions can lead to even larger deviations from the reference scenario, storage demand should be optimised for a greater number of different sets of annual time series. By also analysing the probability of occurrence of certain meteorological conditions, the representativeness of results could be better evaluated.

Storage demand exhibits the highest sensitivity to variations of RES structure. However, scenarios of extremely low diversification – and, thus, extremely high levels of storage demand – are not very likely to occur in reality. For high shares of solar generation, extreme deviations from the reference scenario are observed for all storage technologies. The demand for PSP and AA-CAES increases with higher solar shares. Actually, the rating of PSP charging and discharging capacity is primarily determined by the share of solar generation. Large portions of offshore wind generation apparently reduce the overall demand for storage.

As compared to the generation mix in the reference scenario (where relative shares of onshore wind, offshore wind and solar generation in 2050 amount to 40.8 %, 39.5 % and 19.7 % respectively), a portfolio with considerably more offshore and slightly more solar generation would lead to less storage demand (e. g. variation 11). The smallest total storage capacity is observed for relative shares of 25 % solar and 75 % offshore wind (i. e. 15.7 % and 47.2 % of gross electricity consumption respectively). In order to detect the generation mix with minimum storage demand, the number of

variation scenarios would have to be further increased. However, depending on the costs of the renewable generation portfolio, the respective scenario would not necessarily represent the cost-optimal design of the power system.

Results furthermore show that variations of the general fuel price level by not more than 10 % have comparably small impact on storage demand. A significant increase of storage demand is however observed if higher spreads between gas and coal price are assumed.

The variation of the bonus on storage costs points to the importance of contribution margins earned on alternative markets, like the ancillary services market: In particular, the economic feasibility of AA-CAES and H₂-CCGT decreases significantly if storages have to earn more than 50 % of their revenues through energy arbitrage.

As expected, the assumption of lower power-related and higher energy-related storage investment costs – i. e., above all, the assumption of significantly lower power-related costs of PSP and H₂-CCGT – leads to higher demand for PSP and H₂-CCGT capacities, while the attractiveness of AA-CAES is further reduced.

Thus, none of the examined input parameters can be neglected with regard to their impact on energy storage demand. However, the sensitivity of PSP, AA-CAES and hydrogen storage is observed to differ quite significantly. Being the most efficient and least expensive technology, PSP appear to be comparably robust to varying input parameters. While, all in all, the total share of RES generation is certainly the most important driver of storage demand, the economic feasibility of AA-CAES and H₂-CCGT is also significantly dependent on contribution margins from the ancillary services market.

The structure of RES and the assumed meteorological conditions are apparently also important drivers of storage demand that can significantly influence the proportions – and even the presence – of technologies in the optimised storage portfolio. Aside from modelling results, the analysis of annual time series of generation and demand with regard to FLH, surplus energy, residual energy demand and variability can already provide valuable insight into the characteristics of storage demand.

6 Interpretation of results on energy storage demand from an investor's perspective

The analysis in Chapter 5 demonstrated the high sensitivity of storage capacity expansion to varying input parameters. This chapter intends to interpret this uncertainty about cost-optimal storage demand in the German power system from an investor's perspective: How much revenue can be expected from investments into energy storage?

In the first section, the relevance of modelling results from whole-systems cost minimisation to investors is discussed in general. In order to be useful to private-sector decision makers, modelling results should be based on a discount rate that reflects the expected rate of return of investors. Thus, an appropriate value for the discount rate is determined in Section 6.2. Using this discount rate, storage capacity expansion is optimised anew under the reference scenario. The performance of the obtained storage portfolio is then evaluated under selected scenarios of varying meteorological conditions, RES shares and RES structures.

6.1 Are results from whole-systems cost minimisation of any use to investors?

When energy systems are optimised by means of whole-systems cost minimisation, the question arises as to whether investment decisions which are optimal from a system point of view also prove profitable from an investor's perspective. However, in order to be carried out by a private-sector investor in practice, an investment must increase the expected return of the investor's portfolio and match his risk tolerance.

The applicability of modelling results from whole-systems cost minimisation for real-world energy systems is discussed by Trutnevyte (2014), who, on the one hand, expresses general criticism of the cost-optimality assumption in energy systems modelling: Near-optimal solutions to the optimisation problem “may be significantly different in their attributes”, which means that very different system designs may “have a similarly good performance with respect to the total system costs”.

On the other hand, Trutnevyte (2014) criticises that while the so-called social planner is the underlying assumption of whole-systems cost minimisation, such an omniscient decision maker does not exist in reality. Mai *et al.* (2013) stress that “central-planning decision making” and the prioritisation of “least-cost options” are probably even less suitable to model liberalised and decentralised energy systems of the future.

Furthermore, the long-term equilibrium is reached in whole-systems cost minimisation models, i. e. a state of the system where demand is covered at minimum cost while all generating units earn zero profits (vide Hirth & Ueckerdt 2012). However, as Trutnevyte (2014) argues, real-world energy systems “are not necessarily at equilibrium due to market heterogeneity, imperfect information etc.”

Nevertheless, whole-systems cost minimisation models can still offer valuable insights to private-sector investors. First, modelling results illustrate the demand for certain technologies on a system level, like e. g. the demand for energy storage in a cost-optimal power system. While investment into an asset which is part of the cost-optimal portfolio does not necessarily have to be profitable from an investor's perspective, investments into technologies omitted by the model certainly also do not pay off for private-sector investors: As all generating units earn zero profits in the long-term equilibrium, any capacities that are oversized as compared to this cost-optimal solution – or even installed in the first place – will generate deficits (vide Hirth & Ueckerdt 2012).

Secondly, with regard to storage rating, the specific values of storage duration and the ratio of charging to discharging capacity which are found to be optimal from a system point of view can serve as an adequate indication to investors. Thirdly, whole-systems cost minimisation can be used to test the performance of individual storage projects or storage portfolios under different scenarios (vide Section 6.4): For this purpose, storage dispatch is optimised and the annual profit from storage operation is determined as the difference of costs of charging and revenues of discharging.

In any case, if modelling results are intended to inform private-sector decision makers, a discount rate should be used that reflects the expected rate of return of the respective investor.

6.2 Adapting the discount rate to the investor's perspective

As the whole-systems cost minimisation model IMAKUS represents a classic social planner's approach, a (real) social discount rate of 3 % was applied throughout scenarios in Chapter 5 (vide Section 5.2.1). However, when adopting a private-sector investor's perspective, investment decisions have to be evaluated in comparison to alternative uses of corporate capital (Bruner *et al.* 1998). According to Bruner *et al.* (1998), a company's cost of capital – usually expressed as the WACC – is an adequate benchmark: Investments will not be undertaken “unless a firm can earn in excess of its cost of capital”.

Thus, when whole-systems cost minimisation models are adapted to a private-sector investor's perspective, the discount rate used in the model is commonly fixed at the WACC of a potential investor (e. g. Hand *et al.* 2012): It reflects “the required rate of return on the various types of financing” (Van Horne & Wachowicz 2004) of the respective firm.

In this chapter, the optimisation of storage capacity expansion under the reference scenario as well as the evaluation of performance of the obtained storage portfolio under variation scenarios is conducted using a discount rate which is – by way of example – based on the 2012 WACC of E.ON SE, an investor-owned company and one of the major public utilities in Germany. The company's annual report for 2012 specifies a WACC of 5.6 % after taxes and a pre-tax WACC of 7.7 % (E.ON 2013).

As costs in IMAKUS are assumed to be inflation-adjusted real values of costs (vide Section 3.2.1), a real discount rate is required. Using the average annual inflation rate of 1.6 % for the period 2008–2012 in Germany (Destatis 2014), a real pre-tax WACC of 6.0 % is calculated, which is used as the discount rate in Sections 6.3 and 6.4.

6.3 Results from the reference scenario

Instead of the social discount rate of 3 % applied in Chapter 5, a discount rate of 6 % – which reflects the expected rate of return of a private-sector investor – is used to optimise storage expansion anew under the reference scenario. All other input parameters are assumed as defined in Section 5.2.

As discussed in Section 4.5, higher discount rates can generally be regarded as a disincentive to investments into new build capacity: The NPV of a given investment decreases and, consequently, the competing option of a financial investment with iden-

tical risk becomes more attractive. Moreover, future expenditures associated with a given investment become less important and as much investments as possible are shifted to later years.

Figure 6.1 illustrates the expansion of storage capacity over the whole planning horizon if a discount rate of 6 % is assumed in the reference scenario. As expected, storage expansion is delayed as compared to expansion with an assumed social discount rate of 3 % (vide Figure 5.14, Section 5.4.3): The expansion of PSP is first observed in 2021; the expansion of AA-CAES and H₂-CCGT does not start before 2038 and 2043 respectively.

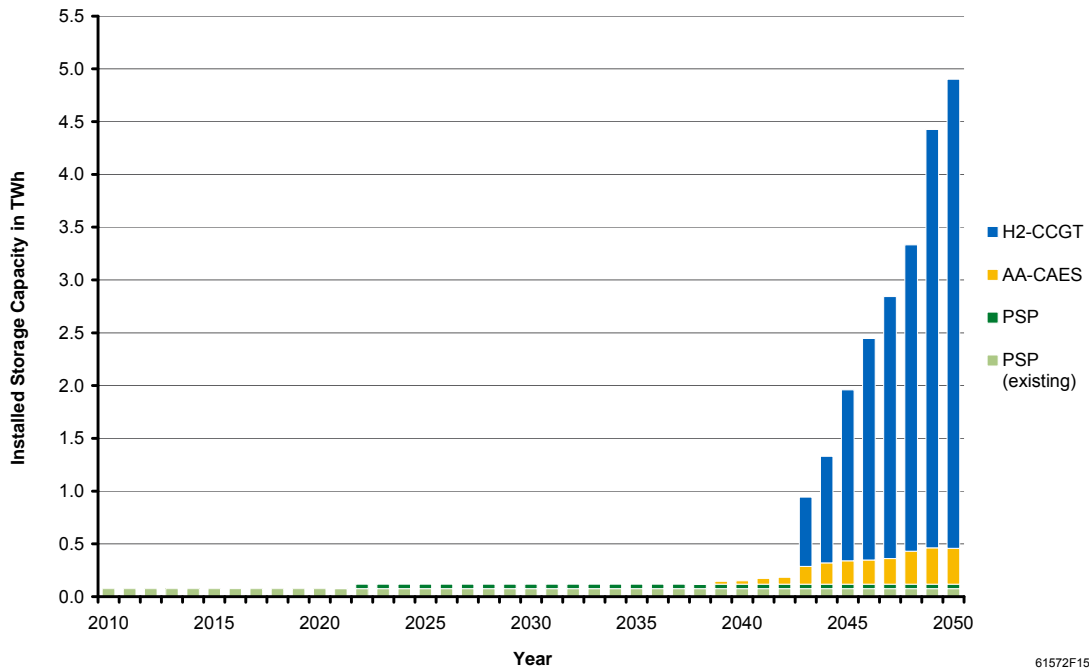


Figure 6.1: Expansion of storage capacity over the planning horizon 2010–2050 in the reference scenario (assuming a 6 % discount rate)

The total installed storage capacity decreases as compared to the social discount rate case: In 2050, the demand for new build storage capacity amounts to 4.8 TWh. With 4.4 TWh, the installed storage capacity is then dominated by H₂-CCGT. For comparative purposes, the total storage capacity of existing PSP (77 GWh) is also included in the figure.

Figure 6.2 presents the expansion of charging and discharging capacity for selected years of the planning horizon. Analogously to storage capacity, total installed charg-

ing and discharging capacities decrease as compared to the social discount rate case: In 2050, the installed charging capacity of new build storages amounts to 29.3 GW and installed discharging capacity reaches 12.7 GW. As in case of a 3 % social discount rate, charging capacity exceeds discharging capacity for all new build technologies (the highest ratio of almost 5:1 is observed for H₂-CCGT in 2050). Again, the figure also includes total charging and discharging capacities of existing PSP (6.2 GW and 6.5 GW respectively).

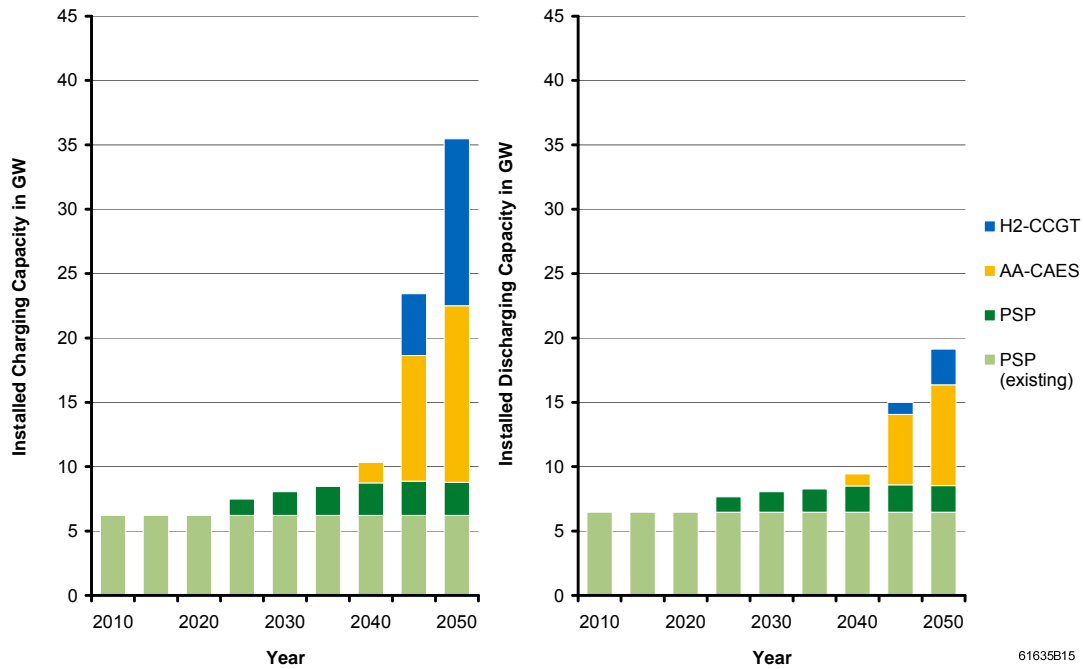


Figure 6.2: Expansion of charging and discharging capacity over the planning horizon 2010–2050 in the reference scenario (assuming a 6 % discount rate)

In the reference scenario, the portion of electricity generation from RES and CHP that cannot be directly utilised accumulates to 1063 TWh over the planning horizon 2010–2050 (vide Section 5.4.2). Due to the lower level of storage expansion in case of a 6 % discount rate, the amount of curtailed energy is only reduced to 630 TWh (as compared to 549 TWh in case of a 3 % social discount rate). In 2050, the curtailed energy reaches a level of 37.8 TWh (as compared to 31.1 TWh in case of a 3 % social discount rate).

The negative impact of a higher discount rate on investment activity is also evident with regard to generation capacity expansion: The overall new build generation ca-

capacity decreases as compared to new build generation capacity in the social discount rate case. Throughout the planning horizon, the share of less capital-intensive gas-fired power plants is considerably larger if a 6 % discount rate is assumed.

6.4 Profitability of investments into storage under variation scenarios

6.4.1 Approach to determining profitability under variation scenarios

The performance of the optimal storage portfolio that was determined for the year 2050 in Section 6.3 shall be evaluated under selected scenarios of varying meteorological conditions, RES shares and RES structures. For this purpose, the dispatch of the obtained storage portfolio is optimised under the variation scenarios and the annual profit from storage operation is determined as the difference of costs of charging and revenues of discharging.

As shown by Hirth & Ueckerdt (2012), in general, all assets of an optimised portfolio earn zero profits in the long-term equilibrium. If zero profits are generated, the NPV of a given investment is zero and, thus, by definition, the internal rate of return (IRR) on this investment is equivalent to the assumed discount rate (vide Van Horne & Wachowicz 2004). If the discount rate was fixed at the investor's WACC as described in Section 6.2, this means that the minimum expected rate of return – the so-called hurdle rate “at which a project is acceptable” (Van Horne & Wachowicz 2004) – is reached.

If additional constraints are introduced to the model – for instance, in case of PSP expansion being limited to a maximum storage capacity of 40 GWh –, assets can also earn rents beyond the hurdle rate. In general, assets will generate additional profits if their installed capacity is lower than the cost-optimal capacity, whereas any capacities that are oversized as compared to the cost-optimal solution will generate deficits, i. e. will not reach the hurdle rate.

Thus, as the storage portfolio optimised under the reference scenario is not necessarily optimal under deviating boundary conditions (e. g. a slow-down of RES expansion), storage units from the reference scenario will either earn rents (i. e. yield an IRR greater than 6 %) or generate deficits (i. e. yield an IRR less than 6 %) when transferred to the variation scenarios in this section.

In order to isolate the impact of a varying environment on the profitability of storages, only the optimised storage portfolio is transferred from the reference scenario. Therefore, generation and storage capacity expansion is first optimised under the

respective variation scenarios. Next, the submodel MESTAS is used to again optimise generation and storage dispatch for the examined year 2050: While the generation portfolios resulting from the previous optimisation of the respective variation scenarios are adopted, the resulting optimal storage portfolios are discarded and, instead, the optimal storage portfolio from the reference scenario (vide Section 6.3) is exogenously fixed. Any further expansion of storage capacity is not allowed.

For each variation scenario, the annual profit from storage operation is then determined as the difference of costs of charging (plus variable O&M costs) and revenues of discharging. It is assumed that the hourly market price of electricity can be approximated by the marginal costs of electricity generation resulting from optimisation (i. e. the shadow prices associated with hourly demand constraints).

By calculating the IRR for each storage technology and comparing it to the hurdle rate of 6 %, the profitability of the optimal storage portfolio from the reference scenario is evaluated with regard to the uncertainty about the boundary conditions. For the calculation of the IRR, it is assumed that 2050 is the first year of operation and that the annual profit from storage operation determined for 2050 can also be realised in all subsequent years of the storage's lifetime.

It should be noted that – as a bonus on storage costs of 50 % is assumed (vide Section 5.2.9) – the calculated IRR is only based on 50 % of the non-variable costs of charging, discharging and storage capacity. Thus, an IRR greater than or equal to the hurdle rate of 6 % implies that the storage project is acceptable with regard to returns on investment that can be expected from energy arbitrage. However, if the assumed bonus on storage costs is justified, the required returns on the other half of the investment are earned on markets that are not endogenously modelled, like e. g. the ancillary services market.

6.4.2 Overview of earned IRR

This section provides an overview of the profitability of the optimal storage portfolio that was determined in Section 6.3 under boundary conditions that deviate from the reference scenario. The profitability of each storage technology is evaluated in terms of earned IRR, as described in the previous section.

The performance of the storage portfolio from the reference scenario is tested under all variations of annual time series (vide Section 5.5.1), under all variations of RES share (vide Section 5.5.2) as well as under variations of RES structure where all three major RES contribute to the generation mix in 2050 (variation scenarios 7, 8 and 11, vide Section 5.5.3).

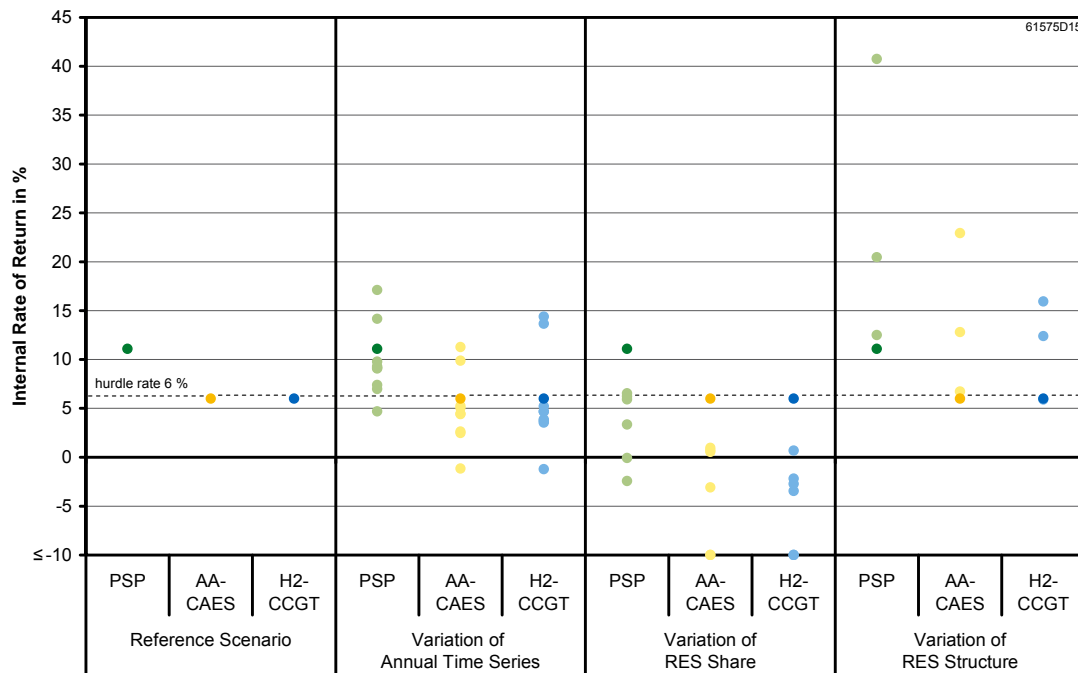


Figure 6.3: Earned IRR on storage investments under the reference scenario and under selected scenarios of varying meteorological conditions, RES shares and RES structures

Figure 6.3 presents the IRR earned with new build PSP, AA-CAES and H₂-CCGT capacities of 2050 under the reference scenario and under the variation scenarios. For illustrative purposes, rates less than -10 % were set to -10 %.

Under the reference scenario, the IRR of both AA-CAES and H₂-CCGT is equivalent to the assumed discount rate of 6 %: These storage technologies are expanded exactly to the optimal capacity level of the long-term equilibrium. By contrast, the IRR of PSP (11 %) well exceeds the 6 % hurdle rate, as the optimal PSP capacity cannot be reached due to the 40 GWh limit on PSP storage capacity (vide Section 5.2.9).

The significant sensitivity of storage expansion to variations of annual time series, RES share and RES structure observed in Chapter 5 suggests that the optimal storage portfolio from the reference scenario might not be suited for operation under deviating boundary conditions. As Figure 6.3 illustrates, in some cases this can lead to storages generating additional profits (i. e. the IRR exceeds 6 %), but mostly storages generate deficits (i. e. the IRR undercuts 6 %).

While PSP yield mostly positive IRR that under the majority of scenarios also exceed the hurdle rate of 6 %, the hurdle rate is only rarely reached in case of AA-CAES and H₂-CCGT and negative values of IRR occur quite often. The profitability of storages is

apparently strongly dependent on the share of RES: Only PSP capacities prove profitable from an investor's perspective for other shares of RES than 80 %. While storage capacities from the reference scenario prove profitable under variations of RES structure where all three major RES contribute to the generation mix, the IRR can be significantly reduced if meteorological conditions vary. The performance of the storage portfolio under variation scenarios is further analysed in the following sections.

6.4.3 Earned IRR under scenarios varying annual time series

As the overview in the previous section already showed, the storage portfolio that was optimised in the reference scenario does not prove profitable under the majority of scenarios varying annual time series. Figure 6.4 presents the IRR on investments into PSP, AA-CAES and hydrogen storage for varying meteorological conditions. The scenarios are sorted in descending order of IRR earned by PSP.

While the profitability of the PSP capacity that was determined in the reference scenario is observed to be very robust to variations of annual time series – the IRR only undercuts the hurdle rate of 6 % in the 2007 scenario –, the IRR of AA-CAES and H₂-CCGT is more often than not reduced significantly if meteorological conditions deviate from the reference scenario. In fact, the optimal storage portfolio from the reference scenario as a whole only proves profitable in two more scenarios, namely under meteorological conditions of 2004 and 2011.

The low and partly negative values of IRR for scenario 2007 are due to considerable differences between the optimal storage portfolio from the reference scenario and the rating of storages that would actually be optimal under scenario 2007: If storage expansion is optimised under the 2007 scenario, AA-CAES is not observed to be part of the optimal storage portfolio in 2050. Also, the 2007 scenario is the only case where a considerably lower ratio of PSP charging to discharging capacity than in the reference scenario would be optimal, which explains the poor performance of PSP capacities. Similarly, significantly lower optimal values of the ratio of charging to discharging capacity and storage duration lead to a poor performance of H₂-CCGT capacities that were optimised for the meteorological reference year 2012.

Apparently, the profitability of a given storage portfolio under varying boundary conditions depends not only on the absolute level of storage demand under these conditions but also on the suitability of storage duration and the ratio of charging to discharging capacity. In case of AA-CAES, the storage duration which is found to be optimal in the reference scenario comes closest to the optimal storage durations of

scenarios 2004 and 2011. As a consequence, the IRR of AA-CAES well exceeds the hurdle rate of 6 % for meteorological conditions of 2004 and 2011.

The high IRR of H₂-CCGT under scenarios 2004 and 2011 can be explained by suitable values of the ratio of charging to discharging capacity and storage duration respectively. Moreover, the 2004 and 2011 scenarios represent two of the very few cases where more H₂-CCGT expansion than in the reference scenario would be optimal (in terms of both storage capacity and charging and discharging capacity).

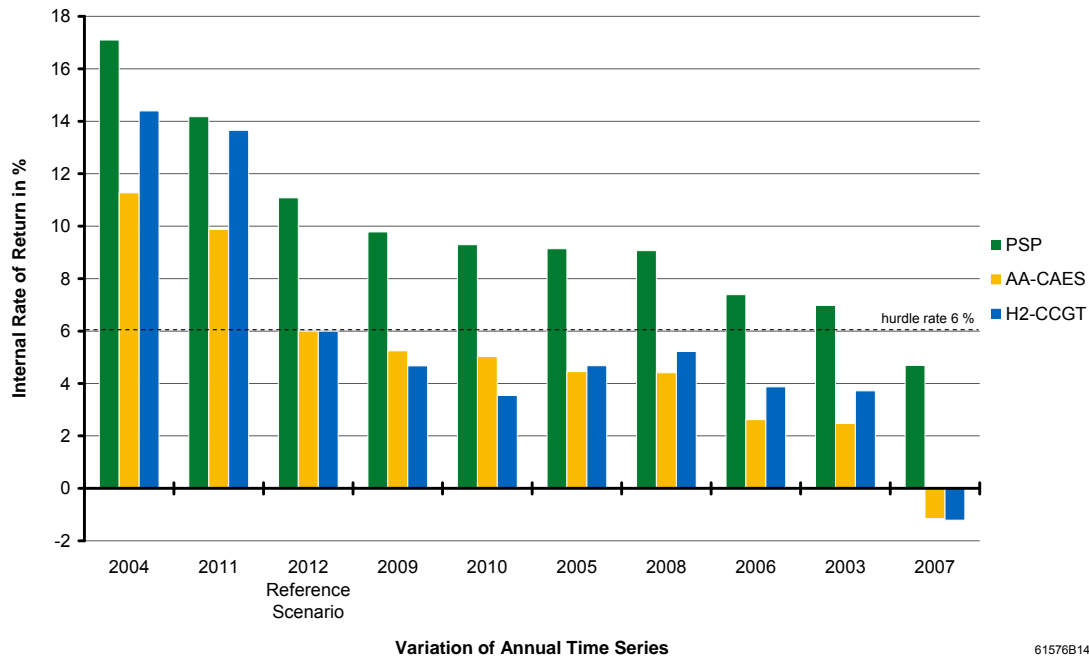


Figure 6.4: Earned IRR on storage investments for variations of annual time series and the reference scenario

6.4.4 Earned IRR under scenarios varying RES share

As the overview in Section 6.4.2 already showed, the profitability of the storage portfolio that was optimised in the reference scenario is strongly dependent on the share of RES: Only PSP capacities prove profitable from an investor's perspective for other shares of RES than 80 %. Figure 6.5 presents the IRR on investments into PSP, AA-CAES and hydrogen storage for varying shares of RES. For illustrative purposes, rates less than -10 % are truncated.

The poor performance of storage capacities from the reference scenario under scenarios with low RES shares in 2050 is not surprising. Results in Section 5.7.2 already

illustrated that – assuming a 3 % social discount rate – there is little to no storage demand under scenarios with RES shares of 50 % or less in 2050: Storage expansion is completely abandoned under the 40 % scenario and only PSP capacity is expanded in case of 50 % RES in 2050. While in the social discount rate case all three storage technologies become part of the optimal portfolio for an RES share of 60 % in 2050, the expansion of hydrogen storage is still not economically feasible if a 6 % discount rate is assumed.

The storage capacities that are optimal under the 80 % reference scenario are clearly oversized in scenarios with RES shares of 60 % or less and, thus, lead to low and partly negative values of IRR. In the 50 % case, the IRR of PSP is virtually zero.

While AA-CAES and H₂-CCGT also perform poorly under the other variation scenarios, the 6 % hurdle rate is exceeded or only narrowly missed (by 0.1 % under the 90 % scenario) by PSP under scenarios with RES shares of 70 % or more. Although the optimal rating under 90 % and 100 % scenarios differs quite significantly from the rating of PSP capacities determined under the reference scenario – larger discharging capacities would be required in both scenarios (vide Section 5.6.2) –, PSP also prove (almost) profitable for these extremely high shares of RES.

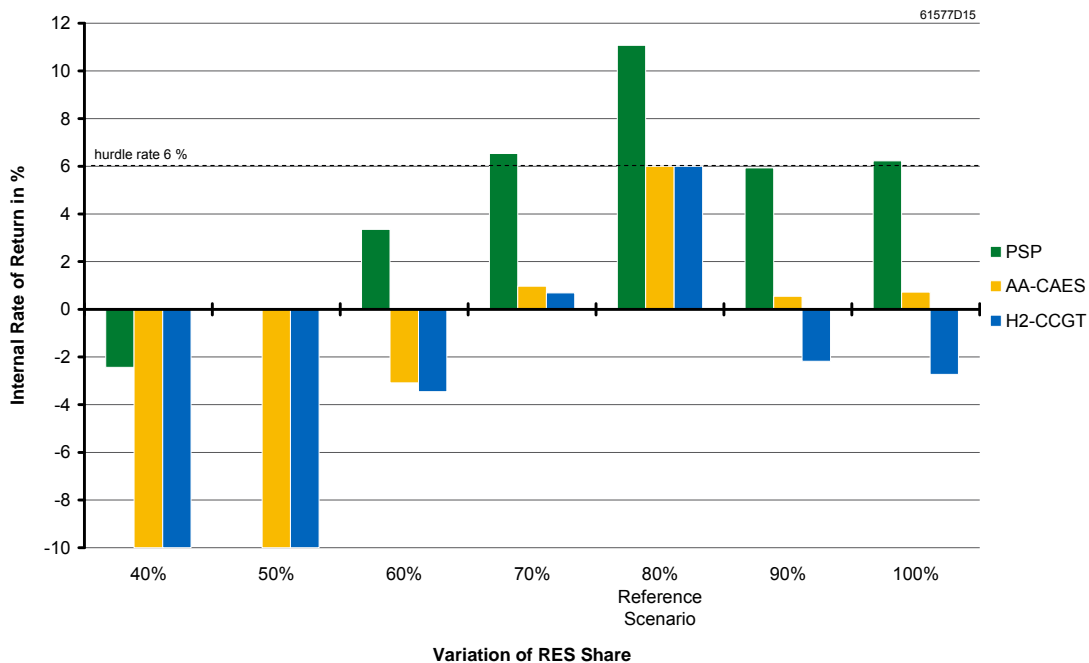


Figure 6.5: Earned IRR on storage investments for variations of RES share and the reference scenario

6.4.5 Earned IRR under scenarios varying RES structure

The overview in Section 6.4.2 already showed that storage capacities from the reference scenario prove profitable under variations of RES structure where all three major RES contribute to the generation mix in 2050 (variation scenarios 7, 8 and 11, vide Section 5.5.3). By contrast, it is to be assumed that the same storage portfolio would perform poorly under scenarios of lower diversification. Figure 6.6 compares the IRR on investments into PSP, AA-CAES and hydrogen storage for variation scenarios 7, 8 and 11 and the reference scenario.

As the RES structure in variation 7 comes closest to the RES structure in the reference scenario (vide Figure 5.22, Section 5.5.3), results on storage expansion are observed to be very similar under both scenarios: Besides a slightly smaller total storage capacity (which is due to a lower level of H₂-CCGT storage capacity), the absolute deviations between optimal capacities under variation scenario 7 and under the reference scenario are comparably small. Analogously, values of the ratio of charging to discharging capacity and storage duration which are found to be optimal in variation scenario 7 come closest to the optimal values in the reference scenario.

Therefore, when the optimal storage portfolio from the reference scenario is transferred to variation scenario 7, storages reach rates of return that are comparable to the rates earned under the reference scenario: While rates of 12.5 % and 6.7 % are observed for PSP and AA-CAES respectively, H₂-CCGT only narrowly miss the hurdle rate with an IRR of 5.9 %.

The RES structure in variation 11 is also relatively similar to the RES structure in the reference scenario. As in case of variation 7, optimal values of the ratio of charging to discharging capacity and storage duration come close to optimal values from the reference scenario. While absolute deviations between optimal capacities under variation scenario 11 and under the reference scenario are still comparably small, particularly charging and discharging capacities are larger than under variation scenario 7 or under the reference scenario. Thus, considerably higher rates are earned by storages under variation scenario 11.

Although optimal values of storage duration in variation scenario 8 differ quite significantly from the ratings optimised under the reference scenario, storage capacities from the reference scenario prove very profitable in this solar-dominated scenario: The optimisation of storage expansion under variation scenario 8 indicates a very high demand for PSP and, in particular, AA-CAES capacity (especially in terms of charging and discharging capacity). Thus, as much larger total capacities would be cost-optimal under variation scenario 8, storages from the reference scenario can generate additional profits.

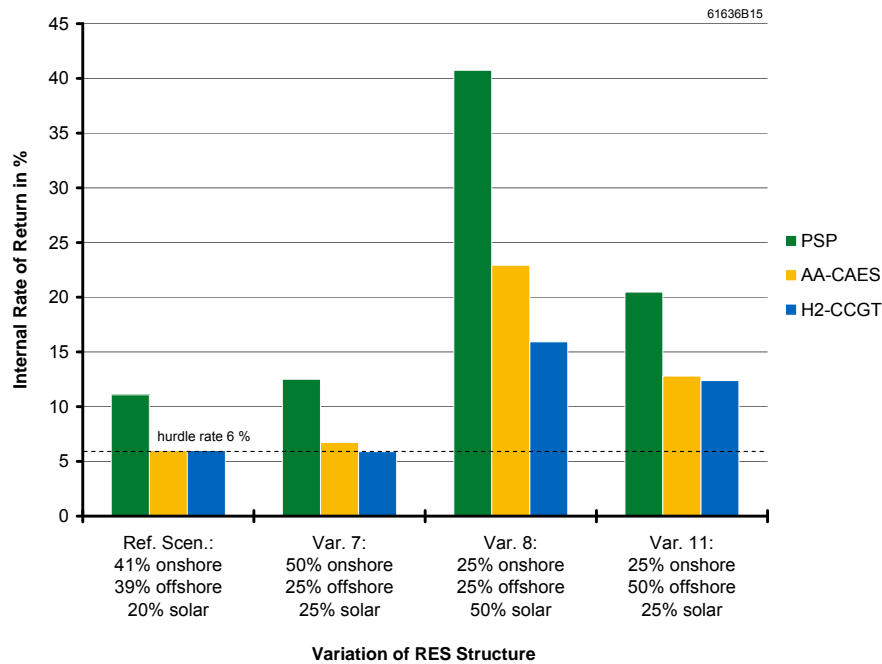


Figure 6.6: Earned IRR on storage investments for variations of RES structure and the reference scenario

6.5 Discussion and conclusion

In this chapter, results on cost-optimal storage demand in the German power system are analysed from an investor's perspective. Whereas investment decisions which are optimal from a system point of view do not necessarily have to be profitable from an investor's perspective, whole-systems cost minimisation models can still offer valuable insights to private-sector decision makers: First, investments into technologies which are omitted by the model certainly also do not pay off for private-sector investors. Secondly, the specific values of storage duration and the ratio of charging to discharging capacity which are found to be optimal from a system point of view can serve as an adequate indication to investors.

Moreover, whole-systems cost minimisation models can be used to test the performance of individual storage projects or storage portfolios under different scenarios. In order to adapt the model IMAKUS to a private-sector investor's perspective in this chapter, the discount rate is set to 6 %, which represents the WACC and, thus, the minimum expected rate of return of a potential investor. Using this discount rate, storage capacity expansion is optimised anew under the reference scenario.

The performance of the obtained storage portfolio is evaluated under selected scenarios of varying meteorological conditions, RES shares and RES structures. For this

purpose, storage dispatch is optimised and the annual profit from storage operation is determined as the difference of costs of charging and revenues of discharging.

The profitability of investment decisions from the reference scenario is determined by calculating the IRR and comparing it to the hurdle rate of 6 %. However, it should be noted that the calculated IRR is only based on 50 % of storage costs and only accounts for returns on investment from endogenously modelled energy arbitrage. The other half of the investment is assumed to be refinanced on markets that are not endogenously modelled, like e. g. the ancillary services market.

As the analysis in this chapter shows, the performance of PSP proves to be comparably robust to variations of input parameters: Under the majority of scenarios, PSP reach an IRR of 6 % or higher. By contrast, the profitability of AA-CAES and hydrogen capacities is rather uncertain under varying boundary conditions, as the IRR only rarely reaches the hurdle rate.

The analysis illustrates that the profitability of a given storage portfolio under varying boundary conditions depends not only on the absolute level of storage demand under these conditions but also on the suitability of storage duration and the ratio of charging to discharging capacity.

The profitability of storages is apparently strongly dependent on the share of RES. Only PSP capacities prove profitable for other shares of RES than 80 % in 2050: Under scenarios with RES shares of 70 % or more, the IRR of PSP exceeds or only narrowly misses the hurdle rate of 6 %. By contrast, all storage technologies prove profitable under variations of RES structure where all three major RES contribute to the generation mix in 2050.

A strong impact on the profitability of storages optimised under the reference scenario is also observed for varying meteorological conditions. In fact, the storage portfolio as a whole only proves profitable in two more variation scenarios. Again, only the performance of PSP proves to be comparably robust to variations.

To conclude, results from whole-systems cost minimisation not only show a significant sensitivity of the optimal storage portfolio to varying boundary conditions (vide Chapter 5) but also demonstrate that – given the uncertainty about these boundary conditions – the profitability of investments into storage technologies other than PSP is highly questionable. While whole-systems cost minimisation models can thus offer valuable insights to private-sector investors, the use of common capital budgeting techniques and the assessment of portfolio risk remain essential to the evaluation of investment projects.

7 Conclusion

This final chapter provides an overview of this thesis and summarises the main results. It concludes by discussing several perspectives for future research and pointing out potential challenges.

7.1 Summary of results

A multitude of studies have been published lately which convey quite contradictory impressions of the future demand for energy storage. A review of eleven recent studies on energy storage demand thus forms the starting point of this thesis. An overview of the general scope and the methodology of these studies is followed by a detailed comparison of results on energy storage demand in the German power system.

However, as studies on storage demand make use of many different methodological approaches and assumptions, it becomes apparent that results are difficult to compare. Moreover, even identical approaches can yield highly contradictory results if input parameters differ. To better understand the broad range of results on storage demand stemming from different studies or even only a single model, it is thus concluded that both the influence of methodological choices and the influence of input parameters on modelling results need further analysis.

In the main part of this thesis, the impact of these factors is therefore analysed qualitatively and quantitatively. While the sensitivity of results to changes in selected input parameters is analysed by means of the whole-systems cost minimisation model IMAKUS, the question of how assumptions and the choice of methodological approaches affect modelling results on storage demand is mostly answered qualitatively. Wherever possible, this qualitative analysis is complemented and underpinned by modelling results. Methodology and formulation of the employed model IMAKUS are described in detail in Chapter 3.

An extensive selection of methodological approaches and assumptions that are commonly encountered in energy systems modelling is analysed in Chapter 4. The question whether a certain methodological choice leads to an increase or decrease of storage capacity expansion is answered for the majority of the considered approaches. The findings of this qualitative analysis are summarised in a table (vide Table 4.1, Section 4.8), which can serve as a quickly accessible guide to better evaluate and compare modelling results on energy storage demand.

The complementary analysis of different approaches and assumptions with IMAKUS indicates significant effects on both scale and structure of storage capacity expansion. It is found that several methodological choices mainly influence the estimated demand for long-duration storage. These are namely: neglecting energy exchange with other countries; planning with perfect foresight; neglecting must-run of conventional generation; and the optimisation of initial storage levels.

In order to analyse the sensitivity of storage demand to changes in input parameters, a scenario framework is established which comprises 42 scenarios, including a suitable reference scenario. As storage demand is largely influenced by the chronological characteristics of renewable electricity generation and electricity demand, the reference scenario is based on a meteorological reference year, i. e. a set of annual time series that is representative of meteorological conditions in Germany. For this purpose, time series are systematically characterised with regard to FLH, surplus energy and residual energy demand as well as intra-annual variability (seasonality).

The sensitivity of storage demand is examined in Chapter 5 with regard to variations of annual time series, RES share, RES structure, fuel costs, the bonus on storage costs and storage investment costs. The analysis demonstrates a significant sensitivity of storage demand to all of the tested input parameters.

However, the sensitivity of PSP, AA-CAES and hydrogen storage is observed to differ quite significantly. Being the most efficient and least expensive technology, PSP appear to be comparably robust to varying input parameters. By contrast, the sensitivity of hydrogen storage capacity to input parameters is generally very high due to the very low level of energy-related investment costs.

While, all in all, the total share of RES generation is certainly the most important driver of storage demand – expansion is completely abandoned for RES shares of 40 % or less in 2050 –, the economic feasibility of AA-CAES and H₂-CCGT is also significantly dependent on contribution margins from the ancillary services market. The structure of RES and the assumed meteorological conditions are apparently also important drivers of storage demand that can significantly influence the proportions – and even the presence – of technologies in the optimised storage portfolio. For instance, higher shares of solar generation in Germany will change the characteristics

of storage demand considerably, leading to, most notably, a higher demand for PSP and AA-CAES capacities.

Moreover, it is shown that a preceding analysis of annual time series can already provide valuable insight into the characteristics of storage demand. The impact of varying meteorological conditions on hydrogen storage capacity can be better explained if – in addition to the amounts of surplus energy and residual energy demand – the low-frequency variability index of residual demand time series is consulted.

The relevance of modelling results from whole-systems cost minimisation to private-sector investors is also discussed in this thesis. Although investment decisions which are optimal from a system point of view do not necessarily have to be profitable from an investor's perspective, whole-systems cost minimisation models can still offer valuable insights to private-sector decision makers, for instance, if used to test the performance of individual storage projects or storage portfolios under different scenarios. In this case, the assumption of a discount rate that reflects the investor's minimum expected rate of return is a necessary prerequisite.

In Chapter 6, the performance of storage capacities optimised in the reference scenario is evaluated under scenarios of varying meteorological conditions, RES shares and RES structures. Whereas the profitability of PSP proves comparably robust to varying boundary conditions, the profitability of AA-CAES and hydrogen capacities is mostly negatively affected.

7.2 Perspectives

Results in this thesis not only show a significant sensitivity of the optimal storage portfolio to varying boundary conditions but also demonstrate that – given the uncertainty about these boundary conditions – the profitability of investments into storage technologies other than PSP is highly questionable.

However, this conclusion should be seen against the background of the methodological approaches and limitations of the model employed in this thesis: As the findings on the influence of methodology and assumptions suggest, the same analysis could yield very different results on storage demand and profitability if conducted with a different model. Whereas some methodological choices might only affect the general level of results, it cannot be ruled out that other choices would also influence the sensitivity of storage demand and profitability to certain input parameters. Moreover, other methodological approaches could open up the analysis to additional technologies, like e. g. the possibility to consider battery storage in case of higher temporal resolutions than hourly resolution.

Of course, the scope of the analysis itself could always be extended. With regard to the qualitative analysis of the influence of methodology and assumptions on modelling results, several other methodological choices can be suspected to affect results on energy storage demand and should thus be subject to further analysis. Further efforts should be made to extend the employed model IMAKUS such that a higher number of alternative methodological approaches are supported and can be compared on a consistent basis.

With regard to the analysis of the sensitivity of storage demand to varying input parameters, a higher number of scenarios varying, in particular, meteorological conditions, RES structure and fuel costs would further improve the validity of results. Alternative scenarios of storage investment costs should also be tested. As to the variation of RES structure, the analysis of additional scenarios should focus on variations where all three major RES contribute to the generation mix. By this means, the comparably low sensitivity of storage demand to realistic variations of RES structure, which is observed in this thesis, could be verified.

By contrast, it must be suspected that the analysis of additional sets of annual time series can lead to even larger deviations of optimal storage demand from the reference scenario. By also analysing the probability of occurrence of certain meteorological conditions, the representativeness of the storage portfolio that is optimised under the reference scenario could be better evaluated.

The high sensitivity of storage demand to varying input parameters actually indicates that the plausibility of future analyses of storage demand could benefit from stochastic programming approaches, which allow to address uncertainty by considering different realisations of input parameters. However, determining the necessary probability distributions of input parameters like renewable generation time series or fuel costs is a major challenge. Moreover, stochastic programming approaches involve a considerably higher computational burden (Dyer & Stougie 2006).

Further efforts should be made to improve whole-systems cost minimisation models with regard to the equally detailed modelling and simultaneous optimisation of generation, storage and transmission. Whereas various models allow for the optimisation of storage expansion and operation while covering a large geographic scope in adequate spatial resolution, improvements are necessary with regard to temporal resolution, modelling the competitive situation between technologies and modelling the transmission of power. Although the DC power flow method represents a suitable approach to approximate physical power flows, the non-linearity of the transmission expansion problem is a major challenge in this case (vide Schaber 2013, Ahlhaus & Stursberg 2013).

As previous studies demonstrated, the coupling of the power sector and the transport (e. g. Kuhn *et al.* 2012) and heating sectors (e. g. Heilek 2014) holds considerable po-

tential to reduce storage demand in the power system. Another important task for future research on storage demand is therefore to also adequately model these sectors. However, the higher computational burden of such extensive models might only be manageable with mathematical decomposition methods.

With model complexity inevitably increasing, the claim for transparency in energy systems modelling becomes even more urgent. Only if transparency of methodological choices and input parameters is provided, can modelling results be interpreted correctly and, thus, offer valuable insight to political and private-sector decision makers. Therefore, systematic analyses of the influence of methodology and parameters on modelling results should form an integral part of future studies on storage demand in particular and on energy systems in general.

A Literature Review

A.1 Complementary aspects of methodology of selected studies

| reference | electricity import and export | operating reserve | security of supply | competing flexible options |
|-----------------------------|---|--|--|---|
| Adamek <i>et al.</i> (2012) | not considered | required amount is fixed exogenously | generation capacity is fixed exogenously such that adequacy requirements are met | flexible loads are considered to be possible implementations of short-duration storage |
| Agora Energiewende (2014) | electricity exchange with regions outside Europe is not considered | required amount is fixed exogenously | generation capacity is fixed exogenously such that adequacy requirements are met | flexible loads are considered, increased flexibility of CHP due thermal storage and electric heaters is assumed |
| EPRI (2012) | not considered in EGEAS, considered in PLEXOS (bordering regions are modelled in less detail) | not considered in EGEAS, considered in PLEXOS | considered | flexible loads are considered |
| Hand <i>et al.</i> (2012) | electricity import from Canada is exogenously fixed | required amount is fixed exogenously in ReEDS, Monte Carlo simulation of outages and forecast errors in GridView | planning reserve constraint ensures adequate capacity in ReEDS | charging of electric vehicles, interruptible load and thermal storage in buildings are considered |
| Klaus <i>et al.</i> (2010) | electricity import considered as backup technology | required amount is fixed exogenously | backup generation capacity is fixed such that adequacy requirements are met | charging of electric vehicles, heat pumps and thermal storage in buildings are considered (dispatch prioritised, not competing) |

| reference | electricity import and export | operating reserve | security of supply | competing flexible options |
|-----------------------------|--|---|--|--|
| Kuhn (2012) | export of surplus energy at exogenously fixed prices can optionally be considered | not considered | adequate capacity is achieved iteratively by comparing firm capacity with peak load and adjusting the minimum capacity constraint (firm capacity is calculated by means of stochastic convolution) | not considered |
| Kuhn <i>et al.</i> (2012) | export of surplus energy at exogenously fixed prices can optionally be considered | not considered | adequate capacity is achieved iteratively by comparing firm capacity with peak load and adjusting the minimum capacity constraint (firm capacity is calculated by means of stochastic convolution) | charging of electric vehicles and operation of other flexible loads can optionally be considered |
| Pieper & Rubel (2011) | not considered | provision of operating reserve is one of the storage applications analysed | not considered | estimated market potential considers availability of alternatives to storage |
| Scholz (2010) | electricity exchange with regions outside Europe and North Africa is not considered | not considered | not considered | not considered |
| Scholz (2012) | electricity exchange with regions outside Europe and North Africa is not considered | not considered | security constraint ensures adequate capacity | not considered |
| Strbac <i>et al.</i> (2012) | electricity exchange with Ireland and Continental Europe is allowed, but annual net balance is constrained to zero | required amount is either fixed exogenously or determined endogenously with stochastic programming approach | security constraint ensures adequate capacity | charging of electric vehicles, heat pumps and other flexible loads can optionally be considered |

B Variability indices

B.1 Determining variability indices of generation and demand time series

The method used in this thesis to calculate variability indices of annual generation and demand time series is largely based on Janker (2015) but improved with regard to the approach of determining the worst case storage capacity. It is applicable for all time series only taking positive values. While, in principle, either scaled or unscaled data can be used, this description refers to time series of generation scaled to installed capacity or time series of demand scaled to annual maximum load.

The main principle underlying this approach to measure the variability of time series, i. e. the temporal distribution of energy, is that the theoretical storage capacity necessary to balance all fluctuations of a time series is dependent on both the amount of energy contained in the time series and the distribution of energy over time. If this theoretical storage capacity is adjusted for energy, the obtained quantity can be used to measure the variability of the time series. The balancing of fluctuations of an annual time series is based on the assumption of a cyclical recurrence of the same annual time series.

Instead of determining only one variability index to characterise all fluctuations, the time series is decomposed into its high-, mid- and low-frequency components and variability indices are calculated for each component. The frequency ranges fr corresponding to these variability indices are defined to comprise all frequency components with period T as follows:

| | | |
|-----------------|----------------------|---------------------------------------|
| <i>high-frq</i> | high-frequency range | $0 \text{ h} < T \leq 24 \text{ h}$ |
| <i>mid-frq</i> | mid-frequency range | $24 \text{ h} < T \leq 30 \text{ d}$ |
| <i>low-frq</i> | low-frequency range | $30 \text{ d} < T \leq 365 \text{ d}$ |

The high-frequency variability index $V_{high-frq}$ measures the intra-day variability of the considered time series. The intra-annual variability or seasonality of the time series

is characterised by the low-frequency variability index $V_{low-freq}$. Fluctuations with period T of more than one day but less than one month are captured by the mid-frequency variability index $V_{mid-freq}$. While the high-, mid- and low-frequency components are zero-mean, a fourth component is obtained from the decomposition which is constant at the mean value of the original time series.

By way of example, Figure B.1 shows the time series of onshore wind generation for the year 2005 in Germany (from the set of annual time series established in Section 5.2.4) as well as its high-, mid- and low-frequency components.

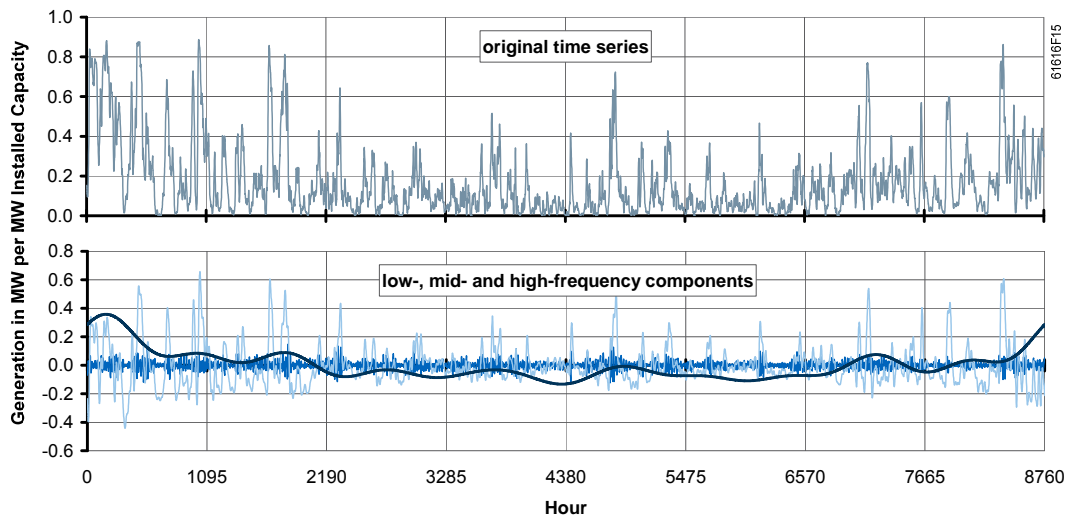


Figure B.1: Time series of onshore wind generation for the year 2005 in Germany and its high-, mid- and low-frequency components (scaled to installed capacity)

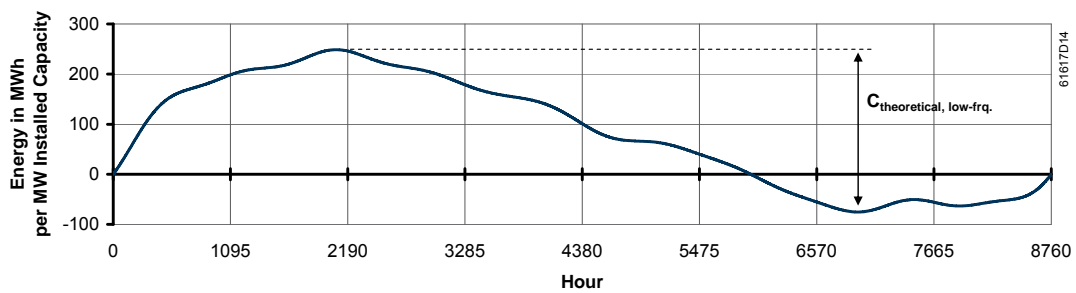


Figure B.2: Storage level of a theoretical storage balancing all low-frequency fluctuations of onshore wind generation for the year 2005 in Germany (scaled to installed capacity)

By integrating each of the three zero-mean components, time series are obtained that represent the hourly storage levels of theoretical storages, which, assuming no storage losses, are operated in such a manner that all fluctuations within the respective frequency ranges are balanced. The necessary capacities of these theoretical storages $C_{theoretical}$ are determined directly from the obtained curves by subtracting the minimum from the maximum storage level.

Figure B.2 shows the time series that is obtained from the integration of the low-frequency component of onshore wind generation in 2005. The figure furthermore illustrates how the theoretical storage capacity $C_{theoretical,low-frq}$ necessary to balance all low-frequency fluctuations of the wind generation time series is determined. As the initial storage level depends on the distribution of energy over the year, the time series of hourly storage levels may include an offset. In this example, the theoretical storage reaches the minimum storage level (meaning that it is completely empty) after approximately 6950 h, while at the end of the year (i. e. at the beginning of the next year) the storage level has reached 23 % of the theoretical storage capacity.

In order to obtain normalised variability indices that are adjusted for energy, the theoretical storage capacities $C_{theoretical}$ are scaled to the corresponding worst-case storage capacity $C_{worst-case}$:

$$V_{fr} = \frac{C_{theoretical,fr}}{C_{worst-case,fr}} \quad (B-1)$$

where V_{fr} variability index for frequency range fr
 $C_{theoretical,fr}$ theoretical storage capacity for frequency range fr
 $C_{worst-case,fr}$ worst-case storage capacity for frequency range fr
 fr set of frequency ranges with members $high-frq$, $mid-frq$ and $low-frq$

The definition of the worst-case storage capacity $C_{worst-case}$ is based upon the observation that, for a given amount of energy contained in a time series, the largest theoretical storage capacity is necessary if all the energy occurs over a contiguous period of time. In order to determine the worst-case storage capacity $C_{worst-case,fr}$ for each frequency range fr , each interval of length $T_{max,fr}$ is tested with regard to the size of the storage capacity that is necessary to balance the energy contained within the individual interval, assuming that the energy occurs over a contiguous period of time. $T_{max,fr}$ is the largest period T included in the respective frequency range fr . While in

the low-frequency case only one interval of 8760 h exists, intervals are overlapping for the mid- and high-frequency ranges.

Janker (2015) uses the original non-negative time series to determine the worst-case storage capacity, where the amount of energy contained within an interval can be measured in FLH and is directly correlated with the necessary size of the storage capacity. However, the energy contained within an interval of the original time series includes energy from all frequency components and thus is not the best basis to estimate the worst-case storage capacity.

By contrast, the approach in this thesis uses the time series of the respective frequency component to determine the worst-case storage capacity for each frequency range fr . As both positive and negative amounts of energy occur in the time series of the high-, mid- and low-frequency components, the worst-case storage capacities $C_{worst-case,iv}$ have to be calculated for each individual interval iv before the largest worst-case storage capacity $C_{worst-case,fr}$ can be detected.

Figure B.3 illustrates the general method to determine the worst-case storage capacity $C_{worst-case,iv}$ for an interval iv of any frequency range fr . While in case of the low-frequency component the one interval of length T_{max} is zero mean, individual intervals of the mid- and high-frequency components are not necessarily zero-mean and consequently mean values P_{mean} not equal to zero are possible.

W_{pos} and W_{neg} represent the positive and negative amounts of energy contained in interval iv of the considered frequency component. In order to determine the worst-case storage capacity $C_{worst-case,iv}$, it is assumed that both positive and negative amounts of energy occur with a certain maximum power P_{max} over a contiguous period of time.

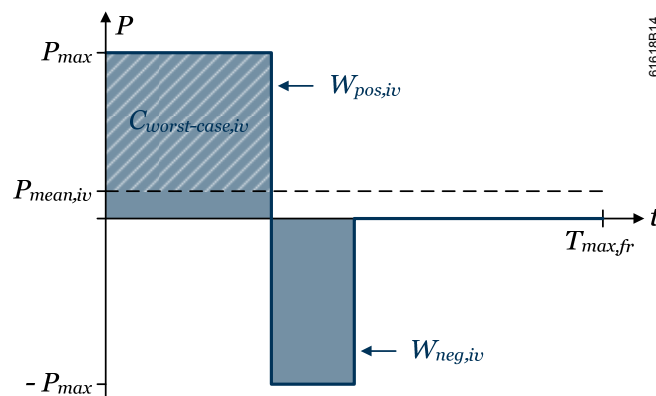


Figure B.3: Determining the worst-case storage capacity in an interval of length T_{max} for any frequency range fr

For time series of generation, P_{max} is defined as the installed capacity, whereas for time series of demand, P_{max} corresponds to the annual maximum load. The following set of equations is used to calculate the worst-case storage capacity $C_{worst-case,iv}$ for an interval iv :

$$P_{mean,iv} = \frac{|W_{pos,iv}| - |W_{neg,iv}|}{T_{max,fr}} \quad (B-2)$$

$$P_{mean,iv} \geq 0 : C_{worst-case,iv} = (P_{max} - |P_{mean,iv}|) \cdot \frac{|W_{pos,iv}|}{P_{max}} \quad (B-3)$$

$$P_{mean,iv} < 0 : C_{worst-case,iv} = (P_{max} - |P_{mean,iv}|) \cdot \frac{|W_{neg,iv}|}{P_{max}} \quad (B-4)$$

| | |
|---------------------|--|
| where $P_{mean,iv}$ | mean value of power in interval iv |
| $W_{pos,iv}$ | positive amount of energy contained in a time series in interval iv |
| $W_{neg,iv}$ | negative amount of energy contained in a time series in interval iv |
| $T_{max,fr}$ | largest period T included in frequency range fr |
| $C_{worst-case,iv}$ | worst-case storage capacity for interval iv |
| P_{max} | maximum power |
| iv | set of intervals of length $T_{max,fr}$ |
| fr | set of frequency ranges with members <i>high-frq</i> , <i>mid-frq</i> and <i>low-frq</i> |

The worst-case storage capacity $C_{worst-case,fr}$ for frequency range fr is the largest capacity detected among the worst-case storage capacities $C_{worst-case,iv}$ for all intervals iv of the respective frequency component. According to equation (B-1), the variability indices for the high-, mid- and low-frequency ranges are obtained by scaling the theoretical storage capacities $C_{theoretical,fr}$ to the corresponding worst-case storage capacities $C_{worst-case,fr}$.

A variability index of zero indicates that the analysed time series is not composed of fluctuations within the respective frequency range. Values greater than zero indicate how close the actual distribution of energy within the respective frequency range is to the worst-case distribution of energy.

While the low-frequency variability index is limited to 1, indices greater than 1 are possible for the mid- and high-frequency ranges. Whereas for the low-frequency range the worst-case storage capacity $C_{worst-case,low-frq}$ is determined based on the whole zero-mean low-frequency component, several 30 d- and 24 h-intervals exist for the mid- and high-frequency components respectively. As individual intervals are not necessarily zero-mean, the energy accumulated by a theoretical storage over several intervals can actually exceed the worst-case storage capacity, which is determined based on only one individual interval, albeit the interval that requires the largest storage capacity.

Thus, variability indices greater than 1 indicate that the theoretical storage capacity necessary to balance all fluctuations of a frequency component over one year is larger than the storage capacity balancing all fluctuations in the worst-case interval. However, usually only the high-frequency variability index is observed to slightly exceed 1 if the analysed time series is strongly governed by a day-night cycle (e. g. solar generation).

B.2 Determining variability indices of residual demand time series

The method used in this thesis to calculate variability indices of residual demand time series is based on the method presented in Appendix B.1 to determine variability indices for time series of generation and demand and was first presented in Kühne *et al.* (2014). It is applicable for all time series taking positive and negative values. While, in principle, either scaled or unscaled data can be used, this description refers to time series of residual demand scaled to the annual maximum load of the original demand time series.

The time series of residual demand is decomposed into its high-, mid- and low-frequency components. The corresponding frequency ranges fr are defined as for time series of generation and demand (vide Appendix B.1). Based on the integrated high-, mid- and low-frequency time series, the theoretical storage capacities $C_{theoretical,fr}$ necessary to balance all fluctuations within the respective frequency ranges are determined. By scaling the theoretical storage capacities $C_{theoretical,fr}$ to the corresponding worst-case storage capacities $C_{worst-case,fr}$ according to equation (B-1), normalised variability indices are obtained that are adjusted for energy.

While the general procedure is identical with the approach for time series of generation and demand, an adaptation is required with regard to the calculation of worst-case storage capacities $C_{worst-case,iv}$ for all intervals iv of length $T_{max,fr}$.

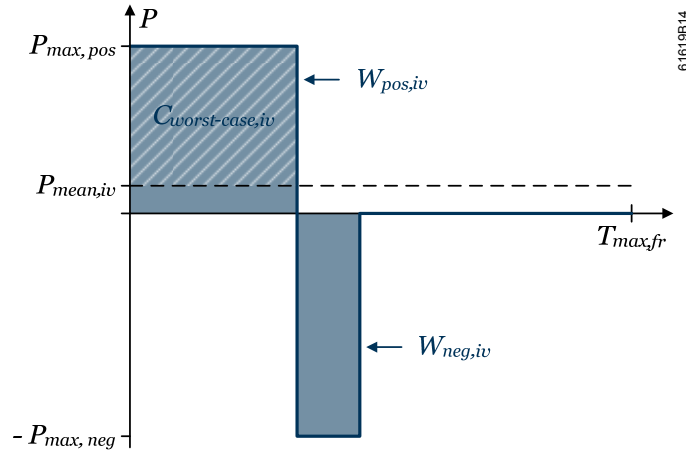


Figure B.4: Determining the worst-case storage capacity in an interval of length T_{max} for any frequency range fr (adapted for time series of residual demand)

Figure B.4 illustrates the general method to determine the worst-case storage capacity $C_{worst-case,iv}$ for an interval iv . Again, W_{pos} and W_{neg} represent the positive and negative amounts of energy contained in interval iv of the considered frequency component. The mean value of power $P_{mean,iv}$ in interval iv can be calculated according to equation (B-2).

Whereas for time series of generation and demand the maximum power is defined symmetrically, an asymmetrical definition is applied in case of residual demand time series. The maximum positive power $P_{max,pos}$ is defined as the annual maximum load of the original demand time series, assuming that the hour of maximum load can coincide with zero generation from RES and CHP. The maximum negative power $P_{max,neg}$ is defined as the total installed capacity of RES and CHP generation, assuming that, in principle, the simultaneous generation from all must-run sources at rated power could coincide with an hour of zero demand.

Thus, for time series of residual demand, the following set of equations is used to calculate the worst-case storage capacity $C_{worst-case,iv}$ for an interval iv :

$$P_{mean,iv} \geq 0: C_{worst-case,iv} = (P_{max,pos} - |P_{mean,iv}|) \cdot \frac{|W_{pos,iv}|}{P_{max,pos}} \quad (B-5)$$

$$P_{mean,iv} < 0: C_{worst-case,iv} = (P_{max,neg} - |P_{mean,iv}|) \cdot \frac{|W_{neg,iv}|}{P_{max,neg}} \quad (B-6)$$

| | | |
|-------|---------------------|---|
| where | $P_{mean,iv}$ | mean value of power in interval iv |
| | $W_{pos,iv}$ | positive amount of energy contained in a time series in interval iv |
| | $W_{neg,iv}$ | negative amount of energy contained in a time series in interval iv |
| | $C_{worst-case,iv}$ | worst-case storage capacity for interval iv |
| | $P_{max,pos}$ | maximum positive power |
| | $P_{max,neg}$ | maximum negative power |
| | iv | set of intervals of length $T_{max,fr}$ |

The worst-case storage capacity $C_{worst-case,fr}$ for frequency range fr is the largest capacity detected among the worst-case storage capacities $C_{worst-case,iv}$ for all intervals iv of the respective frequency component.

As for time series of generation and demand, the low-frequency variability index of residual demand time series is limited to 1, whereas indices greater than 1 are generally possible for the mid- and high-frequency ranges.

C Data

C.1 Parameters of existing PSP in Germany

| No. | plant | round-trip efficiency | turbine capacity | pump capacity | storage capacity | storage duration |
|------------|-----------------------|----------------------------------|-----------------------------|--------------------------|-----------------------------|-----------------------------|
| - | - | <i>in %</i> | <i>in MW</i> | <i>in MW</i> | <i>in MWh</i> | <i>in h</i> |
| 1 | Bleiloch | 61 | 75 | 32 | 753 | 8 |
| 2 | Erzhausen | 74 | 220 | 230 | 940 | 4 |
| 3 | Geesthacht | 68 | 120 | 96 | 600 | 4 |
| 4 | Glems | 73 | 90 | 68 | 560 | 5 |
| 5 | Goldisthal | 80 | 1060 | 1140 | 8480 | 7 |
| 6 | Happburg | 72 | 160 | 126 | 900 | 5 |
| 7 | Hohenwarte 1 | 60 | 55 | 34 | 795 | 11 |
| 8 | Hohenwarte 2 | 68 | 320 | 310 | 2087 | 5 |
| 9 | Koepchenwerk Herdecke | 75 | 153 | 154 | 590 | 3 |
| 10 | Langenprozelten | 70 | 168 | 154 | 950 | 5 |
| 11 | Leitzachwerk 1 | 76 | 42 | 45 | 550 | 11 |
| 12 | Leitzachwerk 2 | 76 | 46 | 37 | 550 | 10 |
| 13 | Markersbach | 73 | 1050 | 1140 | 4018 | 3 |
| 14 | Niederwartha | 53 | 120 | 120 | 591 | 4 |
| 15 | Rabenleite Reisach | 75 | 105 | 81 | 630 | 5 |
| 16 | Rabenleite Tanzmühle | 69 | 35 | 25 | 404 | 10 |
| 17 | Rönkhausen | 75 | 140 | 140 | 690 | 4 |
| 18 | Säckingen | 73 | 363 | 298 | 2064 | 5 |
| 19 | Schwarzenbachwerk | 55 | 41 | 20 | 198 | 4 |
| 20 | Sorpetalsperre | 60 | 9 | 7 | 57 | 5 |
| 21 | Waldeck 1 | 75 | 140 | 96 | 478 | 3 |
| 22 | Waldeck 2 | 80 | 440 | 476 | 3428 | 7 |

| No. plant | round-trip efficiency | turbine capacity | pump capacity | storage capacity | storage duration | |
|---------------------------|------------------------------|-------------------------|----------------------|-------------------------|-------------------------|-------------|
| - | - | <i>in %</i> | <i>in MW</i> | <i>in MW</i> | <i>in MWh</i> | <i>in h</i> |
| 23 Wehr | 76 | 980 | 990 | 6073 | 5 | |
| 24 Wendefurth | 70 | 80 | 72 | 523 | 5 | |
| 25 Werksgruppe Schluchsee | 65 | 452 | 316 | 40030 | 71 | |
| - <i>total</i> | - | <i>6464</i> | <i>6207</i> | <i>76939</i> | - | |

Source: Kuhn *et al.* (2012); own calculations.

C.2 Development of RES and CHP generation capacity

| <i>in MW¹⁾</i> | onshore wind | offshore wind | solar | fossil CHP | biomass | hydro-power | geo-thermal |
|---------------------------|---------------------|----------------------|--------------|-------------------|----------------|--------------------|--------------------|
| 2010 | 24144 | 51 | 13011 | 21688 | 6070 | 4188 | 3 |
| 2011 | 26027 | 1132 | 14771 | 21470 | 6202 | 4188 | 61 |
| 2012 | 27909 | 2212 | 16531 | 21251 | 6334 | 4188 | 118 |
| 2013 | 29792 | 3293 | 18290 | 21032 | 6467 | 4188 | 176 |
| 2014 | 31675 | 4374 | 20050 | 20814 | 6599 | 4188 | 233 |
| 2015 | 33558 | 5455 | 21810 | 20595 | 6731 | 4188 | 291 |
| 2016 | 35441 | 6535 | 23570 | 20376 | 6863 | 4188 | 348 |
| 2017 | 37324 | 7616 | 25329 | 20158 | 6995 | 4188 | 406 |
| 2018 | 39207 | 8697 | 27089 | 19939 | 7128 | 4188 | 463 |
| 2019 | 41090 | 9777 | 28849 | 19720 | 7260 | 4188 | 521 |
| 2020 | 42973 | 10858 | 30608 | 19502 | 7392 | 4188 | 578 |
| 2021 | 44856 | 11939 | 32368 | 19283 | 7524 | 4188 | 636 |
| 2022 | 46739 | 13020 | 34128 | 19064 | 7657 | 4188 | 693 |
| 2023 | 48622 | 14100 | 35887 | 18846 | 7789 | 4188 | 751 |
| 2024 | 50505 | 15181 | 37647 | 18627 | 7921 | 4188 | 808 |
| 2025 | 52388 | 16262 | 39407 | 18408 | 8053 | 4188 | 866 |
| 2026 | 54271 | 17342 | 41167 | 18189 | 8185 | 4188 | 923 |
| 2027 | 56154 | 18423 | 42926 | 17971 | 8318 | 4188 | 981 |
| 2028 | 58037 | 19504 | 44686 | 17752 | 8450 | 4188 | 1038 |
| 2029 | 59920 | 20584 | 46446 | 17533 | 8582 | 4188 | 1096 |
| 2030 | 61803 | 21665 | 48205 | 17315 | 8714 | 4188 | 1153 |

| <i>in MW</i> ¹⁾ | onshore wind | offshore wind | solar | fossil CHP | biomass | hydro- power | geo- thermal |
|----------------------------|-------------------------|--------------------------|--------------|-----------------------|----------------|-------------------------|-------------------------|
| 2031 | 63686 | 22746 | 49965 | 17096 | 8847 | 4188 | 1211 |
| 2032 | 65568 | 23827 | 51725 | 16877 | 8979 | 4188 | 1268 |
| 2033 | 67451 | 24907 | 53485 | 16659 | 9111 | 4188 | 1326 |
| 2034 | 69334 | 25988 | 55244 | 16440 | 9243 | 4188 | 1383 |
| 2035 | 71217 | 27069 | 57004 | 16221 | 9375 | 4188 | 1441 |
| 2036 | 73100 | 28149 | 58764 | 16003 | 9508 | 4188 | 1498 |
| 2037 | 74983 | 29230 | 60523 | 15784 | 9640 | 4188 | 1556 |
| 2038 | 76866 | 30311 | 62283 | 15565 | 9772 | 4188 | 1613 |
| 2039 | 78749 | 31392 | 64043 | 15346 | 9904 | 4188 | 1671 |
| 2040 | 80632 | 32472 | 65802 | 15128 | 10036 | 4188 | 1728 |
| 2041 | 82515 | 33553 | 67562 | 14909 | 10169 | 4188 | 1786 |
| 2042 | 84398 | 34634 | 69322 | 14690 | 10301 | 4188 | 1843 |
| 2043 | 86281 | 35714 | 71082 | 14472 | 10433 | 4188 | 1901 |
| 2044 | 88164 | 36795 | 72841 | 14253 | 10565 | 4188 | 1958 |
| 2045 | 90047 | 37876 | 74601 | 14034 | 10698 | 4188 | 2016 |
| 2046 | 91930 | 38956 | 76361 | 13816 | 10830 | 4188 | 2073 |
| 2047 | 93813 | 40037 | 78120 | 13597 | 10962 | 4188 | 2131 |
| 2048 | 95696 | 41118 | 79880 | 13378 | 11094 | 4188 | 2188 |
| 2049 | 97579 | 42199 | 81640 | 13160 | 11226 | 4188 | 2246 |
| 2050 | 99462 | 43279 | 83400 | 12941 | 11359 | 4188 | 2303 |

1) installed generation capacity assuming annual energy production as defined in the reference scenario and FLH according to the meteorological reference year 2012

Abbreviations

| | |
|----------------------|---|
| AA-CAES | advanced adiabatic compressed air energy storage |
| CAES | compressed air energy storage |
| CAPEX | capital expenditures |
| CCGT | combined cycle gas turbine |
| CHP | combined heat and power |
| CO ₂ | carbon dioxide |
| DC | direct current |
| EU ETS | European Union emissions trading system |
| FLH | full load hours |
| GHG | greenhouse gas |
| H ₂ | hydrogen |
| H ₂ -CCGT | power-to-power hydrogen storage technology (electrolyser, storage cavern and combined cycle gas turbine) |
| HDD | heating degree days |
| kW | kilowatt |
| kWh | kilowatt hour |
| MAC | marginal abatement cost |
| MW | megawatt |
| MWh | megawatt hour |
| NPV | net present value |
| NTC | net transfer capacity |
| O&M | operation and maintenance |

Abbreviations

| | |
|------|----------------------------------|
| OPEX | operating expenditures |
| PSP | pumped-storage hydro power plant |
| PV | photovoltaics |
| RES | renewable energy sources |
| TCS | trade, commerce and services |
| TSO | transmission system operator |
| TWh | terawatt hour |
| WACC | weighted average cost of capital |

Nomenclature

Nomenclature of the models MOWIKA and MESTAS

A few remarks on notation: Variables are denoted by Latin upper-case letters, while parameters are either Latin or Greek lower-case letters. Sets and their elements are denoted by two or more Latin lower-case letters. Superscripts are used to further specify the nature of the respective parameter or variable, whereas subscripts exclusively contain information on the sets for which a parameter or variable is defined.

MOWIKA

| | |
|--------------------------|---|
| C_{pi}^{gen} | generation capacity of new build power plant pi |
| C_{pn}^{gen} | generation capacity of new build power plant pn |
| c_{pe}^{gen} | generation capacity of existing power plant pe |
| $c_{pi}^{gen,max}$ | maximum generation capacity available for installation of new build power plant pi |
| $c_{ys}^{gen,total,min}$ | minimum installed total generation capacity in simulation year ys |
| d | mean value of residual demand |
| $d_{ys,di}$ | mean value of residual demand in discretisation interval di in simulation year ys |
| di | set of discretisation intervals in simulation year ys |
| e_{ys}^{max} | maximum amount of emissions permitted in simulation year ys |
| $e^{max,total}$ | maximum amount of emissions permitted over the whole planning horizon |
| fl | set of fuel types |
| i | real discount rate |
| l | lifetime |

Nomenclature

| | |
|-------------------------------|--|
| l_{pi} | lifetime of new build power plant pi |
| l_{pi}^{rel} | relevant lifetime of new build power plant pi |
| n | number of payment periods (years) |
| P^{gen} | mean value of generating power |
| $P_{pe,ys,di}^{gen}$ | mean value of generating power of existing power plant pe in discretisation interval di in simulation year ys |
| $P_{pefl,ys,di}^{gen}$ | mean value of generating power of existing power plant $pefl$ in discretisation interval di in simulation year ys |
| $P_{pn,ys,di}^{gen}$ | mean value of generating power of new build power plant pn in discretisation interval di in simulation year ys |
| $P_{pnfl,ys,di}^{gen}$ | mean value of generating power of new build power plant $pnfl$ in discretisation interval di in simulation year ys |
| pe | set of existing power plants operational in simulation year ys |
| $pefl$ | set of existing power plants operational in simulation year ys burning fuel fl |
| pi | set of new build power plants available for installation in simulation year ys |
| pn | set of new build power plants operational in simulation year ys |
| $pnfl$ | set of new build power plants operational in simulation year ys burning fuel fl |
| $w_{fl,ys}^{therm,max}$ | maximum amount of thermal energy of fuel fl available for consumption in simulation year ys |
| y^{base} | base year |
| ys | set of simulation years |
| δ_{di} | duration of discretisation interval di in hours |
| $\varepsilon_{pe}^{electr}$ | emissions of existing power plant pe per unit of electricity generated |
| $\varepsilon_{pefl}^{electr}$ | emissions of existing power plant $pefl$ per unit of electricity generated |
| $\varepsilon_{pn}^{electr}$ | emissions of new build power plant pn per unit of electricity generated |
| $\varepsilon_{pnfl}^{electr}$ | emissions of new build power plant $pnfl$ per unit of electricity generated |

| | |
|-----------------------------------|---|
| η_{pefl} | net efficiency of existing power plant $pefl$ |
| η_{pnfl} | net efficiency of new build power plant $pnfl$ |
| κ | costs |
| $\kappa_{pi}^{dec,a}$ | annual savings for decommissioning of new build power plant pi |
| $\kappa_{pi}^{dec,target}$ | target costs for decommissioning of new build power plant pi |
| κ_{ys}^{emi} | carbon emissions price in simulation year ys |
| $\kappa_{pi}^{fix,a}$ | annual fixed costs of new build power plant pi |
| $\kappa_{fl,ys}^{fuel}$ | costs for fuel fl in simulation year ys |
| κ_{pi}^{inv} | investment costs of new build power plant pi |
| $\kappa_{pefl,ys}^{vO\&M}$ | variable O&M costs of existing power plant $pefl$ in simulation year ys |
| $\kappa_{pnfl,ys}^{vO\&M}$ | variable O&M costs of new build power plant $pnfl$ in simulation year ys |
| $\tilde{\kappa}$ | present value of costs |
| $\tilde{\kappa}_{pi}^{dec,total}$ | present value of total decommissioning costs of new build power plant pi |
| $\tilde{\kappa}_{pi}^{fix,total}$ | present value of total fixed costs of new build power plant pi |
| $\tilde{\kappa}_{pi}^{inv}$ | present value of investment costs of new build power plant pi |
| $\tilde{\kappa}_{pi}^{nv}$ | present value of non-variable costs of new build power plant pi |
| $\tilde{\kappa}_{pi}^{sal}$ | present value of salvage value of new build power plant pi |
| $\tilde{\kappa}_{pe}^v$ | present value of variable costs of existing power plant pe |
| $\tilde{\kappa}_{pefl}^v$ | present value of variable costs of existing power plant $pefl$ |
| $\tilde{\kappa}_{pn}^v$ | present value of variable costs of new build power plant pn |
| $\tilde{\kappa}_{pnfl}^v$ | present value of variable costs of new build power plant $pnfl$ |
| ξ_{pe} | reduction coefficient to consider the unavailability of existing power plant pe due to planned maintenance and unplanned outages |
| ξ_{pn} | reduction coefficient to consider the unavailability of new build power plant pn due to planned maintenance and unplanned outages |

MESTAS

| | |
|--------------------------|---|
| b | bonus on non-variable costs of new build storages |
| C_{sn}^{charge} | charging capacity of new build storage sn |
| $C_{sn}^{discharge}$ | discharging capacity of new build storage sn |
| $C_{sn}^{storage}$ | storage capacity of new build storage sn |
| C_{se}^{charge} | charging capacity of existing storage se |
| $C_{sn}^{charge,max}$ | maximum charging capacity available for installation of new build storage sn |
| $C_{se}^{discharge}$ | discharging capacity of existing storage se |
| $C_{sn}^{discharge,max}$ | maximum discharging capacity available for installation of new build storage sn |
| C_{pp}^{gen} | generation capacity of power plant pp |
| $C_{se}^{storage}$ | storage capacity of existing storage se |
| $C_{sn}^{storage,max}$ | maximum storage capacity available for installation of new build storage sn |
| d | mean value of residual demand |
| d_{ts} | mean value of residual demand in time step ts |
| e^{max} | maximum amount of emissions permitted in simulation year |
| fl | set of fuel types |
| i | real discount rate |
| l | lifetime |
| l_{sn} | lifetime of new build storage sn |
| P^{charge} | mean value of charging power |
| $P_{se,ts}^{charge}$ | mean value of charging power of existing storage se in time step ts |
| $P_{se,1}^{charge}$ | mean value of charging power of existing storage se in first time step |
| $P_{sn,ts}^{charge}$ | mean value of charging power of new build storage sn in time step ts |
| $P_{sn,1}^{charge}$ | mean value of charging power of new build storage sn in first time step |
| $P_{ts}^{curtail}$ | mean value of curtailed power in time step ts |

| | |
|-------------------------|--|
| $P^{discharge}$ | mean value of discharging power |
| $P_{se,ts}^{discharge}$ | mean value of discharging power of existing storage se in time step ts |
| $P_{se,1}^{discharge}$ | mean value of discharging power of existing storage se in first time step |
| $P_{sn,ts}^{discharge}$ | mean value of discharging power of new build storage sn in time step ts |
| $P_{sn,1}^{discharge}$ | mean value of discharging power of new build storage sn in first time step |
| P^{gen} | mean value of generating power |
| $P_{pp,ts}^{gen}$ | mean value of generating power of power plant pp in time step ts |
| $P_{ppfl,ts}^{gen}$ | mean value of generating power of power plant $ppfl$ in time step ts |
| $P^{mustrun}$ | conventional must-run capacity in each time step ts |
| pp | set of power plants |
| $ppfl$ | set of power plants burning fuel fl |
| $S_{se,ts}$ | storage level of existing storage se in time step ts |
| $S_{se,ts-1}$ | storage level of existing storage se in time step $ts-1$ |
| $S_{se,1}$ | storage level of existing storage se in first time step |
| $S_{se,8760}$ | storage level of existing storage se in last time step |
| $S_{sn,ts}$ | storage level of new build storage sn in time step ts |
| $S_{sn,ts-1}$ | storage level of new build storage sn in time step $ts-1$ |
| $S_{sn,1}$ | storage level of new build storage sn in first time step |
| $S_{sn,8760}$ | storage level of new build storage sn in last time step |
| se | set of existing storages |
| sn | set of new build storages |
| ts | set of time steps (8760 hours) |
| $w_{curtail,max}$ | maximum amount of curtailed energy permitted in simulation year |
| $w_{fl}^{therm,max}$ | maximum amount of thermal energy of fuel fl available for consumption in simulation year |
| α_{sn}^{max} | upper limit of ratio of discharging to charging capacity of new build storage sn |

Nomenclature

| | |
|---------------------------------|--|
| α_{sn}^{\min} | lower limit of ratio of discharging to charging capacity of new build storage sn |
| β_{sn}^{\max} | upper limit of ratio of storage to discharging capacity of new build storage sn |
| β_{sn}^{\min} | lower limit of ratio of storage to discharging capacity of new build storage sn |
| γ_{sn}^{\max} | upper limit of ratio of storage to charging capacity of new build storage sn |
| γ_{sn}^{\min} | lower limit of ratio of storage to charging capacity of new build storage sn |
| δ_{ts} | duration of time step ts (one hour) |
| $\varepsilon_{pp}^{electr}$ | emissions of power plant pp per unit of electricity generated |
| $\varepsilon_{ppfl}^{electr}$ | emissions of power plant $ppfl$ per unit of electricity generated |
| η_{se}^{charge} | charging efficiency of existing storage se |
| η_{sn}^{charge} | charging efficiency of new build storage sn |
| $\eta_{se}^{discharge}$ | discharging efficiency of existing storage se |
| $\eta_{sn}^{discharge}$ | discharging efficiency of new build storage sn |
| η_{ppfl} | net efficiency of power plant $ppfl$ |
| κ | costs |
| $\kappa^{curtail}$ | revenues of curtailment |
| $\kappa_{sn}^{dec,a}$ | annual savings for decommissioning of new build storage sn |
| $\kappa_{sn}^{dec,target}$ | target costs for decommissioning of new build storage sn |
| κ^{emi} | carbon emissions price |
| $\kappa_{sn}^{fix,a}$ | annual fixed costs of new build storage sn |
| κ_{fl}^{fuel} | costs for fuel fl |
| $\kappa_{sn}^{inv,a,charge}$ | annualised investment costs of charging capacity of new build storage sn |
| $\kappa_{sn}^{inv,a,discharge}$ | annualised investment costs of discharging capacity of new build storage sn |
| $\kappa_{sn}^{inv,a,storage}$ | annualised investment costs of storage capacity of new build storage sn |
| $\kappa_{sn}^{inv,charge}$ | investment costs of charging capacity of new build storage sn |

| | |
|-------------------------------|---|
| $\kappa_{sn}^{inv,discharge}$ | investment costs of discharging capacity of new build storage sn |
| $\kappa_{sn}^{inv,storage}$ | investment costs of storage capacity of new build storage sn |
| $\kappa_{sn}^{nv,charge}$ | non-variable costs of charging capacity of new build storage sn |
| $\kappa_{sn}^{nv,discharge}$ | non-variable costs of discharging capacity of new build storage sn |
| $\kappa_{sn}^{nv,storage}$ | non-variable costs of storage capacity of new build storage sn |
| κ_{pp}^v | variable costs of power plant pp |
| κ_{ppfl}^v | variable costs of power plant $ppfl$ |
| $\kappa_{se}^{v,charge}$ | variable costs of charging of existing storage se |
| $\kappa_{sn}^{v,charge}$ | variable costs of charging of new build storage sn |
| $\kappa_{se}^{v,discharge}$ | variable costs of discharging of existing storage se |
| $\kappa_{sn}^{v,discharge}$ | variable costs of discharging of new build storage sn |
| $\kappa_{ppfl}^{vO\&M}$ | variable O&M costs of power plant $ppfl$ |
| λ_{se} | hourly rate of self-discharge of existing storage se |
| λ_{sn} | hourly rate of self-discharge of new build storage sn |
| ξ_{pp} | reduction coefficient to consider the unavailability of power plant pp due to planned maintenance and unplanned outages |
| ξ_{se} | reduction coefficient to consider the unavailability of existing storage se due to planned maintenance and unplanned outages |
| ξ_{sn} | reduction coefficient to consider the unavailability of new build storage sn due to planned maintenance and unplanned outages |
| σ_{se} | relative storage level of existing storage se at the beginning of the simulation year |
| σ_{sn} | relative storage level of new build storage sn at the beginning of the simulation year |

Other nomenclature

| | |
|------------|---|
| A | energy availability |
| B_0 | initial book value of a given asset |
| B_1 | book value of a given asset at end of first year |
| B_{yl} | book value of a given asset at end of year yl |
| B_{yl-1} | book value of a given asset at end of year $yl-1$ |

Nomenclature

| | |
|-------------------------|--|
| $C_{theoretical}$ | theoretical storage capacity |
| $C_{theoretical,fr}$ | theoretical storage capacity for frequency range fr |
| $C_{worst-case}$ | worst-case storage capacity |
| $C_{worst-case,iv}$ | worst-case storage capacity for interval iv |
| $C_{worst-case,fr}$ | worst-case storage capacity for frequency range fr |
| $C^{discharge}$ | discharging capacity of a given storage |
| $C_{ts}^{discharge,av}$ | available discharging capacity of a given storage in time step ts |
| C^{firm} | firm capacity of a given generation portfolio for a given level of security of supply |
| ΔC^{firm} | deviation of firm capacity from the target value of firm capacity |
| $C^{firm,conv}$ | firm capacity of the conventional generation portfolio for a given level of security of supply |
| $C^{firm,target}$ | target value of firm capacity |
| $C^{gen,conv}$ | total installed conventional generation capacity |
| $\Delta C^{gen,conv}$ | amount of additional or spare conventional generation capacity |
| D_{yl} | depreciation expense in year yl |
| E^a | total annual expenses |
| F^{CCDF} | complementary cumulative distribution function |
| F^{CDF} | cumulative distribution function |
| FOR | forced outage rate |
| fr | set of frequency ranges with members $high-frq$, $mid-frq$ and $low-frq$ |
| I_{yl} | foregone interest in year yl |
| i | real discount rate |
| iv | set of intervals of length $T_{max,fr}$ |
| l | lifetime |
| n | number of payment periods (years) |
| P_{max} | maximum power |
| $P_{max,neg}$ | maximum negative power |
| $P_{max,pos}$ | maximum positive power |

| | |
|-------------------------|--|
| P_{mean} | mean value of power |
| $P_{mean,iv}$ | mean value of power in interval iv |
| R | technical reliability |
| S_{ts} | storage level of a given storage in time step ts |
| T | period |
| T_{max} | largest period T |
| $T_{max,fr}$ | largest period T included in frequency range fr |
| ts | set of time steps (8760 hours) |
| U | energy unavailability |
| U_p | planned energy unavailability |
| U_{up} | unplanned energy unavailability |
| V | variability index |
| V_{fr} | variability index for frequency range fr |
| W_{neg} | negative amount of energy contained in a time series |
| $W_{neg,iv}$ | negative amount of energy contained in a time series in interval iv |
| W_{pos} | positive amount of energy contained in a time series |
| $W_{pos,iv}$ | positive amount of energy contained in a time series in interval iv |
| yl | set of years of the economic lifetime of a given asset |
| δ_{ts} | duration of time step ts (one hour) |
| $\eta^{discharge}$ | discharging efficiency of a given storage |
| $\tilde{K}_1^{inv,avg}$ | present value of average annual investment costs for one year of utilisation |
| ξ | reduction coefficient to consider the unavailability of generation capacity due to planned maintenance and unplanned outages |

List of tables

| | | |
|-------------|--|-----|
| Table 2.1: | General scope of studies selected for review | 19 |
| Table 2.2: | Selected scenarios of storage demand in the German power system and general assumptions for the year 2050 | 32 |
| Table 4.1: | Overview of analysed methodological approaches and an indication of whether they lead to an increase (+) or decrease (-) of estimated storage capacity expansion | 133 |
| Table 5.1: | Electricity generation from RES and CHP in Germany in 2010 and 2050 as assumed in the reference scenario | 138 |
| Table 5.2: | Shares of electricity generation from RES in Germany in 2010 and 2050 as assumed in the reference scenario | 139 |
| Table 5.3: | Relative distribution of installed onshore wind and solar PV capacity across German federal states in 2011 (total installed capacity = 100 %) | 141 |
| Table 5.4: | Annual HDD for the period 2003–2012 | 142 |
| Table 5.5: | Sectoral structure of heat demand in district heating systems in Germany for the period 2003–2012 | 144 |
| Table 5.6: | Sectoral structure of heat demand in district heating systems in Germany for the period 2003–2012 (typical values, based on own assumptions) | 144 |
| Table 5.7: | Annual CHP generation by public utilities and industry in Germany for the period 2003–2012 | 145 |
| Table 5.8: | Total annual CHP generation in Germany for the period 2003–2012 (typical values, based on own assumptions) | 145 |
| Table 5.9: | Energy availability, planned and unplanned energy unavailability and technical reliability of existing power plants by generation technology | 148 |
| Table 5.10: | Variable O&M costs of existing power plants by generation technology | 148 |

| | |
|--|-----|
| Table 5.11: Energy availability, planned and unplanned energy unavailability and technical reliability of existing storages by storage technology | 150 |
| Table 5.12: Variable O&M costs of existing storages by storage technology | 150 |
| Table 5.13: Fuel costs as assumed in the reference scenario..... | 151 |
| Table 5.14: Carbon emission intensity of fossil fuels..... | 152 |
| Table 5.15: Technical parameters of new build power plants by generation technology | 153 |
| Table 5.16: Economic parameters of new build power plants by generation technology | 153 |
| Table 5.17: Energy availability, planned and unplanned energy unavailability and technical reliability of new build power plants by generation technology | 153 |
| Table 5.18: Technical parameters of new build storages by storage technology | 154 |
| Table 5.19: Economic parameters of new build storages by storage technology as assumed in the reference scenario | 155 |
| Table 5.20: Energy availability, planned and unplanned energy unavailability and technical reliability of new build storages by storage technology.. | 156 |
| Table 5.21: Development of annual electricity generation from fossil CHP in Germany by fuel | 157 |
| Table 5.22: Overall CO ₂ emissions target for the planning horizon 2010–2050 (assuming different annual time series of fossil CHP generation)..... | 157 |
| Table 5.23: FLH of demand and generation time series for the period 2003–2012 in Germany | 158 |
| Table 5.24: Minimum power of demand and generation time series for the period 2003–2012 in Germany (scaled to annual maximum load and installed capacity respectively)..... | 160 |
| Table 5.25: Maximum power of demand and generation time series for the period 2003–2012 in Germany (scaled to annual maximum load and installed capacity respectively)..... | 161 |
| Table 5.26: Standard deviation of demand and generation time series for the period 2003–2012 in Germany (scaled to annual maximum load and installed capacity respectively)..... | 161 |
| Table 5.27: Low-frequency variability index of demand and generation time series for the period 2003–2012 in Germany | 163 |
| Table 5.28: Mid-frequency variability index of demand and generation time series for the period 2003–2012 in Germany | 164 |
| Table 5.29: High-frequency variability index of demand and generation time series for the period 2003–2012 in Germany | 164 |

| | |
|---|-----|
| Table 5.30: Installed generation capacities in 2050 (assuming annual energy production as defined in the reference scenario and FLH according to the meteorological reference year 2012)..... | 172 |
| Table 5.31: Total annual electricity generation and total annual electricity consumption in 2050 (assuming different annual time series of generation and demand)..... | 172 |
| Table 5.32: Residual energy demand and surplus energy in 2050 (assuming different annual time series of residual demand)..... | 173 |
| Table 5.33: Low-, mid- and high-frequency variability of residual demand in 2050 (assuming different annual time series of residual demand) | 173 |
| Table 5.34: Shares of electricity generation from RES in 2050 for scenarios varying RES share | 189 |
| Table 5.35: Fuel costs as assumed in variation scenarios (in comparison to fuel costs in the reference scenario) | 194 |
| Table 5.36: Investment costs of new build storages by storage technology as assumed in variation scenarios (in comparison to investment costs in the reference scenario) | 196 |

List of figures

| | |
|---|-----|
| Figure 1.1: Selected study results on the expansion of storage capacity until 2030..... | 11 |
| Figure 2.1: Comparison of study results on charging, discharging and storage capacity in Germany in 2050..... | 33 |
| Figure 3.1: Schematic representation of the whole-systems cost minimisation model IMAKUS | 36 |
| Figure 3.2: Approximation of an annual load duration curve using 15 discretisation intervals of fixed duration vs. using 15 discretisation intervals of variable duration..... | 40 |
| Figure 3.3: Complementary cumulative distribution function of available generation capacity in an exemplary generation portfolio | 75 |
| Figure 3.4: General effect of storage on annual load duration curves and its impact on the level of utilisation of power plants | 82 |
| Figure 3.5: Schematic representation of the iterative process and expected cost reductions in the model IMAKUS | 84 |
| Figure 3.6: Iterative adaptation of conventional generation and storage portfolios in IMAKUS in an exemplary scenario | 86 |
| Figure 3.7: Comparison of annuity method for depreciation and straight-line depreciation (assuming a 20-year planning horizon, 1 million € investment, 20 years lifetime and 5 % interest rate) | 90 |
| Figure 4.1: Comparison of conventional generation portfolios obtained from intertemporal optimisation and from the optimisation of snapshot years in an exemplary scenario..... | 111 |
| Figure 4.2: Comparison of storage portfolios obtained from intertemporal optimisation and from the optimisation of snapshot years in an exemplary scenario | 112 |
| Figure 4.3: Comparison of conventional generation portfolios assuming different real social discount rates in an exemplary scenario | 115 |

| | |
|--|-----|
| Figure 4.4: Comparison of storage capacity expansion assuming different real social discount rates in an exemplary scenario..... | 117 |
| Figure 4.5: Discrete MAC curve and its effect on emissions when exogenously fixing the carbon price | 119 |
| Figure 4.6: Annual emissions targets and annual emissions resulting from an overall emissions target in an exemplary scenario | 121 |
| Figure 4.7: Comparison of storage capacity expansion with and without curtailment of surplus generation in an exemplary scenario | 124 |
| Figure 4.8: Comparison of storage capacity expansion with and without must-run of conventional generation in an exemplary scenario in 2050 | 127 |
| Figure 4.9: Comparison of storage capacity expansion with fixed storage duration and with optimised storage duration in an exemplary scenario in 2050..... | 129 |
| Figure 4.10: Comparison of storage capacity expansion with fixed and with optimised initial storage levels in an exemplary scenario in 2050 | 131 |
| Figure 4.11: Comparison of the storage level of H ₂ -CCGT with fixed and with optimised initial storage levels in an exemplary scenario in 2050 | 132 |
| Figure 5.1: Electricity generation from RES and CHP over the planning horizon 2010–2050 as assumed in the reference scenario..... | 140 |
| Figure 5.2: Development of existing conventional generation capacity in Germany over the planning horizon 2010–2050 | 147 |
| Figure 5.3: Characteristics of existing PSP in Germany..... | 149 |
| Figure 5.4: Comparison of FLH of onshore wind generation based on annual time series and historical values for the period 2003–2012 in Germany | 159 |
| Figure 5.5: Cumulated hourly values of onshore wind generation for the years 2005, 2009 and 2012 in Germany (scaled to annual onshore wind generation) | 162 |
| Figure 5.6: FLH and low-frequency variability of annual time series of onshore wind generation..... | 168 |
| Figure 5.7: FLH and low-frequency variability of annual time series of offshore wind generation..... | 168 |
| Figure 5.8: FLH and low-frequency variability of annual time series of solar generation..... | 169 |
| Figure 5.9: FLH and low-frequency variability of annual time series of electricity demand..... | 170 |
| Figure 5.10: Residual energy demand and low-frequency variability of annual time series of residual demand..... | 174 |

| | |
|--|-----|
| Figure 5.11: Surplus energy and low-frequency variability of annual time series of residual demand..... | 175 |
| Figure 5.12: Economic savings of storage expansion in the reference scenario accumulated over the planning horizon 2010–2050..... | 177 |
| Figure 5.13: Curtailment of generation from RES and CHP in the reference scenario in comparison to cases without storage expansion and without storage..... | 178 |
| Figure 5.14: Expansion of storage capacity over the planning horizon 2010–2050 in the reference scenario | 179 |
| Figure 5.15: Expansion of charging and discharging capacity over the planning horizon 2010–2050 in the reference scenario | 180 |
| Figure 5.16: Development of equivalent full cycles of existing and new build storages over the planning horizon 2010–2050 in the reference scenario..... | 181 |
| Figure 5.17: Development of the conventional generation portfolio over the planning horizon 2010–2050 in the reference scenario | 183 |
| Figure 5.18: Electricity generation over the planning horizon 2010–2050 in the reference scenario | 184 |
| Figure 5.19: Annual carbon emissions and carbon prices over the planning horizon 2010–2050 in the reference scenario | 185 |
| Figure 5.20: Electricity generation from RES and CHP, surplus energy and residual energy demand in 2050 under varying time series of generation and demand | 188 |
| Figure 5.21: Electricity generation from RES and CHP, surplus energy and residual energy demand in 2050 under varying RES shares | 189 |
| Figure 5.22: Graphical representation of relative shares of onshore wind, offshore wind and solar generation as assumed in scenarios varying RES structure | 191 |
| Figure 5.23: Electricity generation from RES and CHP, surplus energy and residual energy demand in 2050 under scenarios varying RES structure | 192 |
| Figure 5.24: Total new build storage capacity in 2050 in the variation scenarios as compared to the reference scenario | 198 |
| Figure 5.25: Range of relative deviations between variation scenarios and the reference scenario – total new build storage capacity in 2050 | 198 |
| Figure 5.26: Range of relative deviations between variation scenarios and the reference scenario – total new build charging capacity in 2050..... | 200 |
| Figure 5.27: Range of relative deviations between variation scenarios and the reference scenario – total new build discharging capacity in 2050 | 200 |

| | |
|---|-----|
| Figure 5.28: Range of relative deviations between variation scenarios and the reference scenario – charging capacity of new build PSP in 2050 | 202 |
| Figure 5.29: Range of relative deviations between variation scenarios and the reference scenario – discharging capacity of new build PSP in 2050... | 202 |
| Figure 5.30: Storage duration of new build PSP in 2050 in the variation scenarios as compared to the reference scenario..... | 203 |
| Figure 5.31: Ratio of charging to discharging capacity of new build PSP in 2050 in the variation scenarios as compared to the reference scenario | 204 |
| Figure 5.32: Storage capacity of new build AA-CAES in 2050 in the variation scenarios as compared to the reference scenario..... | 205 |
| Figure 5.33: Range of relative deviations between variation scenarios and the reference scenario – storage capacity of new build AA-CAES in 2050 | 206 |
| Figure 5.34: Storage duration of new build AA-CAES in 2050 in the variation scenarios as compared to the reference scenario..... | 207 |
| Figure 5.35: Ratio of charging to discharging capacity of new build AA-CAES in 2050 in the variation scenarios as compared to the reference scenario..... | 208 |
| Figure 5.36: Range of relative deviations between variation scenarios and the reference scenario – storage capacity of new build H ₂ -CCGT in 2050 | 209 |
| Figure 5.37: Range of relative deviations between variation scenarios and the reference scenario – charging capacity of new build H ₂ -CCGT in 2050..... | 210 |
| Figure 5.38: Range of relative deviations between variation scenarios and the reference scenario – discharging capacity of new build H ₂ -CCGT in 2050..... | 210 |
| Figure 5.39: Storage duration of new build H ₂ -CCGT in 2050 in the variation scenarios as compared to the reference scenario..... | 212 |
| Figure 5.40: Ratio of charging to discharging capacity of new build H ₂ -CCGT in 2050 in the variation scenarios as compared to the reference scenario..... | 213 |
| Figure 5.41: New build storage capacity in 2050 for variations of annual time series and the reference scenario | 214 |
| Figure 5.42: Surplus energy, residual energy demand and H ₂ -CCGT storage capacity in 2050 for variations of annual time series and the reference scenario | 215 |
| Figure 5.43: Surplus energy, low-frequency variability and theoretical long-duration storage capacity in 2050 for variations of annual time series and the reference scenario | 217 |

| | |
|---|-----|
| Figure 5.44: H ₂ -CCGT storage capacity in 2050 as compared to theoretically expected long-duration storage capacity for variations of annual time series and the reference scenario | 218 |
| Figure 5.45: New build storage capacity in 2050 for variations of RES share and the reference scenario | 219 |
| Figure 5.46: Expansion of storage capacity over the planning horizon 2010–2050 in case of an RES share of 60 % in 2050 | 221 |
| Figure 5.47: Expansion of storage capacity over the planning horizon 2010–2050 in case of an RES share of 80 % in 2050 (reference scenario) | 221 |
| Figure 5.48: Expansion of storage capacity over the planning horizon 2010–2050 in case of an RES share of 100 % in 2050..... | 222 |
| Figure 5.49: New build storage capacity in 2050 for variations of RES structure and the reference scenario | 224 |
| Figure 5.50: Storage capacity of new build AA-CAES in 2050 for variations of RES structure | 225 |
| Figure 5.51: Storage capacity of new build H ₂ -CCGT in 2050 for variations of RES structure | 226 |
| Figure 5.52: Charging capacity of new build PSP in 2050 for variations of RES structure | 227 |
| Figure 5.53: Charging capacity of new build H ₂ -CCGT in 2050 for variations of RES structure | 228 |
| Figure 5.54: Comparison of the storage level of H ₂ -CCGT in 2050 in scenarios with relative shares of 100 % solar and 100 % offshore wind generation..... | 229 |
| Figure 6.1: Expansion of storage capacity over the planning horizon 2010–2050 in the reference scenario (assuming a 6 % discount rate) | 236 |
| Figure 6.2: Expansion of charging and discharging capacity over the planning horizon 2010–2050 in the reference scenario (assuming a 6 % discount rate) | 237 |
| Figure 6.3: Earned IRR on storage investments under the reference scenario and under selected scenarios of varying meteorological conditions, RES shares and RES structures | 240 |
| Figure 6.4: Earned IRR on storage investments for variations of annual time series and the reference scenario | 242 |
| Figure 6.5: Earned IRR on storage investments for variations of RES share and the reference scenario | 243 |
| Figure 6.6: Earned IRR on storage investments for variations of RES structure and the reference scenario | 245 |

References

- Adamek *et al.* 2012 Adamek, F., Aundrup, T., Glaunsinger, W., Kleimaier, M., Landinger, H., Leuthold, M., Lunz, B., Moser, A., Pape, C., Pluntke, H., Roterling, N., Sauer, D., Sterner, M., Wellßow, W. (2012), „Energiespeicher für die Energiewende – Speicherungsbedarf und Auswirkungen auf das Übertragungsnetz für Szenarien bis 2050“, report by Energietechnische Gesellschaft im VDE (ETG), Frankfurt a. M., Germany.
- Agora Energiewende 2014 Agora Energiewende (2014), „Stromspeicher in der Energiewende – Untersuchung zum Bedarf an neuen Stromspeichern in Deutschland für den Erzeugungsausgleich, Systemdienstleistungen und im Verteilnetz“, report by Agora Energiewende, Berlin, Germany.
- Ahlhaus & Stursberg 2013 Ahlhaus, P., Stursberg, P. (2013), “Transmission capacity expansion: an improved transport model”, *2013 4th IEEE PES Innovative Smart Grid Technologies Europe (ISGT Europe)*, New York: IEEE, pp. 1–5.
- Albrecht 2013 Albrecht, J. (2013), „Pumpspeichertechnologien im Vergleich“, in Heimerl, S. (eds), *Wasserkraftprojekte*, Wiesbaden: Springer, pp. 354–362.
- BAFA 2013a BAFA (2013), „Aufkommen und Export von Erdgas“, BAFA statistical publication as at 13 December 2013, Bundesamt für Wirtschaft und Ausfuhrkontrolle (BAFA), Eschborn, Germany, http://www.bafa.de/bafa/de/energie/erdgas/ausgewae_hlte_statistiken/egasmon.pdf [accessed 08.01.2014].

- BAFA 2013b BAFA (2013), „Drittlandssteinkohlepreise“, BAFA statistical publication as at 10 December 2013, Bundesamt für Wirtschaft und Ausfuhrkontrolle (BAFA), Eschborn, Germany, http://www.bafa.de/bafa/de/energie/steinkohle/drittlandskohlepreis/energie_steinkohle_statistiken_preise.pdf [accessed 08.01.2014].
- BDEW 2013 BDEW (2013), „Erneuerbare Energien und das EEG: Zahlen, Fakten, Grafiken (2013)“, BDEW publication series Energie-Info, Bundesverband der Energie- und Wasserwirtschaft e. V. (BDEW), Berlin, Germany.
- BGBL 2011 BGBL (2011), „Dreizehntes Gesetz zur Änderung des Atomgesetzes vom 31. Juli 2011“, *Bundesgesetzblatt Teil I*, **2011** (43), pp. 1704–1705.
- Billinton & Allan 1984 Billinton, R., Allan, R. (1984), *Reliability evaluation of power systems*, New York: Plenum.
- BMWi & BMU 2010 BMWi, BMU (2010), „Energiekonzept für eine umweltschonende, zuverlässige und bezahlbare Energieversorgung“, Bundesministerium für Wirtschaft und Technologie (BMWi), Bundesministerium für Umwelt, Naturschutz und Reaktorsicherheit (BMU), Berlin, Germany, <http://www.bmwi.de/BMWi/Redaktion/PDF/E/energiekonzept-2010> [accessed 09.04.2015].
- BMWi 2013 BMWi (2013), „Zahlen und Fakten – Energiedaten – Nationale und internationale Entwicklung“, BMWi statistical publication as at 20 August 2013, Bundesministerium für Wirtschaft und Technologie (BMWi), Berlin, Germany, <http://www.bmwi.de/DE/Themen/Energie/energiedaten.html> [accessed 17.12.2013].
- Brückl 2005 Brückl, O. (2005), „Die Integration von Windenergie in die allgemeine Stromversorgung – Auswirkungen auf die Versorgungssicherheit“, *Tagungsband zur FfE-Fachtagung 2005 – Sicherheit in der Energieversorgung*, München: Forschungsstelle für Energiewirtschaft e. V. (FfE), pp. 1–11.

- Bruner *et al.* 1998 Bruner, R., Eades, K., Harris, R., Higgins, R. (1998), “Best practices in estimating the cost of capital: survey and synthesis”, *Financial Practice and Education*, **8** (1), pp. 13–28.
- Connolly *et al.* 2010 Connolly, D., Lund, H., Mathiesen, B., Leahy, M. (2010), “A review of computer tools for analysing the integration of renewable energy into various energy systems”, *Applied Energy*, **87** (4), pp. 1059–1082.
- Conrad *et al.* 2014 Conrad, J., Pelling, C., Hinterstocker, M. (2014), „Gutachten zur Rentabilität von Pumpspeicherkraftwerken”, final report, Forschungsstelle für Energiewirtschaft e. V. (FfE), München, Germany.
- Czakainski *et al.* 2013 Czakainski, M., Lamprecht, F., Siefke-Bremkens, J. (2013), „Was ist ein typisches Windjahr?”, *Energiewirtschaftliche Tagesfragen*, **63** (7), p. 21.
- DECC 2011 DECC (2011), “The carbon plan: delivering our low carbon future”, Department of Energy & Climate Change (DECC), London, UK, https://www.gov.uk/government/uploads/system/uploads/attachment_data/file/47613/3702-the-carbon-plan-delivering-our-low-carbon-future.pdf [accessed 19.08.2015].
- Delarue *et al.* 2008 Delarue, E., Voorspools, K., D’haeseleer, W. (2008), “Fuel switching in the electricity sector under the EU ETS: review and prospective”, *Journal of Energy Engineering*, **134** (2), pp. 40–46.
- Delmas & Montes-Sancho 2011 Delmas, M., Montes-Sancho, M. (2011), “U.S. state policies for renewable energy: context and effectiveness”, *Energy Policy*, **39** (5), pp. 2273–2288.
- Delucchi & Jacobson 2011 Delucchi, M., Jacobson, M. (2011), “Providing all global energy with wind, water, and solar power, Part II: reliability, system and transmission costs, and policies”, *Energy Policy*, **39** (3), pp. 1170–1190.
- dena 2010 dena (2010), „dena-Netzstudie II – Integration erneuerbarer Energien in die deutsche Stromversorgung im Zeitraum 2015–2020 mit Ausblick

- auf 2025“, report by Deutsche Energie-Agentur GmbH (dena), Berlin, Germany.
- Destatis 2014 Destatis (2014), „Verbraucherpreisindex für Deutschland“, Destatis statistical publication as at 8 January 2014, Statistisches Bundesamt (Destatis), Wiesbaden, Germany, https://www.destatis.de/DE/ZahlenFakten/GesamtwirtschaftUmwelt/Preise/Verbraucherpreisindizes/Tabelle_n_/VerbraucherpreiseKategorien.html [accessed 08.01.2014].
- Dyer & Stougie 2006 Dyer, M., Stougie, L. (2006), “Computational complexity of stochastic programming problems”, *Mathematical Programming*, **106** (3), pp. 423–432.
- EC 2003 EC (2003), “Directive 2003/87/EC of the European Parliament and of the Council of 13 October 2003 establishing a scheme for greenhouse gas emission allowance trading within the Community and amending Council Directive 96/61/EC”, *Official Journal of the European Union*, **46** (L 275), pp. 32–46.
- Edenhofer *et al.* 2014 Edenhofer, O., Pichs-Madruga, R., Sokona, Y., Farahani, E., Kadner, S., Seyboth, K., Adler, A., Baum, I., Brunner, S., Eickemeier, P., Kriemann, B., Savolainen, J., Schlömer, S., von Strechow, C., Zwickel, T., Minx, J. (eds) (2014), *Climate change 2014: mitigation of climate change – contribution of Working Group III to the Fifth Assessment Report of the Intergovernmental Panel on Climate Change*, Cambridge: Cambridge University Press.
- ENTSO-E 2014 ENTSO-E (2014), “ENTSO-E Yearly statistics & adequacy retrospect 2013“, statistical report, European Network of Transmission System Operators for Electricity (ENTSO-E), Brussels, Belgium.
- E.ON 2013 E.ON (2013), “E.ON 2012 Annual Report“, report, E.ON SE, Düsseldorf, Germany.
- Epe 2011 Epe, A. (2011), *Stochastische Modellierung des Elektrizitätsspeicherzubaus in Deutschland*, Münster: Lit Verlag (ISBN 978-3-643-11306-1).

- EPRI 2012 EPRI (2012), “Midwest Independent Transmission System Operator (MISO) Energy storage study“, phase 1 interim report, Electric Power Research Institute (EPRI), Palo Alto, USA.
- Evans & Sezer 2004 Evans, D., Sezer, H. (2004), “Social discount rates for six major countries”, *Applied Economics Letters*, **11** (9), pp. 557–560.
- Faulstich *et al.* 2011 Faulstich, M., Foth, H., Calliess, C., Hohmeyer, O., Holm-Müller, K., Niekisch, M., Schreurs, M. (2011), „Wege zur 100 % erneuerbaren Stromversorgung“, report, Sachverständigenrat für Umweltfragen (SRU), Berlin, Germany.
- Fezzi & Bunn 2009 Fezzi, C., Bunn, D. (2009), “Structural interactions of European carbon trading and energy prices”, *The Journal of Energy Markets*, **2** (4), pp. 53–69.
- FGH *et al.* 2012 FGH, CONSENTEC, IAEW (2012), „Studie zur Ermittlung der technischen Mindesterzeugung des konventionellen Kraftwerksparks zur Gewährleistung der Systemstabilität in den deutschen Übertragungsnetzen bei hoher Einspeisung aus erneuerbaren Energien“, final report, Forschungsgemeinschaft für Elektrische Anlagen und Stromwirtschaft e. V. (FGH), Mannheim, Consulting für Energiewirtschaft und -technik GmbH (CONSENTEC), Aachen, Institut für Elektrische Anlagen und Stromwirtschaft (IAEW) der RWTH Aachen, Aachen, Germany.
- Giebel 2000 Giebel, G. (2000), “On the benefits of distributed generation of wind energy in Europe”, doctoral thesis, Carl von Ossietzky Universität Oldenburg, Germany.
- Gobmaier 2013 Gobmaier, T. (2013), „Entwicklung und Anwendung einer Methodik zur Synthese zukünftiger Verbraucherlastgänge“, doctoral thesis, Technische Universität München, Germany, <https://mediatum.ub.tum.de/node?id=1166299> [accessed 04.09.2015].
- Graham 2011 Graham, L. (2011), *Accountants’ Handbook – 2011 cumulative supplement*, Hoboken: Wiley.

- Graves *et al.* 1999 Graves, F., Jenkin, T., Murphy, D. (1999), “Opportunities for electricity storage in deregulating markets”, *The Electricity Journal*, **12** (8), pp. 46–56.
- Grinold 1983 Grinold, R. (1983), “Model building techniques for the correction of end effects in multistage convex programs”, *Operations Research*, **31** (3), pp. 407–431.
- Hadjicostas & Adams 1992 Hadjicostas, T., Adams, R. (1992), “The flexible rolling schedule for infinite-horizon optimality in generation expansion planning”, *Transactions on Power Systems*, **7** (3), pp. 1182–1188.
- Hake *et al.* 2015 Hake, J.-F., Fischer, W., Venghaus, S., Weckenbrock, C. (2015), “The German Energiewende – history and status quo”, *Energy* (2015), article in press, <http://dx.doi.org/10.1016/j.energy.2015.04.027> [accessed 18.08.2015].
- Hand *et al.* 2012 Hand, M., Baldwin, S., DeMeo, E., Reilly, J., Mai, T., Arent, D., Porro, G., Meshek, M., Sandor, D. (eds) (2012), “Renewable electricity futures study“, entire report (4 volumes) TP-6A20-52409, National Renewable Energy Laboratory (NREL), Golden, USA.
- Heilek 2006 Heilek, C. (2006), „Entwicklung eines Modells zur Synthese der elektrischen Netzlast“, diploma thesis, Technische Universität München, Germany.
- Heilek 2015 Heilek, C. (2015), „Modellgestützte Optimierung des Neubaus und Einsatzes von Erzeugungsanlagen und Speichern für elektrische und thermische Energie im deutschen Energieversorgungssystem“, doctoral thesis, Technische Universität München, Germany, <https://mediatum.ub.tum.de/node?id=1230817> [accessed 04.09.2015].
- Heilek *et al.* 2016 Heilek, C., Kuhn, P., Kühne, M. (2016), “The role of large-scale hydrogen storage in the power system”, in Töpler, J., Lehmann, J. (eds), *Hydrogen and fuel cell*, Berlin: Springer, pp. 21–37.
- Hillier & Lieberman 2014 Hillier, F., Lieberman, G. (2014), *Introduction to operations research*, New York: McGraw-Hill.

- Hintermann 2010 Hintermann, B. (2010), "Allowance price drivers in the first phase of the EU ETS", *Journal of Environmental Economics and Management*, **59** (1), pp. 43–56.
- Hirth & Ueckerdt 2012 Hirth, L., Ueckerdt, F. (2012), "Redistribution effects of energy and climate policy: the electricity market", *Fondazione Eni Enrico Mattei Working Papers*, paper 733.
- Hobbs 1995 Hobbs, B. (1995), "Optimization methods for electric utility resource planning", *European Journal of Operational Research*, **83** (1), pp. 1–20.
- Höflich *et al.* 2010 Höflich, B., Kreutzkamp, P., Peinl, H., Völker, J., Kühne, M., Kuhn, P., Tzscheuschler, P., Hermes, R., Krahl, S., Meisa, K. (2010), „Analyse der Notwendigkeit des Ausbaus von Pumpspeicherwerken und anderen Stromspeichern zur Integration der erneuerbaren Energien“, report for Schluchseewerk AG prepared by Deutsche Energie-Agentur GmbH (dena), Berlin, Germany.
- Icha 2014 Icha, P. (2014), „Entwicklung der spezifischen Kohlendioxid-Emissionen des deutschen Strommix in den Jahren 1990 bis 2013“, report by Umweltbundesamt (UBA), Dessau-Roßlau, Germany.
- Janker 2015 Janker, K. (2015), „Aufbau und Bewertung einer für die Energiemodellierung verwendbaren Datenbasis an Zeitreihen erneuerbarer Erzeugung und sonstiger Daten“, doctoral thesis, Technische Universität München, Germany, <https://mediatum.ub.tum.de/node?id=1207265> [accessed 04.09.2015].
- Jarass *et al.* 2009 Jarass, L., Obermair, G., Voigt, W. (2009), *Windenergie – Zuverlässige Integration in die Energieversorgung*, Berlin: Springer.
- Kaltschmitt *et al.* 2014 Kaltschmitt, M., Streicher, W., Wiese, A. (eds) (2014), *Erneuerbare Energien – Systemtechnik, Wirtschaftlichkeit, Umweltaspekte*, Berlin: Springer.
- KEMIN 2011 KEMIN (2011), "Energy strategy 2050 – from coal, oil and gas to green economy", Klima- og Energiministeriet

- (KEMIN), Copenhagen, Denmark,
[http://www.kebmin.dk/sites/kebmin.dk/files/news/from-coal-oil-and-gas-to-green-energy/Energy Strategy 2050 web.pdf](http://www.kebmin.dk/sites/kebmin.dk/files/news/from-coal-oil-and-gas-to-green-energy/Energy%20Strategy%202050%20web.pdf) [accessed 19.08.2015].
- Klaus *et al.* 2010 Klaus, T., Vollmer, C., Werner, K., Lehmann, H., Müschen, K. (2010), „Energieziel 2050: 100 % Strom aus erneuerbaren Quellen“, report by Umweltbundesamt (UBA), Dessau-Roßlau, Germany.
- Kuhn 2012 Kuhn, P. (2012), „Iteratives Modell zur Optimierung von Speicherausbau und -betrieb in einem Stromsystem mit zunehmend fluktuierender Erzeugung“, doctoral thesis, Technische Universität München, Germany, <https://mediatum.ub.tum.de/node?id=1093222> [accessed 04.09.2015].
- Kuhn *et al.* 2012 Kuhn, P., Kühne, M., Heilek, C. (2012), „Integration und Bewertung erzeuger- und verbraucherseitiger Energiespeicher“, final report within the framework of the joint research programme „Kraftwerke des 21. Jahrhunderts (KW21) Phase II“, Lehrstuhl für Energiewirtschaft und Anwendungstechnik, Technische Universität München, Germany, <http://mediatum.ub.tum.de/node?id=1115629> [accessed 30.10.2014].
- Kuhn & Kühne 2011 Kuhn, P., Kühne, M. (2011), „Optimierung des Kraftwerks- und Speicherausbaus mit einem iterativen und hybriden Modell“, *Optimierung in der Energiewirtschaft – VDI-Berichte 2157*, Düsseldorf: VDI-Verlag, pp. 305–317.
- Kühne *et al.* 2014 Kühne, M., Janker, K., Hamacher, T. (2014), “Variability of residual load time series and its implications for energy storage demand in Germany”, poster presented at the Energy Systems Conference, 24–25 June 2014, London, UK, <http://mediatum.ub.tum.de/node?id=1233024> [accessed 06.11.2014].
- Mai *et al.* 2013 Mai, T., Logan, J., Blair, N., Sullivan, P., Bazilian, M. (2013), “Re-assume – a decision maker’s guide to evaluating energy scenarios, modeling, and

- assumptions”, report prepared by National Renewable Energy Laboratory (NREL) for International Energy Agency Renewable Energy Technology Deployment (IEA-RETD), Utrecht, Netherlands.
- Mauch *et al.* 2010 Mauch, W., Corradini, R., Wiesemeyer, K., Schwentzek, M. (2010), „Allokationsmethoden für spezifische CO₂-Emissionen von Strom und Wärme aus KWK-Anlagen”, *Energiewirtschaftliche Tagesfragen*, **60** (9), pp. 12–14.
- Nahmmacher *et al.* 2014 Nahmmacher, P., Schmid, E., Hirth, L., Knopf, B. (2014), “Carpe diem: a novel approach to select representative days for long-term power system models with high shares of renewable energy sources“, working paper, Potsdam Institute for Climate Impact Research (PIK), Germany.
- Nitsch *et al.* 2012 Nitsch, J., Pregger, T., Naegler, T., Heide, D., Luca de Tena, D., Trieb, F., Scholz, Y., Nienhaus, K., Gerhardt, N., Sterner, M., Trost, T., von Oehsen, A., Schwinn, R., Pape, C., Hahn, H., Wickert, M., Wenzel, B. (2012), „Langfristszenarien und Strategien für den Ausbau der erneuerbaren Energien in Deutschland bei Berücksichtigung der Entwicklung in Europa und global“, final report, Deutsches Zentrum für Luft- und Raumfahrt (DLR), Stuttgart, Fraunhofer Institut für Windenergie und Energiesystemtechnik (IWES), Kassel, Ingenieurbüro für neue Energien (IFNE), Teltow, Germany.
- Norio *et al.* 2011 Norio, O., Ye, T., Kajitani, Y., Shi, P., Tatano, H. (2011), “The 2011 eastern Japan great earthquake disaster: overview and comments”, *International Journal of Disaster Risk Science*, **2** (1), pp. 34–42.
- Palmintier & Webster 2011 Palmintier, B., Webster, M. (2011), “Impact of unit commitment constraints on generation expansion planning with renewables”, *2011 IEEE PES General Meeting*, New York: IEEE, pp. 1–7.
- Pandžić *et al.* 2013 Pandžić, H., Qiu, T., Kirschen, D. (2013), “Comparison of state-of-the-art transmission constrained unit commitment formulations”, *2013 IEEE PES General Meeting*, New York: IEEE, pp. 1–5.

References

- Pearce & Ulph 1995 Pearce, D., Ulph, D. (1995), "A social discount rate for the United Kingdom", working paper GEC-1995-01, Centre for Social and Economic Research on the Global Environment (CSERGE), University of East Anglia, Norwich, UK.
- Pfenninger *et al.* 2014 Pfenninger, S., Hawkes, A., Keirstead, J. (2014), "Energy systems modeling for twenty-first century energy challenges", *Renewable and Sustainable Energy Reviews*, **33**, pp. 74–86.
- Pieper & Rubel 2011 Pieper, C., Rubel, H. (2011), "Revisiting energy storage – there is a business case", report by Boston Consulting Group (BCG), Boston, USA.
- Roth 2008 Roth, H. (2008), „Modellentwicklung zur Kraftwerksparkoptimierung mit Hilfe von Evolutionsstrategien“, doctoral thesis, Technische Universität München, Germany, <https://mediatum.ub.tum.de/node?id=652674> [accessed 04.09.2015].
- Schaber 2013 Schaber, K. (2013), "Integration of variable renewable energies in the European power system: a model-based analysis of transmission grid extensions and energy sector coupling", doctoral thesis, Technische Universität München, Germany, <https://mediatum.ub.tum.de/node?id=1163646> [accessed 04.09.2015].
- Scholz 2010 Scholz, Y. (2010), „Möglichkeiten und Grenzen der Integration verschiedener regenerativer Energiequellen zu einer 100 % regenerativen Stromversorgung der Bundesrepublik Deutschland bis zum Jahr 2050“, *Materialien zur Umweltforschung*, **42**.
- Scholz 2012 Scholz, Y. (2012), "Renewable energy based electricity supply at low costs – development of the REMix model and application for Europe", doctoral thesis, Universität Stuttgart, Germany.
- Schweppe *et al.* 1988 Schweppe, F., Caramanis, M., Tabors, R., Bohn, R. (1988), *Spot pricing of electricity*, Norwell: Kluwer Academic Publishers.

- Short *et al.* 2011 Short, W., Sullivan, P., Mai, T., Mowers, M., Uriarte, C., Blair, N., Heimiller, D., Martinez, A. (2011), “Regional Energy Deployment System (ReEDS)”, technical report TP-6A20-46534, National Renewable Energy Laboratory (NREL), Golden, USA.
- SKW 2014 SKW (2014), „Entwicklung ausgewählter Energiepreise“, SKW statistical publication as at 8 January 2014, Statistik der Kohlenwirtschaft e. V., Herne, Germany, <http://www.kohlenstatistik.de/files/enpr.xlsx> [accessed 08.01.2014].
- Strbac *et al.* 2012 Strbac, G., Aunedi, M., Pudjianto, D., Djapic, P., Teng, F., Sturt, A., Jackravut, D., Sansom, R., Yufit, V., Brandon, N. (2012), “Strategic assessment of the role and value of energy storage systems in the UK low carbon energy future”, report for Carbon Trust prepared by Energy Futures Lab, Imperial College, London, UK.
- Trutnevyte 2014 Trutnevyte, E. (2014), “Does cost optimisation approximate the real-world energy transition? Retrospective modelling and implications for modelling the future”, paper presented at the International Energy Workshop 2014, 4–6 June 2014, Beijing, China, http://discovery.ucl.ac.uk/1428484/1/Trutnevyte_I EW_2014.pdf [accessed 19.03.2015].
- Van Horne & Wachowicz 2004 Van Horne, J., Wachowicz, J. (2004), *Fundamentals of financial management*, Harlow: Prentice Hall.
- VGB 2010 VGB (2010), „Analyse der Nichtverfügbarkeit von Wärmekraftwerken 2000–2009“, VGB Power Tech e. V., Technisch-wissenschaftliche Berichte (VGB-TW-103-A, Ausgabe 2010), Essen, Germany.
- VIK 2013 VIK (2013), „Statistik der Energiewirtschaft – Ausgabe 2013“, Verband der Industriellen Energie- und Kraftwirtschaft e. V. (VIK), Essen, Germany.
- Voß & Flinkerbusch 2013 Voß, A., Flinkerbusch, K. (2013), „Ist ein niedriger Preis ein Grund, die Treibhausgaszertifikate zu

- verknappen?“, *Energiewirtschaftliche Tagesfragen*, **63** (1/2), pp. 92–96.
- Wenzel & Kunz 2015 Wenzel, B., Kunz, C. (2015), „Metaanalyse: Stromspeicher in Deutschland“, report by Agentur für Erneuerbare Energien e. V. (AEE), Berlin, Germany.
- Witzenhausen *et al.* 2013 Witzenhausen, A., Drees, T., Breuer, C., vom Stein, D., Moser, A. (2013), „Wirtschaftlichkeit unterschiedlicher Speichertechnologien im mittelfristigen Zeitbereich“, *Beiträge des Internationalen ETG-Kongresses 2013 (ETG-Fachbericht 139)*, Frankfurt a. M.: Energietechnische Gesellschaft im VDE (ETG), pp. 1–7.
- Zucker *et al.* 2013 Zucker, A., Hinchliffe, T., Spisto, A. (2013), “Assessing storage value in electricity markets – a literature review“, Joint Research Centre (JRC), Institute for Energy and Transport, Scientific and Technical Research Reports (JRC83688), Petten, Netherlands.